UDC 521–525
YU ISSN 0373–3734

BULLETIN

DE

L'OBSERVATOIRE ASTRONOMIQUE DE BELGRADE

N° 138

BEOGRAD
1988

BULLETIN

DE

L'OBSERVATOIRE ASTRONOMIQUE DE BELGRADE

FOUNDED IN 1936

Published by Astronomical Observatory, Volgina 7,
11050 Belgrade, Yugoslavia

Director of the Astronomical Observatory: M. Mitrović

The publication of this issue is financially supported by the Republic Community of Sciences of Serbia

Printed by

Zavod za grafičku delatnost Instituta za vodoprivredu „Jaroslav Cerni"
Beograd – Bulevar vojvode Mišića 43/III; Tel.: 651–067

BULLETIN

DE

L'OBSERVATOIRE ASTRONOMIQUE DE BELGRADE

N^O 138

Bull. Obs. Astron. Belgrade, N° 138 (1988) UDC 520.245

BELGRADE PROGRAM FOR MONITORING OF ACTIVITY–SENSITIVE SPECTRAL LINES OF THE SUN AS A STAR
I. An Analog Solar Scanning Monochromator

J. Arsenijević, A. Kubičela, I. Vince and S. Jankov

Astronomical Observatory, Volgina 7, 11050 Belgrade, Yugoslavia

(Received: November 9, 1987)

SUMMARY: A scanning attachment for the Belgrade equatorial solar spectrograph based on a tipping glass rotation in front of the focal plane is described. An analog position encoder and an X–Y recorder complete the system of a solar scanning monochromator. The reduction procedure is reviewed and some instrumental parameters estimated, e g.: the flexture, the expected temperature influence, the range of flat field factors, the distorsion of the wavelength scale, and certain components of the instrumental scattered light.

1. INTRODUCTION

A long–term program of observations of some activity–sensitive Fraunhofer lines has been initiated at Belgrade Astronomical Observatory. It is expected that the depth, the half–width and the equivalent width of these spectral lines will be measured throughout the incoming activity cycle. The observations will be done with the solar spectrograph of Belgrade Observatory using the integrated solar light.

For the purpose this instrument, namely an equatorially mounted Littrow–type spectrograph of 9 m effective focal length, with a Baush and Lomb replice grating 154 mm x 206 mm and 600 lines/mm (Kubičela, 1975) has been converted into a scanning monochromator.

2. THE PRINCIPLES

To convert the spectrograph into a monochromator the exit slit, S in Figure 1, has been inserted into the focal plane of the Littrow lens. Being parallel with the spectral lines, and having the constant 2 mm length, the slit has a changeable width controled by a micrometer screw with 5.5 μm divisions along its drum.

Among several known scanning principles: rotation of the grating, linear motion of the exit slit, changing the physical conditions, and optically shifting the image of the spectrum with respect to the exit slit, the last one turned out to be the most suitable for our purpose. It is realized with a tipping glass, actually a 17 mm glass cube, T in Figure 1, in front of the exit slit. The cube rotates around an axis perpendicular to the disperssion, reaching $\pm$ 40^o from the mean position – what corresponds to $\pm$ 4.75 mm shift of the spectrum across the exit slit.

The same rotation axis is connected with an one–wire potentiometer providing a voltage signal of $\pm$ 250 mV corresponding to the mentioned angular rotation. Such a spectral shift to voltage conversion is a nonlinear process where the relation among angular position of the glass cube (or the potentiometer signal), α, the glass refractive index, n, the thickness of the glass, d, (d = 17 mm) and the linear distance within the spectrum at the exit slit along the dispersion direction, x, is the following

$$x = d\,[\sin\,\alpha - \frac{\sin\alpha\cos\alpha}{\sqrt{n^2 - \sin^2}}]\,. \qquad (1)$$

The refractive index of the glass cube has been measured at two wavelengths, 504 nm and 595 nm, amounting to 1.512 and 1.508 respectively, with the possibility of linear interpolation for any wavelength between the two values. Due to the low focal ratio of the spectrograph (about 1:60 at the blazed angle of the grating and using the imaging optics of the spectrophaph, or even close to 1:100 when the imaging is avoided with a periscope) and to the moderate deviation angles of the glass cube (± 40°), the extensión of the spectrograph camera focal length at the two ends of the field of view, followed by a certain loss of spectral resolution, is taken as negligible.

After the exit slit, S in Figure 1, the radiation reaches the photomultiplier, PMT, through a lens, F. The lens projects the camera (Littrow) lens image onto the photomultiplier, but still allowing some motion of the beam across the curved 1P21 cathode during the scanning.

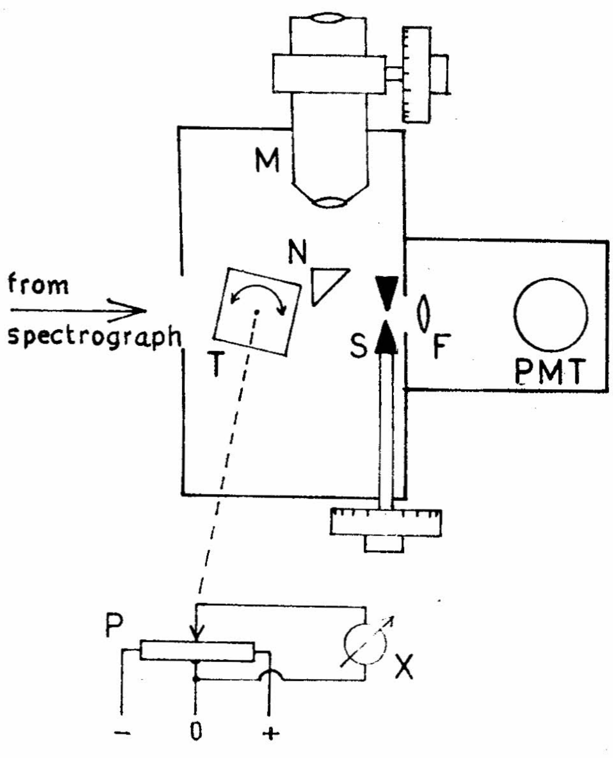

Fig. 1.

An offset microscope, M, with the right–angle prism, N, enables the observer to set the desired spectral feature at the exit slit.

The circular potentiometer, P, has a brass rolling wheel as the working contact and a golden wire as the middle one. The X–coordinate signal is taken from these two contacts. The identity of the potentiometer zero–position with the front glass cube surface being perpendicular to the spectrograph optical axis has been checked optically. The potentiometer wire is fed with 600 mA by an ISKRA RTU 01–20/1.0 D.C. source in the constant current regime.

High voltage to the photomultiplier is supplied and the output signal amplified by the PPI Laboratory Photometer Model 110. The positional, X, and the photometric, Y, signals are recorded at an PHILIPS X–Y recorder Model PM 8120. Using the X–input ranges of 20 mV/cm and 10 mV/cm at the recorder, one magnifies in wavelengths the original spectrum at the middle of the field of view for 30 and 60 times respectively. This gives the possibility to cover by scanning up to 0.48 nm at the 4th order spectrum with about 28 mm/nm dispersion and to record and measure solar spectral line profiles as well as their asymmetries and changes.

Owing to a direct conversion of the glass cube position into the abscissa of an analog record of a spectral feature (not using time as a parameter) the scanning speed can be arbitrary – within some limits given by damping properties of the amplifier and the recorder. It is convenient to cover the whole scanning range during an interval of one minute. In this respect it has to be added that the 3 m long equatorial spectrograph undergoes considerable flexture changes with time noticalbe in the records after several minutes. For example, with the Sun near the meridian, the progressive wavelength shifts up to 256 μm/min at the records, or 4.2 μm/min at the spectrograph focal plane, have been measured. Also, if the temperature extension coefficient of the grating is 10^{-6}/K, a certain temperature influence is expected amounting to about 9 μm/K at the exit slit or about 3.2 pm/K in wavelength and, eventually, about 0.27 mm/K along the X–axis at the recorder (Zajdel' et al., 1976).

3 THE SPECTROPHOTOMETRIC PROCEDURE

As certain spectrophotometric quantities (residual intensities, equvivalent widths, . . .) have to be derived from a scanned and recorded spectrum, the following reduction steps are necessary:

1) Digitalization of the analog records. Besides the simpliest but very tedious procedure of scaling by a ruler, this can be accomplished by any type of the computer digitalizer – what would make all further processing fully automatic.

2) Dark current reduction. This is done by proper positioning and alignment of the coordinate system of the digitalizer.
3) Flat field reduction. That is a necessary position–dependent correction whenever one– or two–dimensional photometric fields are recorded with a non–ideal reciever. In the case of this monochromator, the changeable thickness of galss layer in the light beam during the rotation of the glass cube, some residual motion of the light beam along the curved photopmutiplier cathode and the non–central passing of the light beam through a Barlow lens introduce an unequal response of the reciever to the constant flux produced by the spectrograph within a field of less than 10 mm along the disperssion. Recording a laboratory continuum spectrum, as often as it is necessary, a correction for normalization of any observed signal to the maximum value in the field is obtained at any desired wavelength. The correction factors are usually betwn 1.00 and 1.50 – with the last value corresponding to the very end of the field of view using 20 mV/cm range at the X–input of the recorder.
4) Normalization to the continuum level. In order to express measured intensities in the units of the local continuum intensity, a suitable wavelength interval at each record is chosen and the mean intensity within i taken as the intensity unit. If a record does not contain a local continuum region, another record of such a signal is done at a wavelength up to about 1 nm apart. Selection of such wavelength regions is accomplished according to a high–resolution solar spectrum atlas (e.g. Beckers et al., 1976).
5) Correction of the X–scale. Smaller x–intervals (or wavelength intervals) near the middle, and the longer ones near the edges of the field of view correspond to equal increments of the scanning angle, α, during the rotation of the glass cube. This distorsion of the field can be a posteriori corrected usig (1). The calculation is simple after the digitalization of the analog records. Especially, if an increasing position error from 0 in the middle, to $\pm$ 10 μm near the end of the field at the exit slit (or $\pm$ 0.3 mm and $\pm$ 0.6 mm at the record – depending on the X–input range) is allowed, no interpolation of refractive index between the wavelengths 504 nm and 595 nm is necessary. On the other hand, when, in an exceptional case, the analog records are immediateily analyzed, a special X–scale (a ruler) can be made in order to read equidistant wavelength intervals).
6) Reduction of the instrumental profile. Evaluation of spectral line spectrophotometric quantities, other than the equivalent widths, requires a deconvolution of the observed and instrumental profiles. So far, the instrumental profile has been photographically determined by means of selected telluric lines in the red region, and for two spectral orders separatelly (Jankov, 1985). The results showed that the effective spectrograph resolution in the photographic approach amounted to about 107000 in the 4th order and about 134000 in the 5th order. Preparations are in progress to evaluate the instrumental profile photoelectrically in somewhat shorter wavelengths.
7) Dealing with the scattered light. A previous photospheric velocity research program done with this spectrograph revealed a considerable scattered light within the solar image. However, skipping the imaging optics of the spectrograph and observing the integral solar light, what will be the case in our present and near future research, that problem is avoided.

As the autocollimating spectrographs are known to scatter some amount of light by reflection and difusion from several optical surfaces functioning in the collimator and camera at the same time, two laboratory measurements of such non–selective scattering were undertaken. First, the background signal between the two well separated spectral orders (1st and 2nd) was measured, while the slit was illuminated with a continuum light source through a medium–selective glass filter (filter VG–5, cutting at 450 nm the shortward wavelengths to less than 1%). Second, the background signal well out of the strong Hg I 546 nm emission spectral line was measured. In both cases the measured background intensity was less than 0.5% of the maximum itensity in the adjacent spectrum of the respective light source (1st order spectrum or the green Hg I emission line). That amount of scattered light can, in most cases, be taken as negligible.

According to the certificate, the ghosts of the grating should also be less than 0.5 % at the green Hg I line in the 5th order spectrum.

4. CONCLUDING REMARKS

As far as the accuracy of the whole procedure is concerned, no definitive figures on inner or outer errors have been derived yet. Nevertheless, taking into account the already considered steps of the spectrophotometric reductions with the described scanner, one can expect an inner random error of couple of percents in the intensity measurements, and, perhaps, a similar error in the equivalent widths of spectral lines. The outer errors should be somewhat higher and mainly systematic – because of the problems with instrumental profile, definition of local continuum level, and separation of spectral line blends.

The analog records are, of course, not the most efficient way of processing the spectrophotometric data.

Being aware of that fact but not having possibilities to immediately solve the problem by an on–line digitalization of the signal, and wanting to start a long–term research program as soon as possible, we accepted the analog recording – at least for the present. The other, more efficinet, solutions are still envisaged too.

ACKNOWLEDGEMENTS

This work has been supported by Republic Association for Science in Serbia through the project „Physics and Motions of Celestial Bodies and Artificial Satelites".

REFERENCES

Beckers, M., Bridges, C.A., Gilliam, L.B.: 1976, *A High Resolution Spectral Atals of the Solar Irradiance From 380 to 700 Nanometers,* Volume II: Graphical Form, Sacramento Peak Obs. Project 7649, AFGL, Hanscom AFB, Mass. USA.

Jankov, S.: 1985, *Bull. Astron. Obs. Belgrade,* **135**, 25.

Kubičela, A.: 1975, *Publ. Astron. Obs. Belgrade,* **20**, 47.

Zajdel', A.N., Ostrovskaya, G.V., Ostrovskij, Yu. I.: 1976, *Tehnika i Praktika Spektroskopii,* Nauka, Moskva, 94.

Bull. Obs. Astron. Belgrade, N° 138 (1988) UDC 532.516 : 536.2

ON THE THERMAL INSTABILITY OF A VISCOUS MEDIUM

T. Angelov

Institute of Astronomy, Faculty of Sciences, Beograd

(Received: 2 December, 1987)

SUMMARY: **Thermal instability of a viscous medium with radiation and heat conduction and without volume forces and magnetic field is considered. The characteristic equation for the case of small perturbations is derived, its solutions are discussed and accordingly the instability criteria are given. It is shown that the viscosity has no influence upon the isobaric mode and that it reduces the domain of the isentropic instability mode.**

1. INTRODUCTION

Thermal instability of a given medium with no volume forces, with or without a magnetic field has important nonastrophysical applications. On the other hand formation of a number of astrophysical objects (solar prominences, planetary nebulae, interstellar clouds) cannot be explained by the gravitation condensation mechanism. Another possibility – the instability of the thermal equilibrium has been partly, and for different objects, considered by several authors: Parker (1953), Zanstra (1955a, b) and others. The conditions of a nongravitational condensation, i.e. the criteria of a thermal instability of a nonviscous medium, were proposed by Field (1965) in a detailed analysis. Heating and cooling mechanisms for the interstellar medium have been considered by Oppenheimer (1977), Suchkov and Shchekinov (1979) etc; a review of interstellar medium physics may be found in Spitzer (1978), Kaplan and Pikel'ner (1979).

The subject of the present paper is the instability of the thermal equilibrium of a infinite homogeneous viscous medium with radiation and heat conduction. In Sect. 2 starting basic equations are given and the characteristic equation corresponding to the small perturbations case is derived. Its solutions and the instability criteria are analysed in Sect. 3 and the conclusion is presented in Sect. 4.

2. CHARACTERISTIC EQUATION

The state of a infinite viscous medium with radiation and heat conduction, without a magnetic field and volume forces, is described by the hydrodynamical equations

$$\frac{d\rho}{dt} + \rho\nabla \cdot \vec{v} = 0 \tag{2.1}$$

$$\rho \frac{d\vec{v}}{dt} + \nabla p - \nabla \cdot \tau = 0 \tag{2.2}$$

$$\rho T \frac{dS}{dt} + \rho\mathcal{L} - \nabla \cdot \kappa \nabla T - \Phi = 0 \tag{2.3}$$

with

$$p = p(\rho, S) \tag{2.4}$$

$$\tau_{ik} = \eta \left(\frac{\partial v_i}{\partial x_k} + \frac{\partial v_k}{\partial x_i}\right) + \left(\xi - \frac{2}{3}\eta\right) \delta_{ik} \nabla \cdot \vec{v} \tag{2.5}$$

$$\Phi = \frac{\eta}{2} \left(\frac{\partial v_i}{\partial x_k} + \frac{\partial v_k}{\partial x_i} - \frac{2}{3} \delta_{ik} \nabla \cdot \vec{v}\right)^2 + \xi (\nabla \cdot \vec{v})^2. \tag{2.6}$$

Here ρ, T, S, p are the density, the temperature, the entropy and the pressure of the ideal gas, τ_{ik} and Φ are the components of the viscous stress tensor and the corresponding dissipative function in the Cartesian coordinates (ξ, η are both coefficients of the viscous friction; δ_{ik} is the Kronecker symbol), κ is the heat conduction coefficient, $\mathcal{L}$ (ρ, T) is the total function of gas heating and cooling by radiation (defined as the difference between rate of cooling and rate of heating per gram of material); the operator $d/dt = \partial/\partial t + \vec{v} \cdot \Delta$ and $\vec{v}$ is the hydrodynamical velocity.

In the present paper the stability of the medium is examined with respect to small perturbations. For a homogeneous basic state in the mechanical and thermal equilibrium defined via

$$\rho_0, T_0 = \text{const}; \ \vec{v}_0, \mathcal{L}_0 = 0, \tag{2.7}$$

the linearisation of equations (2.1) – (2.6) yields a perturbation–function system

$$\frac{\partial \rho_1}{\partial t} + \rho_0 \nabla \cdot \vec{v}_1 = 0 \tag{2.8}$$

$$\rho_0 \frac{\partial \vec{v}_1}{\partial t} + \nabla p_1 - \eta_0 \nabla^2 \vec{v}_1$$

$$-(\xi_0 + \frac{1}{3}\eta_0)\nabla(\nabla \cdot \vec{v}_1) = 0 \tag{2.9}$$

$$\rho_0 T_0 \frac{\partial S_1}{\partial t} + \rho_0 \mathcal{L}_\rho \rho_1 + (\rho_0 \mathcal{L}_T - \kappa_0 \nabla^2) T_1 = 0 \tag{2.10}$$

$$p_1 - c^2 \rho_1 - c_\rho^2 S_1 = 0. \tag{2.11}$$

Also, by linearisation of the ideal–gas–state equation, $p = (R/\mu)\rho T$, where both R and μ are constant (these are the gas constant and the mean molecular weight) one obtains

$$v_\rho^2 T_1 = p_1 - v_T^2 \rho_1 . \tag{2.12}$$

In (2.10)–(2.12) $\mathcal{L}_\rho$ and $\mathcal{L}_T$ are the partial derivatives of $\mathcal{L}(\rho, T)$ in ρ and T,$c = (\gamma p/\rho)^{1/2}$ and $v_T = (p/\rho)^{1/2}$ are the adiabatic and izothermal speeds of sound, respectively (γ is the specific heat ratio for the ideal gas), $c_\rho^2 = (\partial p/\partial S)_\rho = (\gamma-1)\rho T$ and $v_\rho^2 = (\partial p/\partial T)_\rho = p/T$; all these quantities, as well as ξ_0, η_0, and κ_0 are calculated in the basic state.

For the case of a perturbation $f_1 \sim \exp(\omega t + i\vec{k}\cdot\vec{r})$ and a potential velocity field, equations (2.8), the divergence of (2.9), and (2.10) with (2.12) yield

$$\omega\rho_1 + i\rho_0 \vec{k}\cdot\vec{v}_1 = 0 \tag{2.13}$$

$$ik^2 p_1 + [\rho_0\omega + (\xi_0 + \frac{4}{3}\eta_0)k^2]\,\vec{k}\cdot\vec{v}_1 = 0 \tag{2.14}$$

$$g_0\rho_1 + h_0 p_1 + \rho_0 T_0 \omega S_1 = 0 \tag{2.15}$$

where

$$g_0 = \rho_0 \mathcal{L}_\rho - v_T^2 h_0 , \ h_0 = (\rho_0 \mathcal{L}_T + \kappa_0 k^2)/v_\rho^2 . \tag{2.16}$$

The condition for the existence of a nontrivial solution for the homogeneous system (2.11), (2.13)–(2.15) is given by the characteristic equation

$$\omega^3 + (\frac{k_T}{k} + \frac{k}{k_\kappa} + \frac{k}{k_\nu})ck\omega^2 +$$

$$+[1 + \frac{k}{k_\nu}(\frac{k_T}{k} + \frac{k}{k_\kappa})]c^2k^2\omega$$

$$+\frac{c^3k^3}{\gamma}(\frac{k_T}{k} + \frac{k}{k_\kappa} - \frac{k_\rho}{k}) = 0 \tag{2.17}$$

where the wave numbers

$$k_T = \frac{(\gamma-1)\mu}{Rc}\mathcal{L}_T, \ k_\rho = \frac{(\gamma-1)\mu}{Rc}\cdot\frac{\rho_0\mathcal{L}_\rho}{T_0}$$

$$k_\kappa = \frac{Rc}{(\gamma-1)\mu}\cdot\frac{\rho_0}{\kappa_0}, \ k_\nu = \frac{\rho_0 c}{\xi_0 + \frac{4}{3}\eta_0} \tag{2.18}$$

are introduced.

3. INSTABILITY CRITERIA

The medium is unstable in the region of purely real, positive, solutions of the characteristic equation (2.17) – aperiodic instability – or in the region $Re(\omega) > 0$ of its complex solutions – periodic instability. Using dimensionless variables

$$z = \frac{\omega}{kc}, \ a_T = \frac{k_T}{k}, \ a_\rho = \frac{k_\rho}{k}, \ a_\kappa = \frac{k}{k_\kappa},$$

$$a_\nu = \frac{k}{k_\nu}, \tag{3.1}$$

one can rewrite (2.17) as

$$z^3 - az^2 + bz - d = 0 \tag{3.2}$$

where

$$a = -(a_T + a_\kappa + a_\nu), \ d = \frac{1}{\gamma}(a + a_\nu + a_\rho),$$

$$b = 1 + \beta, \ \beta = a_\nu(a_T + a_\kappa). \tag{3.3}$$

For the case of a perturbation with $k \in Re$ within the given medium, the cubic equation (3.2) with real coefficients (3.3) has three real solutions (z_k), or one real (y) and two conjugate–complex ones($x \pm iw$). In the latter case from the real and imaginary parts (3.2) one obtains for Re(z)

$$x^3 - ax^2 + \frac{1}{4}(a^2 + b)x - \frac{1}{8}(ab - d) = 0. \tag{3.4}$$

Both equations (3.2), (3.4), have the same form

$$F(u) \equiv u^3 - au^2 + Bu - D = 0 \qquad (3.5)$$

where B and D are the corresponding coefficients in (3.2), (3.4). In such a way the analysis of the general solution of (3.2) is reduced to a discussion of purely real roots of the function F(u). They will be simply identified as abscissae of the intersection of the function

$$f(u) = u^3 - au^2 + Bu \qquad (3.6)$$

with the straight line D = const (where assumptions $|\beta| < 1$ and $a_\rho > 0$ will be used). The elements of the plot f(u) are given in Tab. 1 with

$u_1 = 0,\ u_{2,3} = (a/2)\{1 \pm (1-4B/a^2)^{1/2}\} = |u_{2,3}|\ \mathrm{sign}\ a,$

$u_{I,II} = (a/3)\ \{1 \pm (1-3B/a^2)^{1/2}\} = |u_{I,II}|\ \mathrm{sign}\ a.$

Table 1. Elements of the plot f(u)

region $\|a\|$	zero–points f(u)	extremum abscissae f(u)
$\|a\| > (4B)^{1/2}$	$u_{1,2,3}$	$u_{I,II}$
$(3B)^{1/2} < \|a\| < (4B)^{1/2}$	u_1	$u_{I,II}$
$\|a\| < (3B)^{1/2}$	u_1	–

The identification of the roots of the function F(u) from (3.5) will be done for the corresponding f(u) from Tab. 1. depending on the sign a.

In the case of $a < 0$, F(u) has negative roots for D <0, while for D > 0 F(u) has positive roots – one per each region $|a|$.

If $a > 0$, D must be positive for (3.2), whereas $a > (4B)^{1/2}$ is impossible for (3.4) and F(u) has positive roots only if D > 0: one corresponding to $a < (3B)^{1/2}$, one or three (depending on whether D is larger or smaller than $f(u_I)$, i.e $f(u_{II})$) corresponding to the other two a–regions.

The details of the discussion will not be presented – one merely concludes that F(u) has real, positive and mutually differing roots only if D > 0, independent of sign a. In a special, physically justified, case when for each a_s from (3.1) is valid $|a_s| \ll 1$, F(u) has one and only one univocally defined positive root for D > 0. This is the instability criterion corresponding to the present case and here being looked for. It yields for (3.2) and (3.4), respectively

$$a_T - a_\rho < - a_\kappa, \qquad (3.7a)$$

$$a_T + \frac{1}{\gamma-1}\,a_\rho < -\left(a_\kappa + \frac{\gamma}{\gamma-1}\,a_\nu\right). \qquad (3.7b)$$

Inequalities (3.7) without the terms a_κ and a_ν serve as criteria of the isobaric and isentropic instabilities, respectively (Field, 1965). It is seen that the viscosity does not affect the isobaric instability, but it reduces the domain of the isentropic one: alone (if $a_\kappa = 0$) and combined with the conduction (a_κ and a_ν are positively defined quantities). From (3.7b) and (3.1) it follows that the total effect of both viscosity and conduction stabilizes waves characterized by

$$\lambda < \lambda_c\ ,\ \lambda_c = 2\pi\ \left\{-\frac{1 + \frac{\gamma}{\gamma-1}\cdot\frac{k_\kappa}{k_\nu}}{k_\kappa\left(k_T + \frac{1}{\gamma-1}\,k_\rho\right)}\right\}^{1/2}. \qquad (3.8)$$

The result (3.7a) without the a_ρ term was obtained by Parker (1953), both criteria (3.7) (the second one without a_ν) were obtained by Field in the paper mentioned above.

Now, approximate solutions (real and complex) of the characteristic equation (3.2) written in the form

$$z^3 + z = az^2 - \beta z + d \qquad (3.9)$$

will be found, for $|a_s| \sim \delta$, $\delta \ll 1$ (their solutions for $a_s = 0$ are $z_1(o) = 0$, $z_{2,3}(o) = \pm i$). From (3.9) written in the form

$$z_k(n+1) - z_k(o) = \frac{az_k^2(n) - \beta z_k(n) + d}{\prod\limits_{j\neq k}(z_k(n) - z_j(o))} \qquad (3.10)$$

one obtains by iteration for each k = 1, 2, 3 (already at n = 1)

$$z_1 = d[1 + d(a-d) - \beta] + R(\delta^5), \qquad (3.11)$$

$$z_{2,3} = \pm\, i\,[1 - \frac{a-d}{8}(a+3d) + \frac{1}{2}\beta] +$$

$$+ \frac{a-d}{2}[1 + \frac{a-d}{8}\cdot\frac{a+7d}{2} + \frac{d}{a-d}\,\beta] + R(\delta^4). \qquad (3.12)$$

From the solutions z_1 and $\mathrm{Re}(z_{2,3})$ linear in δ, the criteria for the instability modes (3.7a) and (3.7b), respectively, directly follow.

Now a special case of the function $\mathcal{L}(\rho, T)$,

$$\mathcal{L} = (nL - \Gamma)\,\frac{n}{\rho}\,, \tag{3.13}$$

where are: n–number density of particles, L(T)–cooling function and Γ = const–heating function, is considered. On the basis (3.1) and (2.18) one has

$$a_T = \alpha a_\rho;\ \alpha = \left(\frac{d\ln L}{d\ln T}\right)_0 \tag{3.14}$$

and the criteria (3.7a) and (3.7b) define instabilities within the α–regions

$$\alpha < 1 - \frac{a_\kappa}{a_\rho}\,, \tag{3.15a}$$

and

$$\alpha < -\frac{1}{\gamma-1}\left[1 - \frac{a_\kappa}{a_\rho} + \gamma\,\frac{a_\kappa + a_\rho}{a_\rho}\right]. \tag{3.15b}$$

From the latter inequalities, (3.14) and (3.1) the critical wavelengths $\lambda_c(i)$, i = 1 – isobaric mode, i = 2 – isentropic mode, are

$$\lambda_c(1) = c_1\,(1-\alpha)^{-1/2},\ \lambda_c(2) = c_2\left(|\alpha| - \frac{1}{\gamma-1}\right)^{-1/2} \tag{3.16}$$

with

$$C_1 = 2\pi(k_\rho k_\kappa)^{-1/2} \quad \text{and}$$

$$C_2 = C_1\left(1 + \frac{\gamma}{\gamma-1}\cdot\frac{k_\kappa}{k_\nu}\right)^{1/2}.$$

4. CONCLUSION

Within the framework of the infinite–medium approximation with a homogeneous basic state in the mechanical and thermal equilibrium there are two possibilities for the thermal instability appearance – as the isobaric–condensational mode or as the isentropic–wave mode (Field, 1965). In the present consideration of a viscous medium it is shown how a viscous dissipation can affect the wave mode by reducing the unstable domain. The instability condition ($\lambda > \lambda_c$), as it follows from (3.16) can be more easily fulfilled for the case of a condensational mode, even if viscosity is absent ($\kappa_\nu = \infty$). In several astrophysical applications, when the influences of the conduction and viscosity are insignificant ($a_\kappa, a_\nu \to 0$), the α–criteria of the isobaric and isentropic instabilities are $\alpha < 1$ and $\alpha < -1.5$, respectively, when $\gamma = 5/3$.

This work is part of the research project supported by the Fund for Scientific Research of the S.R. Serbia.

REFERENCES

Field, G.B.: 1965, Astrophys. J. **142**, 531.
Kaplan, S.A. and Pikel'ner, S.B.: 1979, Fizika mezhzvezdnoj sredy (Moskva, „Nauka").
Oppenheimer, M.: 1977, Astrophys. J. **211**, 400.
Parker, E.N.: 1953, Astrophys. J. **117**, 431.
Spitzer, L.: 1978, Physical properties in interstellar medium (New York: J. Wiley and Sons).
Suchkov, A.A., Shchekinov, Yu.A.: 1979, Astron. Zh. **56**, 1179.
Zanstra, H.: 1955a, Gas Dynamics of Cosmic Clouds, ed. J. M. Burgers and H.C. van de Hulst (Amsterdam: North–Holland Publishing Co.), chap. XIII.
––––: 1955b, Vistas in Astronomy, **1**, ed. A. Beer (New York: Pergamon Press), p. 256.

Bull. Obs. Astron. Belgrade, N° 138 (1988) UDC 520.253.028

ANALYSIS OF RESULTS OBTAINED FROM OBSERVATIONS WITH MERIDIAN CIRCLES IN BELGRADE AND BRORFELDE

S.Sadžakov, M. Dačić and Z.Stančić

Astronomical Observatory, Belgrade, Volgina 7, 11050 Belgrade, Yugoslavia

(Received: November 1, 1987)

SUMMARY: Characteristics of the instruments used for the purpose of compilation of the here analysed observational material are given. The systematic errors of $\Delta\alpha$ and $\Delta\delta$ types in the right ascension, declination, magnitude and spectrum are determined.

INTRODUCTION

The results analysed here have been obtained from meridian circle observations in Belgrade and Brorfelde. The characteristics of Belgrade Meridian Circle are the following: objective tube aperture is equal to 190 mm and the focal length to 2578 mm. The eyepiece micrometer system consists of an impresonal micrometer with devices for hand driving allowing motions equivalent to 40 minutes of arc in the azimuth and of an ordinary micrometer whose motion is about 25 minutes of arc in the elevation. The instrument has a graduated metallic circle whose diameter is 80 mm attached to the rotation axis. There are eight microscope micrometers; four of them at the east side and the other four at the west side of the instrument. They have drums divided into 60 parts. The circle is read visually.

The instrument has two collimators of 80 mm diameter and 1000 mm focal length, a level at the rotation axis and a mercury mirror situated under the floor, over which the observer carriage is driven on the rails (Šaletić, 1968). The temperature of the barometer is read visually every 15 minutes during an observation.

The accuracy of determination for 1965 positions of stars within the magnitude range $5^m.5 - 8^m.5$ obtained with the instrument mentioned above and presented in the NPZT–Programme–Star Catalogue (Sadžakov et al., 1981) is equal te $\epsilon_\alpha \cos\delta = \pm 0.^s036$, $\epsilon_\delta = \pm 0.''26$.

The star positions obtained from observations with the automatic meridian circle in Brorfelde (Copenhagen University Observatory) are given in a catalogue by Helmer and others (1983, 1984).

This instrument has a clear aperture of 178 mm and a focal length of 2665 mm is characterized by a photoelectric moving–slit micrometer connected with a computer controlling the observation process. It has a glass circle whose diameter is 2r = 178 mm use of six microscope micrometers scanned under the controlling process and making possible straightforward qualitative interrupting, as well as linear diminishing and the use of the diameter corrections for the purpose of the final reading and measuring of its value.

Another photoeelectric micrometer is used to determine the collimation, the inclination and the flexure of the tube. This collimation micrometer contains a source of light and a single pair of 45^o slits on a plate in front of a photomultiplier. The plate is driven by using a stepping motor controlled by the process controller. Collimation alignment can be realised by using this micrometer to determine the position of a fixed light source in the southern collimator.

The micrometer of the instrument contains a source of light which can be observed by reflection in a mercury pool to provide the nadir direction. The mercury pool is held in a sealed container that opens automatically.

The process controller is linked via an analogue–to–digital converter to the following meteorological sensors: internal and external temepratures -15 to $+35 \pm 0.1^oC$; barometric pressure $650 - 870 \pm 0.1$ mm Hg; relative humidity $0 - 100 \pm 1\%$; wind speed 0.3 ± 1 ms^{-1}; wind direction $0^o–360^o \pm 5^o$.

One should say that this instrument with the accessories is situated within a pavilion furnished with a rain detector being triggered immediately after first rain drops have fallen, otherwise the dome being closed and observing being suspended.

The accuracy of stars position determination with this instrument is equal to $\epsilon_\alpha \cos\delta = \pm 0.^s0139$ and $\epsilon_\delta = \pm 0.''217$ for 1071 stars whose apparent magnitudes are less than or equal to 12.

In the case of both catalogues the observations and the reduction of the observational material were done by use of the relative method.

TREATMENT OF THE OBSERVATIONAL MATERIAL

In the course of our observations always a fraction of 25 – 30% of the total number of observed stars belonged to FK4 stars. The duration of a series was between 4 and 6 hours and the number of observed stars was between 80 and 120. The collimation was always measured twice and the flexure once.

The right ascensions of the programme stars are calculated by use of the Bessel formula

$$\alpha_i = T_i + r_{sec}\,\delta_i + (u + m)_{mean} + n_{mean} \cdot \mathrm{tg}\,\delta_i$$

The declination of the programme stars are calculated by use of the following formula

$$M_i = M + mR_\delta + \Delta\lambda + \rho + f \sin z$$

The refraction is calculated by use of the Pulkovo tables $\log \rho = \mu + \log \mathrm{tg}\, z + \gamma + B + T + E$.

COMPARISON OF STAR POSITIONS

Since all the star positions in both catalogues are given for the equinox 1950.0 and the corresponding observation epoch and in the same system FK4 – they are reduced to the same observation epoch (Belgrade) by using the AGK3 proper motions and the following differences are formed

$$\Delta\alpha = \alpha_{Belgrade} - \alpha_{Brorfelde}$$
$$\Delta\delta = \delta_{Belgrade} - \delta_{Brorfelde}.$$

These differences are composed of contributions of systematic influences (in both equatorial coordinates, magnitude, spectrum and to the origin of coordinates, itself). Thus we can write

$$\Delta\alpha = \Delta\alpha_o + \Delta\alpha_\delta + \Delta\alpha_\alpha + \Delta\alpha_m + \Delta\alpha_{sp}$$

$$\Delta\delta = \Delta\delta_o + \Delta\delta_\delta + \Delta\delta\alpha + \Delta\delta_m + \Delta\delta_{sp}.$$

The systematic influences are calculated by use of the least square method. Then we apply Abbe's criterion to the differences

$$r = \frac{q^2}{s_1^2}$$

where is

$$q^2 = \frac{1}{2(n-1)} \sum_{i=1}^{n-1} (x_{i+1} - x_i)^2;$$

$$s_1^2 = \frac{1}{n-1} \sum_{i=1}^{n} (x_i - x)^2;$$

x_i – i–th systematic differences;
x – mean value of the systematic differences;
n – number of differences,

in order to examine the systematic variations of these differences. Figures 1. – 6. and Tables 1. – 4. contains the results of these calculations. In Tables 1. – 4. Δ is a systematic difference, n is the number of stars.

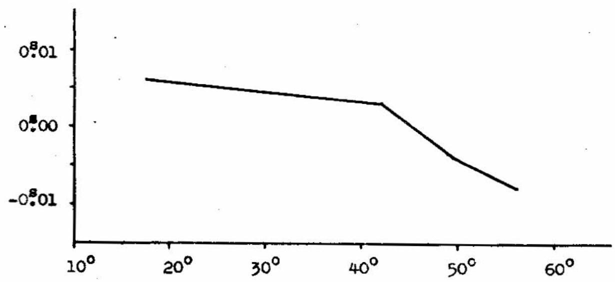

Fig. 1. Systematic Differences $\Delta\alpha_{(BGD\ -\ H82)}$ in Declination

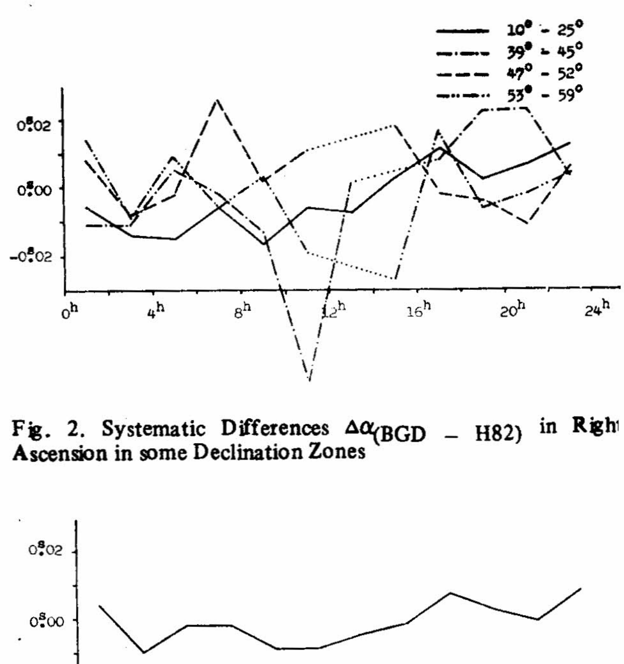

Fig. 2. Systematic Differences $\Delta\alpha_{(BGD\ -\ H82)}$ in Right Ascension in some Declination Zones

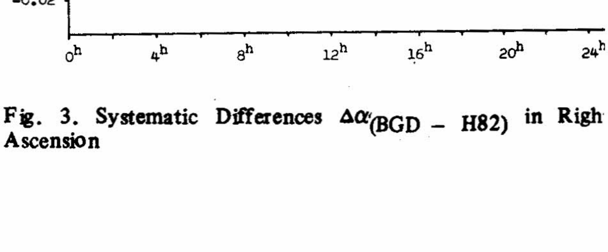

Fig. 3. Systematic Differences $\Delta\alpha_{(BGD\ -\ H82)}$ in Right Ascension

Table 1. Systematic Differences $\Delta\alpha_{(BGD\,-\,H82)}$ in Magnitude

	$m \leqslant 6.5$		6.5 – 7.5		7.5 – 8.5		$8.5 < m$	
	Δ	n	Δ	n	Δ	n	Δ	n
O, B	0^s.005	2	0^s.001	7	0^s.003	5	0^s.012	2
A	0.007	2	–0.001	11	–0.004	42	0.000	14
F	–0.037	1	0.002	16	–0.002	24	0.004	7
G	–0.019	2	0.004	5	0.003	21	–0.007	4
K, M	–0.004	13	0.005	16	0.003	26	0.002	4
$\Delta\alpha_m$	–0,005	20	0.002	55	–0.001	118	0.001	31
r_{sp}	0.923		0.296		0.805		0.926	

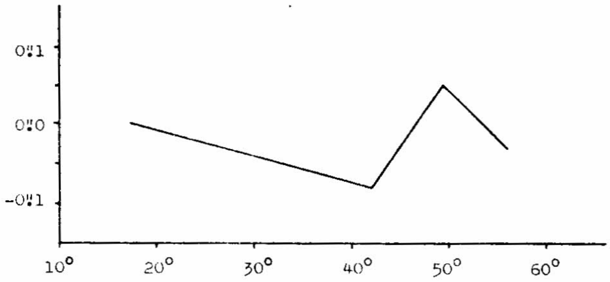

Fig. 4. Systematic Differences $\Delta\delta_{(BGD\,-\,H82)}$ in Declination

Table 2. Systematic Differences $\Delta\alpha_{(BGD\,-\,H82)}$ in Spectrum

	O,B		A		F		G		K, M	
	Δ	n	Δ	n	Δ	n	Δ	n	Δ	n
$m \leqslant 6.5$	0^s.010	2	0^s.012	2	–0^s.032	1	–0^s.014	2	0^s.001	13
6.5 – 7.5	–0.002	7	–0.003	11	–0.001	16	0.002	5	0.003	16
7.5 – 8.5	0.003	5	–0.003	42	–0.002	24	0.003	21	0.004	26
$8.5 < m$	0.011	2	–0.001	14	0.003	7	–0.008	4	0.001	4
$\Delta\alpha_{sp}$	0.003	16	–0.002	69	–0.001	48	0.001	32	0.003	59
r_m	1.039		0.720		0.640		0.945		1.062	

Table 3. Systematic Differences $\Delta\alpha_{(BGD\,-\,H82)}$ in Magnitude

	$m \leqslant 6.5$		6.5 – 7.5		7.5 – 8.5		$8.5 < m$	
	Δ	n	Δ	n	Δ	n	Δ	n
O, B	–0$''$.18	2	0$''$.10	7	–0$''$.24	5	0$''$.13	2
A	0.05	2	–0.07	10	–0.06	40	–0.01	14
F	–0.02	1	–0.08	16	0.05	23	–0.16	6
G	–0.12	2	0.23	5	0.11	20	–0.10	4
K, M	–0.02	13	0.02	18	0.07	27	0.17	2
$\Delta\delta_m$	–0.04	20	0.00	56	0.01	115	–0.03	28
r_{sp}	1.169		1.283		0.313		0.729	

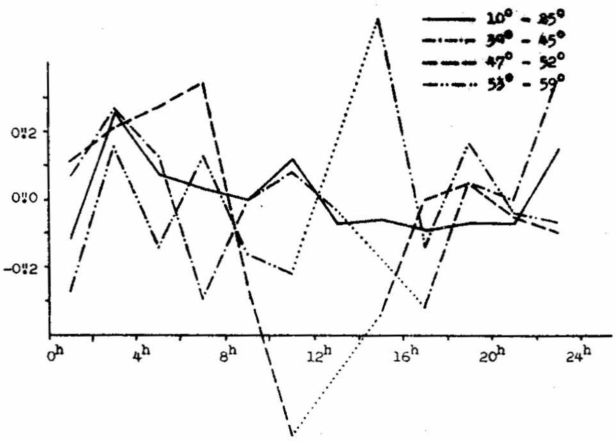

Fig. 5. Systematic Differences $\Delta\delta_{(BGD\,-\,H82)}$ in Right Ascension in some Declination Zones

Table 4. Systematic Differences $\Delta\delta_{(BGD\,-\,H82)}$ in Spectrum

	O, B		A		F		G		K, M	
	Δ	n	Δ	n	Δ	n	Δ	n	Δ	n
$m \leqslant 6.5$	–0$''$.14	2	0$''$.09	2	0$''$.02	1	–0$''$.08	2	0$''$.02	13
6.5 – 7.5	0.09	7	–0.07	10	–0.09	16	0.23	5	0.02	18
7.5 – 8.5	–0.25	5	–0.07	40	0.03	23	0.10	20	0.05	27
$8.5 < m$	0.16	2	0.02	14	–0.13	6	–0.07	4	0.20	2
$\Delta\delta_{sp}$	–0.04	16	–0.05	66	–0.03	46	0.09	31	0.04	60
r_m	1.522		0.934		1.363		1.077		0.502	

Fig. 6. Systematic Differences $\Delta\delta_{(BGD\ -\ H82)}$ in Right Ascension

CONCLUSIONS

On the basis of the results obtained by applying Abbe's criterion, one can say that there are small systematic errors of $\Delta\alpha_{\alpha}$ type in the zones between 0 and 4 hours and between 8 and 10 hours, $\Delta\alpha_{\delta}$ only for the southern zone between 10^{o} and 25^{o}, $\Delta\delta_{\alpha}$ between 2^{h} and 4^{h} and between 18^{h} and 20^{h}; $\Delta\delta_{\delta}$ in the zone between 47^{o} and 52^{o}, whereas for other declination zones, right ascension, magnitude and spectrum they are not evident.

The results of our examination are in favour of the conclusion that the star positions in both catalogues are affected by systematic errors to a very small degree.

ACKNOWLEDGEMENTS

This work has been supported by Republik Association for Science of Serbia through the project „Physics and Motions of Celestial Bodies and Artificial Satelites".

REFERENCES

Helmer, L., Fabricius, C. and all.: 1983, *Astron. Astrophys Suppl. Ser.* **53**, 223.
Helmer, L., Fabricius, C., Einicke, O.H. and all.: 1984, *Astron Astrophys Suppl. Ser.* **55**, 87.
Sadžakov, S., Šaletić, D., Dačić, M.: 1981, *Publ. Astron. Obs. Belgrade,* **30**, 1.
Šaletić, D.: 1968, *Publ. Astron. Obs. Belgrade,* **14**. 88.

Bull. Obs. Astron. Belgrade, No 138(1988) UDC 524.388

THE PROGRAMME OF THE STUDY OF DYNAMICAL STATES OF THE NEARBY TRIPLE STARS

J.P. Anosova

Astronomical Observatory of the Leningrad State University
Bibliotechnaya pl. 2, 198904 Leningrad Petrodvoretz, USSR

(Received: October 15, 1987)

SUMMARY: For the 113 bright ($V \leqslant 10^m5$) and nearby ($r \leqslant 100$ pc) triple stars, included in the Leningrad State University Astronomical Observatory programme dedicated to the study of their dynamical states, the astrometrical and astrophysical observational data have been collected from about 60 catalogues. In the compiled Table the results for all 113 stars are presented, together with the newly collected astrometrical, photometrical and spectroscopical observations, obtained at Pulkovo Observatory (26" refractor), Special Astrophysical Observatory (6m telescope), Crimean Observatory (AST–11 and STS), Burakan Station of LSUAO (AST–14), and Southern Station of MSU (STE and Zeiss).

The LSUAO triple stars programme is included in the Input Catalogue of EAS HIPPARCOS and in General Observer Program at the Hubble Space Telescope, with a purpose of completeness improving and of the essential increasing of data accuracy.

I. STATEMENT OF THE PROBLEM

The study of evolution of the triple stars has a considerable importance, since triple systems are widely distributed in the galactic field as well as in star clusters. The questions related to the age of clusters containing triple stars, as well as to the qualitative picture of their evolution etc. have a special interest.

The numerical studies (Agekian, Anosova, Orlov, 1967–1986) of dynamical evolution of the simulated triple systems with negative total energy ascertained two types of behaviour in these systems:

1. dynamically stable hierarchical systems in which the distant body moves on a nearly Keplerian orbit with respect to the close binary, which retains its identity throughout; in these systems, the dynamical evolution may be effectively studied by analytical methods;
2. dynamically unstable non–hierarchical systems in which the motions of bodies have a complicated character and the minimum two–body separation is alternatively associated with different pairs of bodies; the investigation of these systems requires the computer simulations.

The triple stars and galaxies are thus generally separated to hierarchical and non–hierarchical systems (like, for example, systems of Trapezium type) according to their apparent configurations. From observations, the dynamically stable and unstable triple systems are usually distinguished by the ratio of maximum and minimum angular separations.

The statistical studies of the distributions of configurations in simulated and observed triples have been carried out (Agekian and Anosova, 1964; Anosova, 1968; Anosova and Orlov, 1983), revealing that the results of numerical experiments are in good agreement with the observed data for triple stars. Since the dynamical evolution of the vast majority of the simulated systems terminates in the escape of one of the components (see, for example, Anosova, 1985), the similarity between the distributions of configurations may be considered as an argument for the instability of the observed triples.

However, for the particular triple star and galaxy systems, the apparent configurations are not sufficient to decide on the type of dynamics – the projection effects (Ambartsumian, 1951; Agekian, 1954; Anosova and Orlov, 1983) may hide the true configurations and apparent hierarchical forms of both types may occur, as shown by numerical experiments.

For the study of evolution of actual triple stars one must take into account all the data of astrometric, photometric and spectroscopic observations of the components. The maximum attainable accuracy of parallaxes, relative positions, velocities (from proper motions and radial velocities), and masses of individual components is required in order to exclude the optical triples.

A behaviour of actual triple stars is to be investigated by taking into consideration also the effects of observational errors. The studies of Anosova (1984, 1986) have shown that the reliable results of dynamical investigations can be obtained only for triple stars within the distance of 100 pc from the Sun. For larger distances, the errors are so high at present, that even the correct sign of the total energy cannot be guaranteed with full confidence.

II. THE DATA OF ASTROMETRICAL AND ASTROPHYSICAL OBSERVATIONS FOR TRIPLE STARS

To study the dynamical states and evolution of actual triple stars the list has been compiled at the Leningrad State University Astronomical Observatory of the 113 triple stars with the distance $r \leqslant 100$ pc from the Sun and the magnitudes of components $V \leqslant 0^m0$, out of the 4160 triples in the Index catalogue (43).

The selection of the observational data for the objects included in this program has been made from three sources:

1) the necessary general information has been taken from the available catalogues (6, 17, 19–22, 27, 29, 32, 37, 38, 41, 49, 50, 54–56);
2) the observational information has been obtained from the Center of Astronomical Data of the Astronomical Council of the Academy of Sciences of the USSR, which disposes of the catalogues (the principal ones: 1, 17, 19–38, 41–45) of the Strasbourg Center of Stellar Data; the astrometrical information has been kindly sent by J.Dommanget, C. Worley, G. Soulie, W.Gliese, W. van Altena and R.Harrington. The sample of catalogues looked through is really representative and comprehensive, and one can believe that the majority of observational data for triple stars included in our program has already been collected. However, the analysis of this collection has shown that: a) there is a lack of the systematic astrometric, photometric and spectroscopic observations with accuracy needed – for the most part, the observations of triple stars were made by chance and in the course of the double stars observations. The survey of the catalogues revealed that for the program stars the data accurate enough are not available even for such the well–known stars like α Cen and α Gem (Castor); b) the catalogue data often disagree between themselves, thus requiring a careful analysis; c) the application of criteria for identifying of bounding systems also require the complex of astrometrical and astrophysical observational data.
3) the additional observational information has been collected by means of the systematic observations of nearby triple stars from the LSU list, that have been carried out with our perticipation or after our request, with the aim to enlarge the observed set and to estimate the accuracy of the observed data for the triples components:
   a) the **astrometrical** observations in Pulkovo (26" refractor in 1964–1985) and at Abastumani Observatory (16" refractor in 1966); the observations and their reduction have been performed by means of the Kiselev's method (Kiselev, 1971). The micrometer astrometric observations of triple stars have been made at the Astronomical Observatory in Belgrade (Yugoslavia).
   b) the **photoelectrical UBV photometry** at the Burakan Station of the LSU Astronomical Observatory (AST–14 in 1982–1985), the Southern Station of Moscow University in Crimea (STE and Zeiss in 1984), and the Crimean Astrophysical Observatory (AST–11 in 1984).
   c) the **spectroscopic** observations with the purpose to define the radial velocities and spectral MK classifications of the triples components at the Special Astrophysical Observatory of the USSR (6m Telescope – LTA – with dispersion of 9 A/mm and 28 A/mm in 1982–1986), the Crimean Astrophysical Observatory (2.6 m telescope – STS – in 1984), and the Southern Station of MSU (STE and Zeiss in 1984, 1985).

Let's say, that out of the 113 triple stars of the LSU program, 51 triple stars have been observed by the colleagues from the mentioned Observatories, with our participation or after our request.

The observational data for these objects are summarized in Table 1; our results are marked by an asterisk. The following quantities are included: 1) the file numbers, the ADS catalogue numbers, and the outcomes of the classification of triple systems (Anosova and Popović, 1988): I – real physical systems, II – probable physical systems, III – probable optical systems, IV – real optical systems; 2) the WDS catalogue numbers and the accurate coordinates α and δ of the primary components A in the triple stars at the epoch 1950.0. The epochs T_c of the last astrometrical observation of the distant components C are given too. 3) the positional angles θ and the angular separations ρ of the secondary components B and C with respect to A at the epochs of the last observation T; the cases of the mimimum separation are specially marked; for the most part, the astrometrical data were taken from Worley's catalogue (WDS); the other data were taken from Aitken's, MacAlister's and Soulie's catalogues. Next columns of Table 1. contain the photoelectric UBV photometry data. 4) the apparent magnitudes V; 5) and 6) the color–indexes B–V and U–B (the main sources are 20, 42, 45, and the observations made at Burakan station of LSU); 7) the spectral MK classification data (29, 34, 36, and the

Table 1

No /ADS	WDS/(α,δ)1950,0	Comp.	θ°/ρ"	V	B–V	U–B	Sp	μα"/y	μδ"/y	V_Z km/s
1	00594+0047	A	333.1	7.6	1.42	1.69	K2 II	–0.032	–0.102	–10.3
818	$00^h56^m49^s.413$	B	26.41	9.1			G5 (IV)	0.016	–0.007	
II	00°30'30".89	C*	258.1	10.6			(F6 V)			
	Tc=1907.89		178.03	E(B–V) = 0.13 ±			r = 200 ± 30			
2	01052+1250	A	138.0	9.3			GO (V)	0.046	–0.031	
893	01 02 34.309	B	4.0	10.2			(G6 V)			
I	12 33 52.88	C	83.0	9.7			(G2 V)			
	Tc=1954.89		10.0				r = 95 ± 30			
3	01229–1258	A	313.2	8.4	0.91	0.69	KO V	0.033	0.476	30.6
–	01 20 33.	B	40.55	10.9	1.31	1.26	K6 V	0.031	0.45	
I	13 13.6	C	297.5	13.6			(M4 V)			
	Tc=1973.92		1.60	E(B–V) = 0.02 ± 0.05			r = 22 ± 4			
4	01404+3420	A	319.0	8.1			GO (V)	–0.088	–0.065	
–	01 37 33.067	B	34.84	9.4			(G9 V)	0.044	–0.052	
I	34 05 12.52	C	137	9.9			(K1 V)			
	Tc=1916.97		70.8				r = 55 ± 10			
5	01512+6452	A	35.8	7.15	2.05	2.30	K5 I	0.012	–0.020	
1459	01 47 38.216	B	34.77	9.2	0.23	0.07	B8 III	–0.021	0.005	
II	64 36 27.006	C	254.5	10.4			(B8 V)	0.009	–0.011	
	Tc=1908.54		114.79	E(B–V) = 0.2 ± 0.3			r = 830 ± 100			
6	01586+5545	A	264.3*	10.2						
1565	01 55.2	B	5.69*	10.3						
–	55 31	C	19.48*	10.9						
	Tc=1976.72*		25.644*							
7	02039+4220	A	62.7	2.22	1.37	1.58	K2 III	0.046	–0.047	–11.1
1630	02 00 49.177	B	9.77	4.84	0.03	–0.12	AOp	0.037	–0.051	1.0
I	42 05 27.01	C	109.8	8.3			(F IV)			
	Tc= 1984.086		0.58	E(B–V) = 0.013 ± 0.004			r = 100 ± 10			
8	02158+1046	A	237.7	9.48*	0.72*	–0.10*	GO V	0.041	–0.058	
1727	02 13 00.593	B	14.8	9.92*	0.78*	–0.04*	G5 (V)	0.060	–0.053	
I	10 32 16.24	C	270.8	11.96*	0.90*	0.18*	(G5 V)			
	Tc=1913.01		69.98	E(B–V) = 0.12 + 0.02			r = 75 ± 10			
9	02572–2458	A	328.7	7.35	0.87	0.52	G5 V	0.021	–0.005	
2242	02 55 02.520	B	0.76	7.7			G5 (V)			
I	–25 10 08.78	C	224.0	7.83	0.96	0.74	G5 V	–0.015	–0.022	
	Tc=1954.97		28.54	E(B–V) = 0.22 ± 0.03			r = 21 ± 3			
10	03405+0507	A	57.4	6.58*	1.34*	1.32*	G8 (III)	0.007	–0.005	57.2*
2681	03 37 49.371	B	26.3	9.71*	0.58*	0.04*	G2 (V)	0.004	–0.013	55.5*
11	04 57 55.73	C	300.2	10.44*	0.63*	0.04*	G2 (V)	0.012	–0.035	
	Tc=1973.1		36.1	E(B–V) = 0.07 ± 0.12			r = 120 ± 20			
11	03440+3822	A	83.57	7.54*	1.77*	2.00*	K5 III	0.001	0.000	14.4
2712	03 40 41.664	B	32.64	8.23*	0.27*	0.05*	A5 V	0.024	0.018	13.2
II	38 12 59.78	C	349.9	13.57*	1.29*	0.00*	(K7 V)			
	Tc=1921.899		90.60	E(B–V) = –0.07 ± 0.10			r = 240 ± 80			
12	04009+2312	A	127.7*	6.98*	0.09*	–0.24*	B9 V	0.014	–0.027	7.9*
2926	03 57 54.665	B	7.58*	7.88*	0.13*	0.11*	AO V	0.10	–0.015	10.2*
II	23 03 44.25	C	241.75*	9.67*	0.47*	–0.03*	F2 IV–V	0.022	–0.028	9.6*
	Tc=1982.04*		57.919*	E(B–V) = 0.15 ± 0.03			r = 200 ± 30			
13	04075+3805	A	9.2	7.12	0.85	0.48	G8 V	0.222	–0.220	26.5
2995	04 04 13.915	B	1.47	9.0			K2 (V)			

Table 1 (continued)

No/ADS	WDS/(α,δ)1950,0	Comp.	θ°/ρ"	V	B–V	U–B	Sp	μ_α"/y	μ_δ"/y	V_z km/s
I	37 56 41.48	C	210.4	11.5			KO	–0.009	–0.007	
	Tc=1921.914		232.64	E(B–V) = 0.01 ± 0.04			r = 19 ± 4			
14	04065+1421	A	109.8	8.90*	0.48*	0.04*	GO (V)	0.010	–0.072	
–	04 03 44.264	B	42.07	9.43*	0.55*	0.24*	FO V	–0.005	–0.027	
II	14 14 11.47	C	305.1	7.30*	0.46*	–0.03*	F2 V	0.061	0.051	
	Tc=1908.99		184.88	E(B–V) = 0.00 ± 0.02			r = 90 ± 15			
15	04112+2630	A	273.0	8.7			G3 III	0.048	–0.066	–10.9
3040	04 08 10.112	B	16.24	10.1			(A6 V)			
II	26 22 12.37	C	302.2	10.1			(A6 V)			
	Tc=1940.81		11.04				r = 400 ± 60			
16	04157–0734	A	105.1	4.43	0.32	0.44	G8 Ve	–2.226	–3.425	–42.4
3093	04 12 58.161	B	82.44	9.51	0.03	–0.68	Ay II	–2.184	–3.440	–51.2
I	–07 43 45.67	C	10.2	112.	1.59		M5 Ve	–2.17	–3.42	–47.0
	Tc=1970.734		4.01	E(B–V) = 0.03 ± 0.05			r = 4.8 ± 0.8			
17	04260+4515	A	353.26*	9.52*	0.54*	–0.17*	A(B3 V)	0.017	–0.018	
3198	04 22 26.977	B	37.02*	9.5			A(B3 V)			
IV	45 07 13.69	C	128.97*	10.13*	0.29*	–0.27*	(AO V)			
	Tc=1975.808*		8.11*	E(B–V) = 0.62 ± 0.12			r = 720 ± 100			
18	04590+1432	A	305.36	5.93	0.06	–0.28	B7 II	0.007	–0.019	6.0
3579	04 56 08.995	B	39.307	7.60	0.6	–0.30	B7 IV–V	0.006	0.004	
II	14 28 05.58	C	88.84	9.8			AO (III)	0.001	–0.019	
	Tc=1966.754		54.446	E(B–V) = 0.16 ± 0.01			r = 400 ± 20			
19	05218–2446	A	93.8	5.5	0.67	1.57	G2 III	–0.027	–0.013	4.7
3954	05 19 43.021	B	3.53	6.7			A3 (IV)	–0.039	–0.014	
II	–24 49 13.02	C	104.2	9.8			G5 (IV)	0.004	–0.026	
	Tc=1977.31		63.18	E(B–V) = 0.02 ± 0.01			r = 160 ± 80			
20	05323+4924	A	74.04	7.5	0.5		F5 V	0.007	–0.018	
4119	05 28 29.457	B	7.74	7.5			F2 (III)	0.024	–0.013	
II	49 21 29.32	C	185.2	9.2			F5 (V)			
	Tc=1910.61		118.81	E(B–V) = 0.06 ±			r = 120 ± 10			
21	05354–0525	A	92.6	5.2	–0.10	–0.94	B2 Ve	–0.004	–0.002	37.7
4188	05 32 55.458	B	52.67	6.5	–0.09	–0.92	B2 Ve	–0.008	0.023	30.3
III	–05 26 50.36	C	97.71	9.1	0.05	–0.48	B2 V	–0.011	0.028	30
	Tc=1960.12		128.52	E(B–V) = 0.14 ± 0.05			r = 480 ± 60			
22	05414+7920	A	160.64*	9.3			G5 (V)	–0.012	–0.051	
4189	05 33 56.314	B	11.03*	10.0			(K1 V)	0.03	–0.049	
I	79 18 21.79	C	172.1*	10.7			(K4 V)			
	Tc=1976.052*		1.98*				r = 60 ± 10			
23	05447+0350	A	88.70*	7.7	0.0		B9 V	0.003	–0.016	
4329	05 42 05.317	B	6.82*	9.4			KO (IV)	0.005	–0.006	
II	03 48 40.41	C	149.05*	10.0			F8 (IV)	–0.023	0.000	
	Tc=1966.0*		35.50*	E(B–V) = 0.07 ±			r = 170 ± 50			
24	06047–4505	A	217.3	5.94	0.50		F5 V	–0.014	0.251	21.7
–	06 03 13.789	B	5.21	9.4			(K5 V)	–0.011	0.251	
I	–45 04 39.94	C	320.61	6.32	0.52		F8 V	–0.091	0.244	25.8
	Tc=1950.		196.74	E(B–V) = 0.08 ± 0.03,			r = 25 ± 5			
25	06342+5639	A	252.66*	9.45*	0.14*	0.18*	A2 (V)	–0.006	–0.007	
5177	06 29 58.166	B	9.37*	10.58*	0.26*	0.12*	(A7 V)			
III	56 41 06.04	C	338.31*	11.43*	1.13*	1.25*	(KO IV)			
	Tc=1960.0*		55.95*	E(B–V) = 0.06 ± 0.02,			r = 350 ± 50			

Table 1 (continued)

No/ADS	WDS/(α,γ)1950,0	Comp.	θ°/ρ"	V	B–V	U–B	Sp	μα"/y	μδ"/y	V_z km/s
26	06341+0759	A	277.4	8.5			F8	0.001	0.015	
–	06 31 26.213	B	26.43	9.8			F8 (IV)	0.003	–0.003	
II	08 01 51.30	C	105.6	9.6			(F7 V)			
	Tc=1919.20		43.15				r = 140 ± 30			
27	06386+4021	A	253.2	7.5	1.1		KO (III)	–0.022	–0.238	
–	06 35 06.653	B	48.94	9.4			KO (V)	–0.014	0.006	
I	40 23 03.03	C	90.1	9.2			M2 (V)	–0.004	–0.020	
	Tc=1918.21		61.54				z=25±10			
28	06375+1211	A	151.2	7.6	0.8		G5 V	–0.100	–0.272	52.3
–	06 34 46.052	B	70.29	9.0			G5 (V)	–0.003	–0.004	
II	12 13 42.29	C	168.5	8.3			F8 (V)	–0.054	0.003	10.0
	Tc=1918.15		162.96	E(B–V) = 0.01 ±			r = 65 ± 10			
29	06408+4816	A	54.7	8.4			F8 (V)	0.036	–0.038	
5300	06 37 03.123	B	6.66	10.4			(K2 V)			
	48 18 09.06	C	181.5	9.2			(G6 V)	0.018	0.017	
	Tc=1910.10		194.62				r = 65 ± 10			
30	06451–1643	A	46.0	1.50	0.20	0.05	AO V	–0.545	–1.211	–4.7
5423	06 42 56.713	B	10.10	8.25	0.12	1.03	Ay II			
I	16 38 45.93	C*	144.0	14.0			(M7 V)			
	Tc=1981.230		1.5				r = 3.6 ± 0.3			
31	07040–4337	A	123.6	5.52	0.63	0.06	G2 V	–0.103	0.390	86.4
–	07 02 25.236	B	21.13	6.79	0.80	0.38	G9 V	–0.112	0.378	90.4
I	–43 32 15.77	C	282.0	8.66	1.19	1.13	K5 V	–0.100	0.395	88.0
	Tc=1977.29		184.8	E(B–V) = 0.02 ± 0.03			r = 16 ± 1			
32	07187+6331	A	211.4	10.0			G (5 V)	0.058	–0.046	
5948	07 14 02.114	B	3.17	10.0			(G2 V)			
II	63 36 55.11	C	311.6	9.8			K2 (IV)	–0.040	–0.006	
	Tc=1956.29		127.66				r = 120 ± 20			
33	07264+1830	A	98.11*	7.26*	0.34*	0.18*	FO (III)	–0.018	–0.026	
6073	07 23 32.745	B	60.75*	8.22*	0.33*	0.10*	F1 IV	–0.018	–0.022	39
II	18 37 05.10	C	79.85*	9.92*	0.186*	0.20*	G5 (V)	–0.005	–0.006	
	Tc=1983.84*		49.44*	E(B–V) = 0.03 ± 0.01			r = 140 ± 20			
34	07346+3153	A	86.2	1.98	0.06		A2 IV	–0.171	–0.102	5.9
6175	07 31 24.654	B	2.66	2.85	0.02	0.00	A2 V	–0.175	–0.103	6.4
I	31 59 58.07	C	163.3	9.74	1.49	1.04	KO Ve	–0.204	–0.110	2.2
	Tc=1973.1		71.8	E(B–V) = 0.02 ± 0.01			r = 14.7 ± 0.5			
35	07470+6404	A	339.1	6.82	0.1		A2 V	0.036	–0.042	
6336	07 42 23.428	B	5.42	8.8			(F1 V)			
I	64 10 30.46	C	170.8	9.9			(GO V)			
	Tc=1968.20		16.79	E(B–V) = 0.05 ±			r = 120 ± 20			
36	07490+0040	A	5.1	7.58	0.4		F2 V	–0.016	–0.026	
–	07 46 23.700	B	57.44	8.9			(F7 V)	–0.013	–0.021	
II	00 47 17.10	C	51.6	9.8			G (5 V)	–0.180	–0.	
	Tc=1935.25		94.64	E(B–V) = 80 ± 20						
37	08122+1739	A	234.8	5.6	0.54	0.06	F7 Vp	0.060	–0.140	–12.3
6650	08 09 20.831	B	0.62	6.24			G2 Vp			–5.6
I	17 47 59.38	C	79.4	6.02	0.60	0.13	F8 V	0.099	–0.113	–7.3
	Tc = 1984.06		5.22	E(B–V) = –0.01 ± 0.08			r = 15.8 ± 1.6			

Table 1 (continued)

No/ADS	WDS/(α,δ)1950,0	Comp.	θ^{o}/ρ"	V	B/V	U–B	Sp	μ_{α}"/y	μ_{δ}"/y	V_z km/s
38	081647+4054	A	249.6	9.0			GO (V)	–0.038	–0.058	
6700	08 13 20.783	B	20.40	9.9			(G6 V)	0.042	–0.139	
I	41 02 32.20	C	208.2	10.1			(G7 V)			
	Tc=1957.19		6.12				r = 85 ± 20			
39	08226–1041	A	172.6	9.69			GO (V)			
6777	08 20 17.4	B	2.02	10.1			(G3 V)			
II	–10 31 26	C	9.8	10.3			(G4 V)			
	Tc=1946.71		17.54				r = 120 ± 30			
40	08267+2432	A	48.6	7.02	0.32	0.07	A8 III–V	–0.040	–0.083	14.2
6811	08 23 41.534	B	5.73	7.81	0.53	–0.04	F7 V	–0.044	–0.088	18.0
I	24 41 59.88	C	333.2	8.4			(G2 V)			
	Tc=1973.24		0.156	E(B–V) = 0.05 ± 0.02,			r = 80 ± 10			
41	08543+3034	A	315.7	6.1	1.05		KO III	0.049	–0.024	–60.1
7071	08 51 11.894	B	1.36	6.6			(K2 III)			
II	30 46 12.40	C	199.2	9.2			G5 (IV)	–0.015	–0.032	
	Tc=1953.24		54.78	E(B–V) = 0.025 ±			r = 140 ± 15			
42	08593+4803	A	24.2	3.14	0.19	0.17	A5 Vp	–0.443	–0.235	9.8
7114	08 55 47.627	B	3.90	9.5			M1 V			15.0
I	48 14 22.05	C*	229.0	9.8			(M2 V)	0.017	–0.005	
	Tc=1971.35		0.34	E(B–V) = 0.00 ± 0.01			r = 16 ± 2			
43	09104+6708	A	358.9	4.79*	0.49*	0.02*	F6 IV–V	–0.001	–0.100	–1.8
7203	09 06 01.235	B	3.31	8.2			K2 (V)			0
II	67 20 19.54	C	147.8	10.21*	0.66*	0.26*	(G5 V)			
	Tc=1919.21		204.57	E(B–V) = 0.00 ± 0.03,			r_{AB} = 18 ± 2, r_C = 160 ± 40			
44	09205–0933	A	210.93	4.80	0.93	0.67	G6 III	–0.031	–0.032	23.3
7311	09 18 02.500	B	231.84	6.93	0.38	0.00	P4 V	–0.023	–0.028	16.4
I	09 20 33.49	C	197.7	11.25	1.15		K2 V			
	Tc = 1963.32		9.25	E(B–V) = 0.06 ± 0.05,			r = 65 ± 6			
45	09287+4537	A	162.2	5.41	0.98		G5 III	–0.013	–0.131	38.2
–	09 25 23.875	B	78.13	8.1			F8 IV	–0.027	–0.019	8.3
II	45 99 18.84	C	78.8	9.8			(G3 V)			
	Tc = 1923.856		83.39	E(B–V) = 0.10 ±			r = 80 ± 15			
46	09307+3340	A	129.9	5.85	1.05		G9 III	–0.018	–0.051	2.0
–	09 27 42.271	B	63.13	9.4			KO (V)	0.023	–0.037	
I	33 52 35.92	C	213.2	9.8			(G9 V)			
	Tc=1912.00		97.79	E(B–V) = 0.08 ±			r = 50 ± 10			
47	09343+6647	A	247.5	8.21*	0.45*	0.06*	F5 V	–0.026	–0.021	–54.0
7425	09 30 11.822	B	10.46	8.23*	0.41*	0.03*	F5 V	–0.025	–0.027	
II	67 01 04.59	C	212.5	9.13*	0.47*	–0.03*	GO V	–0.038	–0.030	
	Tc=1968.19		122.29	E(B–V) = –0.04 ± 0.04,			r = 90 ± 15			
48	09354+3957	A	149.38*	6.77	0.35	–0.02	A8 V	–0.008	0.006	–40.2
7438	09 32 15.211	B	24.963*	8.08	0.43	–0.05	F4 V	–0.032	0.000	–10
I	40 11 11.92	C	323.04*	8.36	0.44	–0.06	F5 V	–0.026	–0.018	–6
	Tc=1984.22*		116.85*	E(B–V) = 0.00 ± 0.03,			r = 70 ± 10			
49	10179+7104	A	166.7	6.65*	0.32*	0.20*	A5 III	–0.034	–0.050	12.1
7705	10 13 51.091	B	16.83	7.36*	0.30*	0.19*	A7 III	–0.023	–0.052	13.0
II	71 18 24.21	C	14.5	10.84*	0.47*	–0.03*	(F6 V)			
	Tc=1956.34		149.46	E(B–V) = 0.12 ± 0.02,			r = 150 ± 20			

Table 1 (continued)

No/ADS	WDS/(α,δ)1950,0	Comp.	θ^{o}/ρ''	V	B−V	U−B	Sp	μ_α''/y	μ_δ''/y	V_z km/s
50	11115+6610	A	225.6	8.25	0.70	0.26	G5 V	−0.331	−0.125	25.7
–	11 08 15.327	B	72.86	8.18	1.37	1.01	K2 (V)	0.009	0.002	−2
I	66 17 22.08	C	304.5	8.6			G5 (V)	0.000	−0.004	−1.6
	Tc=1922.182		183.33				r = 40 ± 2			
51	11145+0515	A	256.9	8.4			KO (V)	−0.024	0.005	
8098	11 11 54.533	B	104.31	10.6			K7 (V)			
I	05 32 08.41	C*	352.8	10.8			K8 (V)	−0.105	−0.012	
	Tc=1919.35		3.41				r = 30 ± 10			
52	11154−1807	A	81.31	10.1	0.13	0.12	MO V	0.500	−0.800	6.3
–	11 12 49.9	B	18.762	10.1	0.13	0.12	MO V			16.1
I	−17 51 41	C	320	13.8	0		M5 (V)			
	Tc=1960		83	E(B−V) = −0.04 ± 0.03,			r = 19 ± 2			
53	11432−3926	A	329.4	8.4			F2 (V)	0.008	−0.005	
–	11 40 32.60	B	24.56	8.9			GO (V)	−0.277	0.083	
II	−39 16 02.9	C	241.5	9.8			(G4 V)			
	Tc=1959.33		2.57				r = 95 ± 20			
54	11563+3527	A	142.3	6.80			F2 V	−0.121	−0.004	
8355	11 53 42.781	B	1.45	8.7			(G4 V)			
I	35 43 34.35	C	7.4	-			(F5 V)			
				E(B−V) = 0.04 ±			r = 50 ± 10			
55	12151−0715	A	270.32	7.96*	0.70*	0.56*	G5 III−V	−0.237	−0.060	21.6
8477	12 12 33.210	B	7.019	8.24*	0.94*	0.54*	G8 V	−0.230	−0.075	18.6
I	06 58 43.57	C	175.4	10.47*	1.08*	0.56*	(K3 V)			
	Tc=1925.26		98.11	E(B−V) = 0.08 ± 0.05,			r = 32 ± 7			
56	12225+2551	A	54.8	4.81	0.49	0.27	F6p	−0.012	−0.014	−5.8
8530	12 19 59.615	B	35.73	9.12*	0.49*	0.00*	KO (IV)			−1.0
II	26 07 24.31	C	167.19	8.58*	0.52*	0.01*	GO V	−0.011	−0.023	6
	Tc=1972.270		65.261	E(B−V) = 0.02 ± 0.03,			r = 90 ± 10			
57	12295+2931	A	223.5	9.3	0.54		GO (V)	−0.019	−0.020	
8570	12 27 00.880	B	2.62	9.9	0.52		G5 (V)	0.005	−0.055	
I	29 47 19.81	C	181.5	9.41			(G1 V)			
	Tc=1956.38		72.13	E(B−V) = −0.05 ± 0.06,			r = 90 ± 10			
58	12406+4017	A	2.6	8.65			GO (V)	−0.042	0.086	
8623	12 38 13.454	B	5.65	9.3			(G5 V)			
II	40 33 42.97	C	175.1	9.5			(G6 V)			
	Tc=1910.223		165.15				r = 70 ± 15			
59	12459+1009	A	38.5	9.6	1.05	0.96	KO IV	−0.004	−0.014	
–	12 43 22.524	B	33.60	9.8			KO (IV)	−0.088	−0.004	
II	10 25 14.86	C	96.1	9.9			G5 (IV)	−0.009	−0.045	
	Tc=1913.34		42.68	E(B−V) = 0.04 ±			r = 200 ± 20			
60	12520+1910	A	201.1	7.34*	0.33*	0.13*	A8 (V)	−0.082	0.000	−14.8
8690	12 49 26.488	B	15.68	7.85*	0.54*	0.08*	A8 (V)	−0.070	0.004	−12.2
II	19 26 36.98	C	325.6	8.17*	0.71*	0.34*	G5 (V)	0.018	0.013	
	Tc=1918.68		246.04	E(B−V) = 0.05 ± 0.02,			r = 55 ± 10			
61	12522+1704	A	50.5	6.36	1.61	1.99	K8 (III)	−0.003	−0.022	−0.4
–	12 49 43.043	B	196.47	6.29	0.17	0.09	A5 (IV)	0.033	−0.043	8.2
II	17 20 43.26	C	262	8.9			(F3 V)	−0.013	−0.012	
	Tc=1960.42		27.3	E(B−V) = 0.04 ± 0.02,			r = 120 ± 30			
62	13006+1823	A	35.5	6.23*	0.46*	−0.03*	F5 (III)	−0.229	0.051	0.0
8735	12 58 11.457	B	146.82	9.51*	0.54*	0.06*	G2 V	0.001	−0.047	
II	18 38 28.66	C*	297.3							
	Tc=1926.32		1.94	E(B−V) = −0.01 ± 0.02,			r = 90 ± 10			

Table 1 (continued)

No/ADS	WDS/(α,δ)1950,0	Comp.	θ^o/ρ"	V	B−V	U−B	Sp	μ_α"/y	μ_δ"/y	V_z km/s
63	13136+6717	A	296.4	6.54	1.14	1.08	K1 III	−0.156	−0.003	4.7
–	13 11 17.500	B	179.87	6.96	1.14	1.08	K1 III	−0.158	0.004	4.5
II	67 34 26.78	C	228.9	8.8			F8 (V)	−0.007	0.010	
	Tc=1924.37		114.54	E(B−V) = 0.05 ± 0.05,			r = 140 ± 40			
64	13289+5956	A	119.1	5.41	−0.07	−0.02	A1 V	−0.168	0.035	−7.5
8919	13 26 37.109	B	1.20	11.0			(K3 V)			
I	60 12 12.87	C	110.5	8.8			F8 (V)	−0.168	0.017	
	Tc=1924.10		182.35	E(B−V) = 0.01 ±			r = 75 ± 10			
65	13377+0223	A	31.31	6.9	1.1		KO III	−0.015	−0.036	
8975	13 35 11.498	B	15.926	8.6			KO (IV)	−0.018	−0.012	
II	02 38 10.96	C	138.8	9.3			(F5 V)			
	Tc=1909.321		172.21	E(B−V) = 0.03 ±			r = 120 ± 15			
66	1436−6050	A	279.5	6.70	0.2		A5 V	−0.185	0.004	
8997	13 40 10.333	B	26.21	9.7			(G4 V)			
II	77 05 44.67	C	316.1	9.0			G (OV)	−0.045	−0.014	
	Tc=1956.44		45.92	E(B−V) = 0.04 ±			r = 90 ± 15			
67	14396-6050	A	210.0	0.0	0.66	0.23	G2 IV	−3.608	0.712	−22.2
–	14 36 11.250	B	21.91	1.34	0.89	0.63	K3 V			−21.0
I	−60 37 48.85	C	–	11.0	1.96	1.48	M5 Ve	−3.760	0.815	−15.7
			7850	E(B−V) = 0.04 ± 0.03,			r = 1.3 ± 0.8			
68	14375+4743	A	14.86*	10.00*	0.72*	0.28*	G5 (V)	−0.023	0.002	
9327	14 35 43.036	B	5.583*	11.6			(K6 V)			
I	47 56 01.48	C	117.31*	10.20*	1.06*	0.89*	KO (V)	−0.021	−0.008	
	Tc=1983.10		78.851*	e(B−V) = 0.07 ± 0.02,			r = 60 ± 15			
69	14407+1625	A	108.4	4.93	−0.03	−0.33	B9 III	0.010	0.016	−1.3
9338	14 38 22.547	B	5.69	5.85	0.24		AO (V)	0.000	0.006	−6.1
II	16 37 54.14	C	162.0	10.0			(G4 V)			
	Tc=1960.06		127.74	E(B−V) = 0.10 ± 0.10,			r = 90 ± 15			
70	14584+4403	A	277.9*	8.52*	0.52*	− 0.06*	F8 III	−0.060	−0.078	
9461	14 56 33.428	B	3.81*	9.4			(KO III)			
III	44 14 34.45	C	334.51*	10.90*	0.50*	0.02*	F8 IV			
	Tc=1966.6*		58.912*	E(B−V) = 0.02 ± 0.00,			r = 520 ± 60			
71	15087−0059	A	284.2	8.8			GO (V)	0.015	−0.008	
9514	15 06 08.373	B	0.84	9.5			(G5 V)			
I	−00 47 22.34	C	130.0	10.0			(G8 V)			
	Tc=1922.346		25.49				r = 75 ± 20			
72	15174+4348	A	16.7	9.55*	0.94*	0.79*	G6 (V)	−0.009	−0.041	−14.5*
9573	15 15 37.269	B	8.79	9.33*	1.12*	1.14*	G6 (V)	−0.006	−0.009	−14.6
I	43 58 33.03	C	217.7	(11.63)*	0.45*	0.11*	(G5 V)			
	Tc=1921.45		140.58	9.6	E(B−V) = 0.12 ± 0.10,		r = 60 ± 10			
73	15201+6022	A	197.9	7.4	0.4		FO V	−0.081	0.031	
–	15 19 01.766	B	151.03	7.8	0.4		F2 V	−0.015	0.007	
II	60 31 32.15	C	164.2	9.7			K (OV)	−0.001	−0.039	
	Tc=1919.43		82.83				r = 63 ± 16			
74	15245+3721	A	171.46	4.3	0.31	0.06	FO V	−0.148	0.084	−10.3
9226	15 22 35.995	B	108.917	6.5	0.60	0.13	G5 V	−0.149	0.100	−8.8
I	37 33 05.49	C*	15.0							
	Tc=1957.195		2.13	E(B−V) = −0.05 ± 0.02,			r = 28 ± 2			
75	15462+1525	A	265.2	3.67	0.06		A2 IV	0.066	−0.055	−0.8
9778	15 43 52.58	B	30.67	9.95*	0.96*	0.79*	K3 V			2
I	15 34 38.30	C	209.9	11.02*	0.95*	0.68*	(K2 V)			
	Tc=1960.07		201.12	E(B−V) = 0.00 ± 0.01,			r = 35 ± 5			

Table 1 (continued)

No/ADS	WDS/(α,δ)1950,0	Comp.	θ°/ρ"	V	B–V	U–B	Sp	μ_α"/y	μ_δ"/y	V_z km/s
76	15589+2148	A	61.25*	8.43*	1.34*	1.57*	K3 III	–0.022	0.021	
9865	15 56 42.687	B	55.965*	8.51*	0.28*	0.11*	A5 V	–0.031	0.008	
II	21 55 56.31	C	59.06*	8.9			A5 V	–0.011	–0.008	
	Tc=1983.52*		59.297*	E(B–V) = –0.01 ± 0.03,			r = 360 ± 30			
77	16044–1122	A	19.1	4.16	0.46	0.01	F6 V	–0.064	–0.033	–31.8*
9909	16 01 36.889	B	1.114	5.1			F4 V			–33.6
I	–11 14 12.27	C	60.2	7.30	0.75		G7 (V)	–0.71	–0.021	–31.0*
	Tc=1983.43		7.42	E(B–V) = 0.01 ± 0.01,			r = 22 ± 1			
78	16061+1320	A	323.27	6.6	1.1		KO III	–0.039	–0.021	
9922	16 03 41.399	B	36.727	6.90	1.1		KO III	0.015	–0.017	
II	13 27 47.27	C	137.6	10.5			G5 (V)			
	Tc=1921.37			E(B–V) = 0.02 ±			r = 140 ± 20			
79	16240+6130	A	142.8	2.74	0.91	0.69	G6 III	–0.029	0.064	–14.0*
10058	16 23 18.469	B	5.45	8.8			K1 V			–14.6*
IV	61 37 37.32	C	241.	7.86*	1.61*	1.86*	K2 (III)	–0.008	–0.011	30.4*
	Tc=1923.0		564.9	E(B–V) = –0.01 ± 0.01,			r_{AB} = 23 ± 3, r_C = 600 ± 100			
80	16441+5036	A	43.90*	10.09*	0.48*	0.03*	F6 III	0.000	0.000	
10192	16 42 45.013	B	2.510*	10.3						
II	50 41 51.21	C	204.46*	10.38*	1.29*	1.22*	(K7 III)			
	Tc=1966.0*		43.986*	E(B–V) = –0.02 ± 0.02,			r = 830 ± 120			
81	16476+2538	A	316.17*	9.3	0.65	0.30	GO (V)			
10216	16 45 30.	B	4.885*	9.3			(GO V)			
I	25 44	C	257.21*	10.9						
	Tc=1964.0*		29.738*	E(B–V) = 0.02 ± 0.01,			r = 30 ± 6			
82	16579	A	59.55	7.79	0.99	0.10	K8 V	–0.165	0.270	–6.5*
10288	16 56 30.006	B	4.604	11.1			(M2 V)			
I	47 26 18.92	C	275.77	7.9	1.00	0.82	K4 V	–0.126	0.266	–6.8*
	Tc=1982.6		112.50				r = 16 ± 1			
83	17048+2806	A	231.63	7.29*	1.17*	0.90*	K1 III	–0.001	0.009	1.7
10332	17 02 46.646	B	19.15	9.56*	0.64*	0.10*	(GO IV)			
II	28 09 30.85	C	173.87	10.33*	1.28*	1.31*	(K4 IV)			
	Tc=1982.6		144.79	E(B–V) = 0.09 ± 0.04,			r = 170 ± 30			
84	17130+5407	A	227.8	6.91*	0.31*	0.19*	FO III	–0.013	0.072	–18.8
10410	17 12 02.953	B	2.67	10.0			G5 V			
I	54 11 44.67	C	232.0	8.70*	0.63*	0.12*	G5 IV	–0.023	0.108	–15.6*
	Tc=1964.56		88.6	E(B–V) = 0.01 ± 0.03,			r = 100 ± 10			
85	17411+2431	A	7.0	6.44*	1.18*	1.17*	K1 III	–0.020	0.053	–38.7 *
10715	17 39 02.136	B	16.07	9.43*	0.50*	0.09*	F3 V	–0.025	0.051	
II	24 32 12.35	C	160.6	9.21*	1.35*	1.36*	K1 (V)	–0.002	–0.007	–27.4*
	Tc=1959.55		167.71	E(B–V) = 0.09 ± 0.04,			r = 130 ± 20			
86	17446–0145	A	354.7	8.2			K1 (V)	–0.017	–0.062	–19.1*
–	17 42 05.96	B	55.29	9.3			(K6 V)			
II	–01 43, 11.9	C	147.6	9.5			(K6 V)			
	Tc=1890.46		138.19				r = 22 ± 5			
87	17467–0113	A	115.2	8.86	0.66	0.20	GO V	0.000	–0.003	15.4
10781	17 44 04.274	B	10.03				G5 V			
I	–01 11 48.83	C	197.8	9.7			K2 (V)	–0.025	–0.003	
	Tc=1910.36		105.42	E(B–V) = 0.05 ± 0.05,			r = 55 ± 10			
88		A		4.22	0.86	0.51	KO V	0.256	–1.097	–6.7
11046	18 02 55.761	B		6.3	1.15		K5 V			–14.9
I	02 30 20.29	C								
				E(B–V) = 0.02 ± 0.02,			r = 5.0 ± 1.0			

Table 1 (continued)

No/ADS	WDS/(α,δ)1950,0	Comp.	θ°/ρ"	V	B−V	U−B	Sp	μα"/y	μδ"/y	Vz km/s
89	18237+5138	A	24.6	8.8			G5 (V)	0.047	0.132	−42.2*
11328	18 22 34.82	B	9.40	8.9			(G6 V)			−37.7*
II	51 37 05.4	C	119.0	9.1			(G7 V)			
	Tc=1911.71		86.32				r = 55 ± 10			
90	18472+2826	A	273.5	8.99*	0.62*	0.16*	F8 V	0.015	0.007	−80.2*
–	18 45 16.873	B	18.70	9.84*	0.61*	0.10*	F8 (V)	−0.007	−0.002	−81.1*
II	28 22 05.34	C	163.5	9.69*	1.19*	1.10*	KO (IV)	0.000	−0.004	−1.5*
	Tc=1918.38		74.57	E(B−V) = 0.07 ± 0.03,			r = 115 ± 20			
91	18562+0412	A	102.3	4.60*	0.15*	0.09*	A5 V	0.046	0.032	−45.8
11853	18 53 43.976	B	22.55	4.98*	0.20*	0.07*	A5 V	0.050	0.024	−52.8
I	04 08 13.25	C*	55.8	6.89*	0.57*	−0.04*	G5 (V)	−0.010	−0.093	10.4
z=23,36	Tc=1927.55	Di	414.14	8.0	0.90	0.06	G8 V	0.000	−0.091	18.9
92	19026−2952	A	77.1	2.7	0.08	0.09	A2 III	−0.023	−0.006	26.1
11950	18 59 25.880	B	0.384	3.6			(FO III)			
I	−29 57 12.7	C	301.6	10.0			(K6 V)			
	Tc=1977.51		74.55	E(B−V) = 0.03 ±			r = 28 ± 3			
93	19058+0633	A	153.15	6.91*	0.39*	0.12*	F5 V	0.006	−0.087	−17.8
12029	19 03 21.184	B	9.587	8.83*	0.57*	0.36*	(GO V)	0.022	−0.096	
I	06 28 13.83	C	340.7	(12.07)*	0.79*	0.37*	(G9 V)			
	Tc=1905.56			E(B−V) = −0.03 ± 0.03,			r = 85 ± 5			
94	19298−6719	A	141.64	7.70	1.1		KO III	0.023	−0.012	
–	19 24 42.907	B	26.089	9.5			F (OV)	0.027	−0.044	
II	−64 24 41.38	C	14.0	10.0			(F2 V)			
	Tc=1940.14		36.6	E(B−V) = 0.12 ±			r = 210 ± 30			
95	20001+1736	A	14.8	8.0			K2 III	0.017	0.011	−38.5*
–	19 57 52.820	B	114.3	8.7			F5 (III)			
II	17 28 20.71	C	338.4	9.5			A2 (VI)	−0.011	−0.017	
	Tc=1921.65		79.50				r = 190 ± 10			
96	20098+5657	A	82.45*	9.42*	0.49*	0.08*	F8 (V)	0.022	0.031	
13464	20 06 43.965	B	5.536*	9.76*	0.54*	0.02*	F7 (V)	0.018	0.042	
II	56 48 16.20	C	61.46*	9.54*	1.10*	0.76*	G5 (V)	−0.009	0.010	
	Tc=1969.77*		34.858*	E(B−V) = 0.00 ± 0.02,			r = 120 ± 30			
97	20089+7743	A	120.9	4.38	−0.08	−0.11	B9 III	0.010	0.027	−22.7
13524	20 10 36.574	B	7.30	8.14*	0.26*	−0.42*	A7 V			
II	77 33 42.56	C	336.6	10.34*	0.55*	0.04*	F8 (V)	0.012	0.004	
	Tc=1912.27		169.40	E(B−V) = 0.03 ± 0.01,			r = 130 ± 30			
98	20183+2002	A	75.3	10.4			G5 (V)	−0.009	−0.009	
13661	20 16 03.598	B	4.73	10.6			(G6 V)			
II	19 52 19.43	C	169.2							
	Tc=1904.45		86.62				r = 130 ± 15			
99	20378+6045	A	257.3	7.12*	0.84*	0.57*	GO (III)			−61.4*
14102	20 36 46.131	B	1.92	9.7			(F5 V)			
II	60 34 45.95	C	51.8	10.58*	0.64*	0.18*	(G5 V)			
	Tc=1956.74		42.71	E(B−V) = 0.02 ± 0.01,			r = 140 ± 20			
100	20425+1243	A	86.9	8.26*	0.39*	−0.04*	F5 V	−0.001	−0.022	
14184	20 40 11.118	B	9.00	8.28*	0.43*	0.04*	F5 V	−0.024	−0.028	
I	12 32 54.37	C	345.3	8.88*	1.66*	1.96*	MO (IV)	0.015	−0.008	−35.6*
	Tc=1912.72		167.11	E(B−V) = 0.00 ± 0.03,			r = 90 ± 10			
101	20421+5013	A	185.8	9.5						
14186	20 40 39.9	B	4.50	9.7						
–	50 09 09.6	C	233.8	9.7						
	Tc=1911.64		18.08							

Table 1 (continued)

No/ADS	WDS/(α,δ)1950,0	Comp.	θ^o/ρ"	V	B–V	U–B	Sp	μ_α"/y	μ_δ"/y	V_Z km/s
102	20452–3120	A	218.	8.66	1.44	2.20	K8 Ve	0.267	–0.350	–1.7
–	20 42 03.675	B	3.8	10.52	1.51	0.91	M4 Vep	0.294	–0.327	–4
I	–31 31 03.54	C	–	10.9			M4 Ve			–3
			4600	E(B–V) = 0.00 ± 0.05,			r = 9.8 ± 4.0			
103	20497+5007	A	13.4/	6.62	1.63	1.63	M4 III	–0.049	0.016	
14345	20 48 02.954	B	101.55	9.9			(F1 V)			
II	49 56 24.25	C*	94.2	10.4	0.58	0.01	F8 V			
	Tc=1931.74		2.42	E(B–V) = 0.05 ± 0.01,			r = 210 ± 50			
104	21046+1202	A	236.1	7.60	1.1		KO III	0.023	–0.015	
14601	21 02 13.739	B	74.62	9.8			(F1 V)			
II	11 49 30.15	C*	96.9	10.0			G5 (IV)	0.030	–0.003	
	Tc=1915.82		6.62	E(B–V) = 0.09 ±			r = 210 ± 30			
105	21069+3845	A	146.1	5.22	1.17	1.11	K6 V	4.135	3.250	–64.3
14636	21 04 41.882	B	29.76	6.04	1.38	1.22	K6 V	4.122	3.112	–63.5
II	38 30 33.75	C	255.8	10.5			(M4 V)	–0.004	–0.007	
	Tc=1975.56		48.00	E(B–V) = 0.02 ± 0.01,			r = 3.5 ± 0.2			
106	21154–1021	A	52.0	8.4			KO (V)	–0.008	0.029	
14786	21 12 41.707	B	84.09	9.2			KO (V)	0.045	–0.032	
II	–10 33 24.90	C*	340.1							
	Tc=1930.40		5.50				r = 45 ± 7			
107	21440–5720	A	5.1	6.50	0.48	0.00	P8 V	–0.225	–0.050	
–	21 40 26.841	B	152.2	6.87	0.46	–0.01	P8 V	–0.195	–0.034	
II	–57 33 14.74	C	220.6	6.80	1.1		K2 III	0.042	–0.050	
	Tc=1845.88		205.4	E(B–V) = 0.00 ± 0.04,			r = 55 ± 5			
108	22207+6828	A	7.48*	10.41*	0.51*	0.13*	F5 III	0.003	–0.017	
15868	22 18 40.928	B	5.155*	11.2			(F6 V)			
II	68 09 32.40	C	300.64*	11.68*	0.66*	0.13*	G3 V			
	Tc=1972.721*		39.339*	E(B–V) = 0.00 ± 0.02,			r = 320 ± 50			
109	22294–2839	A	320.	3.90	1.1		KO III	–0.009	–0.019	
15978	22 26 37.643	B	0.3	8.2			(G2 III)			
II	–28 54 56.66	C	297.1	11.1			(F6 V)			
	Tc=1959.79		33.28	E(B–V) = 0.09 ±			r = 230 ± 50			
110	22450+6808	A	201.47*	8.7	0.28	–0.15	A2 V	–0.008	0.046	–17.4
16252	22 43 20.180	B	3.730*							
	67 51 55.79	C	219.50*	10.88	0.45	0.28	GO (V)			
	Tc=1971.870*		20.783*				r = 160 ± 40			
111	22506+5306	A	176.05*	10.00*	0.56*	0.10*	F6 III			
16304	22 48 48.685	B	4.480*				(A8 III)			
III	52 46 42.83	C	225.44*	10.76*	0.20*	0.21*	A8 III			
	Tc=1975.823*		26.578*	E(B–V) = 0.01 ± 0.01,			r = 1000 ± 100			
112	23434+6325	A	287.94*	10.5						
16955	23 41 33.4	B	8.801*	10.5						
–	63 02 44	C	42.42*	10.3						
	Tc=1966.0*		32.387*							
113	23581+2420	A	313.34	7.5	0.9		G5 IV	–0.060	–0.189	–16.1*
17131	23 55 27.835	B	8.710	9.6			GO IV	–0.099	–0.188	–11.8*
II	24 03 40.91	C	253.2	10.5			GO (V)	–0.023	–0.019	
	Tc=1961.82		40.80	E(B–V) = 0.18 ±			r = 90 ± 30			

observations by LSU); 7) the spectral MK classification data (29, 34, 36, and the observations by LTA). The spectral classification data given in the parentheses are hypothetical data corresponding to the situation of existence of a physical relation among the components (Anosova and Sudakov, 1987). Columns 8) and 9) give the components proper motions μ_α and μ_δ in arcsec/yr (17, 21, 27, 43, 56, and the Pulkovo observations); 10) the radial velocities in km/sec (1, 27, 32, 54, 55, and the observations at the Southern Station of MSU and at LTA. The colour excesses E(B–V), the photometric distances r and their rms errors are presented as well. These are their mean values taken over all triple system components.

It has been shown that the 48 triple systems observed in the frame of our programme have the small average (over the three comonents) color excesses E(B–V) = $+0^m.02 \pm 0^m.03$. Our photoelectric UBV data have the errors in V, B–V, and U–B, $\pm 0^m.02$, $+ 0^m.02$,, and $\pm 0^m.04$, respectively.

As a result of the information collection (from the catalogue data and from the observations) it has been found that for the 25 triple star systems the entire observational data complex necessary for the determination of dynamical states is available. The four systems among these are real optical systems (they are accordingly marked in the Table), while the others could be the boundary systems. In order to prove that, and for the study of dynamical evolution of the boundary star systems, one has to provide the additional observations of these systems at the highest accuracy level. The space observations of the multiple star systems by the EAS HIPPARCOS, and by the Hubble Space Telescope are the most promising in this sense, at present.

III. CONCLUSIONS

Let's state in conclusion that the study of the multiple star systems consists of solution of a number of problems:

1) the identification of boundary systems; statistics of physical properties of components;
2) the definition of dynamical states in the multiple systems – deriving of the energy characteristics; the total energy $E_{tr} \pm \sigma_{E_{tr}}$ and the relative pair energies $E_{ij} \pm \sigma_{E_{ij}}$ $(i \neq j)$ taking into account the uncertainties of the observational data;
3) the determination of the dynamical type (for the multiple star systems with negative total energy); the definition of the qualitative evolution trends – the classification of multiple stars into the stable systems (dynamical type I), and the unstable ones (dynamical type II);
4) the study of dynamical evolution in the unstable systems by the computer simulations; the definition of the quantitative characteristics like a life–time etc., the study of the processes of formation, evolution and disruption of binary systems belonging to the multiple star systems, the construction of the trajectories of the components' relative motions etc.

The aforesaid programs are also to be studied according to the indicated sequence.

The necessary conditions for the solution of these problems are:

1. the availability of the space coordinates and velocities for all the components in multiple star system; this condition requires the entire set of the astrometrical and astrophysical observations of these objects;
2. the above problems require the different levels of the observational data accuracy for their solution; the accuracy requirements increase with the above proposed priority of the problem;
3. the final solutions of any of the problems for the multiple star systems are possible only if the observational data were obtained with the maximal accuracy. This maximum level can be reached only under the following conditions:
   a) for the astrometrical observations the accuracy level $\sigma_\rho = \pm 0''.005$, $\sigma_\mu = \pm 0''.0005$ per yr.(ρ, θ, μ – are the relative coordinates and proper motions of components) can be reached for $\rho \geqslant 3'' - 4''$, as shown by Kiselev and Kijaeva (1980) by means of the systematic series consisting of the large number of observations made at the long–focus refractors during 10–15 years; for the multiple systems including the close binary systems with $\rho \leqslant 2''$, the micrometric and speckle – interferometric observations (see 18, 41, 52) are necessary;
   b) the errors $\sigma_{v_r} \approx 0.2 - 0.4$ km/s of star radial velocities may be achieved by their spectroscopic observations with the CORAVEL–type apparatus;
   c) the errors $\sigma(\Delta m) \approx 0.2\ m_\odot$ in masses are quite possible in case of derivation of the relative star masses by using the photoelectric UBV photometry data (the V values) for the nearby multiple star systems with the well–known trigonometric parallaxes for all the components (see the description in 27);
   d) the essential growth of accuracy level for the star parallaxes $\sigma_\pi \approx \pm 0''.002$ may be reached (Dommanget, 1985; Perryman, 1982) by the astrometrical satellite HIPPARCOS observations;
   e) the considerable improvement of the astrometrical and astrophysical data accuracy (σ_π, $\sigma_\mu \cong \pm 0''.0003$, $\sigma_{v_r} \cong \pm 0.1$ km/s) could be reached by the systematic Hubble Space Telescope observations during 10 – 15 years.

The LSU programme of triple stars is included in the Input Catalogue of EAS HIPPARCOS and in General Observer programme for the Hubble Space Telescope, with purpose of increasing the degree of completeness of information about the components.

ACKNOWLEDGEMENTS:

Author wishes to express her deep appreciations to the following colleagues from the USSR observatories and institutes for their interest in this work and for their valuable assistance: A.A.Kiselev, G.N. Salukvadze, A.A. Tokov nin, V.N.Sementsov, G.V.Zaitseva, T.M.Rachkovskaja, N.M. Schahovskoji, A.G. Tcherbakov, E.L. Chenzov, I.D.Karachenzev, V.E. Karachenzeva, A.E. Piskunov, N.D.Kostuk, V.V.Orlov, O.S.Shulov, T.E.Derviz, S.V. Sudakov, V.Y.Terebizh.

Autor is also grateful to J.Dommanget, L.Spitzer, C.Worley, W.Gliese, W.van Altena, N.Bahcall, J.Bahcall, R.Harrington, G.Solie, and especially to G.M.Popovich and D.Zulevich for their interest in this work and for kind putting at our disposal the information on their observations.

REFERENCES

1. Abt H.A. and Biggs E.S.1972, *Kitt Peak Nat. Observ.* New York, (S 3004).
2. Agekian T.A.: 1954, *Astron. Zh.* **31**, 544.
3. Agekian T.A. and Anosova J.P.: 1964, *Trans. Astron. Obs. Leningr. Univ.* **21**, 103.
4. Agekian T.A. and Anosova, J.P.: 1967, *Astron. Zh.* **44**, 1261: *Soviet.Astron.* **2**, 1006.
5. Agekian, T.A. and Anosova, J.P.: 1968, *Astrofizika* **4**, 31.
6. Aitken, R.R.: 1932, *Publ. by Carnegie Inst. of Washington*, 1488.
7. Ambartsumian, V.A.: 1951, *Lect. Acad. Sci. Arm. USSR* **13**, 97.
8. Anosova, J.P.: 1968, *Trans. Astron. Obs. Leningr. Univ.* **25**, 100.
9. Anosova, J.P.: 1984, in *Astrophysical Problems* Saradsk, p. 75.
10. Anosova, J.P.: 1985, in *Totals Sci.Techn.* ser. Astr., **26**, 57.
11. Anosova, J.P.: 1986, *Astrofizika*, **25**, 297.
12. Anosova, J.P. and Orlov, V.V.: 1983, in *Star Clusters and Problems of Stellar Evolution*, Sverdlovsk, p. 121.
13. Anosova, J.P. and Orlov V.V.: 1985, *Trans. Astron. Obs. Leningr. Univ.* **40**, 65.
14. Anosova, J.P., Bertov, D.I., and Orlov, V.V.: 1984, *Astrofizika* **20**, 327; *Astrophys.* **20**, 177.
15. Anosova, J.P., Sementsov, V.N., and Tokovinin, A.A.: 1987, *Astron. Zh.* **64**, 2.
16. Anosova, J.P. and Sudakov, S.V.: 1987, *Trans. Astron. Obs. Leningr. Univ.* **41** 80.
17. Anosova J.P. and Popovich G.M., 1988, *Astrofizika* (in press).
18. *AGK 3*,: 1973, Hamburg–Bergerdorf (S, 1061).
19. Balega, Yu.Yu. and Balega, I.I.: 1985, *Pis'ma Astron. Zh.* **11**, 112.
20. Batten, A.H., Fletcher, J.M., and Mann, P.J.: *Publ. Dom. Astrophys. Obs.* **15**, 121. (S 3016).
21. Blanco, V.M., Demers, S., Douglass, G.G., and Fitzgerald, M.P.: 1968, *Publ.U.S. Nav.Obs.* 2nd ser., Washington, 21 (S 2004).
22. Boss, B.: 1937, *Carnegie Inst. of Washington* (S 1008).
23. Buscombe, W.: 1977, *Northwestern Univ.* (S 3052).
24. Cannon, A.J. and Pickering, E.C.: *Ann.Astron. Obs. Harv. Coll.* 90–100 (S 3001).
25. Cape photogr. catal., *Ann. Cape obs.* 17–22 (S 1004).
26. Catal. of stellar indentifications, 1979, *CDS Inform. Bill.* **17**, 88. 1981, *Astr. Astrophys. Suppl. Ser.* **43**, 259.
27. Davis, R.J., Deutschman, W.A., and Haramundanis, K.L.: 1973, *SAO spec.rep.* **350** (S 2006).
28. Gleese, W.: 1969, *Veroff.Astron. Rechen–Inst. Heidelberg*, **22**, (S 5001).
29. Gronbech, B., and Olsen, E.N.: 1976, *Astron. Astrophys. Suppl. Ser* **25**, 223; 1977, **27**, 443 (S 2033).
30. Haramundanis, K.L.: 1966, *Smith. Inst. Washington, D.C.* (S 1001).
31. Hardorp, J., et al.: 1959–1965, *Hamburg–Bergedorf, I–VI* (S 3015).
32. Hauck, B., and Mermilliod, M.: 1975, *Astr. Astrophys. Suppl. Ser.* **22**, 235 (S 2003).
33. Hoffleit, D.: 1964, *Yale Univ. Obs.* (S 5002).
34. Houck, N.: 1978, *Dept. Astron. Univ. Michigan, Ann. Arbor. Mich.* (S 3051).
35. Houck, N., and Cowley, A.P.: 1975, *Michigan* (S 3031).
36. Jaschek, M.: 1978, *CDS Inform. Bull.* **15**, 12 (S 3042).
37. Jaschek, C., Conde, H., and Sierra, A.C.: 1964, *Publ. La Plata Obs* (S 3018).
38. Jeffers, H.M., van den Bos, W.H., and Greeby, F.M.: 1963, *Univ. of California Publ. Lick Obs.* **21**, 804.
39. Jenkins, L.F.: 1952, 1963, *Yale Univ. Obs.* (S 1010).
40. Kiselev, A.A.: 1971, *Izv. GAO in Pulkovo*, **187**, 49.
41. Kiselev, A.A., and Kiyaeva, O.V.: 1980, *Astron. Zh.* **57**, 1227.
42. McAlister, A.H., and Hartkopf, W.J.: 1984, *Cent. HARA, Geogria State Univ.* Atlanta.
43. Morel, M., and Maghenar, P.: 1978, *Astron. Astrophys. Suppl. Ser.* **34**, 477 (S 2007).
44. Morin, D.: 1973, *CDS Inform. Bull.* **4**, 4(S 5003).
45. Neugebauer, G., and Leighton, R.B.: 1969, *Calif. Inst. of Technology, NASA* (S 2002).
46. Nicolet, S.: 1978, *Astron. Astrophys. Suppl. Ser.* **34**, 1(S 2051).
47. Perryman, M.A.C.: 1982, *Bull. d'Inf.Centre Donn.Stel.* **22**, 87.
48. Petrie, R.M., Crampton, D., Leir, A., and Younger, F.: 1973, *Publ.Dom. Obs.* **14**, 151(S 3029).
49. Rufener, F.: 1976, *Astron. Astrophys. Suppl.Ser.* **26**, 275.
50. *Sky Catalogue 2000.0*, 1982, Cambridge, 604.
51. Soulie, G.: 1983, *Astron. Astrophys. Suppl. Ser.* **54**, 281.
52. Straizys, V., and Kurillene, G.: 1981, *Astrophys. and Space Sci.* **80**, 353.
53. Tokovinin, A.A.: 1983, *Pis'ma Astron. Zh.* **9**, 9.
54. Wackerling, L.R.: 1970, *Mem.Roy.Astron.Soc.* **73**, 153 (S 3017).
55. Wilson, R.E.: 1953, *Carnegie Inst. Washington, D.C.*, 601 (S 3021).
56. Wooley, R., Epps, E.A., Penston, M.J., and Pocock, S.B.: 1970, *Royal Obs. Ann.* 5 (S 5004).
57. Yale, Zone Catalogue, *Trans. Astron. Yale. Univ.* **11**, 27, **30**, 31 (S 1003).

Bull.Obs. Astron. Belgrade, N° 138 UDC 550.34

SEISMOTECTONIC CHARACTERISTCS OF THE PART OF THE CENTRAL SERBIA BETWEEN MOUTH OF SAVA; DUNAV AND ZAPADNA MORAVA RIVERS

B. Sikošek
Seizmološki zavod, p.f. 351, 11000 Beograd, Yugoslavia

V. Knežević
SOUR REIK Kolubara, 14220 Lazarevac, Yugoslavia

N. Banjac
Seizmološki Zavod, p. f. 351, 11000 Beograd, Yugoslavia

(Received: 12 February, 1987)

SUMMARY: Complex investigations of the changes in the mean average geographic coordinates of Beograd include also investigations of seismotectonic characteristics of the part of the central Serbia between mouth of Sava. Danube and Zapadna Morava rivers which is some 55 km wide and about 100 km long. This is seismically a very active area as a result of a considerable dynamics of the crust. This activity is due to the specific configuration of this area within the geotechnic framework of Serbia i.e. European Alpids in general (Knežević et al., 1985) Our results provide informations that might give a possibility (if correlated to the results of other investigations – astronomical, geomagnetic) to detect short time earthquake precursors phenomena.

GEOTECTONIC CONFIGURATION AND SEISMOGENIC CONDITIONS

The investigated area is located between the rivers Sava and Danube in the north and Zapadna Morava in the south, covering a part of the geotectonic complex of the inner Dinarides at the border with Serbo– Macedonian massif, which represents a part of the next geotectonic category of the Alpine orogen (fig. 1.). In this area we can clearly observe the intersection of geotectonic and tectonic units in N–S and W–E directions. But the W–E directions are more significant Plicative and disjunctive tectonic structures have the same axis directions. Such an orientation of tectonic axes is due to the order (paleo and meso alpides) and, more precisely, to young and neotectonic stresses (strains). This influences seismogenic characteristics of this part of Serbia (Sikošek B.,1982) (Fig. 2.).

In the geotectonic and tectonic structures of this area, dominant directions of the tectonic axes in the north are W–E and N–S, and in the south NW–SE.

Our opinion is that the seismic energy is primary generated as tectonic strain by the recent active geotectonic contact between continental plats and, through the faults transmitted in their background. On certain seismic structures, when the strain overcauses the resistance on the fault surfaces, it is released in the form of seismic energy.

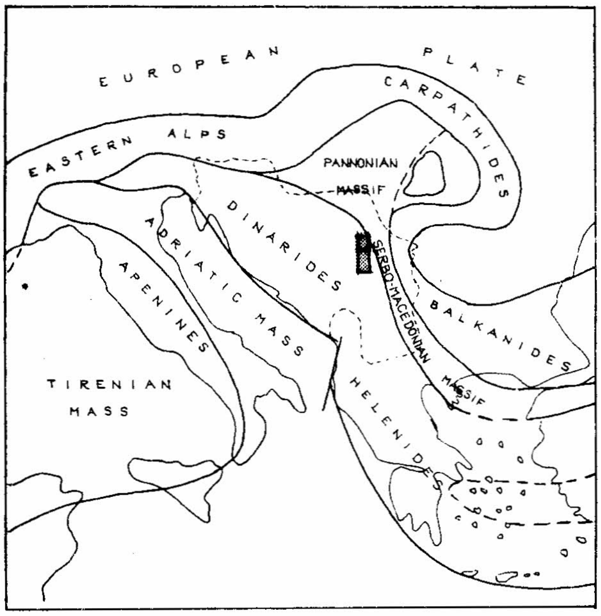

Fig. 1. Geotectonic position of Yugoslavia and investigated area in the European alpine orogenic system (Sikošek,1975).
Scale 1 : 10 000 000

Investigated area

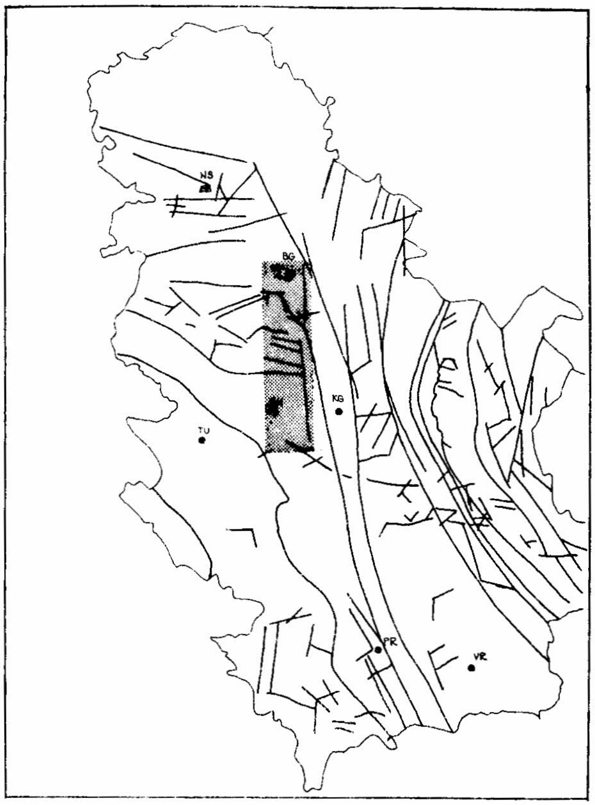

Fig. 2. Geotectonic framework of SR Serbia.
scale 1 : 2 000 000 (Sikošek B.,1982)
investigated area

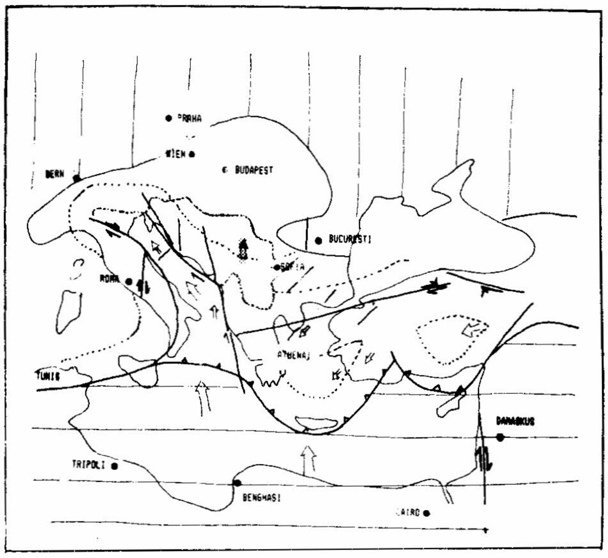

Fig. 3. Present geotectonical conditions on the south border of European plate (After Bergougnan H., Fourquin C., Ricou E., 1978; Sikošek B., 1979)

Area of the european plate.
Alpine south border.
Area of the Afro-Arabian plate.
Yugoslavia.
Investigated area.
Subduction zone.
Strike-slip deep fault.
Main neotectonic fault.
Motions of plates and blocks.
Boundary of primary compression zone.

For Yugoslav region, the primary generator of the tectonic strain is recent geotectonic contact of the Adriatic mass, as the prominent part of African table, and Dinarides body, as the southern part of the European plate (Fig.3.) (Bergougnan et al., 1978; Sikošek, 1979). Strain conditions dictated by this collision contact form three strain zones in Yugoslav area. Depending on the distance of this contact, seismogenetic structures can generate earthquakes with the magnitudes within ranges of $6,5 \leqslant M \leqslant 7,5$ in the first, $5,5 \leqslant M \leqslant 6,5$ in the second and $M \leqslant 5,5$ in the third, the remotest zone, respectively. The width of the first zone is about 200 km and its seismicity is controled primarily by tectonic strains, whereas in the second zone it is controled by tidal effects of the upper part of astenosphere too. The investigated area is located in the second strain zone.

SEISMOTECTONIC FRAMEWORK OF THE INVESTIGATED AREA

Based on the seismic activity of this area, three seismic zones can be detected: 1. Belgrade; 2. Lazarevac and 3. Rudnik zone. Their seismotectonic characteristics are as follows:

1. **Belgrade seismic zone** is a complex seismogenetic block divided by the system of paralel faults in three parts: 1. middle, 2. western and 3. eastern part which are relatively lower than the first part. These secondary blocks are divided by the system of parallel transversal faults (EENE–WWSW, NE–SW, WWNW–EESE) into the smaller complexes that form a jigsaw – puzzle of 10 km x 10 km. Due to this, foci distribution of the small magnitude earthquakes are relatively regular. All these segments are tectonically stabilised, so that there is no very strong seismic activity in the area. Seismoactiv levels are at the dephts of 0–5 km and 5–10 km, i.e. they are shallow. More prominent seismic activity of the area is located in the southern part, north of Kosmaj mountain. The depth of the lithosphere is 26 km.

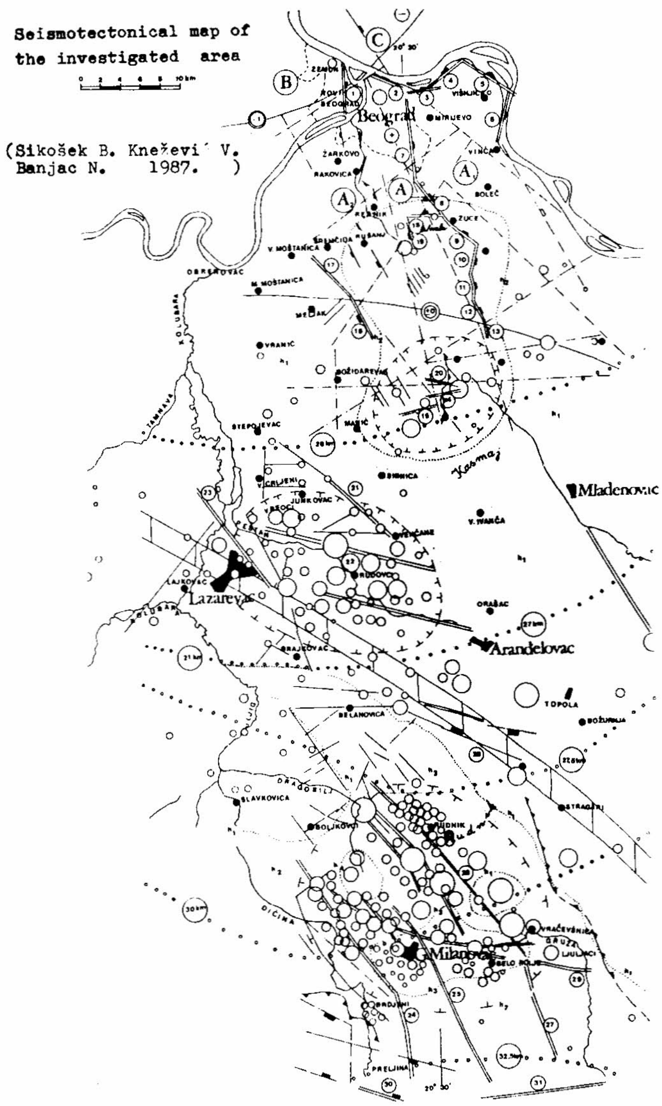

Fig.4.

Legend for the Seismotectonic map of the investigated Part of the Central Serbia.

Earthquake epicenters

- $2{,}2 \leqslant M \leqslant 2{,}8$
- $2{,}9 \leqslant M \leqslant 3{,}5$
- $3{,}6 \leqslant M \leqslant 4{,}2$
- $4{,}3 \leqslant M \leqslant 4{,}8$
- $4{,}9 \leqslant M \leqslant 5{,}4$
- $5{,}4 \leqslant M \leqslant 6{,}0$

faults and overthrust sheets
faults (detected, covered)
faults detected by the remote sensing
dip–slip faults
deep fault
seismicaly active faults
1–20 Beograd seismic zone
21–23 Lazarevac seismic zone
24–31 Rudnik seismic zone
isolines of the seismically active depth zones
h_1 0–5 km, h_2 5 – 10 km, h_3 10–20 km, h_4 more than 20 km.
isolines marking Moho discontinuity (in km.)
zones of higher seismic activity
recent vertical movements tendencies (mm/year)
⊖ subsidence ⊕ uprisal
A Beograd seismic block (A_1 western wing, A_2 eastern wing)
B Srem seismic block gravitational slip
C Banat seismic block gravitational slip

2. Lazarevac zone

The range of the thickness of the lithosphere in this zone is 26 – 27 km. Here a deep fault is detected with direction WNW–ESE whic represents qualitative border between northern and southern parts of the Central Serbia seismic area. Seismic evidence shows that earthquake foci can be classified in 4 magnitude groups: M = 3, M = 4, M = 5 and M = 5,6. Three seismic blocks are registrated: Vreoci, Batoševac and Lazarevac. Length of seismoactive segments are 8 km $\leqslant L \leqslant$ 20 km. Earthquakes are shallow with foci depts from 0 to 5 km. Accordingly, this is the zone which is exposed to considerable seismic danger. Part of higher seismic activity is located along the river Peštan between Vreoci on the north, Venčane on the east, Brajkovac on the south and Lazarevac on the west, mainly concentrated in the region of Rudovac.

3. Rudnik seismic zone

The northern border of this zone is neotectonic rift Mionica–Belanovica–(W–E) whereas at the south the border is complex tectonic rift of the Zapadna Morava river. The system of parallel faults NW–SE (NNW–SSE) that are devided by the transversal fault into segments with length from few up to 22 km, is within these borders.

Magnitudes of historically registrated earthquakes up to now are within the range $2{,}2 \leqslant M \leqslant 5{,}6$. The lithosphere depth is 27,5 km in northern parts and 32,5 km on the south. Foci dephts vary from 0 – 5 km and more then 20 km. This is seismically a vary active zone. Part of higher seismic activity is surrounded by Rudnik mountain in the north, G.Milanovac town in the south and rivers Dičina and Gruža in the west and the east, respectively.

Analysing focal depths of the earthquakes that occured in this part of Central Serbia one can conclude at what depths recent seismotectonic activity should be expected.

The seismotectonic active levels are classified as follows:

- at the depths 0 – 5 km occured in the last 200 years 6% of total number of earthquakes
- at depths from 10 – 15 km occured 68% of all earthquakes
- at depths from 15 – 20 km occured 24% of all earthquakes
- at depths from 20 km and more occured 2% of all earthquakes

Accordingly, the most active level is at the depth of 5 – 10 km which was taken into account for determination of the seismogenetic capacities of the seismotectonic structures.

Velocities of the vertical movements in this zone are from 1 mm/y in the north to 4 mm/y in the south (Jovanović P.,1972).

Seismotectonic framweork of the investigated area in the Central Serbia is shown in Fig. 4.

SEISMIC STRUCTURES AND THEIR SESIMIC CAPACITIES

It was identified 31 seismic structures, as following: in the seismic zone of Beograd 20, in the seismic zone of Lazarevac 3 and in the seismic zone of Rudnik 8.

Their seismic capacities are determinated by interdependence between seismicaly active fault surface and earthquake magnitude generated on it. Correlation is expressed by following equation (at the depth of 10 km) (Sikošek B.,1982):

$$M = \frac{\lg L(km) + 1{,}74}{0{,}84}$$

For Rudnik seismic zone where earthquake foci are deeper we need Shebalin's (1968) equation

$$M = \frac{\log L(km) + 2{,}8}{0{,}7}$$

where L (km) is the length of seismoactive segment and M – magnitude

According to the empiric equation given by Shebalin, the area of the seismic zone is determined as following

$$\text{Log } S_o = M - 3{,}6$$

where S_o is the area of the seismoactive zone in km^2.

Taking this correlations we can obtain the degree of focal compactness, according to Shebalin (1968)

$$Q = M - \text{Log } S_o$$

where

Q is focal depth,
M – magnitude and
S_o – seismoactive fault area in km^2

Classification of focal compactness is following:

1. focies with week compactness	$Q \leqslant 3$
2. focies with normal compactness	$3 < Q \leqslant 4$
3. very compact focus	$Q > 4$

Seismoenergetic capacities of seismic structures in the investigated part of Central Serbia are:

No	Lenght (km)	Magnitude M	Seismoactive area $S_0 km^2$	Compactness Q	
1.	6,0	4,2	4,0	3,6	2
2.	4,5	3,9	2,0	3,6	2
3.	4,5	3,9	2,0	3,6	2
4.	4,5	3,9	2,0	3,6	2
5.	6,5	4,3	5,0	3,6	2
6.	4,5	3,9	2,0	3,6	2
7.	6,5	4,3	5,0	3,6	2
8.	7,0	4,4	6,3	3,6	2
9.	4,0	3,7	1,25	3,6	2
10.	3,0	3,4	0,65	3,6	2
11.	2,5	3,2	0,4	3,6	2
12.	3,5	3,6	1,0	3,6	2
13.	5,0	4,0	2,5	3,6	2
14.	2,5	3,2	0,4	3,6	2
15.	4,0	3,7	1,25	3,6	2
16.	5,0	4,0	2,5	3,6	2
17.	4,5	3,9	2,0	3,6	2
18.	3,0	3,4	0,63	3,6	2
19.	2,5	3,2	0,4	3,6	2
20.	7,5	4,47	7,4	3,6	2
21.	8,0	4,5	8,0	3,6	2
22.	20,0	5,7	126,0	3,6	2
23.	15,0	5,3	50,0	3,6	2
24.	22,0	5,9	200,0	3,59	2
25.	12,0	5,4	87,0	3,6	2
26.	25,0	6,0	251,0	3,6	2
27.	12,0	5,54	87,0	3,6	2
28.	16,0	5,7	126,0	3,6	2
29.	18,0	5,8	158,0	3,59	2
30.	10,0	5,4	63,0	3,6	2
31.	6,0	4,2	4,0	3,6	2

One can bee seen from the table that maximal possible magnitude range is $3{,}2 \leq M \leq 6{,}0$. Maximal magnitudes (M_{max}) increase from the north (Belgrade seismic zone), towards Lazarevac seismic zone, starting with M = 5 up to M = 6,0 in the southern part (Rudnik seismic zone). It follows that the magnification increase follows the increase of thickness of the consolidated part of the earth's outher mantle which also increase from the north toward the south (from 26 km till 32,5 km) (Dragašević, Andrić, 1974).

DYNAMICS OF THE EARTHQUAKE FOCI

During the last 200 years 370 earthquakes occured in the investigated area, with intensities ranging from 3°MCS up to 9°MCS. The most numerous are small foreschocks or afterschocks. Released seismic energy of all these earthquakes is $2{,}0125 \times 10^{16}$ J.

The seismic activity dynamics in this area is characterised by cyclic periods of 100 years, with shorter periods of 25–30 years or even shorter of 6–8 years.

CONCLUSION

The investigated area, where changes in mean geographic coordinates have been detected, is seismically a highly active part of the lithosphere. Here, considerable tectonic strains are cyclically accumulated and released as seismic energy. The seismotectonic patern, the litosphere thickness and the location of this region with geotectonic framework of the southern border of the European plate determine seismic activity which increases from the north (Beograd zone) towards the south area (Rudnik zone) and is expressed through maximal possible magnitudes (M_{max}) that range from M = 4,5 to M = 6,0.

Seismic activity is in 100 years cycles with subcycles of 25–30 years and even shorter ones of 6–8 years.

REFERENCES

Bergougnan H., Fourquin C.: 1978 Paris *Les troncons de la faille nord–anatolienne dans la tectonique recente du Moyen Orient.* C.R Acad. Sc.Fr. **287**,D.

Brković T., Stefanović M., Malešević M., Urošević M., Radovanović Z., Dimitrijević M., Trifunović S., Pavlović Z., Rakić M.: 1970, Beograd, *OGK 1:100 000 list ČAČAK sa tumačem,* Savezni geološki zavod.

Brković T., Radovanović Z., Pavlović Z.: 1980, Beograd, *OGK 1:100.000 list KRAGUJEVAC sa tumačem.* Savezni geološki zavod.

Burchfiel C.: 1980, Amsterdam, *Eastern European Alpine System and the Carpatian Orocline as a Example of Collision Tectonics,* Tectonophysics **63**, 31.

Cvijanović D., Prelogović E., Skoko D.: 1976, Beograd, *Seizmotektonska karta SR Hrvatske,* Acta seismologica Yugosl. **4**,19.

Dragašević T., Andrić B.: 1975, Beograd, *Results of the Earth crust investigations obtained by the recent day by deep seismic sounding,* Acta seismologica Yugoslavica **2–3** 47.

Filipović I., Marković B., Marković O., Pavlović Z., Rodin V.: 1978, Beograd, *OGK 1:100 000 list GORNJI MILANOVAC,* Savezni geološki zavod.

Filipović I., Rodin V., Pavlović Z., Marković B., Miličević M., Atin B.: 1980, Beograd, *OGK 1:100.000 list OBRENOVAC sa tumačem.* Savezni geološki zavod.

Jovanović P.: 1972, Sarajevo, *Pregledna karta brzina vertikalnih kretanja zemljine kore u Jugoslaviji.* C.R. Kongresa geol. inž. i tehn.

Knežević V., Sikošek B.: 1985, Beograd, *Stepen istraženosti seizmičnosti lazarevačkog trusnog područja sa naročitom osvrtom na područje Beograda.* Zbornik savetovanja o geološkim istraživanjima regiona Beograda.

Pavlović Z., Marković B.: 1977, Beograd, *OGK 1:100 000 list SMEDEREVO sa tumačem,* Savezni geološki zavod.

Seizmološki Zavod SRS: 1900–1985, *Katalog zemljotresa,* Fond Zavoda.

Sikošek, B.:1979, Skopje: *Characteristics of the tension conditions of the Yugoslav territory.* Intern. Research Conf. on Intracontinental Earthquakes, 189.

Sikošek B.:1986, Titograd, *Seismotectonical composition and Earthquake source regions in Yugoslavia.* Montenegro Acad. of Sc. and Arts Vol. **2**, 165.

Shebalin N.V.: 1968, Moskva, *Makroseizmicheskoe pole i ochag silnogo zemletryaseniya.* Doktorska disert. ANSSR.

Vukašinović M.: 1972, Beograd. *Seizmotektonske karakteristike terena između Velike Morave i Drine.* Doktorska disertacija. Univerzitet Beograd.

Bull. Obs. Astron. Belgrade, N° 138 (1988) UDC 524.338.2

Be STARS – A CHALLENGE TO THE OBSERVERS AND THEORETICIANS

J. Arsenijević, A. Kubičela and I. Vince

Astronomical Observatory, Volgina 7, 11050
Beograd, Yugoslavia

(Received: December 2, 1987)

SUMMARY: The main historical steps in the investigation of the B stars with emission lines, starting with the year 1922 when IAU Commission 29 introduced the name „Be stars" at the first General Assembly of the Union in Rome and closing with the IAU Colloquium No. 92 „Physics of Be Stars" organized in August 1986 in Boulder, are briefly reviewed. The enormous quantity of the existing observational data and their significant characteristics over broad spectral region from X–ray to radio wavelengths are discussed. One of the main characteristics – photometric and spectral time variability – is analysed with a special attention to long–term changes. The correlation of long–term photometric and spectal changes with the polarimetric ones for some stars has been mentioned. Observational results in confrontation with the theoretical interpretations from Struve's hypothesis to the contemporary empirical Be stars models are presented.

1. INTRODUCTION

The spectral changes observed in the visual spectra of Be stars opened a new question in the classification and modeling of these stars. That this statement is not an exaggeration we'll be convinced by an example, namely the three spectra of 59 Cyg observed in the period 1974–1975, Figure 1. All these spectra are completely different: one is a normal B spectrum with somewhat rotationally widened absorption lines, the second one is an emission spectrum with Balmer lines from H_ϵ to H_{17} and the third one is, so called, shell spectrum with deep narrow absorption up to H_{25}.

Which of the known models can comprise all the three spectra and explain them? What mechanism can be the cause? What has to be observed in order to solve the problems? And what one can say if the data from the other spectral region, radio, IR, UV and X–ray, are added to the picture?

The overall picture is a challenging and at the same time a discouraging one. However, the situation didn't hinder the investigators, including the autors of the present review who were supposed to separate from an enormous quantity of the observational data and a number of interpretation attempts, the most essential and representative facts of the Be stars.

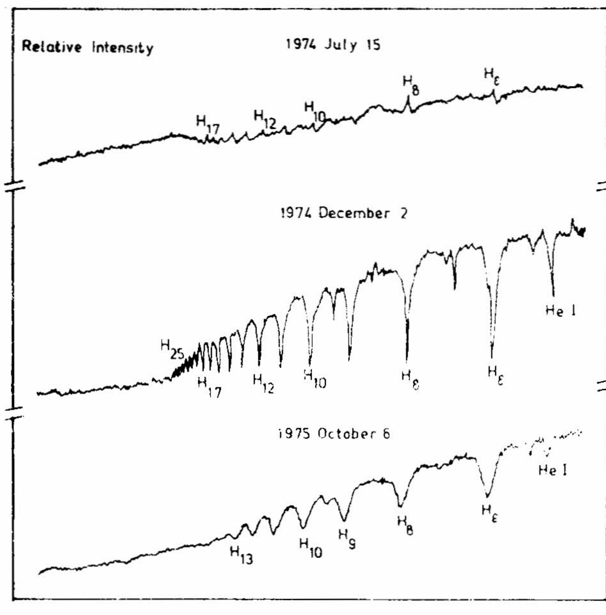

Fig. 1. Three spectra of 59 Cyg: strong Be–emission spectrum in July 1974 (top), shell spectrum in December 1974 (middle) and spectrum of a normal B–phase in October 1975 (bottom). (Based on Thomas, R.N.: 1983) Stellar Atmospheric Structural Patterns. NASA SP–471

2. THE MAIN HISTORICAL PERIODS

The initial period in Be stars research lasted from 1867, when Secchi noticed the H_β emission of γ Cas, and the First General IAU Assembly in Rome 1922 when the IAU Commission 29. introduced the name „Be stars", to the famous O. Struve's interpretation of the fenomenon in 1931:

„Sir James Jeans has shown that under certain conditions a rapidly rotating gaseous body may become lens–shaped and throw off matter at its sharp equatorial edge. It is therefore reasonable to expect that Be stars in extremely rapid rotation will eject gaseous matter at the equator. A gaseous ring will be formed and the system will resemble in appearance the planet Saturn (Struve, 1931)".

Beisdes by Struve, that problem has been treated by Curtis McLaughlin and Merrill. Several bright stars as: γ Cas, Pleione, ζ Tau, β Mon and φ Per have been studied at that time and their interpretation has been founded. The origin of the visual emission lines in an extended disk–like envelope has been finally established. Also, some characteristics of timechanges of the spectral line emission with respect to the neighbouring continuum, E/C, and the ratio V/R of emission peaks on the violet, V, and red, R, wings of the Balmer lines have been noticed.

The period from the begining of 30–ties till the end of 60-ties has been devoted to: a) stellar rotation and its influnece on the star and on the envelope, b) the spectral line formation in the extended atmosphere, more exactly, the stellar envelope, and c) mechanisms of the origin and maintenance of the envelope. The most important result from that period have been summarized in the proceedings of IAU Coll. 4, treating stellar rotations, of IAU Coll. 2, dealing with formation of stellar lines in the extended atmosphere, and of IAU Symp. 51, where much has been talked on the problems of stellar envelopes. Of course, the investigations in some other fields, primarily in the research of hot supergiant instabilities, have largely influenced the interpretation of the Be phenomenon.

The third, still lasting, phase in Be stars research has started in 70-ties. It is characterized by wide application of contemporary observational procedures permitting aquisition of spectral data from a wide frequency range of $\nu = 10^{8}\,s^{-1}$ to $\nu = 10^{18}\,s^{-1}$. Astronomers are forced to deal with an astonishing quantity of observational facts. During this period, three international IAU meetings dedicated to Be stars, Symp. 70 „Be and Shell Stars" 1976, Symp. 98 „Be Stars" 1982, and Coll. 92 „Physics of Be Stars" 1986, have taken place. Among many other meetings treating similar specific problems, the two, attended by some of the authors, will be menetioned: „Observational Basis for Velocity Field in Stellar Atmospheres" Trieste, 1982, and „Fast Changes of Early Type Stars" Hvar, 1983.

In order to better coordinate the research, IAU Commissions 29 and 45 founded the Working Groupe on Be Stars joined by several hundred astronomers. Since begining of 1980, the Working Groupe sponsored by IAU issues „Be Star Newsletter" where a complete bibliography on Be stars in regularly published.

Although a great number of well organized investigators work very intensivelly in a wide range of the electromagnetic spectrum, we are still far from a solution of the Be–phenomenon problem. The problem is a very complex one and we'll try to present it briefly.

3. SPECTRAL CALSSIFICATION

Even such a fundamental matter as spectral classification is not an easy task in Be stars. Xeenan and Morgan (1951) found Be stars among those ones where the two–dimensional spectral classification failed mainly because of wide and difuse absorption spectral lines, widened by fast rotation and disturbed by the presence of emission and shell lines of circum stellar envelopes.

Nevertheless, the spectral classification of the Be stars is done according to the criteria being valid in the case of B stars. However, the accurcy is not high and it is taken that the majority of Be stars belongs to the classes between B2 and B5. Slettebak (1982) completed the spectral classification of all known Be stars brighter then the magnitude 6.0.

4. ABSOLUTE MAGNITUDE

Great problems arise in determination of the absolute visual magnitude of Be stars. Their absolute magnitude, derived from their cluster and binaries adherence, occupy in the H–R diagram luminosity interval from III to V and, in average, they are located to more than one magnitude above the main sequence Figure 2. This fact

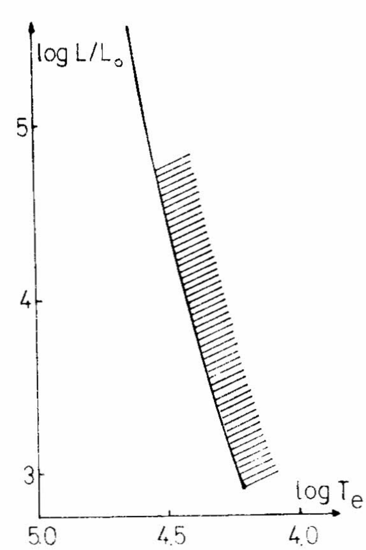

Fig. 2. The region of Be stars in H–R Diagram

couldn't be a manifestation of the evolution processes because of fast (some months or years) any–directional, changes of luminosity classes and spectral subclasses within the H–R diagram observed in Be stars. That would be interpreted as a ratational spread of H–R diagram.

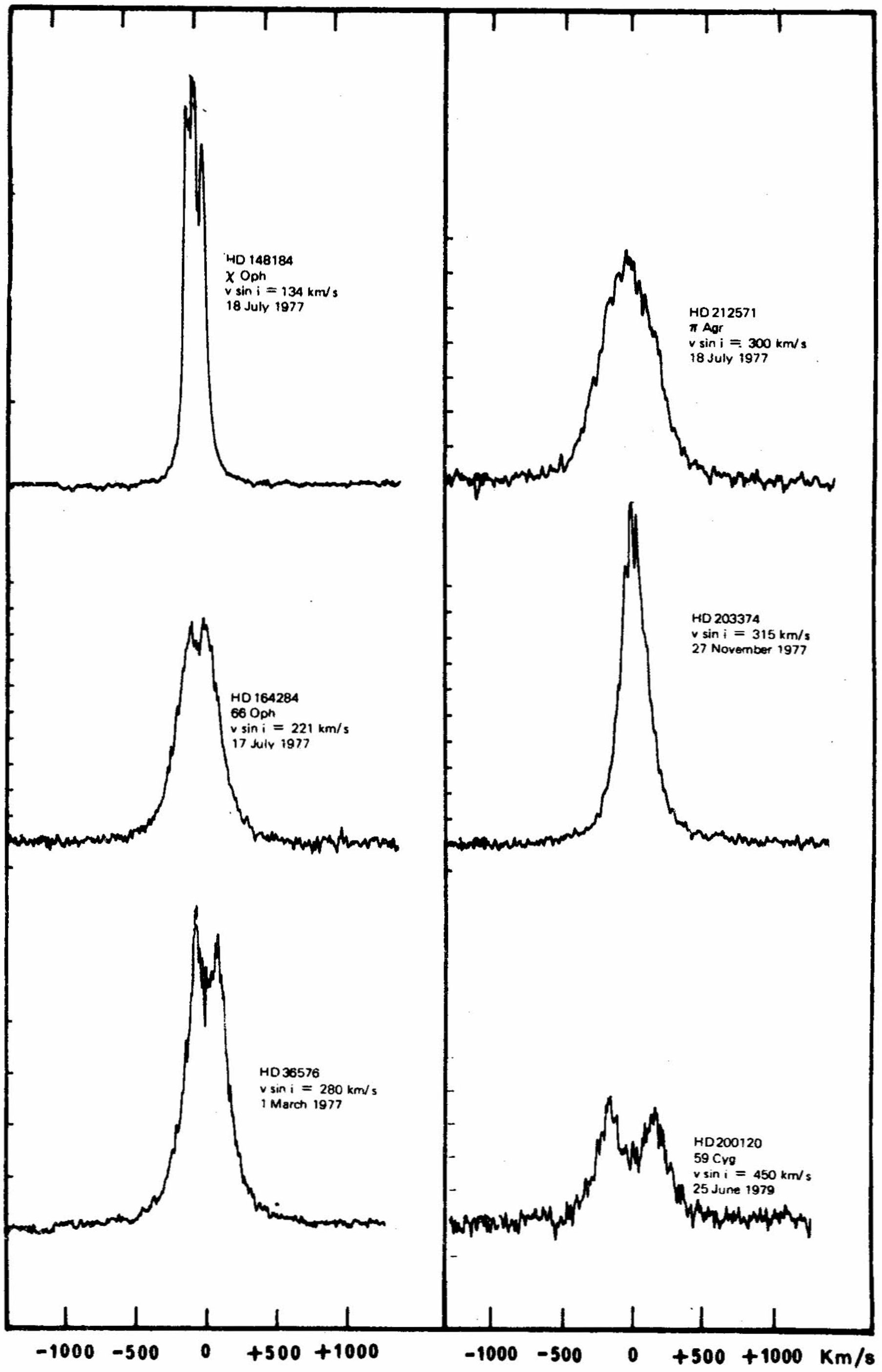

Fig. 3 Various H_α emission line profiles of Be spectra with low and high Vsin i (Doazan, 1982.)

5. SPATIAL DISTRIBUTION OF Be STARS

There are no basic differences in distribution of Be and B stars in space. They can be found in clusters (Pleiades and others), as spectrosopic binary components (ζ Tau), as eclipse binaries (V367 Cyg), and as composite--spectrum system components (K + Be, Wc 7 + Be spectra). Be stars are not concentrated in associations but are evenly distributed along the Milky Way.

In other words, instabilities causing the Be phenomena are the intrinsic properties of the stars and do not depend on distribution of the stars in space.

Egret and Jaschek have completed the New General Catalogue of 1100 Be Stars.

6. LINE–SPECTRUM IN THE VISUAL REGION

The most striking manifestation of Be phenomenon is the existence of Balmer emission lines in the spectrum which would, otherwise, be classified as a normal B one. The Struve's opinion that the emission spectrum originates in an extended (according to him up to 3–5 R, and according to Poeckert and Marlborough up to 50 stellar radii) disk–like gas envelope is widely accepted.

The emission lines form in the envelope due to recombination that follows the ionization by the stellar radiation. Besides the Balmer lines, the metal lines, most often Fe II, are frequently observed. In most cases, the emission appears in H_α, and sometimes only in H_α. The typical profiles of H_α emission in the stars with various rotational velocities (Vsini) are shown in Figure 3. Very often the emission profile is by a cnetral absorption divided into the short–wave, V, and long–wave part, R. It is nicely seen in Figure 4, where such H_α profiles of 59 Cyg are given. The typical shi fts of these lies indicate the expansion velocities about 30 km s^{-1} or more, but never more than 100 km s^{-1}.

The two most important characteristics of the visual emission lines, unsuccossfully interpreted by several different models, are: 1) the ephemeral cyclic changes of the V and R emission peak intensities, V/R, usually in intervals of several years, and 2) too wide spectral line wings, unsatisfactorily explained by any of the existing models.

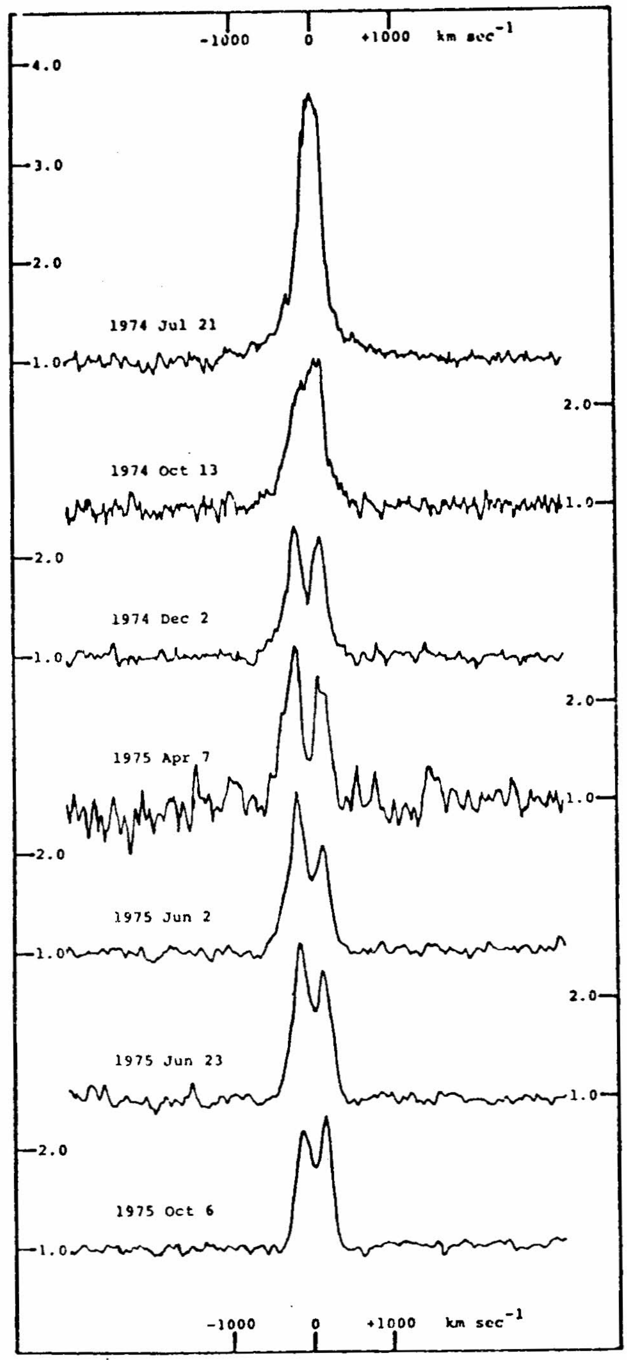

Fig. 4. The illustration of V/R variability in the case of 59 Cyg H_α profile from July 1974 till October 1975. (Barker, P.K.: 1979, Ph.D. Diss. Univ. Colorado, Boulder.)

7. SHELL SPECTRUM

The shell spectral lines, named by Struve, appear in a Be–spectrum from time to time. These are deep, narrow absorption lines (absorption cores) superposed on broad emission and absorption spectral lines. In Figure 5 and Figure 6 the shell lines within the emission and absorption lines are shown. An emission spectrum can smoothly turn into the shell one, and vice versa, what is nicely seen in Figure 7, where H_α emission of

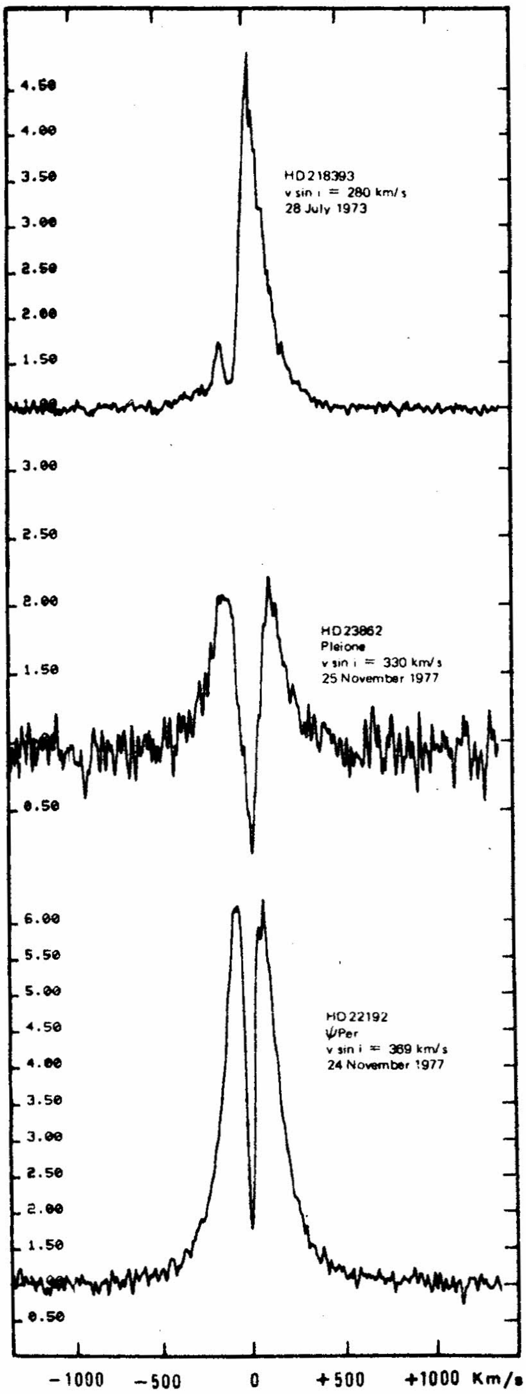

Fig. 5. Typical H_{α} emission line profiles with shell absorption. (Doazan, 1982)

Pleione is presented. Sometimes, a star completely looses its shell–spectrum characteristics. Also, the same object can have all the three types of spectra. The spectral changes from Be to Be–shell and to normal B phase are smooth and can run in any direction.

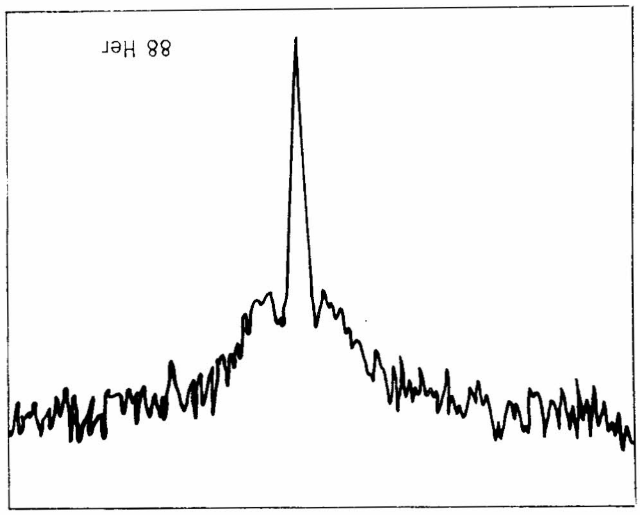

Fig. 6. H_{β} absorption line with the sharp shell absorption. (Doazan, private comunication.)

Some more general characteristics of the shell spectrum have to be mentioned. A well developed shell spectrum seems to be of a later type than the one indicated by the photosperic lines only.

The hydrogen spectral lines, at least the lower members of Balmer series, exhibit a very deep narrow absorption bordered with the emission wings. The ionized metal lines, as Fe II, Ti II, Cr II etc., have deep absorptions with or without the emission wings. The Be absorption spectrum can also contain the lines of Si II, Mg II, He I, Ca II, Na I, Mg I, etc. and, in some cases, even Fe I. Sometimes, deep absorption in Balmer lines is observed in high series numbers, e.g. up to 42 (48 Lib, EW Lac). In some other cases the deep absorption is seen only in high–resolution H_{α}–observations.

There are great time–dependent differences in shell spectra among the Be stars.

8. CONTINUUM SPECTRUM

The unlikeness of B and Be stars are not fully exhausted in their line– spectra. Gerasimovich (1929) has already noticed a quite different spectral energy distribution in the Be and normal B stars. This fact, in some more modern measurements of energy distribution, Schild (1978) for example, giving the same result, is ilustrated in Figure 8. The energy distribution greately deppend on dereddening procedure which is not uniquely accepted till now.

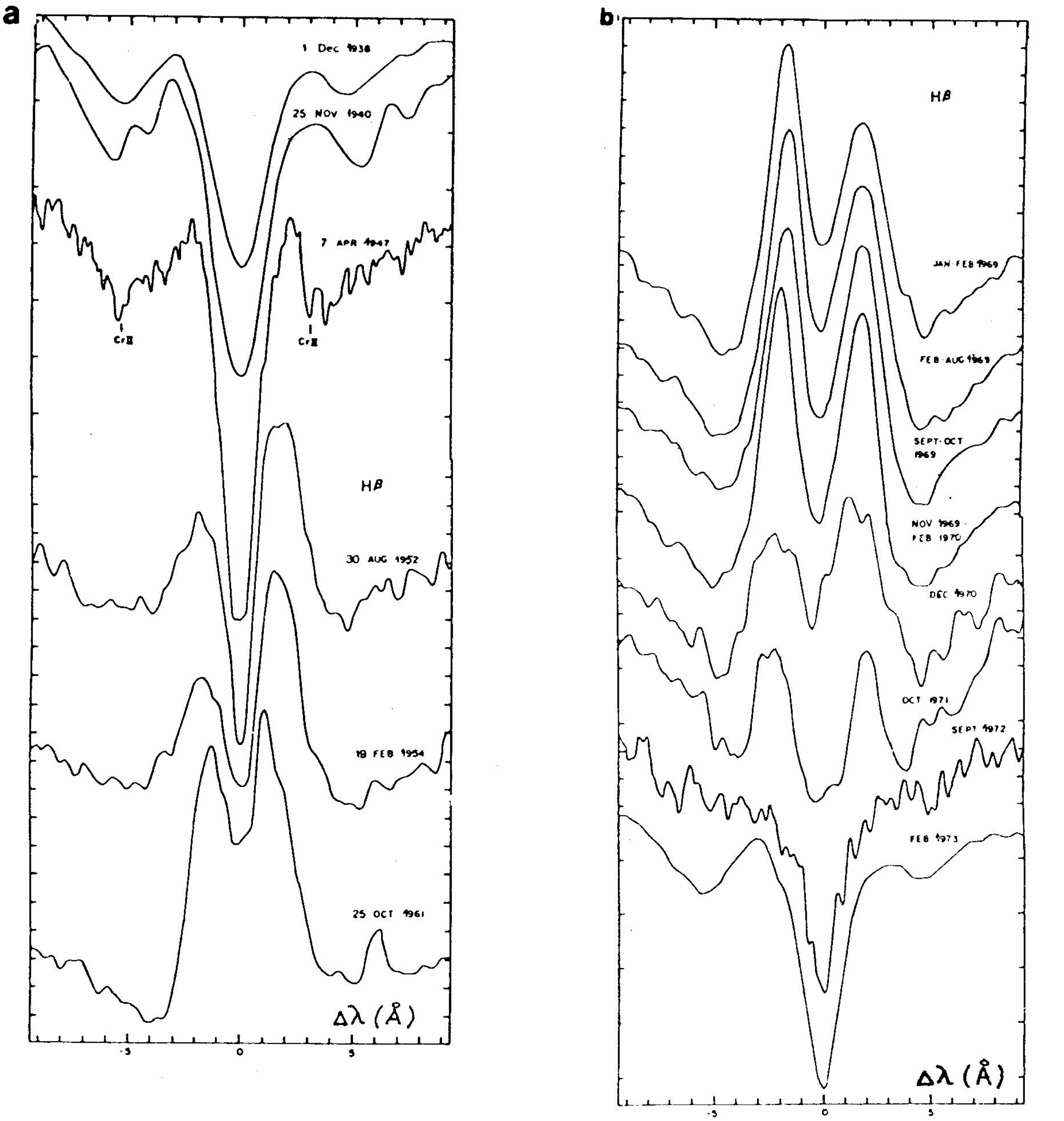

Fig. 7. The changes from the shell to the Be phase (a) and from Be to the shell phase (b) of Pleione. (Gulliver, A.F.: 1977, Astrophys. J. Supplement, **35**, 441.)

A thorough study of spectral energy distribution of Be stars in the region 320–600 nm, based on photographic photometry, has been accomplished by Barbier and Chalonge (1941). They found that the visual emission spectral lines are followed by a continuum reddening, i.e. by the lower temperature than usually found in a normal B spectrum, as well as by changes of the Balmer jump differing in the cases of Be and sh spectra.

In the most cases the Balmer jump in Be stars smaller than in the normal B stars. It could also normal, in emission or absorption, and even deeper th the normal Balmer jump. The characteristic aspects

Be star Balmer discontinuity compared to the normal B case are shown in Figure 9.

In addition, a great number of Be stars have a red excess in the Pashen continuum.

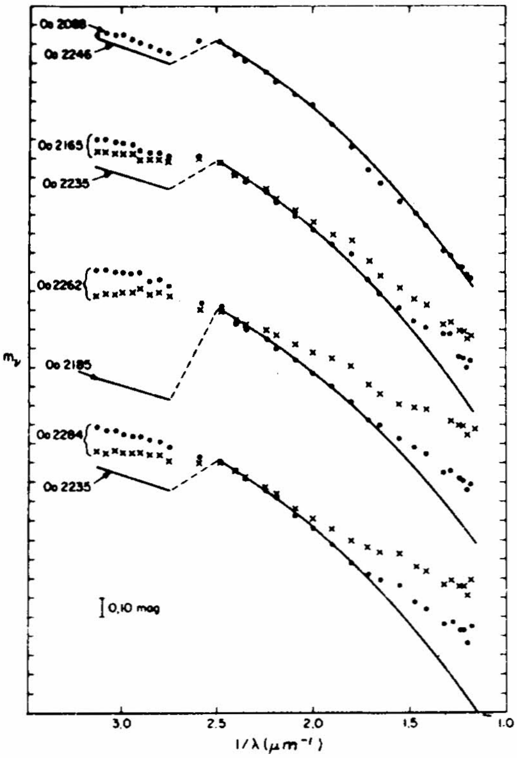

Fig. 8. The energy distribution of some Be stars in the cluster χ Per. Solid curves – normal B stars; dots – dereddening with the best fit to the normal B stars in the 40.0 – 55.0 nm region; crosses – dereddening by using cluster mean reddening. (Schild, 1978, Astrophys. J. Supplement, **37**, 77.)

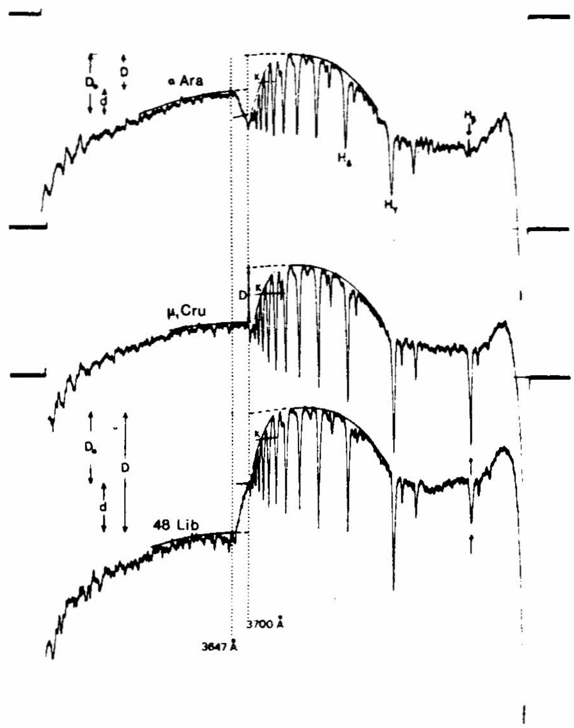

Fig. 9. Three types of Balmer discontinuity in Be stars. Top: αAra – second Balmer discontinuity in emission increasing the level of continuum intensity at $\lambda < 364.7$ nm with respect to the continuum of normal B spectrum.
Middles: μ_1, Cru – normal B star.
Bottom: 48 Lib – Second Balmer discontinuity in absorption.
(Divan, L.: Proc. IAU Coll. 47, Spectral Classification of the Future, eds. M.F.McCarthy, A.G.D.Philip, G.V. Coyne, specol Vaticana, 247.

9. INFRARED SPECTRUM

The presence of an excess in the infrared spectral region is one more indication of the existence of mass outflow from the star. The estimated mass loss rate in IR is about 10^{-8} $M_\odot$/yr.

The infrared excess in K–L colour index of Be stars has been discovered by Johnson (1967). Scargla et al. (1978) explained a 28%-part of the IR excess up to 20 μm of γ Cas as the free–free emission, while the rest, 72%, they attributed to the free–bound emission. They also developed a model of the envelope yielding: $T = 17540$ K, $\tau = 0.5$, $n_e = 10^{12}$ cm^{-3}, $R = 2 \times 10^{12}$ cm. Some of the most recent statistical investigations in the infrared up to 60 μm have been done by Cote and Waters (1987). A good illustration of the infrared excess is the colour–colour diagram given by the same authors, Figure 10. Here the observed position of Be stars agrees well with the one expected in the case of the excess originating in free–free emission of decreasing–density ($\rho \sim r^{-n}$; $2.5 < n < 3.0$) ionized gas envelope. The ionization is supposed to be caused by the photospheric Lyman continuum.

The extremely high infrared excess found in some Be stars with „unusual" spectra require an additional thermal reemission from the envelope particles.

In the case of a typical conventional Be star evelope at about 4R from the star, Gehrc et al. (1974) estimated the electron concentration to about 3×10^{11} cm^{-3}.

A radiation deficit in the shortwave region and an excess in the longwave one is clearly seen in Figure 11, where the observed energy distribution of the star DH 45677 is shown For comparison, the energy distribution of normal B2 III star, γ Ori, is also presented.

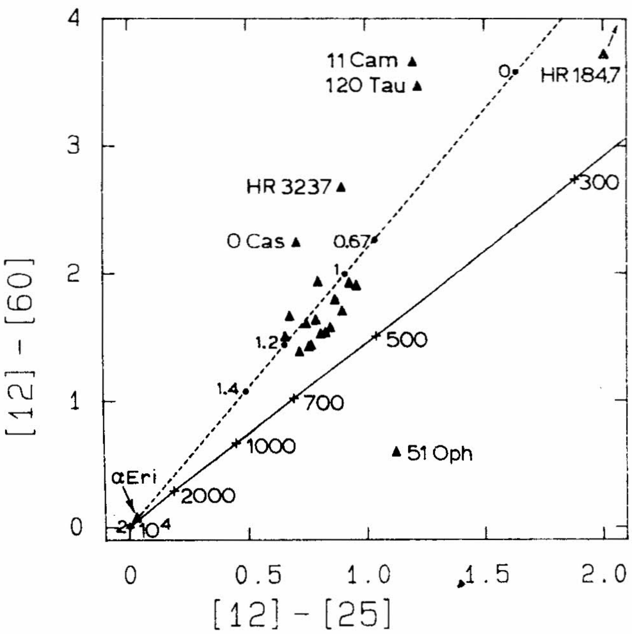

Fig. 10. Far IR colour–colour diagram observed at 12, 25, and 60 μ. Be stars (triangles) occupy smal area outside the blackbody line (solid line with indicated temperatures). (Cote and Waters, 1987).

The infrared line–spectrum of Be stars is very rich, with many more lines than in other spectral regions. For example, the spectrum of γ Cas from 1 μm to 2.5 μm, Figure 12, exhibits numerous lines of Brackett, Paschen and Pfund spectral series. Besides the H I lines, in Figure 12 one can also notice the lines of O I, He I, N I and Si I. Assuming a photoexcitation of some O I energetic levels by Lyman Beta or Gamma lines, Dimitrijević et al. (1987) tried to identify the origin mechanism of two O I lines: 1316.5 nm and 1128.7 nm. In densities of about 10^{13} cm^{-3} one can obtain the intensity of one of the two lines. However, even with much higher densities it is difficult to explain their intensity ration. The work on this problem is going to be continued at Belgrade Astronomical Observatory.

10. RADIOFREQUENCY RADIATION

Extended circumstellar envelopes are common properties of all stars with the observed radioemission. However, there are not many stars observed in the radio wavelength range. Only the upper limits of radio flux, up to 20 mJy, of conventional Be stars have been measured. The radio flux and hydrogen emission data can yield density distribution in the envelope. So estimated densities at the Hβ formation level are of the order $10^6 cm^{-3}$ to $10^8 cm^{-3}$. These densities are much smaller than the ones ($10^{11} cm^{-3}$ to $10^{12} cm^{-3}$) taken as standard in the stellar envelopes. Even in the radio flux case the problem of eliminating the interstellar extinction appears.

Generally speaking, the radiation originating in the outher atmospheres of the emission line stars can differ much from one star to another of the same spectral calss and, also, exhibit some similarities with some other classes.

11. FAR ULTRAVIOLET CONTINUUM RADIATION (90 nm – 300 nm)

The first UV observations were obtained in 1964 (Smith, 1967). Marlborough (1982) has reviewed all the measurements prior to 1982.

Two successful satelites, Copernicus and IUE (International Ultraviolet Explorer) have made an enormous leap in the shortwave radiation field during the last decade.

The evaluation of continuum radiation distribution based on the measured data is loaded with considerable problems because of the necessary correction of interstellar extinction and the different intrinsic luminosity of Be and normal B stars. It is very difficult to exactly apply both corrections, and the UV spectral energy distributions are uncertain.

In a smaple of 25 B and 15 Be shell stars Bottemiller (1972) didn't find essential differences between Be and B stars in the wavelength range 169 nm – 332 nm. Similarly, in the region about 250 nm Lamers et al. (1980) couldn't find the B – Be difference. From the wavelengths 110–360 nm Bless and Savage (1972) found in strong line emission stars an excess longward from 200 nm. Beeckmans (1977, 1978) concluded that the earliest–type Be and latest–type Be shell stars have ultraviolet flux defficiency with respect to the normal B stars. For Be stars having the largest IR excesses Zorec et al. (1982) have found the largest UV color differences with respect to the sequences of normal stars. Doazan (1982) considers this problem as unsolvable untill the mentioned question of interstellar extinction correction and B – Be stars luminosity difference is complstely solved.

12. ULTRAVIOLET LINE–SPECTRUM

In the spectral region 90 nm – 300 nm the differences between Be and normal B stars qualitatively do not exist. In the both types of stars the resonant lines of highly ionized atoms, as CIV O VI, N V or S i IV, have been observed. The ionization is much higher than the one expected on the basis of the star's effective temperature and its thermal radiation.

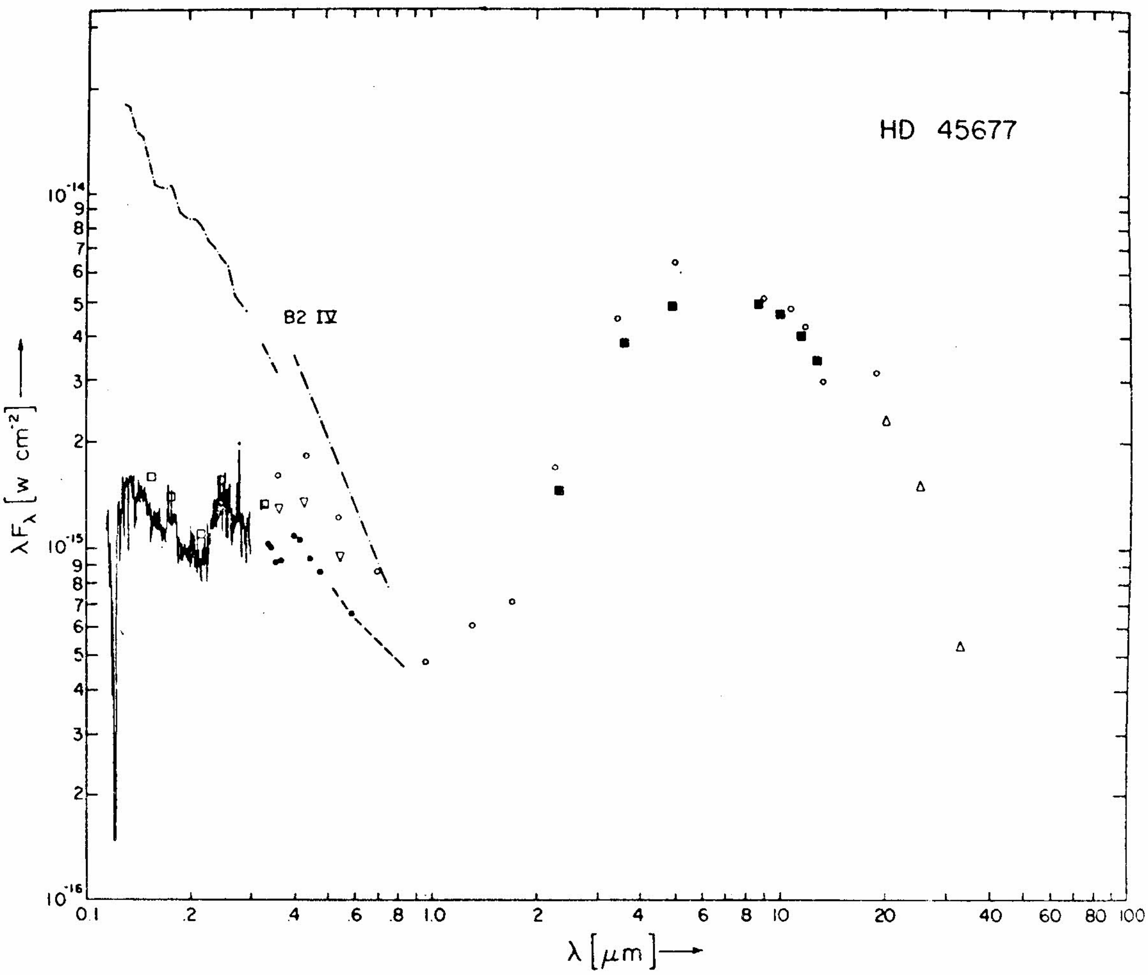

Fig. 11. The energy distribution of Be star HD 45677 shows an IR excess in the region $\lambda > 2\ \mu m$ and a deficiency in the ultraviolet region compared with normal B2 IV star γ Ori. Deficiency depend greately of the deredding procedure. (Sitko, M.L. and Savage, B.D.; 1980, Astrophys. J. **237**, 82.)

Due to high temperature (2×10^5 K according to Lammers and Ragerson (1978) and more than 10^6 K as cited by some other authors) as well as to the large shifts and asymmetries of these spectral lines, the ionized regions where they are formed can not be easily located in the atmosphere. That is one of the dominant problems of Be stars modeling.

One of the characteristics of the spectral lines in this spectral interval is the presence of large wavelength shifts indicating mass outflows with velocities up to some 2000 km s^{-1}. Such a spectral shift of C IV ionized carbon at ω Ori, corresponding to the velocity of 855 km s^{-1} considerably exceeding the escape velocity of the star, is given in Figure 13.

The other characteristic property of these absorption spectral lines is their asymmetry, namely the extended shortwave wings, as can be seen in a C IV spectral line of θ CrB, Figure 14. Assuming formation of the line within a rarefield expanding envelope with the mass outflow, the shortwave end of the line–wing determines the highest approaching ion velocity. Any correlation between such a line–asymmetry and the quantity V sin i has not been found – what is interpreted as an additional confirmation of the mass flow coming not only from the stellar equatorial regions as expected according the Struve's model. This explanation is supported by the fact that the high wavelength shifts of super–ionized lines have been observed in some pole–on stars too. The UV spectra of Be stars have provided the direct indications of a high stellar latitude mass outflow processes. Snow and Marlborough (1976), Marlborough (1977) have shown that the superionization does not depend on absolute bolometric magnitude and effective temperature of a star.

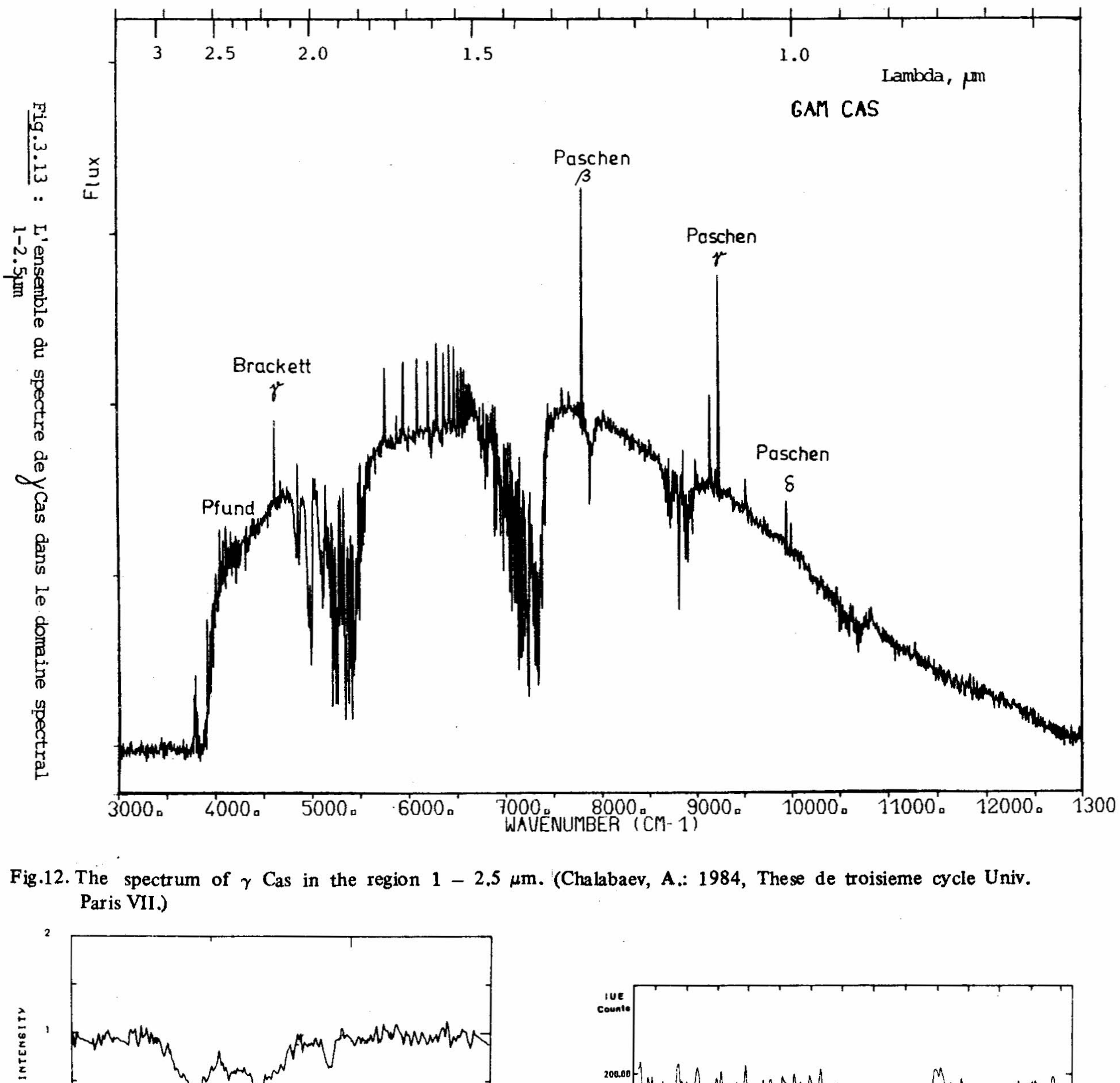

Fig.12. The spectrum of γ Cas in the region 1 – 2.5 μm. (Chalabaev, A.: 1984, These de troisieme cycle Univ. Paris VII.)

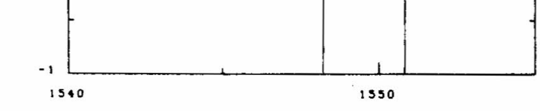

Fig.13. Absorption components of the C IV resonance lines in the pole – on star 66 Oph violet shifted by 700 and 250 km/s. The bars indicate the position of laboratory wavelengths. (Doazan, 1982.)

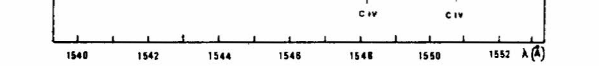

Fig. 14. The C IV resonance lines of θ Cr B with extende wings toward the short wavelengths observed when th spectrum in visual was quasi–normal.(Doazan, 1982.)

The estimation of the mass loss rate observed in UV (Si III and Si IV) yields the values 3 x 10^{-9} to 10^{-11} $M_{\odot}$ year^{-1} (Snow, 1981). This estimation, is for one order of magnitude lower than the velocities obtained from the visual spectral region when an equatorial disk has been considered.

The ultraviolet spectra of some Be shell stars have deep absorption lines resembling the shell lines in the visual region. These lines originate in atoms equally or less excited or ionized than those in the photosphere. For example, some of them are: Fe III, Cr III, Ti III and especially Fe II. The location of such an absorbing region is uncertain yet. Some authors (Doazan and Thomas, 1982) take it as a „post–coronal region" in the outer stellar atmosphere – likewise the extended emission envelope observable in the visual wavelengths.

The resonant lines of Al III, Al II and MGII are also strong. The existence of two ionization states of the same atom indicates a large ionization range within observed layer.

The UV–shell lines can be observed even when the star does not show any shell lines in the visual region. They are present in some pole–on stars too – opposing the rotation model of Be stars. The strength of UV–shell lines of these stars has no correlation to Vsini (Peters, 1976).

13. X – RAYS

Soft (0.2–3.5 keV) and hard (> 3 keV) X–emission have been measured by the satelite EINSTEIN for several hundreds of stars including some of Be types. The main results of these observations can be found in the papers of Rosner and Vaiana (1979), who concluded that all stars radiate X–rays of certain level and that there is no such class of them as „X–Ray stars". Hence, in this respect, no discrepency between Be and normal Be stars exists. UHURU satelite data base was analysed by Peters (1982), who founded that „clasical" Be stars do not apear to be sources of hard X–rays. Upper limits of the energy for the nearest objects are less than 10 erg/s.

It is taken that within the whole HR – diagram the soft X–radiation indicates the existence of stellar coronae, while hard X–rays are interpreted as interaction in a binary system containig a compact component where accretion can heat the matter up to 10^{-7} K or 10^{-8} K (Shklovsky, 1967).

In spite of the hypothesis of binarity of all Be stars (Harmanec and Kriz, 1976) it isn't likely that those mechanisms dominate there. For exmaple, discussing the observed X–radiation of γ Cas, Marlborough (1977) concluded that the radiation does not originate in the accretion disc around the optical component. He rather interpreted the observed X–emission as a consequence of the corona surrounding γ Cas. According to him, this region is a natural extension of the superionized layer above the photosphere observed in the UV wavelengths. It seems that such observations initiated the comprehension of stellar coronae as a normal component of the atmosphere structure and not as an anomaly. Marlborough considers X–radiation of γ Cas as caused by bremstrahlung in the optically thin Maxwell circumstellar envelope with the temperature more than 2 X 10^7 K, and the electron density less than 10^{11} cm^{-3}.

Besides, it has to be noticed that the observed X–emission changes in time, what seems to be general property of all kinds of Be stars radiation.

14. POLARIZATION

In about 50% of polarimetrically measured Be stars the intrinsic optical polarization has been found. The intrinsic character of this polarization has been revealed on three ways:

- by the time–dependent stellar measured polarization (first such polarization has been found in γ Cas by Behr, 1959),
- by specific wavelength–dependence of polarization basically different from the interstellar one, and,
- by the existence of decreased degree of polarization within some Balmer emission lines.

It is generally accepted that the presence of intrinsic polarization of Be strars confirms the basic assumption of an extended non–spherically symmetric envelope, or an equatorial disk around the star, as well as the origin of the polarization in the scattering of non–polarized stellar radiation on the free electron in the envelope.

The properties of the wavelenth–dependent polarization, shown in Figure 15, came from the simultaneous action of the scattering mechanism and radiation transfer processes among which the most efficient is absorption, and in a smaller degree emission. General characteristics of that function are: a steep drop of the polarization percentage after the Balmer series limit and a moderate one after the Paschen series. The changes of the polarization position angle are small. Using high–resolution spectral observation, several authors have been measured a decreased amount of polarization within the emission profiles of the strongest Balmer lines, H–α and Hβ The measurements started in 1975 (Poeckert and Marlborough, 1978 McLean et al , 1979) with an echell–spectrograph and digicon achieved the spectral resolution of 0.05 nm at Hβ. The variations of polarization percentage and position angle along the spectral line profile in the case of γ Cas and φ Per are

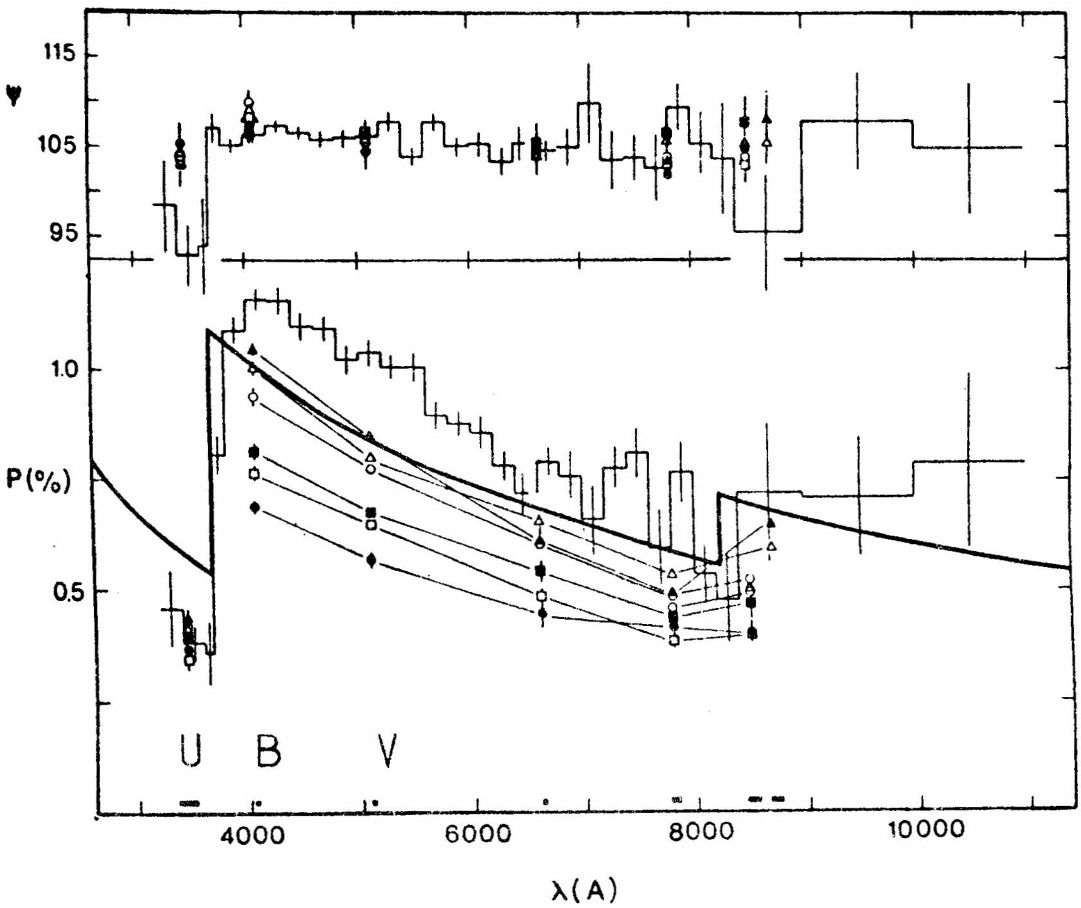

Fig. 15. The polarization percentage as a function of wavelength for γ Cas. The heavy line represents the model calculation by Poeckert and Malborough (1978) The symbols represent different observations. (Poeckert, R. and Marlborough, J.M.: 1978, Astrophys. J., **220**, 940.

shown in Figure 16. The main cause of decreasing of polarization percentage along the profile of spectral line is certainly some amount of unpolarised radiation within the emission line superposed to the polarized continuum. However, the depolarization in spectral lines is lower than expected. This can be explained by partial polarization within the lines, as well as, by partial absorption of the unpolarized line–radiation in the envelope. The changes of the polarization position angle are complex what can be understood taking into account their origin in a radially expanding and differentially rotating envelope, having probably certain geometrical distorsion too.

In spite of the number of polarimetrically measured stars being not to large, some statistical investigations revealed that:

– The intrinsic linerar polarization in the visual region is usually not higher than 2%–what is generally considered to be a low value. Such a low polarization percentage might indicate a not too flattened envelope around a Be star as well as a dominant contribution of the direct stellar unpolarized light, in the total observed flux of the star.

– There are no stars with high intrinsic polarization and low rotation velocities. This fact may mean that a certain minimal stellar rotation velocity is needed to obtain a given flattness.

– There is a tendency that all higher polarized stars exhibit large equivalent width of H_α– emission (McLean, 1979)

– All stars with large infrared excess have an intrinsic polarization. One can conclude: the processes leading to an infrared excess certainly have an influence on the polarization of stellar radiation too.

– There are some indications of a time–lag between a stellar spectral (Poeckert et al., 1979) and photo-

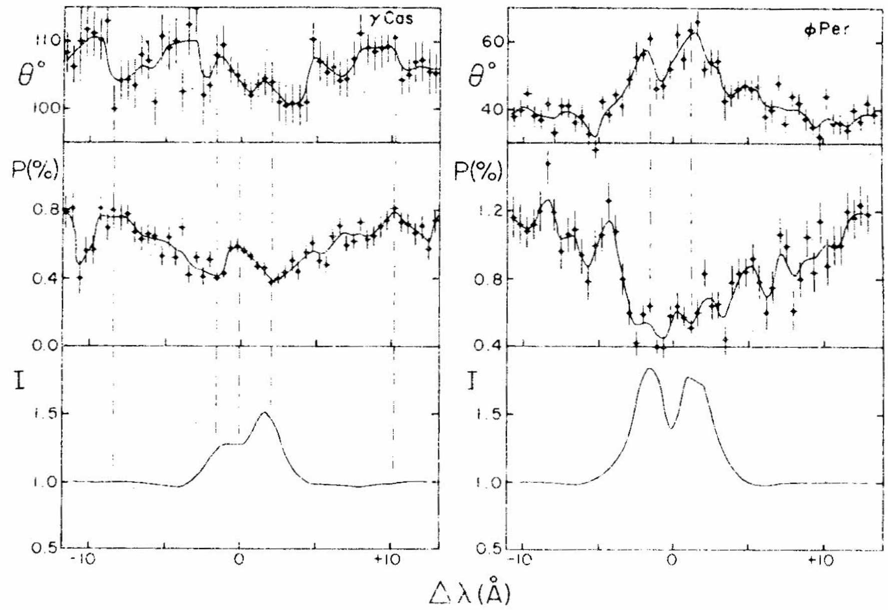

Fig. 16. The position angle, the polarization percentage and the normalized intensity profile across H_β for γ Cas and ΦPer. (McLean, 1979.)

metric (Arsenijević et al., 1987) changes and the accompanied polarization variations.

To get a more detailed insight into intrinsic polarization problems one can consult the rewievs of Coyne (1976) and Coyne and McLean (1982).

15. TIME–VARIATION AS A GENERAL CHARACTERISTIC OF Be STARS

So far, it could be seen that the Be stars have been observed for more than a century, very intensively during the last years, and very successfully in some campaigns simultaneously covering several spectral regions. All these numerous measurements reveal the existence of a common characteristic: time–variation of almost all measured quantities. The nature of the changes does not allow any prediction even for a single star. The time intervals involved are very diverse. There are short–term changes within minutes, hours and days, as well as long–term ones – when months, years or even decades come in question.

One of the long–term variability aspects is the interchange of Be–shell, Be and B–normal phases and vice versa. The duration of any of the phases depends on the given star and the epoch of observation and can be anything between a month and a decade. For example, during almost a century, γ Cas had only two Be–shell phases separated by an interval of four years. In the case of 59 Cyg the interval between two Be–shell phases lasted for only one year, while for Pleione it was 35 years.

The change of the intensity of spectral line emission, E, wiht respect to the adjacent continuum intensity, C, is a characterisic measure of the Be–phase itself. The time–interval between two successive E/C maxima differs from one star to another, and even in one star at different epochs. The shortest of such intervals amounting to about 7 days has been observed on HD174237.

In the spectral lines the most prominent are the changes of the V/R – the ratio of the emission intensities in the two wings of spectral line. The changes are quasi–periodic and the characteristic time is about several years. In the case of γ Cas the period is about 5 years–what is nicely seen in Figure 17. The whole phenomenon (the variability) can last several or more years and then may completely disapear. The ratio V/R has been found to change even without any substantional variation of the total emission. On the other hand, V/R changes are approximately followed by radial velocity variations of central absorption and emission wings in a spectral line. For $V/R < 1$ there is a blueshift, and for $V/R > 1$ the red one can be found.

Struve tried to explain V/R changes and especially the emission line shifts by the apsidal rotation of the eliptical equatorial gas ring. This model has been lately elaborated by Huang (1972, 1973) who obtained a good agreement with the observed changes. However,

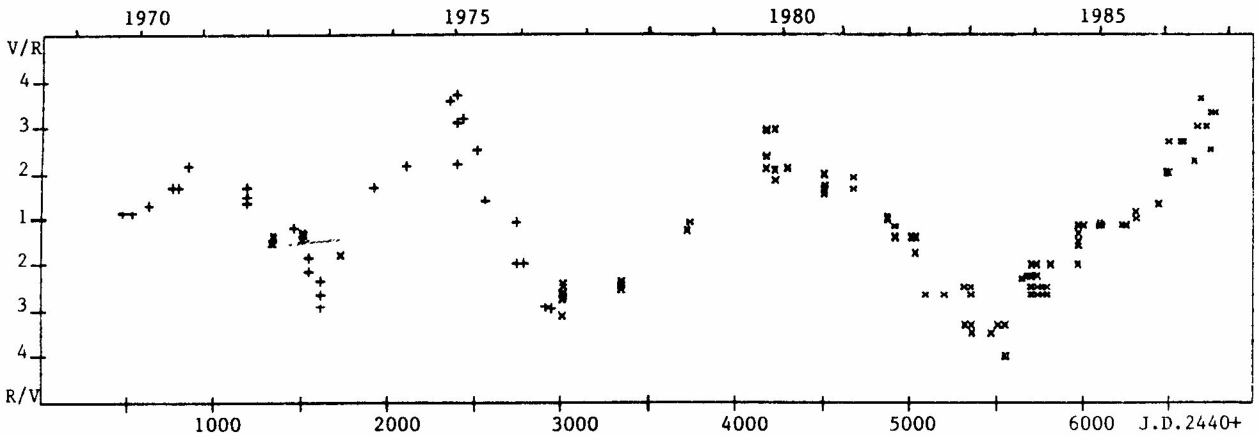

Fig 17. V/R variations of H_β emission line of γCas from 1969 to 1986. (Doazan et al. 1987).

besides the variation of V/R, the model can hardly explain any other phenomenom. Some other models can not cover the V/R changes.

The relative shifts of the shell–lines and emission lines with respect to the stellar photospheric absorption lines indicate an expansion, a contraction or a stationary state of the circumstellar envelope. In the visual spectral region the expansion velocities are small, below 100 km s^{-1}. Radial velocity changes are, generally, unpredictable, time–scales different and behavior of individual stars different. Nevertheless, in some stars, as e.g. 88 Her,

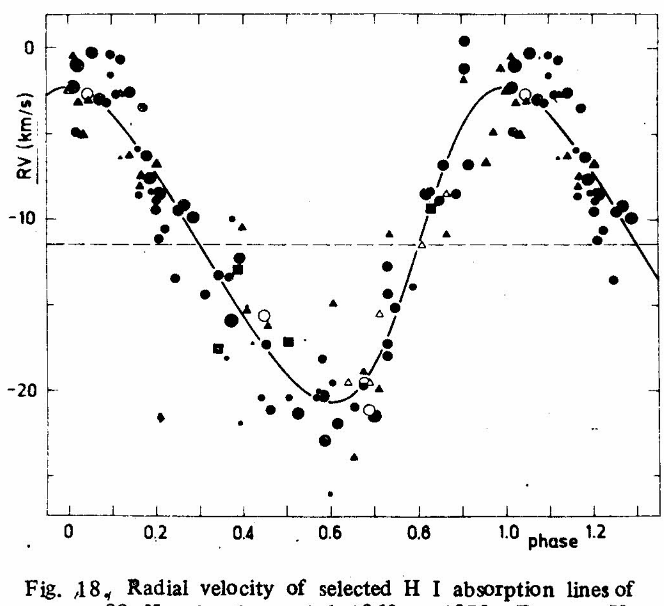

Fig. 18. Radial velocity of selected H I absorption lines of 88 Her in the period 1963 – 1979. (Doazan, V., Harmanec, P., Koubsky, P., Krpata, J., Ždarsky, F.: 1982, Astron. Astropphys., **115**, 138.)

Figure 18, and 4 Her, the periodic changes of radial velocities have been observed. Such a result for 88 Her has been confirmed in the most recent period of collaboration of Paris and Belgrade observatories and Muenster Astronomical Institute for the Balmer and some metal lines.

As shell lines are narrow and sharp, the derived radial velocities are reliable. In many cases systematically different radial velocities, obtained from shifts of the absorption spectral line cores, are found for different Balmer lines. The effect is refered to as Balmer progression (Merill and Sanford, 1944). Usually, the approaching velocities are higher for the lines closer to the series limit, what is interpreted as deceleration of the circumstellar envelope matter with the distance from the star. Balmer progression, undergoes large long–term and mid–term changes (Ballerau and Chanville, 1987).

Photometric changes, sometimes connected with the alteration of stellar phases, usually commence suddenly, strikingly, although with small amplitudes, less then 0.3 magnitude. Exceptionally, γ Cas changed its optical magnitude for more than 1 magnitude in the period 1935–1940. In short–wave region these changes are somewhat larger. Photometric changes have been observed in about 50% of all cases. It has been found that such changes usually precede to a shell–fase and conversion of a purely hydrogen into a metal shell. While the intensity of Balmer emission grows, the stellar visual luminosity, the B–V color index and the reddening in Pashen series increses too. Such a sequence of events has been observed on γ Cas in the period 1936–1942, as well as in number of other stars. However, 88 Her didn't show these characteristics – what again, confirms our present inability to generally and logically comprehend the long–term photometric changes of Be stars. An ilustration of long–term changes of V/R, H_α emission

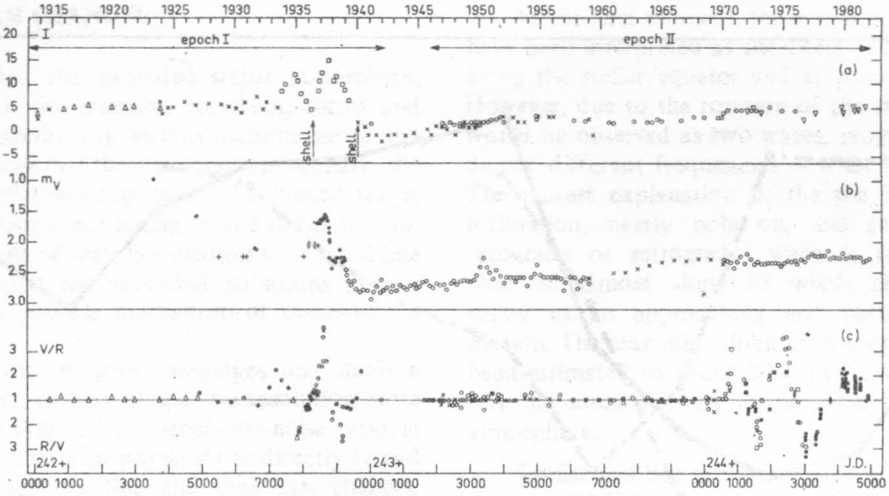

Fig. 19. The long–term variations of intensity (a), visual magnitude (b) and V/R (c) of γCas. (Doazan, V., Franco, M., Rusconi, L., Sedmak, G., Stalio, R.: 1983, Astron.Astrophys. 128)

intensities and brightness of the star γ Cas is given in Figure 19.

16. TIME–VARIATIONS OF STELLAR POLARIZATION

Time changes of linear stellar polarization have been studied since the begining of 60–ties. They yielded an insight into structural and geometric changes of the envelope. Likewise the other observed phenomena, the polarization changes are irregular and characterized by various time–intervals and they also differ from one star to another.

In majority of the observed Be stars the small–amplitude polarization changes in intervals of the order of one day have been noticed. The long–term variations, in intervals of one month to several years, seem to have somewhat larger amplitudes. In most cases, the polarization position angle changes not much and in some cases, due to small polarization percentage, they are measured with an insufficient accuracy. Such long–term changes are rarely examined in a small number of stars, and accordingly in time–intervals of 10 or more years.

Systematic investigation of optical linear polarization of several Be stars at Belgrade Astronomical Observatory has led to few interesting conclusions. One can safelly assert that long–term changes of the intrinsic polarization in the intervals of several years, really exist Arsenijević et al. 1979, 1986, and 1987). It was shown in several stars: 88 Her, o And, γ Cas and ℋ Dra. The polarization percentage changes are mainly below 1%, and the postiion angle changes not more than 20°. These changes are connected with the stellar photometric variations and envelope activity. In the case of 88 Her, where almost simultaneous photometric, polarimetric and spectral observations exist, some such correlations have been noticed. Namely, an anticorelation of polarization percentage and stellar magnitude changes– but with polarization falling behind for about one year – has been found.

On the other hand, almost a perfect correlation of polarization percentage and intensity of H_α emission has been found in the period 1974–1979. These relations are ilustrated in Figure 20 a, b and c.

The minimum values of the polarization percentage have been measured in the periods of normal B stellar phases, when the envelope activity is also at its minimum. During the phase of high envelope activity, what is indicated by strong emission and shell spectrum, an increased value of polarization percentage is observed. Nevertheless, it has to be noted that a correlation between polarization percentage and the strength of absorption shell lines has not been found in the case of 88 Her.

Further work on interpretation of long–term changes of the intrinsic polarization of Be stars is in progress at Belgrade Astronomical Observatory.

The existing theoretical models are still not able to fit the polarization changes in intervals of several years. An attempt to do that with a model based on stochastic behavior of electron globulae in a Be circumstellar envelope (Clarke and McGale, 1986, 1987) is now supposed to be in progress at Glasgow University.

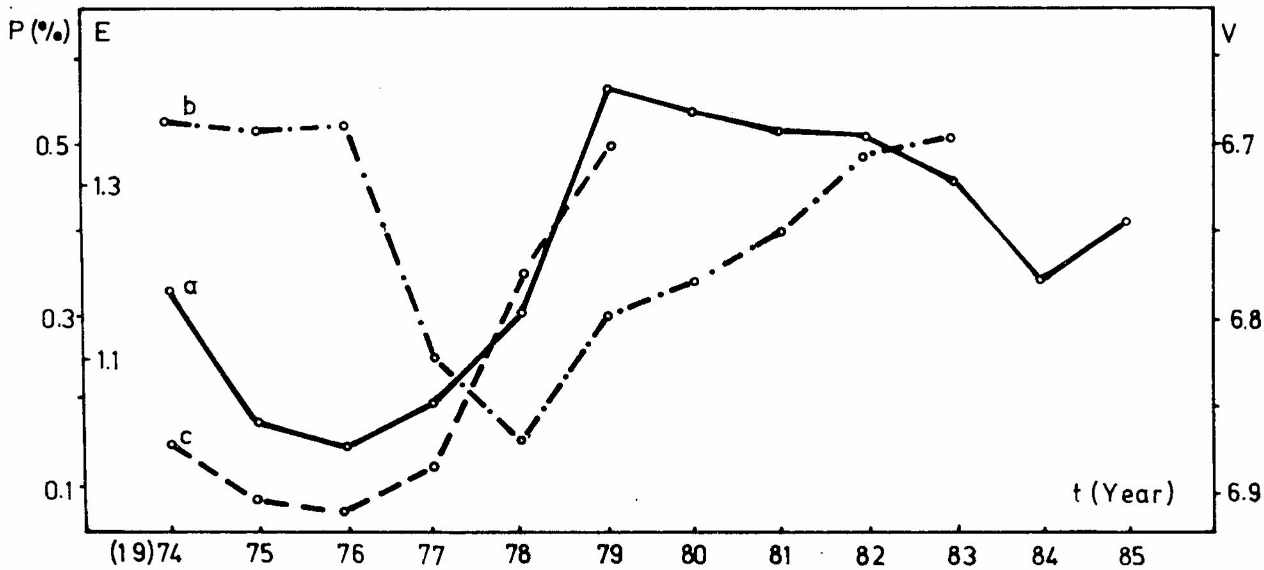

Fig.20. The long–term variation of polarization percentage (a), visual magnitude (b) and intensity of H_α emission (c) of 88 Her.

17. VARIABILITY IN THE UV–REGION

It is generally accepted that changes in the UV–region are much larger than in the visual one. The spectral line shifts and profiles change considerably. For example, the shifts of N V and CIV lines vary in the interval from -200 km s^{-1} to -1000 km s^{-1}. The profile of the resonant CIV line in θCrB changes so much that the line from time to time disappears and reappears, and all that happens in normal B stellar phase without any appreciable changes in the visual spectral region. Some such violet changes in the UV spectrum have been illustrated in Figure 21. The shifts and profiles of spectral lines are just those parameters determining the stellar mass flux and its change, hence the variations of the mass outflow can be taken as quite large.

In comparison with such an unstable, rarefied and highly ionized envelope found in the UV region, the layer of the envelope seen in the visual spectrum looks like being relatively cool, dense and quite.

Doazan et al. (1987) have shown that the high–velocity components of Si IV, C IV and N V resonant lines in the case of γ Cas exhibit some long–term changes connected with the cyclic V/R variations in Balmer emission lines. This is an important observational finding that can indicate an interaction of hot and cool envelope regions, what might affect the modeling of Be stars.

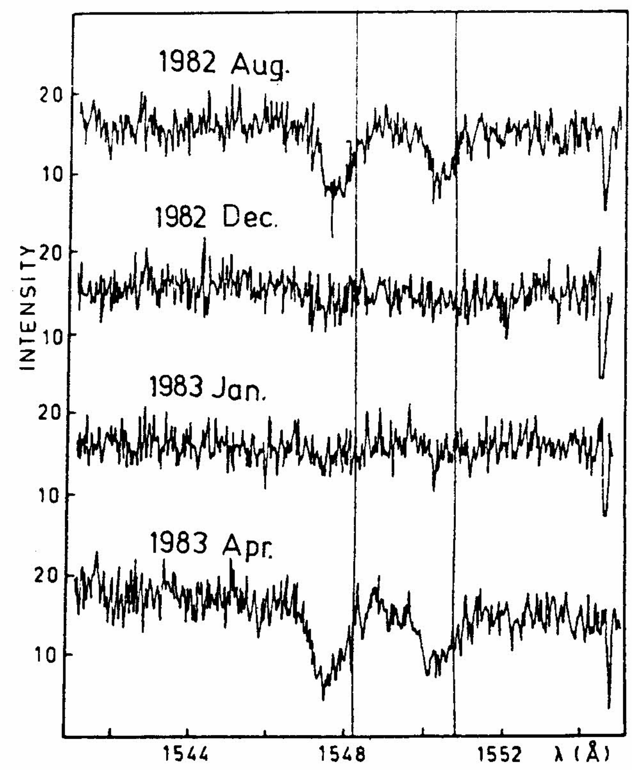

Fig. 21. The violent changes in C IV resonence line of θCrB from August 2, 1982 till April 6, 1983. (Doazan, V., Thomas, R.N.: 1983, Hvar.Obs.Bull. 7, 97.)

18. SHORT–TERM CHANGES

It is clear that the extended stellar atmosphere, revealable through the emission spectrum, forms and destroys itself without any serious disturbance of the star. As it is unlikely that the star rotates irregularly, the cause of changeable mas flux has to be looked for in another variable source not acting on the stellar structure. The observations of very fast changes of spectral line profiles indicate that the nonradial pulsations can be considered as the possible mechanism of the envelope activity.

The application of large telescopes and modern radioation receivers, namely of spectral resolution more than 20000 or 30000 and of signal–to–noise ratio in excess of 200, enabled astrophysicists to directly record details within a spectral line and their fast changes. Typical examples are the two series of He I 667.8 nm profiles of μ Cen obtained successively in the intervals of 20 to 80 minutes, Figure 22 (Baade, 1986). Besides the

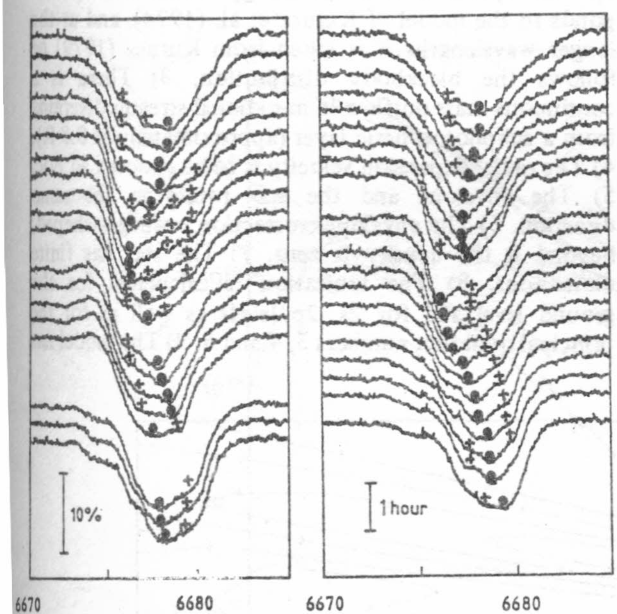

Fig. 22. The oscillatory variations of HeI λ 66.78 nm line–profile of μCen. (Baade, 1987.)

main minima of the absorption line, marked with full circles in the figure, a number of secondary minima or „bumps" are also seen (crosses). They progress from left to right (from violet to red shifts), or vice versa, during only several hours. Although the physical identity of a given line profile feature is not consequentially preserved by the applied marking, the phenomenon is clearly seen.

At the first moment, the events in μ Cen line profile have been interpreted as the direct and retrograde waves along the stellar equator and at planes parallel with it. However, due to the rotation of the star, such a motion would be observed as two waves, prograde and retrograde, of different frequencies – what was not the case. The newest explanation is: the star is seen at a small inclination, nearly pole–on, and an one–directional (prograde or retrograde) wave is at the same time observed almost along its whole circumstellar path, partly as an approaching and partly as a receding motion. The maximla velocities of these oscillations have been estimated to about 20 km s^{-1}, what is approximately the sound velocity in the upper layers of a Be star atmosphere.

Similar fast line profile changes have been noticed in the stars 28 CMa and HR 4074 (Baade, 1984), as well as in the case of Spica (Smith, 1985).

Differentila intensity changes of the spectral line emission components are often connected with the oscillatory features in the wings of the absorption lines. They are of the same nature, and they reveal themselves as V/R changes observable even without the highest spectral resolving power.

The nonradial pulsation hypothesis has been invoked to explain fast, minute spectrophotometric changes in several types of related stars. It appeared as an additional alternative among various hypotheses trying to connect the observed spectral features with the possible binarity of the star, the stellar rotation, or the changes in the circumstellar disk – what was not acceptable for a great number f the observed stars. On the other hand, the radial pulsations have not been taken into account because of much higher brightness changes they would require than it was actually observed in Be stars.

As the nonradial pulsations are thought to originate in the rarefied layers of the stellar atmosphere (transition region, lower corona) the observations of very fine, fast spectrophotometric changes in Be stars allow an insight in some apsects of stellar structure itself – contrary to the rough, long–term changes designated to the circumstellar envelope alone or its interaction with the star. This opens the possibility to immediatelly study the Be stars, to better understand their evolution stage and their position in the HR– diagram.

The fact that the oscillatory motion in stellar atmosphere introduces an additional velocity component which, at some phases at least, might superpose on sub–escape rotational velocities, increasing them to the critical values, and initiating in this way a mass outflow from the stellar atmosphere. So, the old Struve's problem of the Be stars mass loss may perhaps today be solved by this mechanism.

19. THE MODELS

To generally resolve the whole structure and dynamics of the Be star envelope and to get the density, temperature and local velocity as functions of position and time is a very intricate problem. An idea of its complexity, even in the case of a stationary state, spherical symmetry and a very simple radiation transfer can be gained from Cassinelli's and Castor's (1973) and Castor's et al. (1975) papers. But, if the magnetic field plays an important role in the envelope dynamics, as some authors suggest, the solving of the problem becomes more complicated. Still further difficulties are introduced by taking into account the non–thermal energy – what is justified in fast–rotating stars where the meridional circulation might drive an additional turbulent motion slightly below the sound velocities (10 km s^{-1} to 30 km s^{-1}) resulting in the stellar mass outflow.

To simplify the matter, particular solutions under certain assumptions are sought. Most frequently, the models with stationary stellar wind continuously originating along the equatorial belt of the star and being accellerated by the radiation pressure, are applied.

However, the radiation driven stellar winds had to be modified to include the envelope regions with temperature higher than the photospheric one, with high ionization and velocities as high as observed in the UV spectral region (e.g. in the O VI or N V resonant lines). The non–radiative heating, common for all new models, has been introduced. The most frequently taken energy sources are acoustic or MDH waves dissipating as shock–waves in the low–density regions and heating the stellar wind.

The rotation of the envelopes and their radial velocities much higher than the velocity of a radiative stellar wind make the radiation transfer problem more difficult: which equatorial velocity and inclination, or V sin i, to take as well as what effective temperature to choose. V sin i depends on the used spectral line and line profile changes with the rotational velocity. On the other hand, the densities in the envelope are such that collisional processes can not be neglected and the LTE approximation beocmes insufficient.

Marlborough (1969) has given in detail the first model with the stellar wind. However, he – as some other authors also did -- used only H_α emission to constrain his model.

Poeckert and Marlborough (1977, 1978) elaborated Marlbourough's model and applied it on γ Cas using the observed data on polarization in continuum from 300 nm to 900 nm, polarization in H_α emission lines and H_α and H_β line profiles. They also assumed that the following conditions were satisfied: 1) The central star is spherically symmetric and rotates at the critical speed. 2) The optical continuum energy distribution corresponds to the model of Kurucz et al. (1974), and at the longer wavelengths it is taken from Kurucz (1979) or follows the blackbody distribution. 3) There is a continuous mass outflow in meridional streams diverging from a subphotospheric layer (approximatelly at 0.8 R). 4) The radial expansion velocity is to be choosen ad hoc. 5) The envelope and the star rotate in the same direction. 6) The envelope crossection is wedge–shaped; beyond it the density is zero. 7) The star has finite dimenisons. 8) The ionization is calculated for the ground level and for 2s, 2p levels as well as for the principal qunatum numbers 3, 4 and 5. 9) The model has

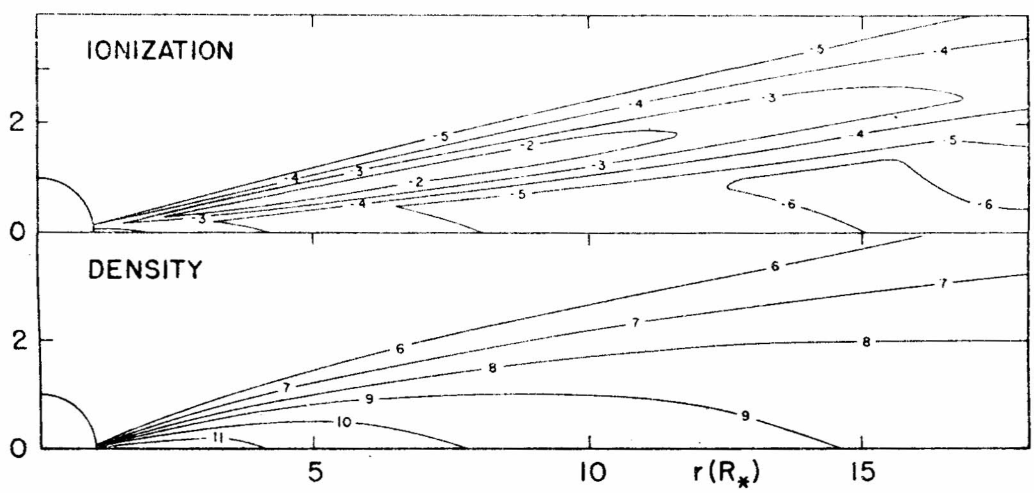

Fig. 23. Poeckert – Marlborough's envelope model: Density (log N) and ionization distribution (log N_H/N). (Poeckert, R.: 1982, Proc. IAU Symp. 98, Be Stars, eds. M.Jaschek, H.G.Groth, Reidel, Dordrecht, with permission)

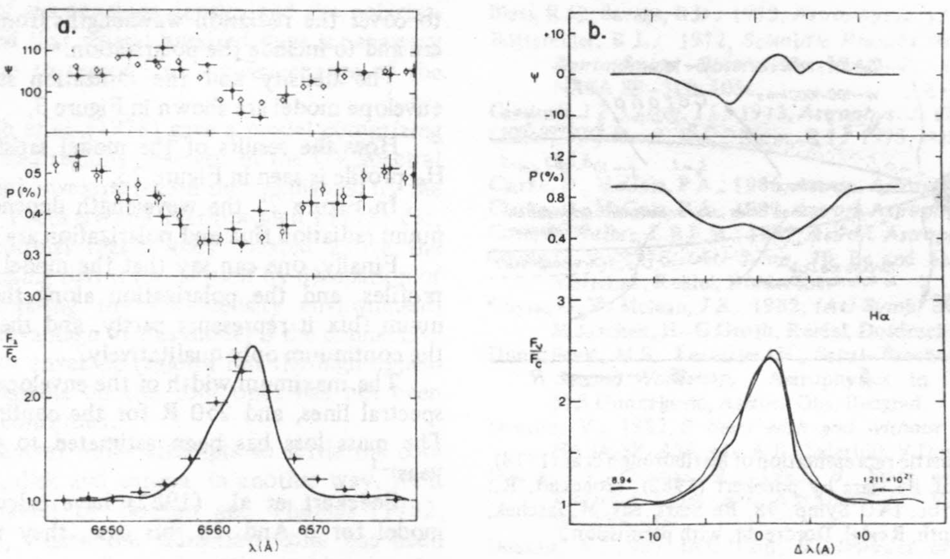

Fig. 24. Observed (a) and computed (b) H_α profile of γCas. Polarization position angle (above) and percentage (middle) and the radiation flux in the continuum flux units (bottom). (Poeckert, R.: 1982, Proc. IAU Symp. 98, Be Stars, eds. M Jaschek, H.G.Groth, Reidel, Dordrecht, with permission)

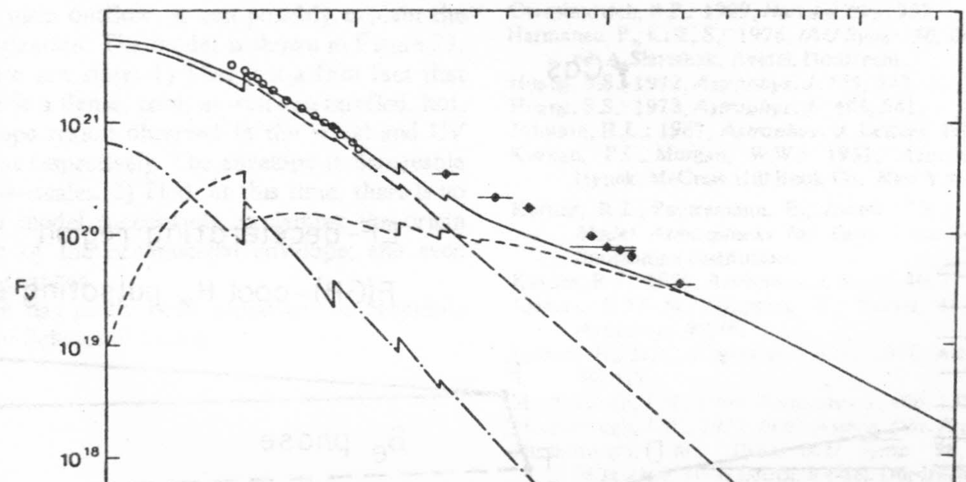

Fig. 25. The continuum polarization percentage (bottom) and energy distribution (above) for γCas. (Poeckert, R : 1982, Proc. IAU Symp. 98, Be Stars, eds. M Jaschek, H.G Groth, Reidel Dordrecht, with permission.)

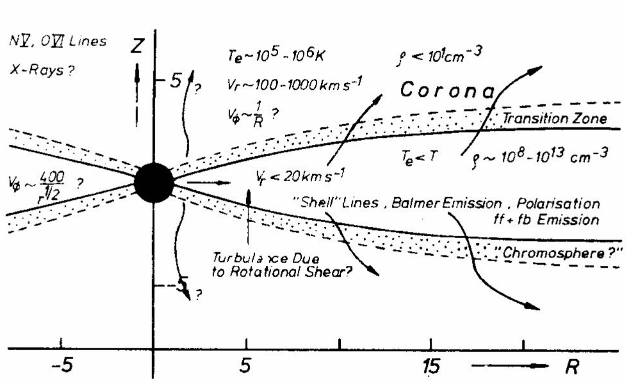

Fig. 26.The chematic representation of Marlborough et al.(1978) model of Be stars by poeckert (1982). (Poeckert, R.: 1982, Proc. IAU Symp. 98, Be Stars, eds. M. Jaschek, H.G. Groth, Reidel, Dordrecht, with permission.)

to cover the radiation wavelengths from 100 nm to 1 cm and to include the polarization.

The density and the ionization structure of thi envelope model are shown in Figure 3.

How the results of the model satisfy the observe H_α profile is seen in Figure 23.

In Figure 25 the wevelength dependence of conti nuum radiation flux and polarization are presented.

Finally, one can say that the model fits well the H_α profiles, and the polarization along them. The conti nuum flux it represents partly, and the polarization i the continuum only qualitatively.

The maximum width of the envelope is 50 R for th spectral lines, and 250 R for the continuum radiatior The mass loss has been estimated to 4.4 x 10^{-8} M year^{-1}.

Poeckert et al. (1982) have calculated a simila model for o And. In this case, they tried to fit th

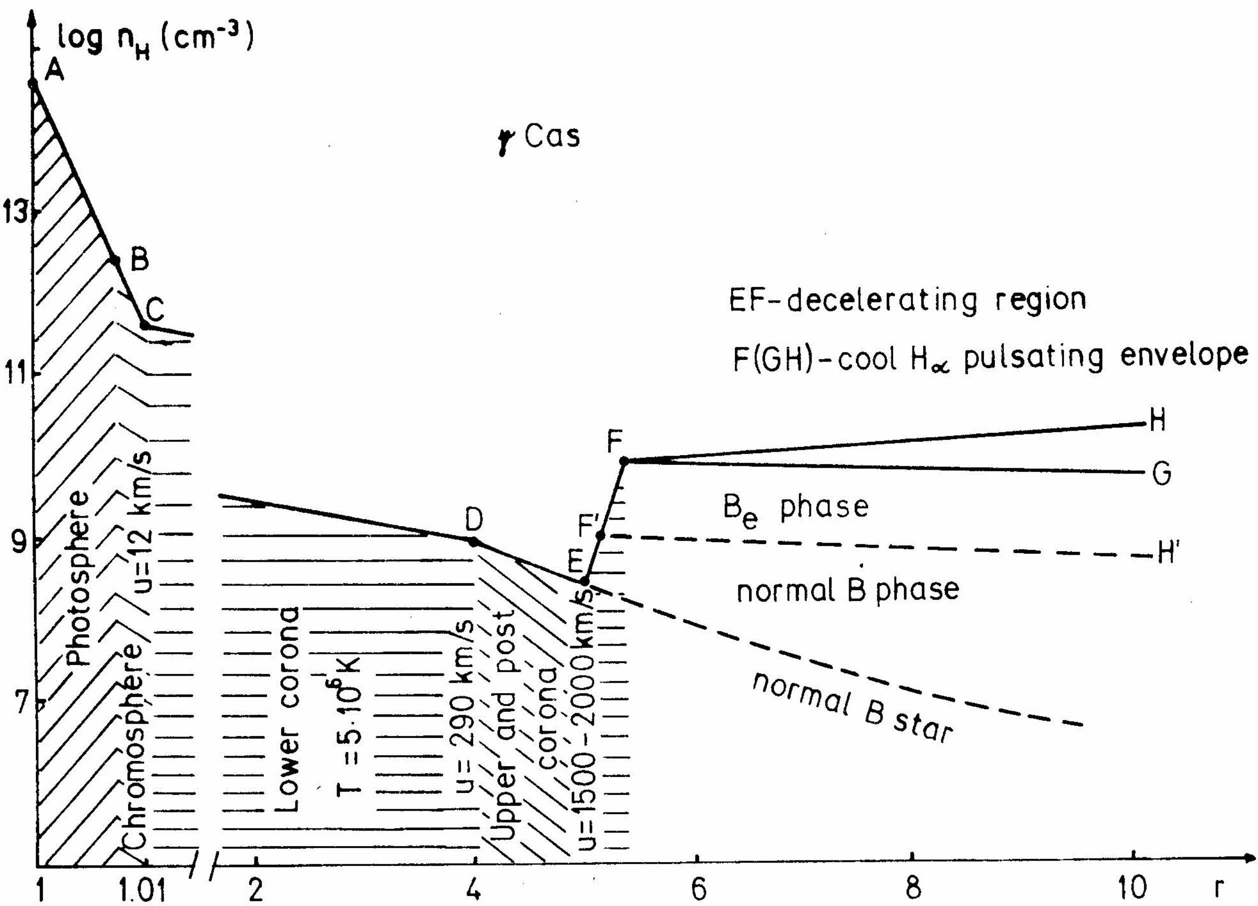

Fig. 27., Doazan (1987) schematic representation of a Be star atmosphere of γ Cas: hydrogen density versus stellar radii. Note the double scale along the abscissa. (Based on Doazan, 1987).

time–changes of the envelope density and the polarization. They found that several hundred days is necessary for the envelope to respond to a given change of the mass flux.

Marlborough et al. (1978) gave a model comprizing hot, highly ionized regions observed in the UV spectral domain. The cool envelope region they explained by the stellar wind, as Poeckert and Marlborough (1978) did, but the hot coronal region they located above the envelope disk taking that it forms itself by dissipation of shock–waves entering the low–density environment, Figure 26. An advantage of this model is the connection between the two envelope regions, but the high dependence of hot regions on the cool ones has not been observationally confirmed.

There are several other attempts to settle the cool and hot regions, disk and corona, in another way. We'll mention the model of Doazan and Thomas (1982, Doazan, 1987), where the transition zone has been placed just above the stellar surface (photosphere) and a hot stellar wind is assumed to flow from almost all stellar latitudes. At the astrocentric distances larger than 10 R, gas is being decelerated to form the cool envelope. If this model allows a non – uniform latitude dependence of the mass outflow, it can possibly explain the observed polarization. The model is shown in Figure 27.

Finally, we can state: 1) That it is a firm fact that Be stars do have a dense, cool, as well as a rarefied, hot, ionized envelope region observed in the visual and UV spectral regions respectively. The envelope is changeable in various time–scales. 2) That, at this time, there is no single Be star model successfully explaining the origin and evolution of the circumstellar envelope, and even less, its time–changes.

This work has partly been supported by Republic Association for Science of Serbia.

REFERENCES

Arsenijević, J., Vince, I., Kubičela, A.: 1979, *Publ.Obs. Astron.* Beograd, **26**, 125.

Arsenijević, J., Jankov, S., Đurašević, G., Vince, I.: 1986, *Bull. Obs. Astron.* Beograd, **136**, 6.

Arsenijević, J., Jankov, S., Vince, I., Đurašević, G.: 1987. *Bull. Obs. Astron.* Beograd, **137**, 49.

Baade, D.: 1984, *Astron.Astrophys.*, **134**, 105.

Baade, D.: 1986, IAU Coll. 92, *Physics of Be stars, eds. A Slettebak,* T.P. Snow, Cambridge Univ. Press, Cambridge.

Ballereau, D., Chanville, J.: 1987, *Astron. Astrophys. Suppl.* Ser., **70**, 229.

Barbier, D., Chalonge, D.: 1941, *Ann. Astrophys.* **4**.75.

Beeckmans, F.: 1977, *Bull. Soc. Roy. Sci. Liege,* **9–10**, 306.

Beeckmans, F.: 1978, Thesis Univ. Liege.

Bless, R.C., Savage, B.D.: 1972, *Astrophys.J.* **171**, 293.

Bottemiller, R.L.: 1972, *Scientific Rresults from the Orbiting Astronomical Observatory (OAO–2),* ed. A.D. Code, NASA SP–310, 505.

Cassineli, J.P. Castor, J.I.: 1973, *Astrophys. J.* **179**, 189.

Castor, J.I., Abott, D.C., Klein, R.I.: 1975, *Astrophys. J.* **195**, 157.

Clarke, D., McGale, P.A.: 1986, *Astron. Astrophys.* **169**, 251.

Clarke, D., McGale, P.A.: 1987, *Astron. Astrophys.* **178**, 294.

Cote, J., Waters, L.B.F.M.: 1987, *Astron. Astrophys.* **176**, 93

Coyne, G.V.: 1976, *IAU Symp.* **70**, Be and Shell Stars, ed. A. Slettebak, Reidel, Dordrecht.

Coyne, G.V., Mclean, J.S.: 1982, *IAU Symp.* **98**, Be Stars. Eds. M.Jaschek, H–G.Groth, Reidel, Dordrecht.

Dimitrijević, M.S. Feautrier, N., Sahal–Brechot, S.: 1987, *The Second Workshop,* Astrophysics in Yugoslavia, ed. M.S.Dimitrijević, Astron. Obs. Beograd.

Doazan, V.: 1982, *B Stars with and without Emission Lines* . NASA SP–456, eds. A.B.Underhill, V.Doazan, 279.

Doazan, V., Thomas, R.: 1982, *B. Stars with and wthout Emission Lines eds.* A.B.Underhill, V.Doazan, NASA SP–456, 409.

Doazan, V.: 1987 IAU Coll. 92, *Physics of Be stars,* eds. A.Slettebak, T.P.Snow, Cambridge Univ. Press, Cambridge.

Doazan, V., Rusconi, L., Sedmak, G., Thomas, R.N., Bourdonneau, B.: 1987, *Astron. Astrophys.* **182**, Letters L25.

Gehrc, R.D., Hackwell, J.A., Jones, T.W.: 1974, *Astrophys. J.*, **191** 675.

Gerasimovich, B.P.: 1929, *Harvard Circ.* 339.

Harmanec, P., Križ, S.: 1976, *IAU Symp. 70,* Be and Shell Stars, ed. A.Slettebak, Reidel, Dordrecht.

Huang, S.S.: 1972, *Astrophys. J.* **171**, 549.

Huang, S.S.: 1973, *Astrophys. J.* **183**, 541.

Johnson, H.L.: 1967, *Astrophys. J.* Letters, **150**, L39.

Keenan, P.C., Morgan, W.W.: 1951, *Astrophysics .ed.* J.A. Hynek, McGraw Hill Book Co. New York.

Kurucz, R.L., Peytremann, E., Avrett, E.H.: 1974, *Blanketed Model Atmospheres for Early Type Stars* Washington Smitsonian Institution.

Kurucz, R.J.: 1979, *Astrophys. J.* Suppl. **40**, 1.

Lamers, H.J.G.M., Faraggina, R., Burger, M.: 1980, *Astron. Astrophys.* **82**,48.

Lamers, H.J.G.M., Rogerson, J.B.Jr.: 1978, *Astron. Astrophys.* **66**. 417.

Marlborough, J.M., 1969, *Astrophys. J.* **156**, 135.

Marlborough, J.M.: 1977, *Publ. Astron. Obs. Pacific,* **89**, 122.

Marlborough, J.M.: 1982, *IAU Symp.* **98**, Be Stars, eds. M.Jaschek, H–G.Groth, Reidel, Dordrecht.

Marlborough, J.M., Snow, T.P., Slettebak, A.: 1978, *Astrophys. J.* **224** 157.

McLean, I.S.: 1979, *Mon. Not. R. Astr. Soc.* **186**, 265.

McLean, I.S., Coyne, G.V., Frecker, Jack E., Serkowski, K.: 1979, *Astrophys.J.* **228**, 802.

Merill, P.W., Sanford, R.F.: 1944, *Astrophys.J.* **100**, 14.

Peters, G.J.: 1976, *IAU Symp. 70,* Be and Shell Stars, ed. A. Slettebak, Reidel, Dordrecht, 209.

Peters, G.J.: 1982, *IAU Symp. 98,* The Be Stars, eds. M.Jaschek, H–G. Groth, Dordrecht, Reidel, 353.

Poeckert, R., Marlborough, J.M.: 1977, *Astrophys. J.* **218**, 220.

Poeckert, R., Marlborough, J.M.: 1978, *Astrophys.J.,* **220**, 940.

Poeckert, R., Bastein, P., Landstreet, J.D.: 1979, *Astron.J.* **84**, 812.

Poeckert, R., Gulliver, A.F., Marlborough, J.M.: 1982, *Publ. Astron.Soc.Pacific* **94** 87.

Rosner, R., Vaiana, G.S.: 1979, *Proc. Int. School of Astrophysics, eds.* G.Sette, R.Giacconi.

Scargle, J.D. Erickson, E.F., Wittebar, F.C., Strecker, D.W.: 1978, *Astrophys. J*, **224** 527.

Schild, R.E.: 1978, *Astrophys. J. Suppl*, **37**, 77.

Shklovsky, I.S.: 1967, *Astrophys.J.Letters*, **148**, L1.

Slettebak, A.: 1982, *Astrophys. J. Suppl, Ser.* **50**, 55.

Smith, A.M.: 1967, *Astrophys. J.*, **147**, 158.

Smith, M.A.: 1985, *Astrophys. J.*, **297**,206.

Snow, T.P.: 1981, *Astrophys. J.*, **251**, 139.

Snow, T.P., Marlborough, J.M.: 1976, *Astrophys. J. Letters*, **203**. 287.

Struve, O.: 1931, *Astrophys. J.* **73** 94.

Zorec, J., Briot, D., Divan, L.: 1982, *IAU Symp. 98*, Be Stars. eds. M.Jaschek, H–G.Groth, Reidel, Dordrecht, 419.

Bull. Obs. Astron. Belgrade, N° 138 (1988) UDC 550.38

ON THE NATURE OF BEHAVIOUR OF THE GEOMAGNETIC AND MAGNETOTELLURIC FIELDS IN TECTONICALY ACTIVE REGIONS

Y.T.Bicskei

Geomagnetic Institute, 11306 Grocka, Yugoslavia

(Received: 23 February, 1987)

SUMMARY: **The purpose of this article is to give a brief review on the features of experimentaly discovered changes in magnetic and telluric fields in tectonicaly active regions with summary of their most likely causes.**

1. INTRODUCTION

Few years ago, in order to explain the possible cause of astronomically observed relative motion of geographical coordinates of Belgrade with respect to Warsaw, a complex multidisciplinary investigation have been realized, including geomagnetic and magnetotelluric field observations, as well as a paleomagnetic investigations, too. The aforementioned investigations were performed in wider area of Belgrade. The investigated territory occupies more than 5000 km^2 in area and might be characterized by a relatively complex geologic and tectonic structure.

The paleomagnetic investigation of the rocks from this area have been performed in order to establish the feature and the distribution of tectonic movements in the studied region in the course of the geological era.

The geomagnetic and magnetotelluric surveys have been used to detect the anomalous geomagnetic field intensity and electrical resistivity variations assotiated with changes of tectonic stresses in the rocks of earth's crust.

2. SECULAR VARIATION ANOMALIES OF THE GEOMAGNETIC FIELD IN TECTONICALY ACTIVE REGIONS

In the frame of modern complex multidisciplinary researches which are in progress at geodynamical polygons by the study of contemporary geodynamic processes which can lead to neotectonic movements and seismic activities, geomatgnetic investigatiions and surveys have a significant role.

Namely, in tectonicaly active regions of world it has been observed and experimentally confirmed that geodynamical processes which take place in the eart's crust may cause a local geomagnetic secular variation anomalies probably related to a strain aliteration in the earth's crust (Shapire and Ivanov, 1973). An anomalous geomagnetic field variation may occur, also, in the vicinity of active faults as a consequence of stress induced changes in rock magnetization (piezomagnetic effect) (Johnston, 1978).

In recent years, it has been demonstrated that the geomagnetic field measurements can be used to study stress in rocks of upper crust. This is borne out by magnetic observations near and around epicentral areas in the vicinity of active faults (Skorovodkin et al. 1971, Johnston et al. 1976, Rikitake 1976, Smith and Johnston 1976, Rikitake 1976). Important in this investigation is the use of high–sensitivity absolute magnetometers, thus making possible the detection of tectonomagnetic variations with amplitudes of one to several nano Tesla's. The amplitude changes in local magnetic field is largely dependent on focal depth, as well as on the relative position of observation sites and the directions of the geomagnetic field and stress axes.

However, the current level of our knowledge does not permits us, to describe the exact analytical form of the dependence between observed surface magnetic field anomalies and relevant stress field changes in the rocks, a tectonomagnetic models have been developed (Stacey 1964) which will explain the observed geomagnetic data. Several mechanisms for the generation of anomalous geomagnetic variations are possible. As piezomagnetic and various other effects are fundamentally different in origine, the amplitudes, periods and characteristic size of the anomalles created by them, may also be different. Based on the experlences of investigations of local geomagnetic field changes at geodynamical polygons around the world as well as on results of our investigations in seismically active region of Kopaonik mountain, it can be stated, that, by their feature, the observed geomagnetic field variations in tectonicaly active regions may be divided and characterized with several types of variations. The revealed types of variations are:

- slow changes at separate sites (locations) which may be explained by compression or tension of individual earth's crustal blocks;
- a variety of field changes with amplitudes of a few nT and periods of 0,5 – 2 years;
- variations, which may be due to different conductivity of rocks,
- anomalous changes in the fracture zones.

Semétimes this anomalous changes are correlated with seismic activity.

3. ANOMALIES OF SECULAR VARIATION AND RECENT MOVEMENTS OF THE EARTH'S CRUST

It is of interest to look for relationship between secular variation anomalies and recent movements of the earth's crust. From the results of the performed investigations on the San Andreas fault zone in USA, and Tajikistan area at the junction of the Pamir and Tien–Shan mount a in structures (the Garm geodynamic polygon) in USSR, it is a known fact, that the active geodynamic processes, taking place in the earth's crust and upper mantle can lead to tectonical activities which are followed by vertical and horizontal crustal movements, as well as with anomalous geomagnetic field variations likely associated with stress distribution and it's changes in crustal rocks. From the experience it seems, that the appropriate geomagnetic field changes are well correlated with observed recent crustal movements and depend on the level of seismic activity (Sadovsky and Ersesov, 1978).

Analyzing the secular variation of geomagnetic field on the territory of GDR, Mundt' (1978) established, that the secular variation anomalies with amplitudes of about 3–4 nT/year are obviously partly located in regions with marked recent vertical and horizontal crustal movements.

These examples make it eveident that there is a correlative relationship between the recent movements of earth's crust and appropriate anomalous geomagnetic field changes.

4. CONCLUSIONS

In the light of treated topics, the following conclusions can be made:

- the geomagnetic measurements enable investigators to identify local changes in the magnetic field having a tectonic origin;
- highly accurate geomagnetic survey is one of the most sensitive methods for studying of modern geodynamic processes in the earth's crust;
- the recent crustal movements and anomalous geomagnetic field changes caused by tectonic activities, are connected with a correlative relationship.

The later statement suggest the idea, that the results of geomagnetic survey, can be used in the investigation of recent vertical and horizontal crustal movements for the network planing of measurements.

REFERENCES

Johnston M.J. S. et al.: 1976, *J. Geomag. Geoelectr.* **28**, 85.
Johnston M.J.S.: 1978, *J. Geomag. Geoelectr.* **30**, 511.
Mundt W.: 1978, *J.Geomag. Geoelectr.* **30**, 523.
Rikitake T.: 1976, in *Earthquake Prediction*, Elsevier, Amsterdam, p.197.
Rikitake T.: 1976, *J. Geomag. Geoelectr.* **28**, 145.
Sadovsky, Ersesov: 1978, *Fizika Zemli,* **8**, 13.
Shapiro , V.A. Ivanov N.A.: 1973, in *Recent Movements of the earth's Crust*, Academy of Science of Estonian S.S.R., Tartu, p. 173.
Skorovodkin Yu. P. et al. 1971, in *Experimental Seismology*, Nauka, Moscow, p. 398.
Smith B.E., Johnston M.J.S.: 1976, *J.Geophys.* **81**, 3556.
Stacey F.D.: 1964, *Pageoph,* **58**, 5.

Bull. Obs. Astron. Belgrade, N° 138(1988) UDC 524.383

MICROMETER MEASUREMENTS OF DOUBLE STARS (Series 41)

G.M. Popović

Astronomical Observatory, Volgina 7, 11050 Belgrade, Yugoslavia

(Received: October 15, 1987)

SUMMARY: 242 measurements of 85 systems (94 pairs), made with the 65/1055 cm refractor of Belgrade Observatory, are presented.

The observations of double stars contained in Table I form the 41th Belgrade series of measurements made with the 65/1055 cm refractor are a continuatinon of my measurements published as Series 39 (Popović G.M., 1986). The arrangement of the material in the Table I is selfexplanatory and the same as in the earlier series of measurements made by the author.

The residuals between observations and orbits have been calculated according to the ephemeris of P.Muller and P.Couteau (1979) and Yan Linshan, Chu Zongyuan and Pan Dasa (1986).

The distribution of the observed pairs by discover's name is following: Σ : 41, OΣ : 15, β : 11, A : 8, Hu : 5, Ho : 4, COU:3, AG, D, Es, h, Hn, J, Ku : 1.

Table 1

Identification:				Observation:					Analysis:
ADS	IDS m (IDS)	Disc.	Mult.	Epoch 1900+	P	ρ	m or Δm	Weight	O – C and notes
48	00002N4516	O Σ 547	AB	85.976	176.2	5.93	0.1	1+1	P.Muller, 1957: – 1°.04, – 0″.03
	9.4 – 9.4			85.978	174.1	5.79	0.1	1+1	
				85.977	175.2	5.86	0.1	2n	
61	00010N5753	Σ 3062		85.976	299.6	1.44	1.0	1+1	Baize, 1957: – 0°.1, – 0″.01
	6.4 – 7.5			86.731	300.2	1.43	7.2 – 8.2	2+2	
				86.479	300.0	1.43	1.0	2n	
-	01233N4249	COU 1359		83.745	319.1	1.15	10.0 – 10.0	1+2	
	–			85.757	319.0	0.89	9.5 – 9.6	3+2	
				85.002	319.0	0.99	9.6 – 9.7	2n	
1254	01308N0708	Σ 138	AB	84.930	53.9	1.55	0.1	1+2	
	7.7 – 7.7			85.768	55.3	1.58	0.1	2+2	
				85.924	55.1	1.57	0.1	2+2	
				86.048	54.4	1.61	0.0	1+1	
				85.666	54.8	1.57	0.1	4n	ΔP/(1985–1830)=+35°/155y
	6.9 – 15.1		AC	85.768	72	–	–	1+1	
1305	01342N3828	Σ 141		85.981	302.0	2.02	0.2	2+2	
	8.2 – 8.7			86.048	301.7	1.64	8.0 – 9.0	1+2	
				86.073	302.2	1.53	0.5	1+1	
				86.024	301.9	1.78	0.5	3n	
1709	02076N4701	Σ 228		85.973	273.7	1.07	0.8	2+1	
	6.4 – 7.3			86.073	270.2	1.00	0.7	1+1	
				86.013	272.3	1.04	0.8	2n	Heintz, 1952: +1°.7, – 0″.03
2416	03089N0022	Σ 367		83.879	146.6	0.98	0.0	1+2	Heintz, 1962: + 5°.0, – 0″.04
	8.9 – 8.9			85.728	142.6	1.14	0.1	1+2	Heintz, 1962: + 2°.0, + 0″.11

Table 1 (continued)

Identification:				Observation:					Analysis:
ADS	IDS m (IDS)	Disc.	Mult.	Epoch 1900+	P	ρ	m or Δm	Weight	O – C and notes
3390	04355N3719	Σ 577		83.794	19.2	0.97	0.0	3+3	Popović, 1965: + 0°.9, – 0".23
	8.6 – 8.6			85.973	16.0	0.99	–	2+2	– 0.5, – 0.20
				86.073	12.2	0.83	0.0	1+1	– 4.3, – 0.36
									Hock, 1966: + 0.4, – 0.13
									– 0.9, – 0.10
									– 4.6, – 0.26
3837	05098N1937	Σ 665		86.057	255.3	1.54	1.0	1+1	
	8.5 – 9.4			86.063	252.6	1.51	0.5	1+1	
				86.060	254.0	1.52	0.8	2n	
4200	05304N2156	Σ 742		86.057	272.7	3.75	0.6	1+1	ΔP/(1986–1837)=+21°/149 y
	7.2 – 7.8			86.063	272.3	3.86	0.2	1+2	Δρ/(1986–1837)=+0".5/149 y
				86.061	272.5	3.82	0.4	2n	
7067	08460N7071	Σ 1280	AB	85.258	138.1	1.01	0.1	1+1	Heintz, 1973: – 1°.7, – 0".11
	9.3 – 9.4								
				86.238	142.0	1.06	0.2	1+2	
				86.303	142.0	0.97	9.0 – 9.2	1+2	
				86.270	142.0	1.02	0.2	2n	Heintz, 1973: – 2°.6, – 0".08
7307	09147N3837	Σ 1338	AB	86.312	261.8	0.99	–0.1	1+1	
	6.6 – 6.8			86.317	262.8	0.99	0.0	1+1	
				86.315	262.3	0.99	–0.1	2n	Starikova, 1966: –9°.9, + 0".22
									Arend, 1953: –2.2, – 0.07
			AC	86.312	347	10±		1+1	
7477	09352N3884	Σ 1374		86.311	304.2	2.90	1.2	1+1	ΔP/(1986–1838)=+30°/148y
	7.3 – 8.6			86.312	304.8	3.02	1.0	2+1	Δρ/(1986–1838)=–0".4/148 y
				86.317	303.5	2.74	1.2	1+2	
				86.314	304.2	2.88	1.1	3n	
7536	09440N6065	Σ 1381		86.306	193.7	0.83	–	1+1	ΔP/(1986–1832)=–22°/154 y
	9.2 – 9.4			86.309	195.8	0.89	0.1	3+2	Δρ/(1986–1832)=–0".6/154 y
				86.308	195.2	0.87	0.1	2n	
7685	10075N2755	0 Σ 213		86.306	126.8	0.65	1.5	1+1	
	8.4 – 10.4			86.309	128.4	0.83	1.5	2+2	
				86.308	127.9	0.77	1.5	2n	Heintz, 1962: +2°.9, – 0".11
7704	10108N1774	0 Σ 215		86.238	182.8	1.30	0.3	1+1	
	7.3 – 7.5			86.246	182.0	1.43	0.2	1+1	
				86.303	182.6	1.36	0.2	1+2	
				86.268	182.5	1.36	0.2	3n	Wierzbinski, 1953: +0°.4, – 0".[illegible]
									Zaera, 1957: + 3.1, – 0.[illegible]
7745	10171N4873	Es 917		86.306	147.1	2.03	–	1+1	
	10.3 – 10.6			86.309	147.6	1.98	0.7	2+2	
				86.308	147.4	2.00	0.7	2n	
8100	11088N7361	0 Σ 539	AC	84.303	325.2	–	–	1+1	
	7.5 – 11.0			85.362	318.8	6.35	–	2+2	
				85.365	319.8	5.37	–	1+1	
				85.098	320.6	6.02	–	3/2n	Probably optical!
8128	11138N1449	Σ 1527		85.259	39.8	1.08	0.7	1+1	
	6.9 – 8.1			85.362	41.4	1.11	7.5 – 8.5	2+2	
				85.365	42.0	1.16	8.0 – 9.0	2+2	
				85.343	41.3	1.12	0.9	3n	Hopmann, 1958: +8°.4, – 0".24

Table 1 (continued)

ADS	IDS m (IDS)	Disc.	Mult.	Epoch 1900+	P	ρ	m or Δm	Weight	O – C and notes
	Identification:			Observation:					Analysis:
8148	11187N1065	Σ 1536		85.259	135.7	1.04	3.0	1+1	
	4.1 – 7.3			85.363	130.3	1.22	–	1+1	
				85.428	133.6	1.18	–	1+1	
				85.350	133.2	1.15	3.0	3n	Baize, 1951: – 8°.2, – 0″.16
8242	11319N4761	Ku 39		85.448	90.2	1.74	9.5 – 9.8	1+1	
	11.1 – 11.4			86.208	88.1	1.49	–	1+2	
				85.904	88.9	1.59	9.5 – 9.8	2N	Zulević, 1986: –0°.5, –0″.15
8355	11511N3560	0 Σ 241	AB	86.317	143.6	1.51	2.5	1+1	ΔP/(1986–1849)=+24°/137 y
	6.8 – 8.7			86.380	138.1	1.52	2.0	1+1	
				86.348	140.8	1.52	2.2	2n	
8539	12194N2568	Σ 1639	AB	85.409	327.4	1.48	0.7	1+1	
	6.6–7.8			85.428	326.4	1.48	7.5–8.5	1+2	
				85.420	326.8	1.48	0.8	2n	Aller, 1947: + 2°.2, – 0″.06
8553	12222N2735	Σ 1643		86.303	12.9	2.41	0.1	1+2	
	9.2–9.5			86.306	11.7	2.50	0.2	1+1	
				86.309	12.9	2.57	0.2	2+2	
				86.306	12.6	2.50	0.2	3n	Optical.
8887	13189N2945	Ho 260		86.303	72.5	1.07	0.5	1+1	
	9.6–9.8			86.309	72.3	1.09	0.3	1+2	
				86.312	72.4	1.22	0.3	2+2	
				86.457	70.4	1.17	–	1+1	
				96.336	72.0	1.15	0.4	4n	Ambruster, 1978: – 3°.9, + 0″.02.
9000	13380N0363	Σ1777		86.465	229.5	2.63	2.5	1+1	
	5.7–8.1			86.468	231.5	2.77	2.0	1+1	
				86.470	229.7	2.79	7.0–9.0	2+1	
				86.468	230.2	2.74	2.1	3n	
9063	13519N3467	β 936		85.428	93.4	3.95	9.0–11.5	1+1	
	9.6–13.4			85.431	94.8	3.78	9.0–12.0	1+1	
				85.447	94.3	3.58	9.5–13.0	2+2	
				85.438	94.2	3.72	9.2–12.4	3n	
9067	13527N3455	β 937		85.428	130.4	0.89	0.2	1+1	
	9.2–9.4			85.431	128.8	1.05	0.1	1+1	
				85.447	130.3	0.99	0.2	1+2	
				85.437	129.9	0.98	0.2	3n	ΔP/(1985–1880) = +25°/105 y
9071	13539N5229	A 1614		85.483	311.2	1.26	–	1+1	
	9.4–9.5			86.386	314.1	1.25	0.1	1+1	
				86.468	311.4	1.18	0.1	1+1	
				86.112	312.2	1.23	0.1	3n	Mourao, 1970: –1°.2, 0″.11
9174	14095N2934	Σ 1816		86.312	84.1	0.69	0.1	2+1	ΔP/(1986–1831) = + 6°/155 y
	7.5–7.6			86.462	87.4	0.71	0.3	1+1	Δρ/(1986–1831) = –1″.2/155 y
				86.479	88.1	0.75	0.3	1+1	
				86.402	86.2	0.71	0.2	3n	
9167	14097N5548	Σ 1820		86.459	111.9	2.45	0.1	3+3	
	8.8–9.1			86.473	111.9	2.36	0.3	1+1	
				86.462	111.9	2.43	0.2	2n	Hopmann, 1954: –1°.7, + 0″.16

Table 1 (continued)

Identification:				Observation:					Analysis:
ADS	IDS m (IDS)	Disc.	Mult.	Epoch 1900+	P	ρ	m or Δm	Weight	O – C and notes
9418	14478N4480	0 Σ 287		84.467	348.3	0.98	0.2	2+1	
	8.5–8.6			85.365	348.9	0.91	0.2	2+2	
				85.409	347.1	0.93	0.1	1+1	
				86.479	351.0	0.90	0.3	1+1	
				85.331	348.8	0.93	0.2	4n	Heintz, 1959: + 1°.6, – 0".15
9578	15140N2672	Σ 1932	AB	85.448	252.7	1.29	0.1	1+1	
	7.1–7.6			86.386	253.0	1.39	–0.2	1+2	
				86.408	252.4	1.52	0.0	1+2	
				86.468	252.6	1.42	0.0	1+1	
				86.479	253.0	1.35	0.0	1+1	
				86.264	252.7	1.40	0.0	5n	Heintz, 1964: –0°.8, – 0".07
9595	15161N1545	Hu 1160		85.366	255.6	0.59	2.5	3+1	
	8.8–11.4			85.429	256.1	0.58	2.0	2+1	
				85.393	256.2	0.59	2.3	2n	Popović, 1986: – 2°.9, – 0".17
9600	15165N2126	Hu 146		85.521	125.9	0.68	0.2	3+1	
	9.3–9.6			86.386	126.4	0.62	0.3	1+1	
				85.809	125.9	0.66	0.2	2n	ΔP/(1985–1900) = –46°/85 y
9626	15207N3742	Σ 1938	BC	85.409	15.1	2.37	0.5	1+1	
	7.2–7.8			85.483	13.1	2.15	0.8	1+2	
				85.519	14.9	2.04	0.3	1+1	
				85.521	15.8	2.09	0.8	1+2	
				85.487	14.7	2.15	0.5	4n	Baize, 1951: + 0°.5, – 0".05
9641	15228N2376	A 82		85.366	345.8	0.66	10.0–11.0	2+2	
	10.0–11.0			86.470	347.4	0.66	10.0–11.0	1+1	
				85.734	346.3	0.66	10.0–11.0	2n	ΔP/(1985–1900) = +24°/85 y
9639	15230N4421	0 Σ 296	AB	85.366	280.1	1.87	8.0–9.5	2+2	
	7.6–9.2			85.432	281.9	1.85	8.0–9.0	1+1	
				85.521	279.5	2.00	8.0–9.5	1+1	
				85.421	280.4	1.90	8.0–9.4	3n	
				86.457	280.5	1.86	8.0–9.2	2+2	
				86.460	279.8	1.77	8.0–10.0	2+2	
				86.462	281.1	1.77	1.5	1+1	
				86.459	280.3	1.81	1.6	3n	
		0 Σ 296	AC	86.460	313.6	77.0	8.0–11.0	2+2	
	7.4–12.5			86.462	314.8	–	–	1+1	
				86.461	314.0	77.0	8.0–11.0	2/1n	
9952	16069N1523	A 1799		85.519	113.4	0.65	9.3–9.2	1+1	
	9.2–9.3			86.465	114.4	0.58	–0.1	1+2	
				86.087	113.8	0.61	–0.1	2n	ΔP/(1986–1908) = –57°/78 y
9982	16111N0737	Σ 2026		85.431	22.8	2.88	0.5	1+1	
	9.1–9.6			85.519	23.6	2.85	0.3	2+1	
				85.521	24.0	2.85	9.0–9.3	3+2	
				85.502	23.6	2.86	0.3	3n	Heintz, 1962: +1°.2 – 0".06
10075	16245N1837	Σ 2052	AB	85.483	132.2	1.62	0.1	1+1	
	7.8–7.8			86.471	131.1	1.59	8.0–8.5	2+2	
				86.142	131.5	1.60	0.4	2n	Siegrist, 1950: + 0°.8, + 0".01
10087	16259N0172	Σ 2055		85.486	17.8	1.18	–	1+1	
	3.9,-6.0			86.465	18.4	1.24	1.0	1+1	
				85.976	18.1	1.21	1.0	2n	Baize, 1973: 0°.0, – 0".17

Table 1 (continued)

Identification:				Observation:					Analysis:
ADS	IDS m (IDS)	Disc.	Mult.	Epoch 1900+	P	ρ	m or Δm	Weight	O – C and notes
10188	16408N4340	D 15		85.486	137.0	0.95	0.0	3+3	
	9.1–9.1			86.460	136.0	0.95	8.0–8.0	2+2	
				86.465	137.0	1.04	9.1–9.0	3+3	
				86.097	136.8	0.98	0.0	3n	Wierzbinski, 1955: + 0°3, – 0″07
10235	16479N2850	Σ*2107	AB	85.448	88.8	1.26	8.0–9.0	1+1	
	6.7–8.2			86.460	88.1	1.24	1.5	1+1	
				86.613	89.3	1.36	1.0	1+1	
				86.174	88.9	1.29	1.2	3n	Rabe, 1926: – 2°3, – 0″10
10341	17015N0047	β 823	AB	85.429	131.5	0.80	8.5–9.0	1+1	
	8.7–9.7			85.448	132.1	0.79	0.5	1+1	
				85.527	133.3	0.89	0.5	1+1	
				85.468	132.3	0.83	0.5	3n	Arend, 1955: + 8°4, – 0″23
10429	17114S00 20	A 2984		85.522	359.7	1.13	–	1+1	PAa ~ 0°
	4.9 – 7.9			86.711	360.6	0.97	3.0	3+2	
				86.371	360.3	1.02	3.0	2n	ΔP/(1986–1915) = +62°/71 y. Δρ/(1986–1915) = +0″5/71 y.
10456	17142N3235	β 45		85.527	289.8	4.51	0.2	1+1	
	9.8–10.4			86.632	290.8	4.69	0.3	1+2	
				86.635	290.7	4.46	0.3	1+1	
				86.728	289.8	4.36	9.5–9.7	2+2	
				86.467	290.2	4.50	0.2	4n	
10459	17146N3246	β 628		85.522	278.9	0.42	0.5	2+2	Zulević, 1986: – 2°0, – 0″04
	9.4–9.9								
10722	17381N4142	Σ 2203		85.366	297.2	0.71	0.3	2+2	
	7.6–7.9			85.519	298.2	0.65	0.2	2+2	
				85.639	297.6	0.79	0.2	1+2	
				85.642	298.1	0.78	0.1	1+2	
				85.527	297.8	0.72	0.2	4n	ΔP/(1985–1830) = – 36°/155 y
10743	17394N2239	Hu 1285		85.366	219.8	0.57	9.0–9.0	3+2	
	9.0–9.0			85.519	224.2	0.59	0.0	2+1	
				85.522	223.2	0.53	0.1	2+2	
				85.642	217.4	0.61	0.3	1+1	
				85.483	221.4	0.57	0.1	4n	ΔP/(1985–1905) = – 30°/80 y
10796	17426N1504	Hu 1288		85.519	152.9	0.47	0.5	2+1	ΔP/(1985–1905) = +37°/80 y.
	8.7 – 9.2								
11010	17596N4414	β1127		85.486	73.9	0.86	2.0	1+1	
	7.4–9.3			85.519	78.1	0.84	1.5	1+1	
				85.502	76.0	0.85	1.8	2n	Popović, 1970: –1°0, – 0″24
11291	18176N1410	AG 222		85.675	141.8	1.57	0.1	1+1	
	9.3–9.5			85.677	143.3	1.55	0.2	1+1	
				85.680	144.3	1.56	0.2	2+2	
				85.694	142.6	1.51	0.2	1+1	
				85.696	146.0	1.35	0.1	1+1	
				86.613	152.6	1.39	0.2	1+1	
				85.816	145.0	1.50	0.2	6n	
11292	18176N1123	Σ 2311	AB	85.677	113.0	2.74	0.7	1+2	
	9.8–10.8			85.680	111.4	2.81	9.0–10.0	2+2	
				85.694	112.0	2.91	1.0	1+1	
				85.696	113.7	2.97	9.0–10.0	2+1	
				85.686	112.5	2.85	1.0	4n	Optical. μ = 0″135/y in 9° according A.

Table 1 (continued)

Identification:				Observation:					Analysis:
ADS	IDS m (IDS)	Disc.	Mult.	Epoch 1900+	P	ρ	m or Δm	Weight	O – C and notes
11483	18314N1654	0 Σ 358	AB	85.716	162.7	1.61	0.2	2+2	
	6.8–7.2			86.460	162.3	1.61	8.0–8.2	2+2	
				86.471	162.6	1.78	–0.1	1+1	
				86.613	162.1	1.64	0.0	1+1	
				86.239	162.4	1.64	0.1	4n	Starikova, 1966: +5°.1, + 0″.16 Hopmann, 1970: +3.8, + 0.13
11811	18505N3715	β 137	AB	85.366	157.7	1.56	0.2	2+1	
	8.2–8.7			85.519	155.4	1.42	0.7	2+2	
				85.642	155.8	1.53	0.3	2+2	
				85.702	155.9	1.52	0.2	1+1	
				85.550	156.1	1.50	0.4	4n	ΔP/(1985–1875) = +32°/110 y.
–	18546N4315	COU 1794		80.681	33.6	1.76	10.5–10.7	1+2	
	–			80.711	33.8	1.86	0.0	1+1	
				80.693	33.7	1.80	0.1	2n	
12447	19225N2707	Σ 2525		85.749	291.9	1.73	–	1+1	
	8.5–8.7			85.751	291.8	1.89	0.2	1+1	
				85.750	291.8	1.81	0.2	2n	Job Tamburini, 1967: –0°.5, –0″.09
13082	19494N1502	Σ 2596		85.751	304.1	1.96	8.0–9.5	1+1	
	7.3–8.7			86.725	306.1	1.86	8.0–9.0	1+1	
				86.238	305.1	1.91	8.0–9.2	2n	ΔP/(1986–1831) = – 48°/155 y.
13196	19547N3300	Σ 2606		85.645	140.3	0.83	0.7	1+1	
	7.6–8.3			85.702	141.1	0.84	0.5	1+1	
				85.705	141.4	0.77	0.5	1+2	
				85.687	141.0	0.81	0.6	3n	ΔP/(1985–1832) = +10°/153 y
13198	19550N3750	Σ 2609		85.645	24.4	2.00	7.0–8.0	1+2	
	6.6–7.7			85.669	24.9	1.89	7.0–8.2	2+2	
				85.672	24.4	1.92	1.0	1+1	
				85.675	24.6	1.88	0.8	1+2	
				85.665	24.6	1.92	1.0	4n	
13542	20092N1551	Σ 2651		85.645	279.1	1.10	0.0	1+2	
	8.5–8.5			85.669	279.9	1.07	0.1	3+2	
				85.677	278.5	1.14	0.0	1+1	
				85.680	278.6	1.02	0.1	1+1	
				85.694	277.4	1.06	0.0	1+1	
				85.670	279.0	1.08	0.1	5n	Orbital motion; i ~90°
13543	20094N2356	Σ 2653		85.645	271.3	2.48	7.0–10.0	1+1	
	6.6–9.7			85.669	272.6	2.54	7.0–10.0	2+2	
				85.678	273.0	2.38	7.0–10.0	1+1	
				85.680	273.3	2.55	7.0–10.0	1+1	
				86.730	273.0	2.63	3.0	2+2	
				85.972	272.7	2.54	3.0	5n	ΔP/(1986–1831) = +17°/155 y.
13723	20166N4503	Σ 406		85.770	117.7	0.55	8.0–8.7	2+2	
	7.4–8.3			86.730	116.2	0.57	0.7	3+2	
				86.303	116.9	0.56	0.7	2n	Heintz, 1975: + 2°.1, – 0″.02
13986	20282N1336	β 670	AB	85.522	13.9	0.81	0.3	2+1	
	8.9–9.2			85.702	13.7	0.73	0.2	1+1	
				85.732	15.7	0.87	0.5	1+1	
				85.633	14.4	0.80	0.3	3n	ΔP/(1985–1877) = –44°/108 y

Table 1 (continued)

Identification:				Observation:					Analysis:
ADS	IDS m (IDS)	Disc.	Mult.	Epoch 1900+	P	ρ	m or Δm	Weight	O – C and notes
14558	20580N3852	Σ 2746		86.706	314.9	1.20	8.5–9.0	1+1	
	8.0–8.6			86.714	316.2	1.22	0.7	1+1	
				86.710	315.6	1.21	0.6	2n	ΔP/(1986–1830) = +40°/156 y. Δρ/(1986–1830) = +0″.3/156 y.
14573	20580N0108	Σ 2744	AB	85.768	125.3	1.35	7.0–7.5	3+3	
	7.0–7.5			85.817	124.4	1.26	0.7	2+2	
				85.788	124.9	1.31	0.6	2n	Popović, 1962: +2°.9, +0″.05
14784	21114N5753	Σ 2783		85.754	6.9	0.82	–0.1	2+2	
	7.8–7.8			85.770	5.5	0.75	0.1	2+2	
				85.762	6.2	0.78	0.0	2n	ΔP/(1985–1831) = – 37°/154 y Δρ/(1985–1831) = – 0″.5/154 y
14889	21166N3202	0 Σ 437		85.716	25.7	2.16	0.2	1+3	
	6.9–7.6			85.732	24.8	2.33	0.2	1+2	
				85.751	25.1	2.42	0.5	1+1	
				85.768	25.1	2.19	0.3	2+2	
				85.741	25.2	2.25	0.3	4n	ΔP/(1985–1945) = – 42°/140 y Δρ/(1985–1845) = + 0″.9/140 y
14926	21194N5708	A 764	AB	85.519	3.2	0.86	2.0	2+2	
	8.4 –9.6			85.670	5.5	0.85	8.0–10.0	2+2	
				85.594	4.4	0.86	2.0	2n	Heintz, 1961: – 1°.8, + 0″.15
			AB–C	85.670	192	100 ±	m_C = 8.5	2+1	
15007	21240N1039	Σ 2799	AB	85.642	266.9	1.71	0.0	1+2	
	7.5–7.5			85.645	267.5	1.83	0.0	1+1	
				85.670	267.8	1.72	0.1	2+2	
				85.680	267.2	1.65	0.0	1+1	
				85.660	267.4	1.72	0.0	4n	Popović, 1986: + 0°.8, + 0″.03
15008	21243N1840	J 579		85.645	182.9	3.52	0.3	1+2	
	9.4–9.5			85.670	184.1	3.47	10.0–10.5	1+2	
				85.658	183.5	3.50	0.4	2n	ΔP/(1985–1911) = + 5°/74 y.
-	22058N4224	COU 1828		84.788	276.3	0.70	0.1	2+2	COU 1828 = BD + 42°4310 (9ᵐ.3)
15962	22232N1144	β 701	AB	85.754	206.8	0.78	–	1+1	
	7.3–10.3			86.709	211.8	0.82	2.5	1+1	
				86.728	204.4	0.77	3.0	2+1	
				86.444	207.2	0.79	2.8	3n	
			AB–C	85.754	132.5	–	–	1+1	
16037	22280N2554	Ho 475	AB	85.732	310.1	0.98	0.3	1+1	
	9.3–9.5			85.752	309.3	0.94	0.5	1+1	
				85.742	309.7	0.96	0.4	2n	ΔP/(1985–1893) = – 15°/92 y
	8.7–10.9	Ho 475	AC	85.732	226.2	8.16	–	1+1	
16317	22474N6109	Σ 2950	AB	85.732	288.7	1.59	1.0	1+2	
	6.1–7.4			85.752	286.3	1.41	1.0	1+2	
				85.742	287.5	1.50	1.0	2n	ΔP/(1985–1832) = – 31°/153 y Δρ/(1985–1832) = – 0″.5/153 y
	5.8–10.7		AC	75.732	355.1	–	–	1+1	

Table 1 (continued)

Identification:				Observation:					Analysis:
ADS	IDS m (IDS)	Disc.	Mult.	Epoch 1900+	P	ρ	m or Δm	Weight	O – C and notes
16326	22480N5712	A 632	AB	85.770	168.1	0.94	1.0	3+2	
	8.2–9.0			86.709	162.7	0.95	8.0–8.4	2+2	
				86.714	168.3	0.82	8.2–9.0	1+1	
				86.283	166.2	0.92	0.8	3n	Heintz, 1961: + 3°.2, + 0".20
16373	22508N1515	Hu 987		85.754	86.0	0.81	0.3	3+2	
	9.1–9.3			85.757	85.1	0.79	8.7–8.9	1+1	
				85.754	85.7	0.80	0.3	2n	Heintz, 1965: + 3°.4, + 0".13
16561	23055N3156	β 385	AB	85.754	88.8	0.65	0.3	2+1	
	7.3–8.1			85.757	92.2	0.68	0.3	2+1	
				85.756	90.5	0.66	0.3	2n	ΔP/(1985–1876) = – 45°/109 y
	–9.0	h 5532	AB–C	85.754	77.1	–	–	2+1	
16877	23326N4353	0 Σ 500	AB	83.895	358.7	0.54	7.0–8.5	2+2	Zulević, 1981: – 1°.2, + 0".03
	6.3–7.2								
16951	23380N1117	A 1242		85.770	328.6	0.97	0.6	3+2	
	9.6–9.6			86.712	325.1	0.87	0.2	2+2	
				86.189	327.0	0.93	0.4	2n	Zulević, 1977: – 1°.7, +0".18
17020	23438N6420	0 Σ 507AB		85.770	309.3	0.79	8.0–9.0	2+2	
	6.9–7.6			86.728	308.5	0.78	0.4	1+1	
				86.089	309.0	0.79	0.8	2n	Zulević, 1977: +2°.7, +0".05
	6.4–8.6		AC	85.770	350.2	–	–	2+2	
17037	23455N4252	0 Σ 509		80.793	103.7	5.09	8.5–10.0	1+2	
	7.8–9.7			80.810	104.8	5.24	8.0–10.0	2+2	
				80.889	104.6	5.20	8.5–10.0	2+2	
				80.834	104.4	5.18	8.5–10.0	3n	
17178	23563N3905	Hn 60		85.754	178.9	1.12	9.0–9.4	2+2	
	9.2–9.6			85.757	178.1	1.04	8.0–8.7	2+2	
				85.756	178.5	1.08	8.5–9.0	2n	Heintz, 1961: – 1°.3, – 0".01
17179	23572N3225	Ho 209	AB	83.891	351.9	1.08	2.0	2+2	
	8.9–11.4			86.731	353.0	1.31	8.5–10.5	3+2	
				85.464	352.5	1.21	2.0	2n	

ACKNOWLEDGEMENTS

This work has been supported by Republic Association for Science in Serbia through the project „Physics and Motions of Celestial Bodies and Artificial Satelites".

REFERENCES:

Popović, G.M.: 1968, *Bull. Obs. Astron. Belgrade,* No. 136.

Muller P., Couteau, P.: 1979, *Quatrieme catalogue d'ephemerides d'etoiles doubles,* Pub. Obs. Paris, CERGA, Observatoire de Nice.

Yan Linshan, Chu Zongyuan, Pan Dasa: 1986, *General Catalogue of Ephemerides and Apparent Orbits of 736 Visual Binary Stars.*

Bul. Obs. Astron. Belgrade, N° 138 (1988) UDC 524.383

MICROMETER MEASUREMENTS OF DOUBLE STARS
(Series 42)

D.J. Zulević

Astronomical Observatory, Volgina 7, 11050 Belgrade, Yugoslavia

(Received: November 11, 1987.)

SUMMARY: Presented here are 420 measurements of 154 double stars made with 65/1055 cm refractor of Belgrade Observatory

The present series of measurements is the continuation of my own measurements published under Series 40 (D. Zulević 1986). The measurements were made with the 65/1055 cm refractor of the Belgrade Observatory between 1985 May 5 and 1986 September 25. In Table I the columns give ADS or DM number, double star designation, position angle, separation, estimated magnitudes, weight and number of nights and motes. Under Notes comparisons are presented with the most recent available orbits (Muller, P., Couteau, P. 1979). In the present work the distribution of 420 measurements over distance is as follows:

Distance	Measurements
0.00 to 0.50	28
0.50 ,to 1.00	154
1.00 to 1.50	123
1.50 to 2.00	56
2.01 or greater	59
	420

Table I Micrometer Measurements of Double Stars

ADS	Disc. IDS	Mult.	Epoch 1900+	P	ρ	Est. Mag.	Weight	Notes
48	STF 547		85.976	175°.9	5″.95	8.3–8.3	1+1	
	00002N4516		85.979	176.0	5.92		1+1	Güntzel–Lingner, 1954: –0°.2, –0″.02
			85.978	176.0	5.93		2n	Hopmann, 1961: –1°.1, +0″.03
61	STF 3062		85.976	300.0	1.35	6.9–8.0	1+1	
	00010N5753		86.731	302.5	1.38		3+2	
			86.515	301.8	1.37		2n	Baize, 1957: +0°.2, –0″.08
283	HJ 1018		85.765	87.8	1.45	8.6–9.2	1+1	
	00154N6707		85.768	88.6	1.46		2+2	
			85.767	88.3	1.46		2n	Muller, 1956: +2°.0, –0″.05
588	STT 18		85.973	198.6	1.51	7.7–9.8	2+2	
	00372N0337		85.976	200.9	–		1+1	Baize, 1956: –5°.6, +0″.00
			85.974	199.4	1.51		2n	Sokolova, 1960: –9°.0, +0″.25
862	STT 21		85.973	176.5	0.89	6.7–8.0	2+2	
	00573N4650		86.731	174.7	0.92	6.9–8.0	2+2	
			86.352	175.6	0.91		2n	Heintz, 1964: +0°.4, –0″.02
999	BU 1100		85.760	203.9	0.57	8.3–8.3	1+1	Muller, 1954: +0°.6, +0″.06
	01085N6025		86.731	203.1	0.53		2+2	Eggen, 1961: –10°.8, –0″.01
			86.407	203.3	0.54		2n	Zulević, 1972: –1°.1, –0″.04
–	COU 1359		85.757	326.5	0.94	9.7–9.7	2+2	
	01233N4249							
1254	STF 138	AB	85.768	234.8	1.52	7.7–7.7	2+2	
	01308N0708		85.924	235.2	1.52		2+2	
			86.048	234.1	1.67		1+1	
			85.886	234.8	1.55		3n	

Table 1 (continued)

ADS	Disc. IDS	Mult.	Epoch 1900+	P	ρ	Est. Mag.	Weight	Notes
1305	STF 141		85.981	305.°5	1.″55	8.0–8.5	2+2	
	01342N3828		86.048	303.0	1.58		1+1	
			86.073	306.1	1.49		1+1	
			86.021	305.0	1.54		3n	
1310	BU 1167		85.981	53.5	1.30	Δm = 1.0	1+1	
	01344N3813		86.731	55.2	1.37		3+3	
			86.543	54.8	1.35		2n	
1538	STF 186		85.973	55.6	1.16	6.8–6.8	2+2	
	01507N0121		86.731	55.8	1.17		3+3	Palacios, 1947: +0.°4, + 0.″07
			86.428	55.7	1.17		2n	Fretas–Mourao, 1976: –0.°3, –0.″15
1709	STF 228		85.973	272.1	1.01	6.6–7.1	1+1	
	02076N4701		86.073	269.5	1.02		1+1	Heintz, 1952: +0.°2, –0.″05
			86.023	270.8	1.02		2n	Heintz, 1982: –1.°8, –0.″05
2034	STT 43		85.760	4.9	0.85	7.9–9.1	3+3	
	02349N2612		86.731	4.4	0.86		3+3	
			86.245	4.6	0.86		2n	Heintz, 1961: –0.°4, –0.″14
2446	STT 53		85.973	262.1	0.68	7.2–8.0	2+2	
	03113N3816		86.731	259.7	0.71		3+3	Rabe, 1948: –1.°3, –0.″14
			86.428	260.7	0.70		2n	Zulević, 1984: +1.°2, –0.″16
2995	STT 531		85.973	5.5	1.73	6.5–8.2	1+1	
	05009N3749		86.731	6.1	1.66		3+3	
			86.543	5.9	1.68		2n	Rabe, 1955: +9.°0, +0.″10
3390	STF 577		85.973	12.4	0.99	8.6–8.6	2+2	
	04355N3719		86.073	14.9	0.89	8.6–8.6	1+1	
			86.006	13.2	0.94		2n	Hock, 1966: –3.°6, –0.″15
3837	STF 665		86.057	259.0	1.52	8.3–9.1	1=10	
	05098N1937							
4200	STF 742		86.057	273.0	3.85	7.2–7.8	1+1	Hopmann, 1974: +1.°1, –0.″18
	05304N2156							
7067	STF 1280	AB	86.303	142.7	1.09	9.3–9.4	1+1	Heintz, 1973: –2.°1, 0.″00
	08460N7111							
7307	STF 1338	AB	8.314	265.3	0.94	7.0–7.2	1+1	Starikova, 1966: –6.°9, +0.″18
	09147N3837							
7477	STF 1374		86.312	303.4	2.80	7.0–8.3	2+2	
	09352N3884		86.314	304.2	2.80		2+1	
			86.313	303.8	2.80		2n	
7536	STF 1381		86.306	196.4	0.93	8.5–8.7	1+1	
	09440N6065		86.309	194.5	0.96		2+2	
			86.308	195.1	0.95		2n	
7685	STT 213		86.306	125.1	0.84	7.5–9.5	1+1	
	10075N2755		86.309	128.2	0.83		2+2	
			86.308	127.2	0.83		2n	Heintz, 1962: +2.°2, –0.″05
7704	STT 215							
	10108N1814		86.076	182.3	1.35	7.3– 7.5	1+1	
			86.084	182.4	1.41		1+1	
			86.303	181.7	1.37		1+1	Wierzbinski, 1953: +2.°1, –0.″04
			86.154	182.1	1.38		3n	Zaera, 1957: +2.°7, –0.″01

Table 1 (continued)

ADS	Disc. IDS	Mult.	Epoch 1900+	P	ρ	Est. Mag.	Weight	Notes
7724	STF 1424	AB	86.076	125°.3	4".41	2.3– 3.5	1+1	Rabe, 1956: +1°.5, +0".08
	10145N2021							
7745	Es 917		86.306	152.5	1.91	9.0– 9.3	1+1	
	10171N4873		86.309	151.7	1.90		3+2	
			86.308	151.9	1.90		2n	
8148	STF 1536		85.428	136.3	1.12	3.9– 7.1	1+1	Baize, 1951: –4°.8, –0".20
	11187N1105							
8242	KU 39		85.401	87.7	1.44	11.0–11.2	1+1	
	11319N4761		85.404	86.5	1.42		2+2	
			85.445	88.7	1.36		1+1	
			85.448	88.2	1.36		1+1	
			85.486	91.0	1.43		2+2	
			85.439	8.5	1.41		5n	Zulević, 1986: –1°.3, –0".03
8355	STT 241	AB	86.317	141.9	1.49	Δm = 3.0	1+1	
	11511N3560							
8446	STF 1606		85.404	245.7	0.49	7.3– 8.0	1+1	V.D. Wiele, 1974: –0°.8, +0".18
	12058N4027							
8539	STF 1639	AB	85.406	325.7	1.48	6.6– 7.8	2+2	
	12194N2608		85.409	326.2	1.47		2+2	
			85.428	326.4	1.47		2+2	
			85.414	326.1	1.47		3n	Aller, 1947: +1°.5, –0".07
8553	STF 1643		86.304	11.8	2.45	8.4– 8.7	1+1	
	12222N2735		86.306	11.6	2.47		2+2	
			86.309	12.2	2.50		3+2	
			86.307	11.9	2.48		3n	Hopmann, 1959: –56°.0, +0".60
8655	A 1783		86.317	215.9	1.42	9.0– 9.1	1+1	
	12402N4358		86.386	217.7	1.68		1+1	
			86.351	216.8	1.55		2n	
8680	HU 640		85.409	156.3	0.63	10.1–10.1	2+2	
	12458N2105		85.428	155.9	0.61	10.2–10.2	1+1	
			85.415	156.2	0.62		2n	Baize, 1973: +11°.4, 0".11
8887	Ho 260		85.401	74.1	0.96	8.6– 9.0	1+1	
	13189N2945		85.404	74.2	0.98		2+2	
			85.406	74.1	0.98		1+1	
			86.304	77.0	1.19		1+1	
			86.309	75.3	1.04		2+2	
			86.312	77.9	1.10		2+2	
			85.907	75.6	1.04		6n	Ambruster, 1978: –0°.1, –0".08
9000	STF 1777		86.465	229.2	2.85	5.8– 8.2	2+2	
	13380N0363		86.468	228.0	2.92		1+1	
			86.470	229.3	2.82		1+1	
			86.467	228.9	2.86		3n	
9067	BU 937		85.428	132.2	0.91	9.2– 9.4	1+1	
	13527N3455		85.431	131.1	0.88		2+2	
			85.445	131.4	0.83		1+1	
			85.434	131.5	0.88		3n	
9071	A 1614		85.404	133.2	1.21	9.4– 9.5	3+3	
	13539N5229		85.406	133.4	1.16		2+2	
			85.483	130.1	1.25		1+1	

Table 1 (continued)

ADS	Disc. IDS	Mult.	Epoch 1900+	P	ρ	Est.Mag.	WEIGHT	Notes
			86.386	131°.6	1″.21		1+1	
			86.468	131.1	1.21		1+1	
			85.670	132.4	1.20		5n	
9136	STF 1808 14056N2664	AB	86.473	82.2	2.39	8.0– 9.0	1+1	
9167	STF 1820 14097N5548		86.459	110.9	2.50	8.2– 8.5	3+3	
			86.473	112.9	2.33		1+1	
			86.463	111.4	2.46		2n	Hopmann, 1954: –2°.2, +0″.19
9174	STF 1816 14095N2934		86.312	87.2	0.74	7.0– 7.1	2+2	
			86.462	89.4	0.66		1+1	
			86.479	87.0	0.74		1+1	
			86.391	87.7	0.72		3n	
9229	STF 1834 14166N4858		85.401	101.6	1.33	7.9– 8.0	2+2	
			85.404	103.9	1.37		3+3	
			85.406	103.7	1.38		2+2	
			85.404	103.2	1.36		3n	Van den Bos, 1936: –0°.9, +0″.08
9418	STT 287 14478N4520		85.404	349.2	0.95	8.5– 8.5	3+3	
			85.409	343.3	0.95		2+2	
			85.513	349.3	0.97		1+1	
			86.479	346.7	1.05		2+2	
			85.688	347.1	0.98		4n	Heintz, 1959: –0°.2, –0″.10
9578	STF 1932 15140N2672		85.448	251.6	1.52	7.1– 7.6	2+2	
			85.505	253.4	1.55		1+1	
			85.513	252.4	1.54		1+1	
			86.386	255.5	1.44		2+2	
			86.468	252.5	1.45		1+1	
			86.479	254.3	1.35		2+2	
			86.012	253.5	1.46		6n	Heintz, 1964: +0°.1, –0″.01
9595	HU 1160 15161N1545		85.428	254.5	0.61	9.0–10.0	1+1	
			85.431	258.9	0.59		1+1	
			85.429	256.7	0.60		2n	Popović, 1986: –2°.4, –0″.16
9600	HU 146 15165N2126		85.494	128.0	0.54	9.3– 9.6	1+1	
			85.521	130.5	0.60		2+2	
			86.386	133.5	0.78		1+1	
			85.731	130.6	0.64		3n	
9626	STF 1938 15207N3742	BC	85.401	12.3	1.96	7.0– 7.6	2+2	
			85.404	14.1	2.13		3+3	
			85.409	14.6	2.11		1+1	
			85.483	15.0	2.20		1+1	
			85.415	13.8	2.09		4n	Baize, 1952: –0°.1, –0″.12
9639	STT 296 15230N4421	AB	85.431	281.9	1.93	7.6– 9.2	1+1	
			85.505	282.2	1.95		1+1	
			85.513	281.9	1.93		1+1	
			86.459	280.0	2.06		2+2	
			86.462	280.1	1.99		1+1	
			85.970	281.0	1.98		5n	
9641	A 82 15228N2376		86.470	345.6	0.66	8.5– 9.5	2+2	
9802	BU 621 15466N4449		86.574	28.6	0.55	8.1– 9.3	2+2	

Table 1 (continued)

ADS	Disc. IDS	Mult.	Epoch 1900+	P	ρ	Est. Mag.	Weight	Notes
9880	STT 303		86.573	169°5	1"40	7.5– 8.0	2+2	
	15562N1335		85.576	168.9	1.35		1+1	
			85.579	169.4	1.35		1+1	
			86.574	168.9	1.24		2+2	
			85.741	169.2	1.33		4n	
9925	BU 812		86.574	105.4	0.56	8.2– 8.2	2+2	
	16026N1670							
9952	A 1799		85.494	128.1	0.58	9.2– 9.3	2+2	
	16069N1523		85.519	127.3	0.61		2+2	
			85.530	127.3	0.61		2+2	
			85.565	127.0	0.59		1+1	
			86.465	124.7	0.64		2+2	
			85.731	126.8	0.61		5n	
9969	STF 2021	AB	85.576	350.4	4.10	7.5– 7.7	2+2	
	16086N1346		85.579	350.7	4.11		2+2	
			85.577	350.5	4.11		2n	Hopmann, 1970: –0°8, 0"09
9982	STF 2026		85.404	23.6	2.88	9.1– 9.6	3+3	
	16111N0737		85.431	23.3	2.85		1+1	
			85.497	22.5	2.93		2+2	
			85.519	22.7	2.79		2+2	
			85.521	22.9	2.87		2+2	
			85.472	23.0	2.87		5n	Heintz, 1962: +0°5, –0"05
10075	STF 2052	AB	85.401	132.8	1.43	7.8– 7.8	2+2	
	16245N1837		85.404	132.9	1.49		3+3	
			85.483	131.8	1.45		1+1	
			85.511	131.5	1.45		1+1	
			86.470	131.4	1.51		2+2	
			86.558	131.2	1.59		1+1	
			86.564	131.3	1.55		1+1	
			85.825	132.1	1.49		7n	Scardia, 1984: +0°2, –0"13
10087	STF 2055		85.486	17.7	1.20	4.2 5.2	1+1	
	16259N0212		85.505	17.3	1.35		1+1	
			85.513	16.5	1.26		1+1	
			86.465	16.8	1.38		1+1	
			85.742	17.1	1.30		4n	Baize, 1973: –0°7, –0"08
10158	A 349		85.573	165.3	0.58	10.6–11.2	1+1	
	16374N3018		86.569	163.7	0.52		2+2	
			86.237	164.2	0.54		2n	Couteau, 1974: –3°3, –0"02
10159	J 738		86.558	243.8	1.52	9.5–9.5	1+1	
	16372N2207		86.564	247.4	1.57		1+1	
			86.569	248.7	1.58		2+2	
			86.565	247.2	1.56		3n	
10188	D 15		85.401	141.0	1.13	9.1–9.1	1+1	
	16408N4540		85.404	139.0	1.10		3+3	
			85.486	138.6	1.02		3+3	
			85.497	137.1	1.09		2+2	
			85.571	140.8	1.12		1+1	
			86.460	136.5	1.00		2+2	
			86.465	137.1	1.00		2+2	
			85.745	138.5	1.06		7n	Wierzbinski, 1955: +1°5, 0"00

Table 1 (continued)

ADS	Dis. IDS	Mult.	Epoch 1900+	P	ρ	Est. Mag.	Weight	Notes
10235	STF 2107	AB	85.404	90°.1	1".30	6.7–8.2	3+3	
	16479N2850		85.448	93.6	1.23		1+1	
			85.497	91.7	1.28		2+2	
			85.511	93.0	1.27		1+1	
			85.571	90.8	1.26		1+1	
			86.460	90.6	1.24		1+1	
			85.577	91.3	1.27		6n	Rabe, 1926: +0°.5, −0".12
10279	STF 2118		85.527	70.1	1.21	Δm = 0.1	2+2	
	16559N6511		86.728	69.0	1.22		2+2	
			86.128	69.5	1.22		2n	Giannuzzi, 1955: +1°.3, −0".11
10341	BU 823	AB	85.428	132.3	0.80	8.7–9.7	1+1	
	17015S0047		85.448	132.0	0.86		1+1	
			85.497	132.1	0.86		1+1	
			85.527	132.9	0.77		1+1	
			86.558	132.4	0.82		1+1	
			86.564	131.4	0.78		1+1	
			85.987	132.2	0.81		6n	Arend, 1955: +7°.7, −0".25
10345	STF 2130	AB	85.584	38.2	1.88	5.8–5.8	1+1	
	17033N5436		86.728	35.9	1.89		2+2	
			86.337	36.4	1.89		2n	Heintz, 1965: +5°.1, 0".00
10429	A 2984		86.465	358.0	0.84	4.6–7.6	1+1	
	17114S0020		86.711	0.0	0.85		1+1	
			86.588	359.0	0.85		2n	
10456	BU 45		85.527	291.2	4.70	Δm = 0.6	1+1	
	17142N3235		86.728	290.1	4.65	Δm = 0.1	2+2	
			86.128	290.5	4.67		2n	
10459	BU 628		85.494	285.9	0.41	9.4–9.9	2+2	
	17146N3240		85.522	280.0	0.42		2+2	
			85.530	281.9	0.37		3+3	
			85.565	282.9	0.39		2+2	
			85.568	282.5	0.43		2+2	
			85.544	282.6	0.40		5n	Zulević, 1986: +2°.7, +0".02
10460	STF 2153		85.584	253.0	1.52	9.3–9.8	2+2	
	17154N4925		86.566	251.9	1.56		2+2	
			86.075	252.5	1.54		2n	
10472	BU 630		85.527	223.6	1.34	9.5–11.0	1+1	
	17155N3227		86.719	223.1	1.48		1+1	
			86.123	223.3	1.41		2n	
10487	KR 46		96.575	64.1	1.70	8.8–9.0	3+3	
	17180N5838		86.719	64.4	1.57		1+1	
			86.611	64.2	1.67		2n	
10504	Ho 414		86.575	100.6	0.72	8.4–8.8	2+2	
	17181N2611		86.711	100.6	0.75		3+3	
			86.719	102.2	0.73		1+1	
			86.722	103.2	0.73		3+3	
			86.685	101.6	0.73		4n	
10540	BU 1250		85.494	108.8	1.80	9.3–9.8	1+1	
	17210N3049		85.505	110.1	1.79		1+1	
			85.511	108.6	1.80		1+1	
			85.565	110.2	1.80		2+2	
			85.526	109.6	1.80		4n	

Table 1 (continued)

ADS	Dis. IDS	Mult.	Epoch 1900+	P	ρ	Est. Mag.	Weight	Notes
10646	HU 923		85.584	107°.7	0".97	9.2–9.7	2+2	
	17318N1917		86.566	104.9	0.86		2+2	
			86.722	105.1	0.97		3+3	
			86.350	105.8	0.94		3n	
10669	BU 1121		86.465	208.6	0.49	8.5–9.0	1+1	
	17328N1237		86.722	208.3	0.49		2+2	
			86.636	208.4	0.49		2n	
10699	STF 2199		85.573	61.3	1.73	7.8–8.4	2+2	
	17368N5549		85.576	61.7	1.78		2+2	
			85.579	61.5	1.78		2+2	
			85.576	61.5	1.76		3n	
10722	STF 2203		85.519	298.4	0.73	7.6–7.9	2+2	
	17381N4142		85.530	301.4	0.68		3+3	
			85.573	300.8	0.73		2+2	
			86.697	301.1	0.74		2+2	
			85.796	300.9	0.72		4n	
10743	HU 1285		85.494	222.3	0.53	9.0–9.0	2+2	
	17394N2239		85.519	222.0	0.49		2+2	
			85.522	221.4	0.56		2+2	
			85.565	222.0	0.51		3+3	
			85.529	221.9	0.52		4n	
10755	HU 1286		85.565	272.1	3.10	9.5–9.8	3+3	
	17403N2239							
10773	Ho 70		86.566	94.6	0.47	8.1–8.1	1+1	
	17410N3034		86.722	92.0	0.49	9.0–9.0	3+3	
			86.683	92.8	0.49		2n	
10796	HU 1288		85.494	152.9	0.43	8.7–9.2	1+1	
	17426N1504		85.519	153.0	0.47		2+2	
			85.511	153.0	0.46		2n	
10814	HU 1182		86.567	323.4	0.56	8.7–9.1	1+1	
	17451N3538		86.722	324.4	0.57	8.8–9.2	3+3	
			86.683	324.2	0.57		2n	
10850	STT 338		86.558	347.5	0.96	6.6–6.9	1+1	
	17475N1521		86.564	356.3	0.76		1+1	
			86.572	352.9	0.86		1+1	
			86.565	352.2	0.86		3n	
10880	AC 9		85.573	240.3	1.06	8.6–9.1	2+2	
	17503N2950		85.576	240.3	1.08		2+2	
			85.579	240.5	1.07		2+2	
			85.585	239.6	1.08		3+3	
			85.579	240.1	1.07		4n	
1001	STF 2267		86.564	262.3	0.69	8.0–8.0	1+1	
	17584N4011		86.567	263.4	0.75		1+1	
			86.697	258.2	0.74		1+1	
			86.609	261.3	0.73		3n	
11010	BU 1127		85.486	74.5	0.88	7.4–9.3	1+1	
	17596N4414		85.519	73.4	0.82		2+2	
			85.508	73.7	0.84		2n	Popović, 1970: –4°.5, –0".25

Table 1 (continued)

ADS	Disc. IDS	Mult.	Epoch 1900+	P	ρ	Est. Mag.	Weight	Notes
11012	Ho 565	AB	86.465	105°.3	0".34	8.3–8.3	1+1	
	17592N2603							
11051	J 1220		86.465	130.5	1.55	9.2–9.2	2+2	
	18010N1242		86.572	128.4	1.47		1+1	
			86.706	130.9	1.47		1+1	
			86.552	130.1	1.51		3n	
11059	J 758		86.572	128.7	2.93	9.2–9.4	1+1	
	18019N3805		86.719	125.7	3.04		1+1	
			86.645	127.2	2.98		2n	
11110	STF 2283		86.572	63.3	0.97	7.2–7.7	1+1	
	18047N0608		86.725	63.0	0.84		1+1	
			86.638	63.2	0.90		2n	
11123	STF 2289		85.574	221.1	1.20	6.5–7.2	2+2	
	18057N1627		85.576	221.0	1.21		1+1	
			85.579	221.1	1.18		2+2	
			85.576	221.1	1.19		3n	Hopmann, 1956: +1°.4, –0".04
11128	HU 674		85.495	223.6	0.61	7.5–8.0	2+2	
	18072N5023		85.519	227.9	0.70		2+2	
			85.530	226.2	0.67		3+3	
			85.517	225.9	0.66		3n	
11186	STF 2294		86.569	94.9	1.03	7.4–7.7	2+2	
	18094N0009		86.708	94.8	1.07	8.6–8.7	2+2	
			86.636	94.8	1.05		2n	Wilson, 1935: +1°.5, +0".03
11239	A 577		85.724	296.4	0.75	9.0–11.0	2+2	
	18143N4353							
11247	A 578		86.708	267.8	0.30	9.2–9.9	2+2	Zulević, 1976: +2°.0, +0".04
	18148N4348							
11249	A 579		85.495	342.2	1.32	8.5–11.0	2+2	
	18151N4332							
11260	HU 197		85.585	118.4	0.36	8.5–9.6	1+1	
	18150N1014		86.709	112.8	0.35		1+1	
			86.147	115.6	0.35		2n	Baize, 1970: +2°.3, +0".05
11291	AG 222		85.680	146.6	1.40	Δm = 0.0	2+1	
	18176N1410		85.694	147.4	1.53	Δm = 0.3	1+1	
			85.697	147.1	1.50	9.3–9.5	2+2	
			85.691	147.0	1.47		3n	
11292	STF 2311		85.680	115.1	2.58	8.0–9.0	2+1	
	18176N1123		85.694	113.3	2.69		1+1	
			85.697	114.2	2.70		2+2	
			85.691	114.3	2.66		3n	
11432	STT 354		86.564	206.6	0.60	7.2–8.0	1+1	
	18272N0643		86.575	197.2	0.71		1+1	
			86.706	199.9	0.69		1+1	
			86.615	201.2	0.67		3n	
11479	STT 359		86.569	6.2	–	6.6–6.9	1+1	
	18314N2331		86.709	10.0	0.72		2+2	
			86.662	8.7	0.72		2n	Symms, 1963: +0°.4, +0".08

Table 1 (continued)

ADS	Disc. IDS	Mult.	Epoch 1900+	P	ρ	Est. Mag.	Weight	Notes
11483	STT 358	AB	85.401	162°.0	1".62	6.8–7.2	1+1	
	18314N1654		85.404	160.0	1.58		3+3	
			85.497	160.9	1.65		1+1	
			86.460	161.9	1.53		1+1	
			86.471	159.6	1.57		1+1	Starikova, 1966: +3°.1, + 0".11
			85.720	160.6	1.59		5n	Hopmann, 1970: +1°.8, + 0".08
11568	STF 2384	AB	85.404	313.7	0.48	8.6–9.1	2+2	
	18385N6702		85.530	313.0	0.47		1+1	
			85.585	313.3	0.44		1+1	
			85.481	313.4	0.47		3n	Heintz, 1975: +1°.1, –0".01
11778	STF 2412		86.465	56.5	1.41	8.4–8.5	1+1	
	18480N1353		86.698	56.1	1.44		1+1	
			86.581	56.3	1.43		2n	
11811	BU 137		85.519	154.7	1.39	8.2–8.7	2+2	
	18505N3715		85.702	156.6	1.45		2+2	
			85.721	156.2	1.46		3+3	
			86.717	156.1	1.45		1+1	
			85.790	155.9	1.44		4n	
11869	STF 2422		86.465	73.2	0.76	7.6–7.7	2+2	
	18531N2558		86.567	74.9	0.80		1+1	
			86.698	75.0	0.77		1+1	
			86.549	74.1	0.77		3n	
12033	HU 940		85.401	203.7	0.50	9.6–9.6	1+1	
	19018N3343		85.404	204.6	0.50		2+2	
			85.566	205.2	0.49		2+2	
			85.724	206.5	0.58		3+3	
			85.564	205.4	0.53		4n	Muller, 1953: +3°.4, – 0".05
33°3323	DZ 1		85.401	165.2	1.15	11.0–11.2	1+1	
	19029N3346		85.404	165.9	1.29		2+2	
			85.403	165.7	1.24		2n	
12040	STF 2454	AB	85.574	280.2	1.17	8.5–9.7	2+2	
	19023N3017		85.576	280.5	1.17		1+1	
			85.579	280.6	1.17		2+2	
			86.717	280.3	1.19		1+1	
			86.766	280.4	1.17		4n	Baize, 1975: +0°.1, – 0".07
12447	STF 2525		85.568	291.6	1.88	8.5–8.7	3+3	
	19225N2707		85.740	292.6	1.89		1+1	
			85.749	293.7	1.65		1+1	
			85.751	294.5	1.73		1+1	
			85.692	293.8	1.83		3+3	
			85.692	293.0	1.83		5n	Job Tamburini, 1967: +0°.7, –0".08
12567	A 713		85.495	271.7	0.42	7.7–8.2	2+2	
	19284N4716		86.714	278.7	0.38		1+1	
			86.204	274.0	0.41		2n	
12618	A 597		85.740	97.5	1.51	8.4–10.9	1+1	
	19305N4208		85.760	97.9	1.61		3+3	
			85.755	97.8	1.59		2n	
12746	HU 953		85.721	235.0	0.36	8.8–9.2	2+2	
	19352N3501		86.711	233.9	0.37		2+2	
			86.216	234.5	0.37		2n	

Table 1 (continued)

ADS	Disc. IDS	Mult.	Epoch 1900+	P	ρ	Est. Mag.	Weight	Notes
12889	STF 2576	AB	85.404	353°.2	2".09	9.3–9.3	3+3	
	19418N3322		85.530	354.0	2.06		2+2	
			85.568	353.7	2.19		3+3	
			85.576	353.2	2.13		2+2	
			85.579	352.6	2.15		2+2	
			85.524	353.4	2.13		5n	Rabe, 1943: +1°.6, −0".08
13012	J 124	AC	85.716	222.5	22.91	5.3–13.5	1+1	
	19462N1010							
13082	STF 2596		85.740	304.7	2.03	7.3–8.7	1+1	
	1949N1502		85.751	304.9	2.01		1+1	
			85.762	304.3	2.06		1+1	
			86.725	304.7	1.98		1+1	
			85.994	304.7	2.02		4n	
13183	ROE		85.721	40.4	1.46	11.0–11.5	1+1	
	19542N3539							
13184	AG 244	AB	86.706	272.7	1.29	9.0–10.7	1+1	
	19540N2152		86.723	272.3	1.42		1+1	
			86.715	272.5	1.35		2n	
13194	L		86.723	302.0	1.98	9.8–10.5	1+1	
	19542N2146							
13196	STF 2606		85.702	140.7	0.92	7.5–8.2	2+2	
	19547N3300		85.721	143.1	0.88		3+3	
			85.765	143.1	0.90		2+2	
			85.728	142.4	0.90		3n	
13200	Ho 583		85.702	257.1	1.33	9.0–10.7	1+1	
	19547N2150		86.698	257.0	1.32		1+1	
			86.723	257.0	1.36		1+1	
			86.374	257.0	1.34		3n	
13277	STT 395		86.567	124.0	0.84	5.8–6.2	1+1	
	19578N2439		86.575	122.2	0.78		1+1	
			86.719	123.4	0.84		1+1	
			86.620	123.2	0.82		3n	
13542	STF 2651		85.680	280.7	1.00	8.0–8.0	2+2	
	20092N1551		85.694	280.7	1.05		1+1	
			85.724	281.5	1.10		3+3	
			86.698	280.2	1.13		2+2	
			85.953	280.9	1.08		4n	
13543	STF 2653		85.680	273.0	2.48	7.5–9.6	1+1	
	20094N2356		86.730	278.3	2.59		2+2	
			86.380	276.5	2.55		2n	
13649	BU 984		85.530	246.3	0.76	9.0–9.3	1+1	
	20134N2604		85.568	247.5	0.61		2+2	
			85.585	247.2	0.60		1+1	
			85.563	247.1	0.64		3n	
13665	A 1205		85.724	102.5	0.56	9.2–10.0	3+3	
	20141N2854		86.698	102.8	0.58		1+1	
			86.731	102.4	0.59		2+2	
			86.222	102.5	0.57		3n	Heintz, 1978: +3°.2, −0".10

Table 1 (continued)

ADS	Disc. IDS	Mult.	Epoch 1900+	P	ρ	Est. Mag.	Weight	Notes
13723	STT 406		85.530	117°.3	0".58	7.4–8.3	2+2	
	20166N4509		85.568	115.0	0.59		1+1	
			25.770	116.4	0.55		3+3	
			86.730	116.4	0.53		2+2	
			85.925	116.4	0.56		4n	Heintz, 1975: +1°.5, –0".02
13986	STF 670	AB	85.522	10.9	0.69	8.5–8.8	2+2	
	20282N1336		85.702	14.9	0.73		1+1	
			85.732	14.6	0.78		1+1	
			85.619	12.8	0.72		3n	
14270	STF 2725		85.577	9.4	5.83	7.3–8.0	1+1	
	20416N1532		85.579	9.6	5.79		2+2	
			85.716	9.7	5.91		2+2	
			85.633	9.6	5.85		3n	Hopmann, 1973: +0°.0, –0".10
14296	STT 413		85.530	12.4	0.82	4.8–6.1	1+1	
	20435N3607		86.709	14.0	0.84		1+1	
			86.720	13.4	0.83		1+1	
			86.320	13.3	0.83		3n	Rabe, 1946: +1°.1, –0".02
14499	STF 2737	AB	86.725	290.2	1.01	–	1+1	Van den Bos, 1932: +5°.1, –0".01
	20541N0355							Zeller, 1957: +5°.1, +0".00
14558	STF 2746		86.567	317.2	0.97	8.0–8.6	1+1	
	20580N3852		86.706	319.5	1.01		1+1	
			86.714	317.9	1.04		1+1	
			86.662	318.2	1.01		3n	
14573	STF 2744	AB	85.579	126.7	1.24	7.0–7.5	2+2	
	20580N0108		85.724	126.2	1.26		2+2	
			85.765	126.2	1.27		1+1	
			85.768	126.7	1.26		3+3	
			85.711	126.5	1.26		4n	Popović, 1962: +4°.4, +0".00
14766	A 884		85.566	126.0	0.38	9.3–9.4	1+1	
	21098N4630							
14784	STF 2783		85.754	5.9	0.81	7.8–7.8	2+2	
	21114N5753		85.760	4.8	0.73		3+3	
			85.771	5.6	0.75		3+3	
			85.763	5.3	0.76		3n	
14889	STT 437		85.585	23.1	2.32	6.9–7.6	2+2	
	21166N3202		85.716	25.2	2.19		2+2	
			85.721	24.9	2.12		3+3	
			85.732	25.4	2.11		1+1	
			85.740	25.5	2.24		1+1	
			85.751	25.5	2.22		1+1	
			85.768	25.0	2.14		3+3	
			85.715	24.8	2.18		7n	
14926	A 764		85.519	4.8	0.83	8.4–9.6	1+1	
	21194N5708		85.585	359.4	0.72		2+2	
			85.724	5.1	0.72		1+1	
			85.603	2.2	0.74		3n	Heintz, 1961: –4°.0, +0".03
15007	STF 2799		85.680	268.7	1.57	8.2–8.2	1+1	
	21240N1039		85.722	267.2	1.63		2+2	
			85.765	268.7	1.55		2+2	
			85.730	268.1	1.59		3n	Popović, 1986: +1°.6, –0".10

Table 1 (continued)

ADS	Disc. IDS	Mult.	Epoch 1900+	P	ρ	Est. Mag.	Weight	Notes
15076	STF 2804	AB	86.720	353°.4	3″.14	7.6–8.6	2+2	
	21284N2016							
15156	HU 372		86.720	220.7	0.30	9.9–9.9	1+1	
	21338N2309							
15769	STF 2881		86.725	80.8	1.35	–	1+1	
	22100N2905							
15961	J 580		86.723	112.1	4.18	10.0–10.5	1+1	
	22231N1154		86.728	110.8	4.17		2+2	
			86.726	111.7	4.17		2n	
15962	BU 701	AB	85.754	199.3	0.65	7.3–10.3	1+1	
	22232N1144		86.728	200.6	0.65		2+2	
			86.338	200.0	0.65		2n	
16037	Ho 475	AB	85.732	310.7	0.88	8.0–8.2	1+1	
	22280N2554		85.751	308.8	0.94		1+1	
			85.757	309.8	0.96		3+3	
			85.760	310.7	0.93		3+3	
			85.754	310.1	0.94		4n	
16185	STF 2934		85.566	68.2	0.87	8.5–9.2	2+2	
	22370N2054		85.585	68.3	0.95		2+2	
			85.724	68.2	0.97		2+2	
			85.765	68.9	0.97		1+1	
			85.913	69.1	0.97		1+1	
			85.678	68.8	0.94		5n	Heintz, 1960: +3°.3, –0″.02
16317	STF 2950	AB	85.732	286.3	1.53	5.7–10.0	1+1	
	22474N6109		85.751	286.3	1.39		1+1	
			85.742	286.4	1.46		2n	
16326	A 632	AB	85.771	165.7	0.82	8.0–8.8	2+2	
	22480N5712		86.709	164.8	0.77		2+2	
			86.714	166.4	0.83		1+1	
			86.335	165.5	0.81		3n	Heintz, 1961: +2°.4, +0″.09
16373	HU 987		85.754	89.9	0.76	8.6–8.8	3+3	
	22508N1515		85.757	89.8	0.76		2+2	
			85.760	89.7	0.73		3+3	
			85.765	89.6	0.82		2+2	
			85.759	89.8	0.76		4n	Heintz, 1965: +7°.5, +0″.09
16561	BU 385		85.754	91.1	0.68	7.3–8.1	3+3	
	23055N3156		85.757	90.5	0.68		1+1	
			85.760	91.2	0.64		3+3	
			85.765	90.9	0.67		1+1	
			85.758	91.0	0.66		4n	
16649	BU 79	AB	85.585	21.9	1.46	8.4–10.0	2+2	
	23125S0204		86.711	20.6	1.49		2+2	
			86.148	21.2	1.47		2n	Heintz, 1959: –0°.7, –0″.06
16951	A 1242		85.771	327.1	0.79	9.0–9.0	3+3	
	23380N1117		86.712	327.7	0.75		2+2	
			86.147	327.3	0.77		2n	Zulević, 1977: –1°.4, +0″.02

Table 1 (continued)

ADS	Disc. IDS	Mult.	Epoch 1900+	P	ρ	Est. Mag.	Weight	Notes
17020	STT 507 23138N6420	AB	85.771 86.728	306°.9 306.4	0".72 0.73	6.8–7.5	2+2 2+2	
			86.249	306.6	0.73		2n	Zulević, 1977: +0°.2, –0".01
17149	STF 3050 23544N3310	AB	85.913 86.728	314.8 316.9	1.47 1.47	6.5–6.6	1+1 3+3	
			86.320	315.9	1.47		2n	Franz, 1954: –2°.6, –0".38 Heintz, 1973: –2°.0, –0".13
17178	HLD 60 23563N3905		85.566 85.722 85.724 85.754 85.757 85.760	180.4 178.7 181.2 179.9 179.3 179.4	0.97 1.06 0.97 1.04 0.99 0.98	9.2–9.6	2+2 2+2 2+2 2+2 2+2 3+3	
			85.717	179.8	1.00		6n	Heintz, 1961: 0°.0, –0".09
17179	Ho 209	AB	86.731	350.4	1.39	$\Delta m = 0.2$	3+3	

ACKNOWLEDGEMENTS

This work has been supported by Republic Association for Science in Serbia through the project „Physics and Motions of Celestial Bodies and Artificial Satelites".

REFERENCES

Zulević, D J.,: 1986, *Bull. Obs. Astron. Belgrade*, **136**. 91.

Muller, P., Couteau, P.: 1979, *Quatrieme catalogue d ephemerides d etoile doubles*, Publ. Obs. Paris, Cerga, Obs. de Nice.

Aitken, R.: 1932, *New General Catalogue of Double Stars*, Vol. I, II Washington.

Jeffers, H.M., Van den Bos, W.H., Greeby, F.M.: 1963, *Index catalogue of visual double stars*, 1961.0, *Publ. of the Lick Obs.* 21.

THE ORBIT OF THE VISUAL DOUBLE STAR IDS 17225S6022

V. Erceg and D. Olević

Astronomical Observatory, Volgina 7, 11050 Belgrade, Yugoslavia

(Received: October 7, 1987)

SUMMARY: Presented are preliminary orbital elements, dynamical parallaxis, absolute magnitudes, masses, ephemeris and residuals for visual double star IDS 17225S6022.

The orbital elements for visual double star IDS 17225S6022 ara deduced by the Thiele–Innes, Van den Bos method. On the bases of orbital elements dynamical parallaxes, absolute magnitudes and stellar masses are determinated.

The orbital elements of the star are published in No 103 of C.I. comm. des etoiles doubles.

In Table I the orbital elements, Thiele–Innes constants, dynamical parallaxes, absolute magnitudes and the stelar masses are listed.

In Table. II are the ephemeris for 10 years.
Table III contains data on observations, the observers names' abreviations, the references and the residuals.

We are grateful to Charles E. Worley from the U.S. Naval Observatory which supplied us by measurements, and to Dj. Božičković for the adaptation of computer programmes.

This work has been supported by RZNS through the project „Physics and Motions of Celestial Bodies and Artificial Satelites".

ORBIT OF IDS 17225S6022 = I 600
App. mag.: 9.3–9.4; Sp. FO

Table I

P = 611.0 years		
n = 0°.5892	A = −0".3425	πdyn.orb. = 0".005
T = 1966.00	B = −0".0375	M_A = 2.7
e = 0.36	F = −0".1610	M_B = 2.8
a = 0".494	G = +0".4540	m_A = 1.57 ☉
i = 131°.5	C = ∓0".3528	m_B = 1.54 ☉
Ω = 120°.5	H = ±0".1110	a = 107.4 A.U.
ω = 287°.5		
T_{Ω}, Ω = 2028.38; 1854.72		

Table II

t	θ°	ρ"
1988.0	153°.7	0".28
1989.0	152.6	0.28
1990.0	151.5	0.28
1991.0	150.4	0.29
1992.0	149.4	0.29
1993.0	148.3	0.29
1994.0	147.3	0.30
1995.0	146.3	0.30
1996.0	145.4	0.30
1997.0	144.4	0.31

Table III

N.	t	θ°	ρ''	Obs.n Reference	$(O-C)_\theta$ $(O-C)_\rho$
1.	1909.7	260°.0	0''.4 I	1 Transvaal Obs.Circ.No1, 1909.	−11°.7 +0''.07
2.	1913.66	260.0	0.5 I	2 Union Obs.Circ. **1** 185, 1915.	− 8.3 +0.18
3.	1926.70	281.0	0.40 B	1 Union Obs.Circ.**5**, 312, 1949.	+ 26.3 +0.13
4.	1927.75	262.6	0.34 B	1 Union Obs.Circ.**5**, 312. 1949.	+ 9.2 +0.07
5.	1928.58	253.2	0.27 B	4 Union Obs.Circ.**5**, 312, 1949.	+ 0.9 +0.01
6.	1929.74	247.1	0.23 B	3 Union Obs.Circ.**3** 183, 1931.	− 3.7 −0.03
7.	1930.48	65.6*	0.17 JSP	2 Publ. Univ. Michigan Obs. **9**, 73, 1964.	− 4.2 −0.09
8.	1930.69	239.6	0.18 B	4 Union Obs.Circ.**3** 183, 1931.	−10.0 −0.08
9.	1931.61	249.9	0.21 B	5 Union Obs.Circ.**3** 273, 1932.	+ 1.6 −0.04
10.	1933.03	245.0	0.23 B	4 Union Obs.Circ.**4** 61, 1934.	− 1.3 −0.02
11.	1933.62	244.9	0.26 FIN	4 Union Obs.Circ.**4** 31, 1934.	− 0.6 +0.01
12.	1939.24	237.2	0.20 VOU	2 Ann.Bosscha Obs. Lembang, **6**, Pt.4, D1, 1947.	+ 0.4 −0.03
13.	1944.25	225.6	0.28 VOU	2 J.Obs.**38**, 109, 1955.	− 2.6 +0.06
14.	1945.25	207.9	0.21 VOU	4 J.Obs.**38**, 109, 1955.	−18.4 −0.01
15.	1952.48	197.6	0.22 B	1 Union Obs.Circ.**6**, 266, 1956.	−14.9 +0.01
16.	1960.08	189.7	0.22 ,B	4 Union Obs.Circ.**6**, 353, 1961.	− 7.8 +0.01
17.	1974.304	172.7	0.24 HLN	1 Pub.Astron.Soc.Pacific, **86**, 907, 1974.	+ 0.6 0.00
18.	1979.21	170.9	0.30 ,HEI	3 Astrophys.J.Suppl.**44**, 111, 1980.	+ 6.0 +0.05

*Quadrant changed

REFERENCES

Bos, van den, W.H.: 1926, *Orbital elements of Binary Stars, Union Observatory Circ.* N. 68.

Parenago, P.P.: 1954, *Kurs zvezdnoj astronomiji*, Moskva.

Bull. Obs. Astron. Belgrade, N° 138 (1988) UDC 523.4.521.3

RESULTS OF DIURNAL MEASUREMENTS FOR THE SUN, MERCURY, VENUS AND MARS OBTAINED IN THE PERIOD 1984–1986

S. Sadžakov, M. Dačić and Z. Stančić

Astronomical Observatory, Volgina 7, 11050 Belgrade, Yugoslavia

(Received: October 21, 1987)

SUMMARY: In the paper we present the results $(O-C)_\alpha$ and $(O-C)_\delta$ obtained in the period 1984–1986 in Belgrade from diurnal observations of the Sun, Mercury, Venus and Mars with the large meridian circle „Askania" No 88077, 2r = 190 mm, f = 2578 mm.

The observations of the Sun, Mercury, Venus and Mars are done visually in both coordinates (right ascension and declination) with the large meridian circle „Askania" (d = 190 mm, f = 2578 mm). The pavilion, the instrument, the way in which the observations were carried out and the treatment of the observational material have been described elsewhere (Sadžakov et al., 1976).

Before 1985 for the purpose of solar observations a Sukharev filter was used and afterwards another one from high–quality glass.

Both edges–the front and the rear one in the right ascension – the lower and the upper one in the declination – were observed. Mercury was mostly observed by central bisection of its image. In those cases when the seeing was satisfactory, the part of the planet illuminated by the sunshine was observed. Venus was observed in the same way as the Sun, or only one edge. In both cases of observing one edge only, the diameter correction was applied.

The ephemeric of the Sun, Mercury, Venus and Mars were calculated after 1984. We obtain ephemeris from Institute of Theoretical Astronomy, Leningrad.

The apparent right ascensions and declinations obtained from our observations are compared to the ephemeris places and the results are presented in Tables I–IV.

Each of the four tables contains eleven columns. Their description is given below.

Column I – date of observation;
Column II – observers: Sofija Sadžakov (SS), Miodrag Dačić (MD), Zorica Stančić (ZS), and Dušan Šaletić (DŠ)
Column III – atmospheric pressure in mm Hg;
Column IV – mean air temperature in the pavilion;
Column V – number of reference star transits;
Column VI – ephemeris right ascension (α);
Column VII – $(O-C)_\alpha$ in right ascension;
Column VIII – ephemeris declination (δ);
Column IX – $(O-C)_\delta$ in declination;
Column X – observation epoch;
Column XI – clamp position.

ACKNOWLEDGEMENTS

This work been supported by Republic Association for Science of Serbia throught the project „Physics and Motions of celestial Bodies and Artificial Satelites".

Table I. Data on the Sun observations

Date of observ.	ob- serv.	Ba	t°C	n	α	$(O-C)_\alpha$	δ	$(O-C)_\delta$	Ep	cla- mp
1984.									1980+	
15.03.	SS.MD.	742.3	5.3	3	$23^h41^m48^s343$	0.024	−01°58′16″02	−0″06	4.21	W
16.03.	SS.MD.	738.8	6.2	2	23 45 27.677	−0.010	−01 34 34.39	−0.25	4.21	W
20.03.	MD.	746.0	3.6	2	00 00 03.162	−0.015	00 00 14.64	0.00	4.22	W
29.03.	SS.MD.	741.4	17.4	3	00 32 48.624	−0.042	03 23 18.07	−0.17	4.24	W
16.04.	SS.MD.	742.6	18.8	–	01 38 47.011	0.018	10 16 02.57	0.27	4.29	W
20.04.	SS.MD.	746.8	12.6	–	01 53 39.453	0.014	11 39 25.45	−0.23	4.30	W
26.04.	SS MD.	740.7	12.7	1	02 16 11.671	−0.032	13 38 41.42	0.40	4.32	W
03.05.	SS.MD.	742.4	18.7	–	02 42 52.492	0.005	15 47 35.94	−0.19	4.34	W
07.05.	SS.MD.	737.9	21.4	–	02 58 19.196	−0.027	16 55 37.12	−0.17	4.35	W
18.05.	MD.	743.2	18.6	1	03 41 33.388	−0.045	19 38 21.15	−0.83	4.38	W

Table 1 (continued)

Date of observ.	ob-serv.	Ba	t°C	n	α	(O–C)α	δ	(O–C)δ	Ep	cla-mp
19.05.	MD.ZS.	739.0	21.6	–	03 45 32.619	–	19 51 14.08	–0.36	4.38	W
14 06.	SS.MD.	739.8	20.2	1	05 31 52.000	–0.028	23 17 01.40	0.09	4.46	E
27.06.	SS.MD.	748.0	18.8	5	06 25 54.964	–	23 18 27.72	0.81	4.49	E
28.06.	SS.MD.	742.9	23.7	3	06 30 03.951	0.027	23 15 41.37	0.21	4.49	E
10.07.	MD.	745.3	22.2	–	07 19 29.152	–0.011	22 11 04.34	–0.60	4.53	W
11.07.	SS.MD.	745.9	24.4	–	07 23 33.738	–0.018	22 03 08.72	0.29	4.53	W
12.07.	SS.MD.	745.6	27.4	3	07 27 37.865	0.033	21 54 50.45	0.31	4.53	W
13.07.	SS.MD.	744.8	28.7	–	07 31 41.521	0.000	21 46 09.72	–0.05	4.54	W
19.07.	SS.MD.	744.9	19.1	–	07 55 52.983	–0.001	20 46 24.64	–0.17	4.55	W
23.07.	SS.MD.	744.3	25.3	–	08 11 50.028	–0.017	19 59 31.36	–0.25	4.56	W
06.08.	SS.ZS.	743.7	25.9	–	09 06 25.383	0.001	16 35 15.99	0.06	4.60	E
09.08.	SS.ZS.	743.3	24.1	1	09 17 51.559	0.009	15 44 14.58	–0.52	4.61	E
16.08.	SS.ZS.	741.5	21.3	–	09 44 12.618	0.000	13 36 38.46	0.13	4.63	E
20.08.	SS.	746.4	20.8	–	09 59 04.721	0.007	12 18 51.15	0.24	4.64	E
23.08.	SS.MD.	743.8	21.0	1	10 10 09.009	–0.034	11 18 25.82	–0.10	4.65	E
29.08.	SS.MD.	746.9	19.3	1	10 32 06.516	0.008	09 12 52.25	–0.22	4.66	W
03.09.	SS.ZS.	746.4	22.2	2	10 50 14.641	–	07 24 09.74	0.20	4.66	W
05.09.	SS.ZS.	739.2	26.2	1	10 57 27.858	0.018	06 39 48.85	0.02	4.68	E
06.09.	SS.MD.	740.1	25.4	1	11 01 04.103	0.028	06 17 28.61	0.10	4.69	E
12.09.	SS.ZS.	744.2	20.4	1	11 22 37.809	–0.028	04 01 29.43	0.32	4.70	E
13.09.	SS.ZS.	744.9	22.1	2	11 26 13.009	–0.024	03 38 32.78	0.00	4.71	E
14.09.	SS.ZS.	743.6	23.2	1	11 29 48.151	0.007	03 15 32.15	–0.36	4.71	E
09.10.	SS.MD.	753.2	15.6	–	13 00 05.235	0.022	–06 24 52.53	–0.18	4.78	E
10.10.	SS MD.	752.0	16.8	1	13 03 45.668	0.006	–06 47 35.93	–0.14	4.79	E
17.10.	SS.MD.	750.2	11.4	1	13 29 43.303	0.026	–09 23 47.59	–0.09	4.80	E
18.10.	SS.MD.	745.4	12.5	2	13 33 28.150	–0.010	–09 45 37.49	–0.15	4.80	E
19.10.	MD.ZS.	745.4	15.6	2	13 37 13.633	0.035	–10 07 19.03	–0.03	4.80	E
23.10.	SS.DŠ.	746.7	16.0	2	13 52 22.210	–0.022	–11 32 33.53	–0.51	4.82	E
24.10.	SS.MD	745.3	16.6	3	13 56 11.085	–0.009	–11 53 27.17	0.36	4.82	E
25.10.	SS.MD.	745.5	16.9	4	14 00 00.676	–0.015	–12 14 09.97	–0.52	4.82	W
26.10.	SS.MD.	744.4	18.0	2	14 03 50.992	–0.032	–12 34 41.52	0.09	4.82	W
08.11.	MD.	743.8	13.4	–	14 54 54.897	0.049	–16 41 15.97	0.41	4.86	W
09.11.	MD.ZS.	742.7	13.6	–	14 58 56.276	–0.037	–16 58 26.47	0.05	4.86	W
05.12.	MD.ZS.	753.2	4.7	1	16 48 19.818	–0.017	–22 25 22.69	–0.10	4.93	W
13.12.	MD.ZS.	745.0	4.6	1	17 23 27.449	0.020	–23 10 44.17	–0.31	4.96	W
1985.								1980.+		
04.04.	SS MD.	745.6	17.8	–	00 53 47.573	0.028	05 45 26.13	0.10	5.26	E
05.04.	SS.MD.	741.1	20.1	–	00 57 26.592	0.036	06 08 14.04	–0.36	5.26	E
08.05.	SS.MD.	740.7	20.5	5	03 01 19.971	–0.021	17 07 57.43	0.05	5.35	W
17.05.	SS.MD.	741.7	21.9	–	03 36 36.982	0.024	19 21 54.92	0.32	5.38	W
20.05.	MD.ZS.	742.1	22.7	2	03 48 34.726	0.002	20 00 50.13	–0.18	5.38	W
21.05.	SS.MD.	738.6	23.0	1	03 52 35.074	–0.032	20 13 07.88	–0.36	5.39	W
28.05.	MD.	741.9	24.7	3	04 20 51.598	0.028	21 29 16.57	–0.49	5.41	W
05.06.	SS.MD.	744.1	22.6	2	04 53 36.472	–0.042	22 33 52.63	0.09	5.43	E
06.06.	SS.ZS.	742.3	24.5	2	04 57 43.735	–0.036	22 40 12.24	–0.18	5.43	E
07.06.	MD.	740.9	25.4	4	05 01 51.316	0.014	22 46 08.07	0.02	5.43	E
10.06.	MD.	745.2	23.5	3	05 14 15.782	0.035	23 01 31.50	–0.40	5.44	E
01.07.	MD ZS.	743.1	24.6	3	06 41 29.981	0.037	23 05 56.42	0.20	5.50	E
10.07.	SS.MD.	741.8	22.6	4	07 18 29.852	–0.030	22 12 57.86	0.26	5.53	W
15.07.	SS.MD.	746.0	26.0	1	07 38 49.408	0.005	21 30 01.29	–0.15	5.54	W
16.07.	SS.MD.	746.2	25.8	3	07 42 51.901	0.019	21 20 19.14	0.32	5.54	W
17.07.	SS.MD.	745.2	28.0	2	07 46 53.882	0.030	21 10 15.21	0.00	5.54	W
19.07.	SS.MD.	741.0	23.1	3	07 54 56.238	–0.018	20 49 02.95	–0.38	5.55	W
22.07.	SS.MD.	751.2	21.8	3	08 06 55.529	0.036	20 14 37.19	–0.23	5.56	W
23.07.	SS.MD.	748.6	22.6	4	08 10 54.113	0.040	20 02 27.64	0.21	5.56	W
25.07.	SS.MD.	745.3	24.2	1	08 18 49.466	–0.020	19 37 08.67	0.08	5.56	W
26.07.	SS.MD.	743.3	25.1	2	08 22 46.226	0.037	19 23 59.82	–0.46	5.57	W
29.07.	SS MD.	740.1	29.6	1	08 34 32.808	–0.055	18 42 39.22	0.27	5.57	W
30.07.	SS.ZS.	739.8	30.0	3	08 38 27.099	–0.002	18 28 15.29	0.16	5.58	W
01.08.	SS.ZS.	742.7	24.1	5	08 46 13.836	0.007	17 58 33.47	0.72	5.58	W

Table 1 (continued)

Date of observ.	ob-serv.	Ba	t°C	n	α	(O–C)$_\alpha$	δ	(O–C)$_\delta$	Ep	cla-mp
13.08.	SS.ZS.	746.5	28.0	4	09 32 04.793	–	14 37 06.50	0.44	5.62	W
14.08.	SS.ZS.	747.0	28.5	4	09 35 50.401	–0.061	14 18 40.68	0.25	5.62	W
15.08.	SS.ZS.	746.4	28.4	4	09 39 35.475	0.006	14 00 01.15	0.07	5.62	W
16.08.	SS.ZS.	745.1	28.2	8	09 43 20.017	0.035	13 41 08.25	0.55	5.62	W
19.08.	MD.ZS.	744.7	21.9	4	09 54 30.516	–0.046	12 43 12.60	0.26	5.63	W
21.08.	MD.ZS.	746.3	23.3	7	10 01 54.995	–0.014	12 03 34.72	0.28	5.64	W
22.08.	SS.ZS.	746.7	24.9	7	10 05 36.512	–0.001	11 43 28.56	–0.21	5.64	W
23.08.	SS.MD.	744.1	27.6	7	10 09 17.562	–0.067	11 23 11.37	–0.03	5.64	W
19.09.	SS.MD.	750.4	22.8	3	11 46 53.901	–0.070	01 25 03.21	0.22	5.72	E
20.09.	SS.MD.	745.7	22.4	2	11 50 29.132	0.061	01 01 45.42	0.18	5.72	E
30.09.	MD.	750.8	16.3	2	12 26 27.632	–0.036	–02 51 41.92	–0.59	5.75	W
02.10.	SS.MD.	750.6	18.3	3	12 33 41.887	0.014	–03 38 12.90	0.69	5.75	W
03.10.	SS.MD.	749.3	19.9	1	12 37 19.489	–0.001	–04 01 24.98	0.09	5.76	E
04.10.	SS.MD.	746.7	21.8	3	12 40 57.437	–0.014	–04 24 34.34	–0.52	5.76	E
07.10.	SS.MD.	747.1	19.8	2	12 51 53.567	–0.046	–05 33 42.66	–0.37	5.77	E
14.10.	SS.MD.	750.2	11.2	3	13 17 40.332	0.012	–08 12 19.59	–0.44	5.79	E
22.10.	SS.MD.	748.8	14.3	2	13 47 40.961	0.007	–11 06 35.34	0.24	5.81	E
07.11.	SS.MD.	739.9	8.3	2	14 49 57.025	–0.055	–16 19 36.13	–0.14	5.85	E
03.12.	SS.ZS.	749.3	10.9	2	16 38 34.618	0.037	–22 07 34.80	0.55	5.92	W
04.12.	SS.ZS.	749.5	11.0	2	16 42 55.225	–0.020	–22 15 47.46	0.28	5.93	W
09.12.	MD.ZS.	744.6	11.5	3	17 04 46.682	0.044	–22 50 18.31	–0.18	5.94	W
13.12.	SS.ZS.	752.2	7.5	1	17 22 24.250	0.040	–23 09 50.63	0.15	5.95	W
24.12.	SS.MD.	744.7	4.0	2	18 11 11.354	0.036	–23 25 13.15	0.55	5.98	W
25.12.	SS.MD.	743.0	8.0	2	18 15 37.736	–0.018	–23 23 47.68	0.19	5.98	W
1986.									1980+	
06.01.	MD.ZS.	734.3	4.2	4	19 08 38.618	0.037	–22 30 28.04	0.68	6.02	W
08.01.	MD.ZS.	739.6	2.0	2	19 17 23.902	–0.015	–22 15 13.12	–0.38	6.02	W
21.01.	SS.MD.	750.3	6.8	6	20 13 19.206	–0.043	–19 55 04.79	0.05	6.06	W
27.01.	SS.MD.	745.0	3.4	6	20 38 25.823	0.010	–18 28 32.46	0.30	6.07	W
29.01.	SS.MD.	744.9	5.3	3	20 46 41.610	0.021	–17 56 57.55	–0.07	6.08	W
07.04.	SS.ZS.	743.6	22.1	–	01 03 51.909	0.028	06 48 02.12	0.04	6.27	W
09.04.	SS.MD.	736.8	22.8	–	01 11 11.661	–0.014	07 32 56.72	–0.27	6.27	W
21.04.	MD.ZS	742.1	13.2	–	01 55 35.483	–0.062	11 50 02.95	–0.27	6.30	W
22.04.	MD.ZS.	743.6	17.8	4	01 59 19.870	0.015	12 10 19.82	0.55	6.31	W
23.04.	SS.MD.	744.8	19.9	5	02 03 04.695	0.024	12 30 24.62	–0.14	6.31	W
24.04.	SS.MD.	745.0	22.9	3	02 06 49.979	0.028	12 50 17.07	0.01	6.31	W
25.04.	SS.MD.	743.3	23.8	3	02 10 35.739	–0.013	13 09 56.87	–0.05	6.31	W
28.04.	SS.MD.	735.0	23.6	5	02 21 56.030	–0.022	14 07 37.64	–0.26	6.32	W
05.05.	MD.ZS.	740.9	20.7	5	02 48 42.211	–0.048	16 13 53.57	0.49	6.34	W
06.05.	SS.MD.	741.6	20.3	4	02 52 33.919	0.012	16 30 53.98	0.47	6.34	W
07.05.	SS.MD.	743.8	20.7	5	02 56 26.203	0.016	16 47 37.94	–0.30	6.35	W
08.05.	SS.MD.	743.8	20.2	3	03 00 19.063	0.032	17 04 05.15	0.27	6.35	E
13.05.	SS.MD.	744.8	18.8	1	03 19 51.963	0.000	18 21 58.71	0.03	6.36	E
14.05.	MD.ZS.	743.2	21.0	4	03 23 48.240	0.027	18 36 38.79	0.36	6.37	E
26.05.	MD.ZS.	750.8	19.8	3	04 11 45.542	–0.013	21 06 48.99	–0.17	6.40	E
29.05.	MD.ZS.	749.8	24.7	–	04 23 56.424	–0.040	21 36 26.50	–0.29	6.41	W
30.07.	SS.MD.	743.3	24.1	–	08 37 30.485	0.028	18 31 47.97	–0.35	6.58	E
31.07.	SS.MD.	743.7	26.0	1	08 41 24.429	0.033	18 17 09.94	–0.38	6.58	E
04.08.	MD.	744.5	28.0	3	08 56 54.255	0.046	17 05 40.56	0.42	6.59	E
05.08.	SS.MD.	743.2	28.5	3	09 00 45.211	0.034	16 59 35.40	–0.27	6.59	E
11.08.	MD.	744.2	27.1	3	09 23 38.314	0.032	15 17 28.89	0.49	6.61	E
12.08.	SS.MD.	742.1	28.2	1	09 27 25.089	0.026	14 59 34.85	–0.34	6.61	E
13.08.	SS.MD.	739.6	26.7	1	09 31 11.288	0.037	14 41 26.55	–0.32	6.62	E
18.08.	MD.ZS.	741.0	27.3	3	09 49 53.958	–0.030	13 07 22.56	–0.78	6.63	W
28.08.	SS.MD.	739.8	25.8	3	10 26 43.247	0.005	09 44 21.73	–0.84	6.66	E
02.09.	SS.MD.	745.5	19.2	1	10 44 53.844	0.019	07 56 39.75	0.27	6.67	E
04.09.	SS.MD.	742.3	20.6	3	10 52 08.026	–0.018	07 12 38.51	0.32	6.68	E
17.09.	MD.ZS.	742.7	26.9	2	11 38 51.701	0.011	02 17 07.69	0.31	6.71	E
18.09.	MD.ZS.	744.0	26.6	2	11 42 26.730	0.002	01 53 55.95	–0.33	6.71	E

Table 1 (continued)

Date of observ.	ob-serv.	Ba	t°C	n	α	(O–C)$_\alpha$	δ	(O–C)$_\delta$	Ep	cla-mp
29.09.	MD ZS.	753.8	16.5	2	12 21 58.593	–0.018	–02 22 44.46	0.41	6.74	W
01.10.	MD.	752.0	15.7	4	12 29 12.407	–0.020	–03 09 18.33	–	6.75	W
03.10.	SS MD.	746.8	18.4	5	12 36 27.392	0.036	–03 55 52.20	0.19	6.76	W
06.10.	SS.MD.	751.1	16.6	2	12 47 22.387	0.040	–05 05 15.76	–0.30	6.76	W
07.10.	SS.MD.	748.1	17.4	3	12 51 01.459	0.044	–05 28 16.38	–0.18	6.77	W
10.10.	SS.MD.	746.8	17.5	3	13 02 01.117	–0.020	–06 36 51.05	–0.11	6.77	E
10.11.	SS.MD.	751.2	9.8	6	15 01 02.983	0.037	–17 07 21.35	0.33	6.86	W
11.11.	SS.MD.	752.4	11.1	2	15 05 05.673	–0.016	–17 24 05.49	0.18	6.86	W
17.11.	SS.MD.	755.2	12.4	3	15 29 39.453	0.019	–18 57 58.95	0.19	6.88	E
30.12.	SS.MD.	738.4	9.6	2	18 36 43.390	0.040	–23 10 37.62	–0.06	6.99	W

Table II. Data on the Mercury observations

Date of observ.	ob-serv.	Ba	t°C	n	α	(O–C)$_\alpha$	δ	(O–C)$_\delta$	Ep	cla-mp
1984.									1980+	
16.04.	SS.MD.	742.6	19.0	–	$02^h09^m41^s.145$	–0.042	15°55'10".62	0.15	4.29	W
14.06.	SS.MD.	739.8	20.1	1	04 46 53.331	0.052	22 03 48.17	–0.23	4.46	E
28.06.	MD.	742.9	24.2	3	06 58 56.635	–0.021	24 26 23.24	–0.28	4.49	E
10.07.	MD.	745.3	23.2	–	08 38 07.564	–0.017	20 12 54.54	0.20	4.53	W
11.07.	SS MD.	745.9	25.9	–	08 45 09.324	0.043	19 42 04.02	–0.21	4.53	W
12.07.	SS.MD.	745.6	29.5	–	08 51 59.673	–0.010	19 10 18.62	0.09	4.53	W
13.07.	SS.MD.	744.8	29.9	–	08 58 38.747	–0.003	18 37 44.77	0.18	4.54	W
19.07.	MD ZS.	744.9	20.4	–	09 34 44.285	–0.020	15 10 48.89	–0.01	4.55	W
23.07.	MD ZS.	744.3	26.4	–	09 55 18.179	–	12 48 12.27	0.09	4.56	W
09.08.	SS.ZS.	743.3	25.4	1	10 49 41.392	–0.033	04 11 08.08	–0.20	4.61	E
12.09.	SS.ZS.	744.2	18.9	1	10 16 18.368	–0.018	10 49 16.38	0.11	4.70	E
13.09.	SS.ZS.	744.9	20.6	2	10 19 49.670	0.035	10 45 20.16	–0.06	4.71	E
14.09.	SS.ZS	743.6	21.9	1	10 23 48.672	–0.056	10 37 26.49	0.06	4.71	E
1985.									1980+	
08.05.	MD.ZS.	740.7	19.0	5	01 26 10.130	0.013	05 46 43.68	–0.01	5.35	W
28.05.	MD.	741.9	24.3	3	03 31 54.035	0.042	18 04 32.94	0.29	5.41	W
01.07.	MD.ZS.	743.1	25.1	3	08 20 53.659	–0.067	20 58 19.10	–0.25	5.50	E
17.07.	SS.MD.	745.2	28.5	2	09 32 11.906	–0.071	13 17 40.85	–0.80	5.54	W
22.07.	SS.MD.	751.2	22.4	3	09 42 23.849	–0.022	11 16 27.75	0.21	5.56	W
23.08.	SS MD.	744.1	26.2	7	09 02 05.837	0.069	14 59 52.81	–0.58	5.64	W
09.12.	MD.	744.6	10.2	3	15 48 57.101	–0.015	–17 13 21.10	–0.08	5.94	W
25.12.	ZS.	743.0	7.5	2	16 49 45.389	0.028	–21 17 27.62	–0.26	5.98	W
1986.									1980+	
21.01.	MD.	750.3	6.4	6	19 45 26.297	0.038	–23 01 07.93	0.17	6.06	W
07.04.	SS.ZS.	743.6	19.8	–	23 27 40.670	0.011	–04 52 07.08	–0.53	6.27	W
09.04.	SS.MD.	736.8	20.4	–	23 33 23.123	–0.060	–04 36 49.75	0.14	6.27	W
21.04.	MD.ZS.	742.1	11.1	–	00 21 42.484	0.062	–00 35 44.75	0.55	6.30	W
22.04.	MD.	743.6	16.0	4	00 26 35.827	–0.026	–00 05 57.72	0.61	6.31	W
23.04.	SS.MD.	744.8	17.8	5	00 31 36.009	0.016	00 25 05.12	0.38	6.31	W
24.04.	SS.MD.	745.0	21.2	3	00 36 42.938	–0.032	00 57 21.22	–0.20	6.31	W
25.04.	MD.ZS.	743.3	21.9	3	00 41 56.560	0.026	01 30 48.06	–0.19	6.31	W
05.05.	MD.ZS.	740.9	19.3	5	01 40 29.870	0.037	08 00 38.48	–0.09	6.34	W
06.05.	SS.MD.	741.6	19.3	4	01 47 01.769	0.005	08 44 07.03	–0.17	6.34	W
07.05.	MD.ZS.	743.8	19.4	5	01 53 41.868	0.035	09 28 11.03	–0.26	6.35	W
13.05.	MD.ZS.	744.8	18.3	1	03 36 49.015	0.044	14 00 26.30	0.05	6.36	E
14.05.	ZS.	743.2	20.2	4	02 44 33.419	–0.012	14 46 10.28	–0.38	6.37	E
26.05.	ZS.	750.8	19.8	3	04 28 54.574	0.036	22 44 51.24	0.03	6.40	E
29.05.	MD.	749.8	25.2	–	04 56 46.459	0.040	24 01 46.49	0.58	6.41	W
31.07.	SS.MD.	743.7	24.6	1	07 49 02.797	–0.015	16 50 44.14	0.22	6.58	E
04.08.	MD.	744.5	27.1	3	07 48 43.435	–0.012	17 47 13.75	0.06	6.59	E
11.08.	MD.	744.2	26.3	3	08 05 36.602	–0.020	18 54 49.87	–0.07	6.61	E
28.08.	MD.	739.8	25.1	3	09 57 40.490	0.045	14 12 36.07	0.10	6.66	E
02.09.	SS.MD.	745.5	19.0	1	10 35 35.845	0.028	10 46 58.85	–0.45	6.67	E

Table III. Data on the Venus observations

Date of observ.	ob-serv.	Ba	t°C	n	α	$(O-C)_\alpha$	δ	$(O-C)_\delta$	Ep	cla-mp
1984									1980+	
15.03.	MD.	742.3	4.6	3	22h13m58.s686	0.058	−12°05' 47".03	0.48	4.21	W
16.03.	MD.	738.8	4.8	2	22 18 44.080	0.015	−11 40 59.25	0.25	4.21	W
29.03	SS.MD	741.4	15.6	3	23 19 20.968	−0.037	−05 53 53.52	0.35	4.24	W
16.04.	MD	742.6	17.8	–	00 41 08.602	0.007	02 47 17.74	−0.70	4.29	W
20.04.	MD.	746.8	11.5	–	00 59 18.179	−0.027	04 43 29.92	0.47	4.30	W
26.04.	MD.	740.7	11.7	1	01 26 43.243	0.018	07 34 50.50	−0.18	4.32	W
03.05.	SS.MD.	742.4	17.4	–	01 59 08.162	−0.009	10 47 10.33	0.38	4.34	W
07.05.	SS.MD.	737.9	21.1	–	02 17 56.090	0.053	12 31 54.27	0.34	4.35	W
18.05.	SS.MD.	743.2	18.2	1	03 10 56.055	0.016	16 53 08.22	0.70	4.38	W
19.05.	SS.MD.	739.0	21.5	–	03 15 51.522	–	17 14 33.34	0.36	4.38	W
28.06	MD.	742.9	24.1	3	06 45 15.672	−0.055	23 42 47.90	0.40	4.49	E
10.07.	MD.	745.3	22.2	–	07 49 05.444	0.029	22 09 11.01	0.41	4.53	W
11.07.	SS.MD.	745.9	26.0	–	07 54 19.813	−0.008	21 57 02.04	−0.36	4.53	W
12.07.	SS.MD.	745.6	28.4	3	07 59 33.252	−0.055	21 44 14.82	−0.58	4.53	W
13.07	SS.MD.	744.8	29.2	–	08 04 45.727	0.004	21 30 49.84	−0.08	4.54	W
19.07.	MD.ZS.	744.9	20.1	–	08 35 38.773	0.022	19 57 36.14	0.37	4.55	W
23.07.	MD.ZS.	744.3	25.8	–	08 55 51.907	0.034	18 44 01.31	0.41	4.56	W
06.08.	SS.ZS.	743.7	27.4	–	10 04 10.647	−0.001	13 25 29.58	−0.13	4.60	E
09.08.	SS.ZS.	743.3	25.3	1	10 18 20.327	0.032	12 07 00.77	0.28	4.61	E
16.08.	MD.ZS.	741.5	21.8	–	10 50 49.539	−0.001	08 53 15.73	−0.25	4.63	E
20.08.	SS.	746.4	21.2	–	11 09 05.752	−0.015	06 57 05.39	−0.47	4.64	E
23.08.	MD.ZS.	743.8	22.2	1	11 22 41.292	−0.003	05 27 56.26	0.44	4.65	E
29.08.	MD.ZS.	746.9	20.4	1	11 49 39.715	−0.022	02 25 50.48	0.47	4.66	W
05.09.	SS.ZS.	739.2	27.3	1	12 20 56.037	0.023	−01 10 03.22	−0.55	4.68	E
06.09.	MD.ZS.	740.1	27.0	1	12 25 23.804	−0.065	−01 40 58.38	−0.19	4.69	E
12.09.	SS.ZS.	744.2	21.1	1	12 52 13.142	0.029	−04 45 43.56	−0.29	4.70	E
13.09.	SS.ZS.	744.9	22.4	2	12 56 42.237	−0.065	−05 16 16.86	−0.24	4.71	E
14.09.	SS.ZS.	743.6	24.1	1	13 01 11.699	0.042	−05 46 44.22	0.15	4.71	E
09.10.	SS.	753.2	16.4	–	14 57 18.339	−0.044	−17 19 50.41	0.39	4.78	E
10.10.	MD.	752.0	17.3	1	15 02 09.699	−0.055	−17 43 20.24	0.42	4.79	E
17.10.	MD.	750.2	12.0	1	15 36 42.445	−0.011	−20 14 47.44	0.27	4.80	E
19.10.	MD.ZS.	745.4	17.9	2	15 46 45.419	−0.006	−20 53 30.51	−0.25	4.80	E
23.10.	SS.MD.	746.7	17.1	2	16 07 05.345	0.025	−22 04 14.77	0.91	4.82	E
24.10.	MD.	745.3	17.5	3	16 12 13.139	−0.031	−22 20 28.05	0.42	4.82	E
25.10.	SS.MD.	745.5	18.0	4	16 17 22.010	−0.045	−22 36 04.88	−0.73	4.82	W
26.10.	MD.	744.4	19.2	2	16 22 31.924	−0.080	−22 51 04.63	−0.07	4.82	W
08.11.	MD.	743.8	15.4	–	17 30 55.568	−0.058	−25 05 33.76	−0.30	4.86	W
09.11.	MD.ZS.	742.7	13.5	–	17 36 15.157	−0.020	−25 10 59.63	0.26	4.86	W
05.12.	MD.	753.2	5.0	1	19 52 54.810	−0.032	−23 16 07.85	0.18	4.93	W
1985.									1980+	
04.04.	SS.MD.	745.6	16.9	–	00 38 32.303	−0.056	12 27 21.29	−0.19	5.26	E
05.04.	SS.MD.	741.1	20.0	–	00 36 24.533	−0.006	12 05 32.91	0.51	5.26	E
08.05.	MD.	740.7	17.2	5	00 32 28.130	0.024	04 18 01.84	0.84	5.35	W
17.05	MD.ZS	741.7	19.4	–	00 52 53.949	−0.024	05 00 20.65	−0.64	5.38	W
20.05.	MD.	742.1	18.9	2	01 00 57.003	0.017	05 26 52.00	0.10	5.38	W
21.05.	MD.	738.6	20.4	1	01 03 44.946	0.017	05 36 51.35	0.23	5.39	W
28.05.	MD.	741.9	22.3	3	01 24 45.358	−0.044	07 00 20.84	−0.02	5.41	W
05.06.	MD.ZS.	744.1	19.8	2	01 51 20.541	0.056	08 57 53.89	−0.66	5.43	E
06.06.	MD.	742.3	21.8	2	01 54 50.073	0.024	09 13 46.67	0.36	5.43	E
07.06.	MD.ZS.	740.9	22.3	4	01 58 21.695	0.017	09 29 51.45	0.70	5.43	E
10.06.	MD.	745.2	16.7	3	02 09 08.679	−0.046	10 19 06.62	0.15	5.44	E
01.07.	MD.	743.1	21.0	3	03 32 07.551	0.014	16 10 30.53	−0.53	5.50	E
10.07.	SS.MD.	741.8	19.0	4	03 58 02.123	−0.001	18 22 04.01	−0.46	5.53	W
15.07.	MD.	746.0	22.2	1	04 33 59.030	−0.014	19 24 34.81	−0.23	5.54	W
16.07.	SS.MD.	746.2	24.0	3	04 38 34.985	0.019	19 35 59.18	−1.00	5.54	W
17.07.	SS.MD.	745.2	24.3	2	04 43 12.265	−0.036	19 46 59.96	0.25	5.54	W
19.07.	SS.MD.	741.0	22.0	3	04 52 30.686	0.046	20 07 48.03	0.39	5.55	W
22.07.	SS.MD.	751.2	19.1	3	05 06 37.513	0.002	20 35 46.56	0.50	5.56	W

Table III. (continued)

Date of observ.	ob-serv.	Ba	t°C	n	α	(O−C)α	δ	(O−C)δ	Ep	cla-mp
23.07.	MD.	748.6	19.9	4	05 11 22.122	0.011	20 44 11.99	0.28	5.56	W
25.07.	SS.MD.	745.3	21.4	1	05 20 54.667	−0.018	20 59 38.26	−0.51	5.56	W
26.07.	SS.MD.	743.3	22.3	2	05 25 42.543	−0.016	21 06 38.05	0.28	5.57	W
29.07.	MD.	740.1	26.2	1	05 40 12.195	0.054	21 24 38.04	0.24	5.57	W
30.07.	SS.ZS.	739.8	27.2	3	05 45 03.969	0.030	21 29 36.68	−0.38	5.58	W
01.08.	SS.ZS.	742.7	21.8	5	05 54 50.128	−0.020	21 37 59.18	0.23	5.58	W
02.08.	SS.ZS.	741.0	24.8	3	05 59 44.433	0.036	21 41 22.19	−0.12	5.58	W
13.08.	SS.ZS.	746.5	24.5	–	06 54 22.067	–	21 41 28.79	−0.27	5.62	W
14.08.	SS.ZS.	747.0	25.2	4	06 59 22.434	0.037	21 38 00.84	−0.22	5.62	W
15.08.	SS.ZS.	746.4	25.1	4	07 04 22.977	−0.002	21 33 57.53	0.16	5.62	W
16.08.	SS.ZS.	745.1	25.2	8	07 09 23.645	−0.055	21 29 18.81	−0.03	5.62	W
19.08.	MD.ZS.	744.7	19.5	4	07 24 25.890	0.007	21 11 50.17	−0.01	5.63	W
21.08.	MD.ZS	746.3	21.0	7	07 34 27.127	−0.006	20 57 14.44	0.42	5.64	W
22.08.	SS.ZS.	746.7	22.2	7	07 39 27.541	0.012	20 49 3.87	−0.22	5.64	W
23.08.	MD.ZS.	744.1	24.4	7	07 44 27.764	−0.061	20 40 18.36	−0.28	5.64	W
19.09.	MD.	750.4	19.9	3	09 56 35.424	0.006	13 21 48.37	0.26	5.72	E
20.09.	MD.	745.7	18.8	2	10 01 20.053	−0.045	12 59 04.21	−0.50	5.72	E
02.10.	MD.	750.6	16.4	3	10 57 26.623	−0.001	08 00 03.03	0.36	5.75	W
03.10.	MD.ZS.	749.3	17.8	1	11 02 03.707	−0.046	07 33 16.43	−0.13	5.76	E
04.10.	MD.	746.7	20.3	3	11 06 40.373	0.035	07 06 15.75	−0.15	5.76	E
07.10.	MD.	747.1	18.3	2	11 20 28.138	−0.036	05 43 56.21	0.03	5.77	E
14.10.	MD.ZS.	750.2	10.0	3	11 52 30.247	0.014	02 25 49.15	−0.07	5.79	E
07.11.	MD.ZS.	739.9	7.8	2	13 43 05.337	0.007	−09 06 06.87	0.27	5.85	E
03.12.	SS.ZS.	749.3	10.5	2	15 51 15.516	−0.061	−19 20 48.70	−0.06	5.92	W
04.12.	SS.ZS.	749.5	10.6	2	15 56 26.901	0.012	−19 38 37.81	−0.25	5.93	W
09.12.	MD.	744.6	10.7	3	16 22 41.197	−0.016	−20 59 13.86	−0.52	5.94	W
13.12.	MD.	752.2	7.2	1	16 44 00.081	−0.002	−21 52 51.00	0.11	5.95	W
24.12.	SS.MD.	744.7	3.8	2	17 43 44.521	−0.006	−23 25 20.94	−0.53	5.98	W
1986.									1980+	
06.01.	MD.	734.3	4.0	4	$18^h55^m11^s.737$	0.037	−23°22′43″.62	0.18	6.02	W
08.01.	MD.ZS.	739.6	8.0	2	19 06 08.400	−0.055	−23 11 21.38	0.36	6.02	W
27.01.	SS.MD.	745.0	3.6	6	20 47 22.310	−0.020	−19 07 56.68	−0.28	6.07	W
29.01.	MD.ZS.	744.9	5.4	3	20 57 38.525	0.044	−18 29 28.72	−0.14	6.08	W
07.04.	SS.MD.	743.6	22.8	–	02 16 34.162	0.040	13 18 00.23	0.46	6.27	W
09.04.	MD.	736.8	22.8	–	02 26 02.941	−0.020	14 10 42.69	0.39	6.27	W
23.04.	MD.	744.8	21.3	5	03 34 17.089	−0.016	19 35 14.83	0.48	6.31	W
24.04.	MD.	745.0	23.4	3	03 39 17.447	0.005	19 54 55.87	0.43	6.31	W
25.04.	SS.MD.	743.3	24.1	3	03 44 18.870	0.019	20 14 05.21	0.09	6.31	W
28.04.	SS.MD.	735.0	24.1	5	03 59 29.449	0.037	21 08 16.62	−0.06	6.32	W
05.05.	ZS.	740.9	21.2	5	04 35 28.571	−0.030	22 54 16.52	−0.06	6.34	W
06.05.	MD.	741.6	20.7	4	04 40 40.567	−0.026	23 06 56.26	0.18	6.34	W
07.05.	ZS.	743.8	21.6	5	04 45 53.346	−0.060	23 18 57.20	−0.40	6.35	W
08.05.	MD.	743.8	21.5	3	04 51 06.866	0.035	23 30 18.87	0.03	6.35	E
13.05.	MD.	744.8	19.6	1	05 17 23.883	0.005	24 17 03.35	0.55	6.36	E
14.05.	ZS.	743.2	21.8	4	05 22 40.793	0.037	24 24 20.86	0.15	6.37	E
26.05.	ZS.	750.8	20.7	3	06 26 14.545	0.044	24 56 33.70	0.26	6.40	E
30.07.	MD.	743.3	25.2	–	11 27 50.503	−0.028	03 56 37.88	0.70	6.58	E
04.08.	MD.	744.5	28.6	3	11 47 09.329	−0.017	01 27 28.09	0.27	6.59	E
05.08.	MD.	743.2	27.9	3	11 50 58.056	0.005	00 57 31.29	0.25	6.59	E
11.08.	MD.	744.2	28.0	3	12 13 30.017	−0.026	−02 02 04.32	−0.38	6.61	E
12.08.	MD.	742.1	30.1	1	12 17 11.999	0.044	−02 31 53.45	0.47	6.61	E
13.08.	MD.	739.6	28.1	1	12 20 53.030	−0.015	−03 01 38.94	0.47	6.62	E
18.08.	MD.	741.0	29.4	3	12 39 03.778	−0.050	−05 29 09.39	0.06	6.63	W
28.08.	MD.	739.8	27.6	3	13 14 09.926	−0.014	−10 13 46.45	0.62	6.66	E
17.09.	MD.	742.7	28.1	2	14 17 19.631	−0.039	−18 27 08.71	−0.27	6.71	E
18.09.	MD.	744.0	27.7	2	14 20 05.793	0.026	−18 47 59.36	0.53	6.71	E
01.10.	MD.	752.0	17.2	4	14 50 15.177	0.032	−22 48 34.17	–	6.75	W
03.10.	SS.MD.	746.8	20.0	5	14 53 38.913	−0.017	−22 59 06.07	−0.27	6.76	W
06.10.	SS.MD.	751.1	17.6	2	14 57 56.011	−0.045	−23 32 35.76	0.28	6.76	W
07.10.	MD.	748.1	18.9	3	14 59 07.651	−0.015	−23 42 14.48	−0.10	6.77	W
10.10.	SS.MD.	746.8	18.4	3	15 01 56.409	0.036	−24 06 11.79	0.36	6.77	E
10.11.	MD.	751.2	9.3	6	14 24 07.464	0.045	−18 28 37.26	0.32	6.86	W
11.11.	MD.	752.4	10.9	2	14 22 16.398	−0.026	−18 03 55.17	0.17	6.86	W

Table IV. Data on the Mars observations

Date of observ.	ob-serv.	Ba	t°C	n	α	(O–C)α	δ	(O–C)δ	Ep	cla-mp
1984.									1980+	
16.04.	MD.	742.6	14.7	8	$15^h 42^m 24^s.191$	–0.026	–18 46 26.46	0.39	4.29	W
21.04.	MD.	746.7	7.7	9	15 38 54.093	0.009	–18 44 58.15	–0.05	4.31	W
21.05.	SS.MD.	736.4	16.1	21	14 57 47.360	0.048	–17 33 05.88	0.09	4.39	W
31.05.	SS.MD.	738.6	14.5	19	14 45 17.641	–0.026	–17 06 08.83	0.05	4.42	E
03.06.	SS.MD.	737.8	19.2	20	14 42 21.907	–0.056	–17 00 27.27	0.05	4.43	E
05.06.	SS.MD.	739.7	20.7	12	14 40 39.881	–	–16 57 30.02	0.04	4.43	E
10.06.	SS.MD.	746.0	16.3	20	14 37 20.898	0.030	–16 53 23.86	–0.28	4.44	E
13.06.	SS.MD.	748.7	16.0	14	14 36 01.003	0.041	–16 53 19.83	–0.55	4.45	E
21.06.	MD.ZS.	738.9	23.2	3	14 34 53.031	0.045	–17 02 13.73	0.26	4.47	E
25.06.	SS.MD.	743.0	13.7	3	14 35 36.724	0.024	–17 11 35.89	–0.05	4.49	E
27.06	SS.MD.	745.5	17.8	5	14 36 17.425	0.029	–17 17 28.72	0.40	4.49	E
28.06.	SS.MD.	739.0	22.5	6	14 36 42.396	0.022	–17 20 42.63	–0.20	4.49	E
01.07.	MD.	746.2	18.6	4	14 38 15.387	–	–17 31 32.34	0.14	4.50	W
02.07.	SS.MD.	738.6	23.3	10	14 38 52.285	0.054	–17 35 30.84	–0.17	4.51	W
09.07.	SS.MD.	744.2	18.9	10	14 44 28.832	–0.014	–18 07 59.89	0.35	4.52	W
10.07.	SS.MD.	744.6	22.0	15	14 45 27.542	–0.002	–18 13 14.61	–0.12	4.53	W
11.07.	MD.ZS.	745.3	22.4	14	14 46 28.772	0.027	–18 18 37.45	–0.25	4.53	W
12.07.	SS.MD.	744.8	27.2	17	14 47 32.476	–0.019	–18 24 08.05	0.18	4.53	W
19.07.	MD.	744.9	23.1	20	14 56 04.475	0.037	–19 05 53.67	0.25	4.55	W
22.07.	MD.	744.6	22.0	3	15 00 17.490	–0.007	–19 25 13.77	0.81	4.56	W
25.07.	MD.	743.0	21.4	3	15 04 49.542	–0.033	–19 45 14.68	0.17	4.57	W
01.08.	SS.	743.0	25.3	4	15 16 34.356	0.001	–20 33 53.00	0.25	4.59	E
09.08.	SS.	741.0	24.1	5	15 31 49.717	–0.004	–21 30 55.68	–0.01	4.61	E
22.08.	MD.	748.0	20.2	11	16 00 13.732	–0.042	–23 00 20.33	0.87	4.65	E
23.08.	MD.	742.8	21.3	21	16 02 34.957	0.054	–23 06 48.56	0.23	4.65	E
28.08.	MD.	747.0	17.6	26	16 14 41.362	0.022	–23 37 52.71	0.23.	4.66	W
03.09.	SS.	744.6	24.5	18	16 29 55.276	–0.056	–24 11 44.50	–0.33	4.68	W
04.09.	MD.	740.5	24.7	28	16 32 31.770	–0.034	–24 16 7.63	–0.04	4.68	W
05.09.	SS.	739.2	23.3	3	16 35 09.395	–0.009	–24 22 02.76	0.09	4.68	E
06.09.	SS.	739.4	22.7	4	16 37 48.127	0.016	–24 26 59.64	0.06	4.69	E
12.09.	SS.ZS.	744.2	21.0	3	16 54 02.697	0.021	–24 53 34.02	0.07	4.70	E
13.09.	SS.ZS.	744.8	21.5	3	16 56 48.659	–0.021	–24 57 26.47	–0.11	4.71	E
18.10.	SS.	745.4	13.2	4	18 41 31.490	–0.003	–25 06 38.53	0.00	4.80	E
19.10.	MD.ZS.	745.4	16.5	5	18 44 39.807	–0.022	–25 02 48.06	–0.44	4.80	E
23.10.	MD.	746.7	16.8	5	18 57 15.294	–0.029	–24 44 59.35	–0.12	4.82	E
24.10.	MD.	745.3	16.5	3	19 00 24.634	–0.016	–24 39 55.33	0.75	4.82	E
25.10.	MD.	744.8	16.6	4	19 03 34.124	–0.087	–24 34 36.55	–0.01	4.82	W
26.10.	MD.	744.4	17.9	5	19 06 43.743	0.094	–24 29 03.03	–0.39	4.82	W
08.11.	MD.	743.8	13.8	–	19 47 50.134	0.009	–22 54 43.06	–0.11	4.86	W
09.11.	MD.	742.8	13.0	–	19 50 59.293	0.056	–22 45 47.80	–0.32	4.86	W
05.12.	MD.	753.2	3.8	1	21 11 32.763	–0.009	–17 38 34.16	–0.60	4.93	W
1985.									1980+	
05.04.	SS.MD.	741.1	21.2	–	02 51 03.437	–0.055	16 44 09.46	0.21	5.26	E
19.09.	MD.ZS.	750.4	21.2	3	10 32 33.902	0.042	10 27 23.83	–0.46	5.72	E
03.10.	MD.ZS.	749.3	17.8	1	11 05 39.819	0.035	07 07 19.20	0.49	5.76	E
07.11.	ZS.	739.9	6.6	2	12 26 29.689	–0.036	–01 33 57.59	–0.08	5.85	E
1986.									1980+	
11.08.	MD.	743.0	23.9	4	18 51 51.172	0.034	–28 34 21.76	0.26	6.61	E
12.08.	MD.	739.6	25.6	4	18 51 50.483	–0.056	–28 32 32.18	0.25	6.61	E
18.08.	MD.	738.9	26.9	4	18 53 04.782	0.032	–28 18 3.71	–0.10	6.63	W
19.08.	MD	738.0	26.1	4	18 53 29.892	0.037	–28 15 45.89	0.29	6.63	W
21.08.	MD.	744.4	17.1	4	18 54 30.619	0.071	–28 09 47.70	0.16	6.64	W
25.08.	MD.	744.0	17.1	3	18 57 12.856	–0.012	–27 56 24.22	–0.24	6.65	W
26.08.	MD.	740.5	18.0	4	18 58 01.649	–0.033	–27 52 45.71	–0.45	6.65	E
28.08.	MD.	738.5	23.9	4	18 59 48.785	–0.049	–27 45 07.89	0.31	6.66	E
02.09.	MD.	745.5	16.9	3	19 05 09.958	0.032	–27 24 02.36	0.11	6.67	E
03.09.	MD.	743.3	19.3	4	19 06 22.914	–0.015	–27 19 28.32	–0.36	6.67	E
10.11.	MD.	751.0	7.5	4	21 31 15.542	–0.032	–16 41 24.89	–0.03	6.86	W
17.11.	SS.	756.4	9.5	5	21 48 59.664	–0.013	–14 58 20.16	0.30	6.88	E

Bull. Obs. Astron. Belgrade N° 138 (1988) UDC 523.45. 48

RESULTS OF PLANET OBSERVATIONS WITH THE BELGRADE VERTICAL CIRCLE (Supplement I)

V. Trajkovska

Astronomical Observatory, Volgina 7, 11050 Belgrade, Yugoslavia

(Received: October 7, 1987)

SUMMARY: Results of observations of five major planets with the Belgrade Vertical Circle, carried out in the period April 1985 to December 1986, are presented. The O–C differences for the observed planets, as well as the mean errors of observations are given. Differences of the observed apparent and the ephemeris apparent semi–diameters of the planets Mars, Jupiter and Saturn are given, too.

1. INTRODUCTION

This paper is second in the series, where results are presented of the observations of solar system bodies with the Belgrade Vertical Circle (Askania, 190/2578 mm). First results, containing planet observations obtained during the period 1983–1984 were published by Trajkovska (1986). In the present paper results are given of the observations of Mars, Jupiter, Saturn, Uranus and Neptune, carried out in 1985 and 1986.

2. RESULTS OF OBSERVATIONS

The method and organization of observations have been explained in the preceding paper (Trajkovska, 1986). Here, therefore, only the results of planet observations are given. Apparent places have been computed according to the IAU recommendations from 1976.

The list of the observed stars, being selected from FK4, is displayed in Table I, where n is the number of observations and m – apparent magnitude. On the average 7 to 8 stars were observed per each planet's transit.

During this period, in total, Mars has been observed 4 times. Jupiter – 12, Saturn – 18, Uranus – 17 and Neptune 15 times.

The O–C differences, shown in Table II, were computed by using the ephemeris declinations of the planets supplied by the Leningrad Institute of Theoretical Astronomy. The Table II gives besides:

- ephemeris date at the moment of culmination with a precision of 10^{-5} day;
- Julian ephemeris date up to 10^{-5} day;
- initial instrument position (E or W);
- δ – observed apparent geocentric declination;
- order of the observed edges (N, S, C – centre of the disc, combination of four settings: I – NSSN, II – SNNS);
- $\Delta\pi$ – correction for the parallax;
- n – the number of the reference stars for the given observation;
- note on the circumstances of observation (1 – through the clouds, 2 – image unsteady, 3 – image indistinct, 4 – settings dubious).

Table I. Reference stars observed with the planets

№	N_{FK4}	m	n	№	N_{FK4}	m	n
1	1357	5.7	3	31	1487	3.3	2
2	515	5.2	1	32	1493	6.2	15
3	1365	6.4	1	33	706	2.1	1
4	1366	6.4	1	34	710	3.6	20
5	1369	5.7	2	35	720	3.0	20
6	1381	6.2	2	36	722	5.0	8
7	1387	5.3	3	37	727	4.6	3
8	1391	6.0	3	38	731	5.7	2
9	559	4.7	11	39	736	4.7	4
10	1407	5.9	13	40	1512	5.5	3
11	1413	5.0	15	41	1517	5.1	8
12	1415	5.1	19	42	1522	5.0	9
13	1419	5.5	9	43	753	4.6	1
14	597	2.9	5	44	1529	6.0	8
15	607	3.1var.	3	45	762	3.2	1
16	1430	5.8	4	46	773	5.3	3
17	624	5.0	19	47	1547	4.8	1
18	1437	7.6	6	48	1548	6.0	8
19	1447	6.2	1	49	789	6.3	3
20	1449	6.1	11	50	1552	4.2	4
21	644	3.4	11	51	1561	4.3	9
22	1457	4.3	6	52	1569	4.8	3
23	1461	5.7	4	53	812	3.8	9
24	1463	4.9	19	54	818	5.4	3
25	1464	4.4–5.0	1	55	819	3.0	9
26	1470	6.3	13	56	1580	6.4	1
27	682	4.0	1	57	840	4.3	3
28	687	2.8	1	58	1595	5.3	3
29	692	2.9	17	59	864	3.8	3
30	1485	5.8	11	60	1608	4.5	3

Table II.

Date	JED	Initial instr. position	δ	0–C	Edge	Δπ	n	Note
	2446		MARS					
1968 9 5.78438	679.28438	E	–27°09' 43."76	–0."22	II/I	15."11	3	
1986 9 8.77908	682.27908	W	26 54 35.49	–0.20	II/I	14.69	5	
1986 10 2.74436	706.24436	W	24 10 36.63	–0.46	II/I	11.70	6	
1986 10 3.74313	707.24313	E	–24 01 58.71	0.50	II/I	11.59	7	2)
	2446		JUPITER					
1985 7 16.00859	263.50859	W	–17°16' 7."99	0."12	II/I	1."88	9	
1985 7 22.98720	269.48720	W	17 31 39.80	0.36	I/II	1.90	8	
1985 7 25.97798	272.47798	E	17 38 32.45	0.49	I/II	1.90	7	
1985 9 5.84952	314.34952	W	19 2 44.07	0.35	I/II	1.87	11	
1985 9 13.82601	322.32601	E	19 11 49.46	–0.17	I/II	1.84	9	
1985 9 19.80872	328.30872	E	19 16 35.07	–0.53	II/I	1.81	11	2)
1985 9 20.80587	329.30587	E	19 17 11.96	–0.09	I/II	1.81	9	
1985 10 3.76964	342.26964	E	19 20 32.38	–1.01	II/I	1.74	10	
1985 10 4.76692	343.26692	W	19 20 26.25	–0.05	II/I	1.73	10	
1986 10 4.86987	709.36987	E	7 19 51.93	–0.02	II/I	1.70	8	
1986 10 17.83138	721.33138	E	7 44 50.49	0.77	I/II	1.67	7	2), 3)
1986 11 13.75566	748.25566	E	– 7 56 38.39	–0.17	II/I	1.54	8	
	2446		SATURN					
1985 7 4.79718	251.29718	E	–16° 3' 31."33	0."94	II/I	0."83	8	2)
1985 7 5.79436	252.29436	E	16 3 15.19	1.95	I/II	0.82	8	2)
1985 7 8.78591	255.28591	E	16 2 35.26	0.59	II/I	0.82	6	
1985 7 9.78311	256.28311	W	16 2 24.84	0.17	II/I	0.82	5	
1985 7 11.77751	258.27751	W	16 2 8.41	–0.48	I/II	0.82	5	1)
1985 7 16.76358	263.26358	W	16 1 53.82	–0.78	II/I	0.81	7	3)
1986 5 14.98118	565.48118	W	19 32 8.36	0.54	I/II	0.88	7	2)
1986 5 21.96060	572.46060	W	19 27 17.42	0.11	II/I	0.88	8	2)
1986 6 19.87540	601.37540	W	19 8 22.47	0.52	I/II	0.87	7	
1986 6 20.87248	602.37248	W	19 7 49.75	0.41	II/I	0.87	5	2)
1986 7 23.77802	635.27802	W	18 57 34.62	–0.73	I/II	0.84	3	2)
1986 7 24.77523	636.27523	E	18 57 31.28	0.84	I/II	0.83	1	2), 3)
1986 7 25.77244	637.27244	E	–18 57 31.55	–0.13	II/I	0.83	3	
	2446		URANUS					
1985 6 30.87390	247.37390	E	–22°38' 7."19	–0."28	C	0."45	11	
1985 7 4.86256	251.36256	E	22 37 12.64	1.15	C	0.45	6	2)
1985 7 5.85972	252.35972	E	22 36 59.37	0.13	C	0.45	9	
1985 7 6.85891	253.35891	E	22 36 46.24	–0.15	C	0.44	8	
1985 7 8.85123	255.35123	E	22 36 20.40	1.24	C	0.44	6	4)
1985 7 15.83148	262.33148	W	22 34 55.50	–0.39	C	0.44	9	
1985 7 16.82866	263.32866	W	22 34 44.25	–0.43	C	0.44	7	
1985 7 22.81181	269.31181	W	22 33 41.91	1.18	C	0.44	9	
1985 7 29.79224	276.29224	W	22 32 40.79	–0.31	C	0.44	9	
1985 7 30.78945	277.28945	W	22 32 33.27	–0.18	C	0.44	8	
1986 6 19.91956	601.41956	E	23 9 40.71	–0.30	C	0.45	7	
1986 7 23.82316	635.32316	E	23 4 17.84	–0.04	C	0.44	6	
1986 7 25.81754	637.31754	W	23 4 3.22	–0.40	C	0.44	7	
1986 7 28.80913	640.30913	W	23 3 41.86	–0.36	C	0.44	8	
1986 7 29.80633	641.30633	W	23 3 35.05	–0.32	C	0.44	9	
1986 7 30.80353	642.30353	W	23 3 28.08	0.09	C	0.44	8	
1986 8 1.79794	644.29794	W	–23 3 15.27	0.40	C	0.44	8	
	2446		NEPTUNE					
1985 6 30.92503	247.42503	E	–22°15' 54."73	–0."54	C	0."28	11	4)
1985 7 3.91660	250.41660	W	22 16 1.73	–0.75	C	0.28	7	3), 4)
1985 7 4.91379	251.41379	E	22 16 4.14	0.34	C	0.28	6	4)
1985 7 5.91098	252.41098	E	22 16 6.56	0.01	C	0.28	9	
1985 7 6.90817	253.49817	E	22 16 8.99	0.24	C	0.28	8	
1985 7 8.90256	255.40256	W	22 16 13.85	–0.33	C	0.28	6	
1985 7 15.88292	262.38292	E	22 16 30.95	1.39	C	0.28	9	4)
1985 7 22.86331	269.36331	W	22 16 49,16	–0.83	C	0.27	9	3)
1985 7 29.84374	276.34374	W	22 17 7.42	–1.23	C	0.27	9	3)
1986 6 19.96338	601.46338	W	22 15 16.70	–0.52	C	0.28	7	3)
1986 7 23.86791	635.36791	E	22 17 26.06	1.48	C	0.28	6	3)
1986 7 28.85392	640.35392	W	22 17 47.24	–0.19	C	0.27	8	3), 4)
1986 7 29.85112	641.35112	W	22 17 50.60	0.28	C	0.27	9	
1986 7 30.84833	642.34833	W	22 17 53.87	0.83	C	0,27	8	
1986 8 1.84274	644.34274	W	–22 18 2.74	–0.40	C	0,27	8	

Table III Differences of the observed and ephemeris apparent semi–diameters of the planets

Date	R_o-R_e	Date	R_o-R_e
MARS			
5.9.1986	2".574	2.10.1986	2".585
8.9.1986	1.810	3.10.1986	2.975
JUPITER			
16.7 1985	2".373	20. 9.1985	1".614
22.7.1985	2.852	3.10.1985.	2.064
25.7.1985	2.053	4.10.1985	1.854
5.9.1985	2.006	4.10.1986	1.948
13.9.1985	1.503	17.10.1986	1.748
19.9.1985	2.958	13.11.1986	1.894
SATURN			
22.4.1985	1".802	16.7.1985	1".730
16.6.1985	1.738	24.4 1986	3.029
30.6.1985	1.900	14.5.1986	3.119
4.7.1985	1.867	21.5.1986	3.239
5.7.1985	2.837	19.6.1986	2.395
6.7.1985	1.680	20.6.1986	2.300
8.7.1985	1.217	23.7.1986	2.255
9.7.1985	1.675	24.7.1986	2.445
11.7.1985	1.290	25.7.1986	2.405

The differences of the observed apparent semi–diameters are listed in Table III. The mean square errors σ of the O–C values for each planet, as well as mean square errors σ_1 of the differences R_o-R_e, are shown in Table IV. The O–C and R_o-R_e values, along with number of observation n are also given in the same Table.

Observation of the solar system bodies with Vertical Circle are continually going on the results of observations will be regularly published.

Table IV Mean square errors σ and σ_1

Planet	Year	$\overline{O-C}$	σ	$\overline{R_o-R_e}$	σ_1	n
Mars	1985	–	–	–	–	–
	1986	–0.10	±0".41	2".49	±0".49	4
	1985–86	–0.10	0.41	2.49	0.49	4
Jupiter	1985	–0.06	0.48	2.14	0.50	9
	1986	0.19	0.51	1.86	0.10	3
	1985–86	0.00	0.47	2.07	0.47	12
Saturn	1985	0.40	0.99	1.77	0.44	10
	1986	0.22	0.52	2.65	0.41	8
	1985–86	0.30	0.83	2".16	±0".61	18
Uranus	1985	0.20	0.70	–	–	10
	1986	–0.13	0.30	–	–	7
	1985–86	0.06	0.58	–	–	17
Neptune	1985	–0.19	0.79	–	–	9
	1986	0.25	0.78	–	–	6
	1985–86	0".07	±0".74	–		15

ACKNOWLEDGEMENTS

The author would like to express her sincere thanks to the colleagues from the Institute of Theoretical Astronomy, Leningrad, as well as to B. Jovanović for useing his computer program for calculation of apparent places. The author would also like to thank Mrs. S. Bogić for her help with the observations.

This work has been supported by the Republic Association for Scinece of Serbia through the project „Physics and Motions of Celestial Bodies and Artificial Satelites".

REFERENCES

Trajkovska, V.: 1986, *Bull. Obs. Astron. Belgrade,* **136,** 100.

Bull. Obs. Astron. Belgrade, Nº 138(1988) UDC 523.44

ESCAPE VELOCITY FOR FRAGMENTS OF COLLISIONALLY SHATTERED SOLAR SYSTEM BODIES

P. Farinella

Dipartimento di Matematica, Universita di Pisa, Via Buonarroti 2, I–56100 Pisa, Italy

P. Paolicchi

Istituto di Astronomia, Universita di Pisa, Piazza Torricelli 2, I–56100 Pisa, Italy

A. Cellino and V. Zappala

Osservatorio Astronomico di Torino, I–10025 Pino Torinese (Torino), Italy

(Received: October 5 1987)

SUMMARY: When a small solar system body is shattered by a catastrophic impact, its fragments can either escape self–gravitation and achieve independent orbits, or fall back and reaccumulate into a „pile of rubble". The choice between these alternative outcomes depends on the ratio between the ejection velocity of the fragments and the escape velocity from the gravitational well of the parent body. This escape velocity in turn depends on the initial position of the fragment, and usually is only a fraction of that for a particle starting from the surface of the parent body. The average escape velocity can be estimated by applying the conservation of total energy to a population of fragments whose (differential) mass distribution is parametrized by the exponent q of a power law. When q varies from 1.5 to 1.9, the average escape velocity is found to range from 44 to 76% of the surface value.

In the last decade planetary scientists have realized that self–gravity plays an important role in determining the structure and evolution of asteroids and small satellites (see, e.g., Farinella *et al.*, 1981, 1983a; Catullo *et al.*, 1984; Farinella, 1987). This is the case in particular when collisional fragmentation occurs. Such events are rare but of crucial importance in determining the structure and evolution of many small bodies of the solar system, ranging from asteroids to small satellites of the outer planets (Farinella *et al.*, 1982, 1983b; Fujiwara, 1982; Zappala *et al.*, 1984; Davis *et al.*, 1985). Immediately after a catastrophic breakup, the fragments can either escape the mutual self–gravitational binding and achieve independent heliocentric (or planetocentric) orbits, or fall back and reaccumulate into a gravitationally bound *'pile of rubble'*. The choice between these alternative outcomes depends on the ratio between the ejection velocity of each fragment and the escape velocity from the gravitational well of the parent body. This escape velocity in turn depends on the initial position of the fragment, and usually is only a fraction of the value which holds for a particle starting from the surface of the parent body. For instance, if the parent body is spherical and homogeneous, and the fragment starts at a distance from the centre such that half of the total mass lies deeper than it, it is easy to show that the resulting escape velocity is $2^{-1/3} \cong 0.794$ times the escape velocity from the surface, given by

$$V_{E,PB} = (2GM_{PB}/R_{PB})^{1/2} = (2GM_{PB}{}^{2/3}/Q)^{1/2} \quad (1)$$

where R_{PB} and M_{PB} are the radius and mass of the parent body, G is the gravitational constant and

$$Q = R_{PB}/M_{PB} = (3/4\pi\rho)^{1/3} \quad (2)$$

ρ being the density. A more accurate method to estimate an *average* value of the escape velocity is needed when studies on the ejection velocity field (Zappala *et al.*, 1984; Paolicchi *et al.*, 1987) or on the energy partition (Fujiwara, 1982; 1986) in collisional fragmentation events are to be carried out. This can be done in the following way. Let us assume that the break–up of the parent body gives rise to a population of fragments whose (differential) mass distribution can be parametrized by the exponent q of a power–law relationship. In other words, we shall assume that the number of fragments dN in the mass interval [m, m+dm] is given by

$$dN = A\, m^{-q}\, dm \qquad (3)$$

where the exponent q lies in the range $1.5 < q < 2$, as indicated by extensive evidence from laboratory experiments and from studies on asteroid families (see Zappala *et al.*, 1984; Capaccioni *et al.*, 1986; Fuliwara, 1986; and references quoted therein). The normalizing factor A can be estimated by requiring that

$$\int_M^m dN = A\, M^{(1-q)}/(q-1) = 1/2 \qquad (4)$$

where q is assumed to be larger than 1 and M (corresponding to a radius R) is the upper limit of the mass distribution. In fact, a continuous mass distribution like (3) could not be rigorously applied to the few largest fragments, which are usually well separated in mass; however, as discussed by Kresak (1977), the distribution (3) can be easily discretized, and eq. (4) provides just a way to make approximate computations. The total mass of the fragments, which is also the mass of the parent body, is then

$$M_{PB} = \int_0^M m\, dN = \frac{(q-1)}{2(2-q)}\, M \qquad (5)$$

Notice that $M_{PB} \geqslant M$ only for $q \geqslant 5/3$ (since according to eq. (4), there is only a 50% probability of finding a fragment of mass larger than M) and that M_{PB} becomes much larger than M for $q \to 2$. The total self–gravitational binding energy of the parent body, assumed again to be a homogeneous sphere, is

$$W_{PB} = -\,3GM_{PB}{}^2/5R_{PB} = -\,3\,M_{PB}{}^{5/3}/5Q \qquad (6)$$

while the total self–gravitational energy of the fragments is

$$W_{FR} = -\frac{3G}{5Q}\int_0^M m^{5/3}\, dN = -\frac{3G}{5Q}\,\frac{3(q-1)}{2(8-3q)}\, M^{5/3}$$

$$= -\frac{3G}{5Q}\,\frac{3(q-1)}{2(8-3q)}\left[\frac{2(2-q)}{(q-1)}\right]^{5/3} M_{PB}{}^{5/3} \qquad (7)$$

Thus the gravitational binding energy of the fragments tends to zero when $q \to 2$. In this case we could just say that the target has been comminuted to dust. If we require that no reaccumulation of this dust occurs after the initial explosion, we have to guarantee that the fragments are ejected with a total kinetic energy larger than $-W_{PB}$. From this condition and eq. (6), we can infer that the r.m.s. velocity of the fragments is then larger than

$$V_{E,DUST} = (6GM_{PB}{}^{2/3}/5Q)^{1/2} \cong 0.775\, V_{E,PB} \qquad (8)$$

However, this is clearly a limiting case, and when the fragments (with $q < 2$) retain some self–gravitational energy according to eq. (7), the corresponding „average escape velocity" $V_{E,Fr}$ will be somewhat lower. In general we shall use the condition

$$M_{PB} V_{E,FR}{}^2/2 = -\,W_{PB} + W_{FR} \qquad (9)$$

which yields

$$V_{E,FR} = \left[\frac{6\,GM}{5\,R}\right]^{1/2} \left\{\left[\frac{(q-1)}{2(2-q)}\right]^{2/3} - \frac{3(2-q)}{(8-3q)}\right\}^{1/2}$$

$$= \left[\frac{6G\,M_{PB}}{5\,R_{PB}}\right]^{1/2} \left\{1 - \frac{3\,(q-1)}{2\,(8-3q)}\left[\frac{2\,(2-q)}{(q-1)}\right]^{5/3}\right\} \qquad (10)$$

Fig. 1 shows, as a function of the exponent q of the mass distribution, the behaviour of the ratio between $V_{E,FR}$ and the escape velocity of the largest fragment and of the parent body, respectively, as obtained from eq. (10). As expected, the ratio $V_{E,FR}/V_{E,PB}$ approaches the limit given by eq. (8) as q approaches 2, while $V_{E,FR}/(2GM/R)^{1/2}$ tends to infinity when $q \to 2$. The latter ratio is smaller than the former one when q

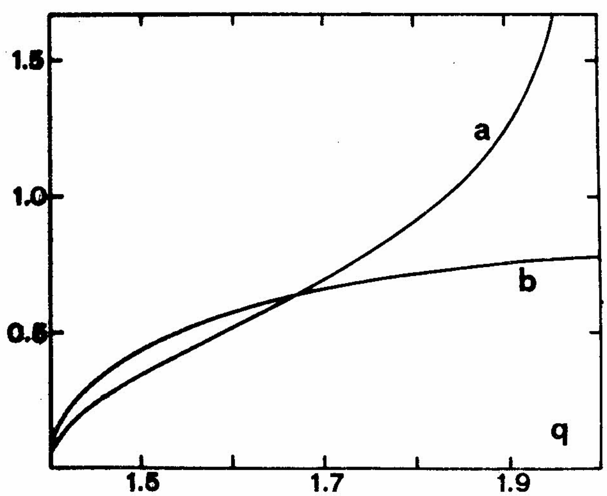

Fig. 1. The ratios $V_{E,FR}/(2GM/R)^{1/2}$ and $V_{E,FR}/V_{E,PB}$ derived from eq. (10) are plotted vs the exponent q of the differential mass distribution (3.). They correspond to the curves a) and b) respectively.

Table I

q	1.5	1.6	5/3	1.8	11/6	1.9
$V_{E,FR}/V_{E,PB}$	0.438	0.572	0.632	0.716	0.731	0.756
$V_{E,FR}/(2GM/R)^{1/2}$	0.348	0.520	0.632	0.902	0.993	1.248

$< 5/3$, since in this case $M_{PB} < M$. Table I gives the values of the two ratios for some representative values of q. We recommend that these values are used in the investigations mentioned above, either by estimating q from the observed mass distribution and reconstructing the total mass M_{PB} or, when this is not possible, by assuming some intermediate value like $q \cong 11/6$ and then deriving the average escape velocity from the mass of the largest observed fragment.

ACKNOWLEDGEMENTS

This work has been supported in part by the National research Council of Italy (C.N.R.) and by the Italian Ministry of Public Education.

REFERENCES

Capaccioni, F., Cerroni P., Coradini M., DiMartino M., Farinella P., Flamini E., Martelli G., Paolicchi P., Smith P.N., Woodward A., and Zappala V.: 1986, *Icarus* **66**, 487–514.

Catullo V., Zappala V., Farinella P., and Paolicchi P.: 1984, *Astronomy and Astrophysics* **138**, 464–468.

Davis D.R., Chapman C.R., Weidenschilling S.J., and Greenberg R.: 1985, *Icarus* **62**, 30–53.

Farinella P. : 1987, *In The Evolution of the Small Bodies of the Solar System,* M. Fulchignoni and L. Kresak, eds., North Holland, Amsterdam pp. 276–300.

Farinella, P., Paolicchi, P., Tedesco E.F., and Zappala V.:1981, *Icarus* **46**, 114–123.

Farinella, P., Paolicchi P., and Zappala V.: 1982, *Icarus* **52**, 409–433.

Farinella,P., Milani A., Nobili A.M., Paolicchi P., and Zappala V.: 1983a, *The Moon and the Planets* **28**, 251–258.

Farinella,P., Milani A., Nobili A.M., Paolicchi P., and Zappala V.: 1983b, *Icarus* **54**, 353–360.

Fujiwara,A.: 1982, *Icarus* **52**, 434–443

Fujiwara, A.: 1986, *Ital.Astron.Soc.***57**, 47–64

Fujiwara, A.: 1987, *Icarus*, Submitted.

Kresak, L.: 1977, *Bull. Astron. Inst. Czech.* **28**, 65–82.

Paolicchi, P., Cellino A., Farinella P., and Zappala V.: 1987, to be published

Zappala, V., Farinella P., Knežević Z., and Paolicchi, P.: 1984, *Icarus* **59**, 261–285.

Bull. Obs. Astron. Belgrade, N° 138(1988) UDC 550.38

MAGNETIC AND PALEOMAGNETIC INVESTIGATIONS OF THE MAGMATIC SYSTEMS IN THE AREA AROUND BELGRADE

D.S.Veljović

Geomagnetic Institute, 11306 Grocka, Yugoslavia

(Received: 23 February, 1987)

SUMMARY: A brief review of paleomagnetic investigation is given. This investigation have been performed in order to establish the geophysical aspects of the geomagnetic field changes in the studied area in the course of the geological era.

More than 75 oriented samples from more than 9 localities of various magmatic tertiary rocks which are found in the area around Belgrade were investigated in order to get a data about the magnetic and paleomagnetic characteristics of the investigations, as well as about the geophysical aspects of the changes in the magnetic

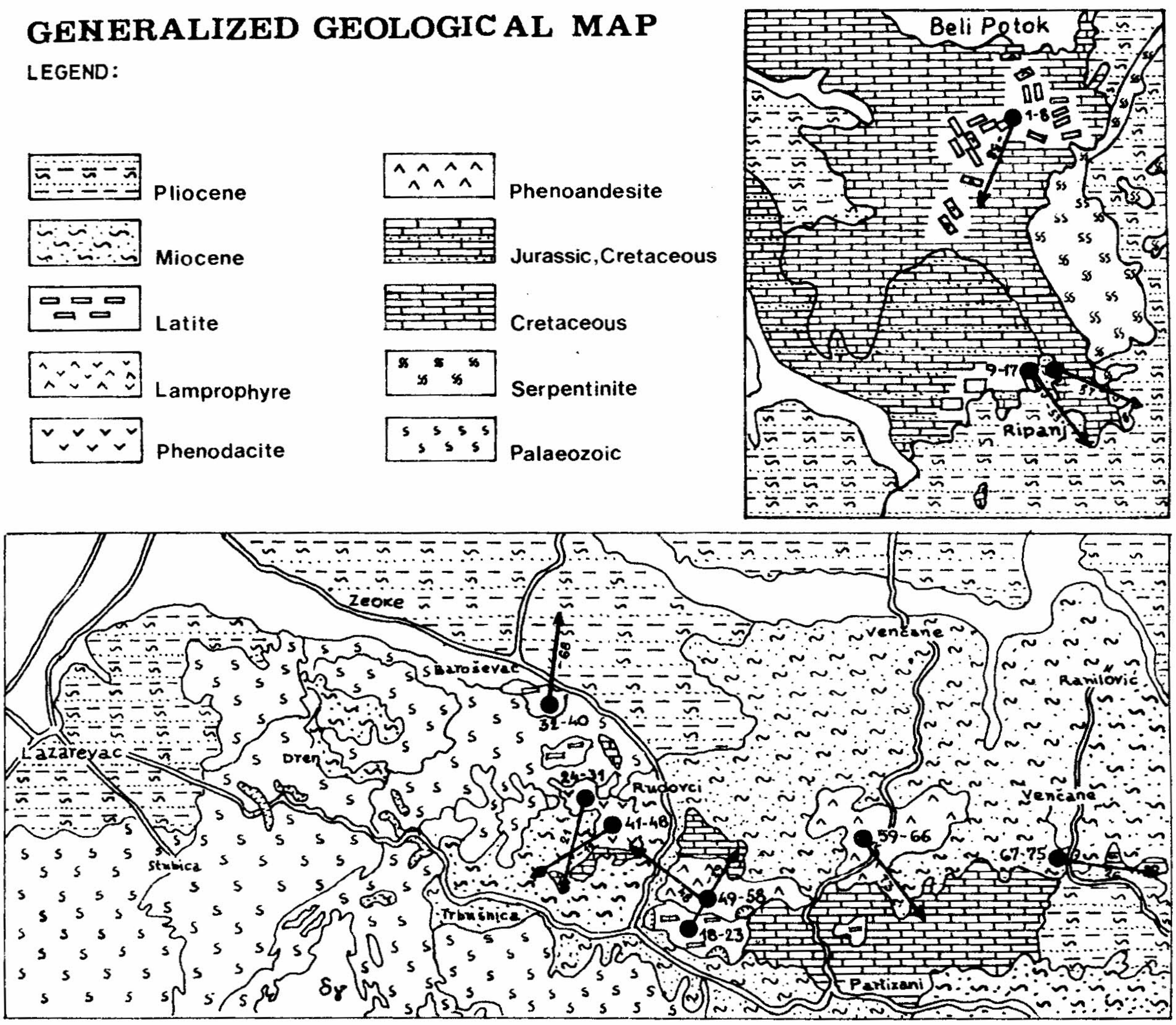

Fig. 1. Generalized geological map on which all the sample localities are marked.

field and its evolution at the time these rocks were formed. Figure 1 shows a generalized geological map on which all the sample localities are marked.

The terrain subjected to paleomagnetic investigation belongs, geotectonically, to the Vardar zone. The Mesozoic sediments folded and broke in the Laramian phase, during which the main tectonic appearance of this area was shapped. According to the majority of those who investigated this area all the tectonic events in the Belgrade area can be divided into premiocenic and postmiocenic. Premiocenic movements would include tectonic movements at the end of the Cretaceous and Paleocene. It is considered that at this time disturbances arose in the Upper Cretaceous sediments accompanied by disjunctive movements, which enabled the magmatic rocks to break through. The paleomagnetically investigated magmatic rocks present equivalents of the Granodiorite magma and are connected with the intrusions which occurred in the period between Upper Cretaceous and Neogene. The magmatic activity continued in the Neogene as well the formation of tufas.

The laboratory investigation of these rocks (number 1–9, Table 1) shows that the thermoremanent magnetization is stable, that they are suitable for paleomagnetic investigation and that they were formed in a normal as well as a reverse geomagnetic field. The analysis of the magnetic characteristics of these rocks showed that during demagnetization in the alternating magnetic field changes arose in the intensity and direction of the natural remanent magnetization, which indicates that these rocks have two types of remanent magnetization of different orientation and stability.

It is interesting to follow the process of demagnetization in the alternating magnetic field of the samples RZ – 32 – 40, whose intensity in turns decreases by 20–50% and then increases in some cases up to 1–1,5 times its original value. Meanwhile, the direction of the reverse, as well as the normal magnetization, groups itself during demagnetization around the following mean values: D = 9° and I = – 68°. Such behaviour of the samples indicates that the viscose remanent magnetization was most probably parallel to the direction of the magnetic field at the rock collection site. In this case we can conculde that the VRM had a great intensity which affected a complete reorientation of the natural remanent magnetization vector in respect to the original direction of the thermoremanent magnetization and that in the demagnetization process a gradual change is affected in the direction of the remanent magnetization which is observable up to the values of demagnetization fields of 16–24 · 10^3 A/m. In these fields the VRM was practically demagnitized and afterwards we could observe only the lowering of intensity without the change of direction of the natural remanent magnetization. However, at the localities 5, 7, 8 and 9, (Table 1) we have

TABLE 1

	Nº of SAMPLES	Type of rocks locality	N	$\chi_m \cdot 10^{-6} \cdot 4\pi$ (SI)	$I_r \cdot 10^{-3}$ (A/m)	PALEOMAGNETIC directions D (°)	PALEOMAGNETIC directions I (°)	K	α_{95}	Polarization	PALEOMAGNETIC pole φ_p (N)	PALEOMAGNETIC pole λ_p (E)	Ovals of confidens dp	Ovals of confidens dm
1	2	3	4	5	6	7		8	9	10	11	12	13	14
1	RZ-9-12	Lamprofiri – Ripanj	9	54	4	146	– 53	17	23,2	R	62	280	22,4	32,3
	RZ-13-17			48	2	113	57	24	15,8	N	12	69	16,6	22,9
2	RZ-18-23	Latiti – Kruševica	6	4	4	30	– 29	82	7,5	R	24	169	4,5	8,2
3	RZ-67-75	Kvarclatiti-žuti Oglavak	9	36	600	98	26	26	10,3	N	4	95	6,0	11,2
4	RZ-1 – 8	Andeziti-tufiti–Avala	8	15	1	202	– 58	50	9,6	R	73	123	10,5	14,2
5	RZ-24-31	Fenodaciti – Rudovci	8	5	3	197	21	296	3,2	N	33	181	1,8	3,4
6	RZ-32-40	Fenodaciti-Baroševac	9	610	16	9	– 68	230	3,4	R	5	15	4,7	5,7
7	RZ-41-48	Fenodaciti – Trbusnica – Rudovci	8	544	673	243	– 12	93	5,8	R	23	126	3,0	5,9
8	RZ-49-58	Fenoandeziti – Kruševica	10	1594	620	305	48	151	3,9	N	44	290	3,3	5,1
9	RZ-59-66	Fenoandeziti – Partizani	8	1409	5790	147	73	534	2,4	N	17	38	3,8	4,3

only one type of magnetization and rocks which are magnetically homogenous and isotropic, because in the process of demagnetization the intensity is lowered but the direction of the natural remenent vector is not affected.

As it is known, in paleomagnetic investigations the magnetic field is not represented only by declination (D^o) and inclination (I^o) of the geomagnetic field which has conditioned the given remanent magnetization but it is also represented with respect to the geocentric dipole, that is, by the paleomagnetic pole, Since the rocks are magnetized under the influence of the gemagnetic field at the time and place of their formation (or, in the case of magmatic rocks, their cooling), the tectonically undisturbed rocks can show some slight deviations of the paleopoles given in Table 1 (φp, λp) satisfy Fisher's statistic model, to which the samples RZ–1–8 and RZ–9–17 are an exception. Great dispersion of the paleomagnetic poles can be observed (Fig. 2), which leads to the conclusion that we have here rocks which have undergone great tectonic disturbances.

On the basis of the data in Table 1, the vectors of the stable component of the remanent magnetization are represented in the horisontal plane as unit vectors with designated inclination values (Fig. 1). It is known that remanent magnetization is also created in the rock formation process and in the magnetically homogenous rocks it has the direction of the magnetizing field. If in the geological past of the investigated rocks a layer is broken along some plane, in which process a part of the layer is rotated as well, then the remanent magnetization vectors are also rotated along with the layer. In this case the slant of the remanent magnetization vector will not change with respect to the layer, while the viscose remanent magnetization vector will change in respect to the horizontal plane by the degree of rotation. If we have translatory movements along the vertical axis (radial movement), then the vector orientation does not change because the layer plane remains horizontal. It is obvious that, if we are dealing with complex tectonic disturbances, which cause respective rotations, we have greater or lesser dispersions of the vector directions determined by the investigation of orientated samples taken on different localities within the same layer or outflow. During the paleomagnetic and magnetic investigations of the magmatic rocks from the area arond Belgrade no corrections were made for the elements of stretching and deep of the layer. It can be observed in Fig. 1 that the directions of the unit vectors are greatly dispersed and that very few are approximately parallel to each other like RZ–9–12 and RZ–59–66 ar RZ–1–8 and RZ–24–31 or RZ–13–17 and RZ–67–75. In these cases we can talk of very intensive local tectonic shifts which took place during and after the otupouring of these rocks. This is confirmed by the positions of the paleopoles in Fig. 2.

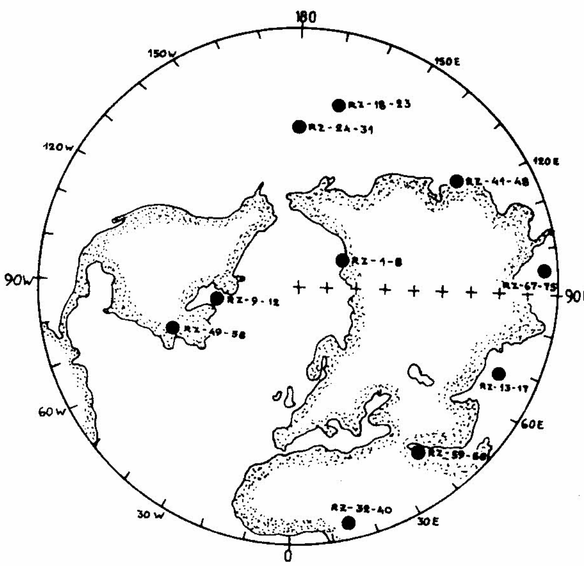

Fig. 2. Mean positions of paleomagnetic poles for the investigated samples of the volcanic rocks from the Area around Belgrade.

On the basis of the magnetic and paleomagnetic investigations of the magmatic rocks from the area around Belgrade that have been carried out so far it can be concluded that the investigated area has very complex tectonics (local tectonic shifts) and that the outpouring of these rock in the geological sense took place over a long time period.

Bull.Obs.Astron.Belgrade, N° 138(1988) UDC 550.38

GEOMAGNETIC AND MAGNETOTELLURIC INVESTIGATIONS IN THE WIDER AREA OF BELGRADE

M.Popeskov, M.Stojković and T.Bicskei

Geomagnetic Institute, 11306 Grocka, Yugoslavia

(Received: 23 February, 1987)

SUMMARY: A breif review of geomagnetic and magnetotelluric invesitgations carried out in the wider area of Belgrade is given. Although the obtained results are indicative, no definite conclusion could be derived on the relationship between geomagnetic and telluric field changes and contemporary tectonic activity in the area concerned.

1. GEOMAGNETIC INVESTIGATIONS

1.1. Introduction

Since the beginning of intensified multidisciplinary studies aimed to establish both theoretical and experimental basis for earthquake prediction, geomagnetic methods proved to be one of useful means for monitoring precursory phenomena. As it is well known, under the effect of mechanical stress – compressional or tensional– the magnetization of crustal rocks changes reversibly or irreversibly. On the earth's surface these changes are reflected as small magnitude geomagnetic field changes, nowdays generally refered to as tectonomagnetic effect. Therefore, with sensitive instruments and adequate measuring and data reduction techniques it should be possible to identify geomagnetic field changes of tectonic origin and that is how geomagnetic methods can be used for monitoring tectonic processes, which is of particular interest in seismically–active regions.

Based on the afore–mentioned concept of relationship between tectonic forces and geomagnetic field changes, the idea was to detect possible relative motions between tectonic blocks in the wider area of Belgrade, in order to obtain additional data which could help in clarifying the problem of relative motion of geographical coordinates of Belgrade with respect to Warsaw.

Before discussing the results of geomagnetic investigations, it has to be pointed out that what has been done so far should be considered only as a preliminary stage of more complex and long–term investigations which should be continued in future if a final goal is to be achieved. It is quite clear that on a small time–scale of two years, only very intensive tectonic processes – such as preparatory stage of a strong earthquake – might give detectable geomagnetic changes while some others could be, due to their small magnitude, masked within field changes of other origin.

1.2. Discussion of results

In the area of about 4000 km^2, at nine I order stations, three surveys of declination (D), horizontal component (H) and total intensity of the geomagnetic field (F) have been carried out in the period August 1981 – October 1982. Total field intensity was additionally measured at 19 newly established measuring sites in order to cover evenly the whole investigated area. Standard measuring equipment was used such as declinator, horizontal torsion magnetometer and proton precession magnetometer. All instruments were calibrated at Grocka observatory before going into field and after coming back. All the data were reduced to the epoch 1980.0 by the use of observatory magnetograms and other relevant data. When discussing the spatial and temporal distribution of particular field component, the basic geological nad tectonic characteristics of the surveyed area will be considered only to the extent which is essential for the interpretation of geomagnetic data.

Total field intensity values for the successive epochs I and II are presented in Figs. 1 and 2. An anomaly with maximum intensity of 47500 nT dominates over the obtained pattern of distribution. It is most probably caused by the presence of serpentines whose appearance coincides with the region of F values between 47200 and 47500nT. This anomaly, with smaller intensity, extends further in the NNW–SSE direction towards Vrčin, Ralja and Kosmaj, coinciding with dislocation in the zone Stragari–Kosmaj–Ripanj–Belgrade as one of two main boundary dislocations in this area which separates Central from Internal Vardar subzone and is clearly marked with linear magnetic anomalies. System of faults in the NW–SE and NE–SW direction dominates in the SW part of the investigated area where sedimentary rocks are mostly present. Neogene and Quartary complexes of Belgrade's Posavina and Kolubara basin in the

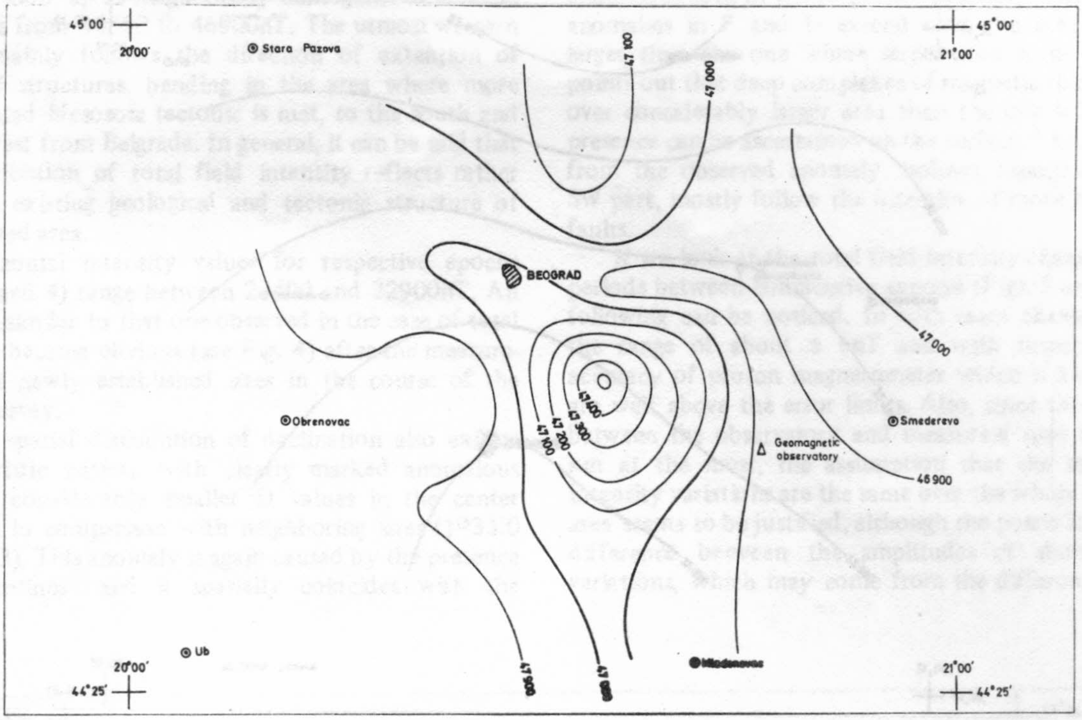

Fig. 1. Total geomagnetic field intensity distribution for the epoch I (unit: nT)

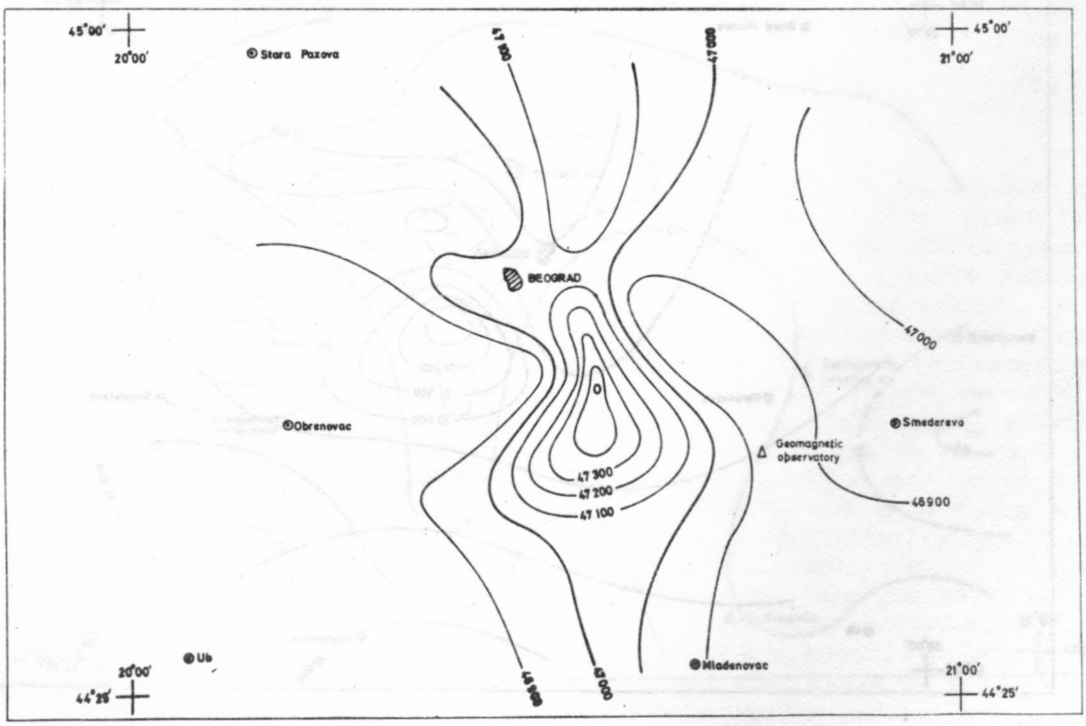

Fig. 2. Total geomagnetic field intensity distribution for the epoch II (unit: nT)

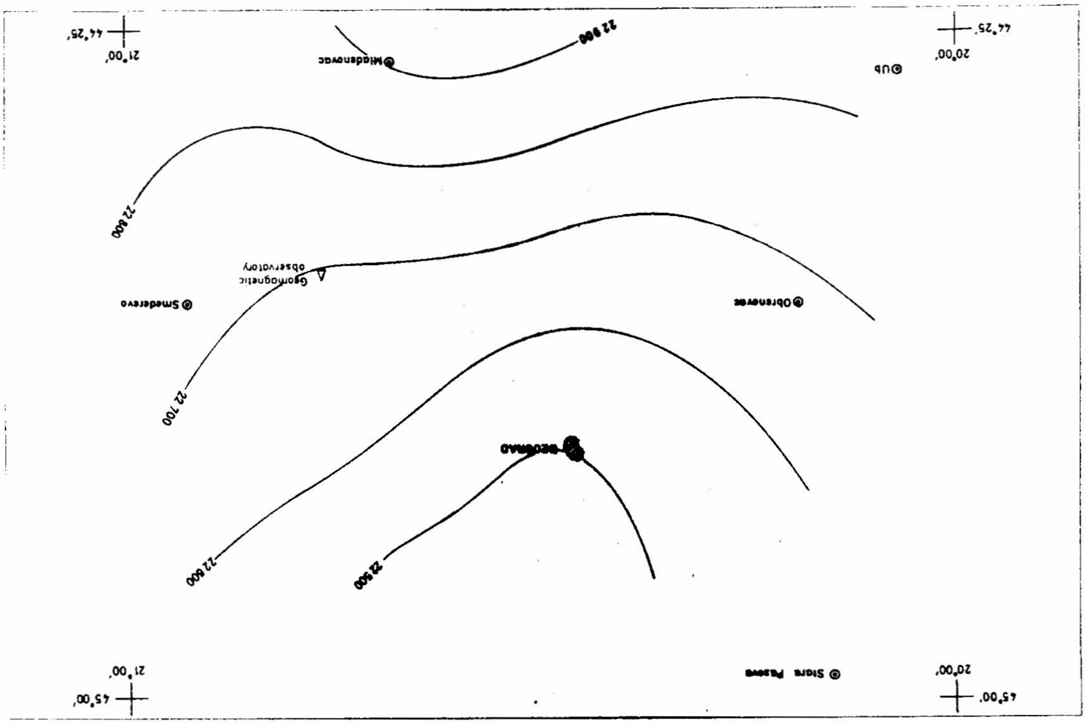

Fig. 3. Horizontal geomagnetic field intensity distribution for the epoch I (unit: nT)

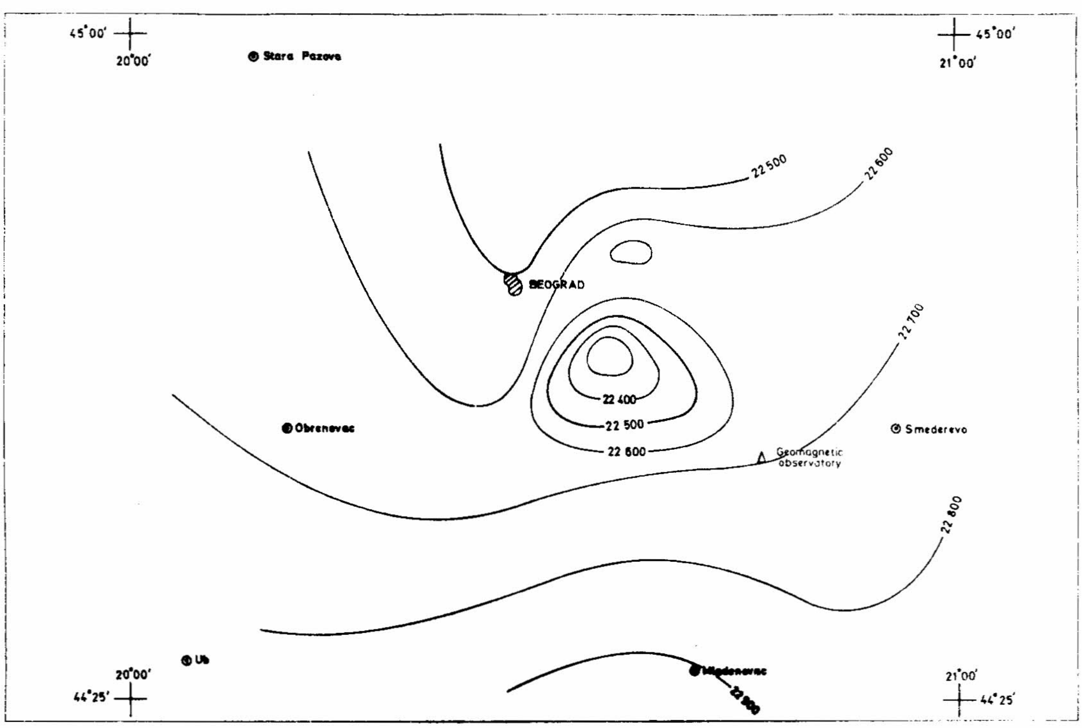

Fig. 4. Horizontal geomagnetic field intensity distribution for the epoch II (unit: nT)

F chart show up as magnetically homogeneous areas in the range from 46800 to 46900nT. The utmost western isoline mainly follows the direction of extention of fractured structures, bending in the area where more complicated Mesosoic tectonic is met, to the south and south–west from Belgrade. In general, it can be said that the distribution of total field intensity reflects rather well the existing geological and tectonic structure of investigated area.

Horizontal intensity values for respective epochs (Figs. 3 and 4) range between 22400 and 22900nT. An anomaly similar to that one observed in the case of total intensity became obvious (see Fig. 4) after the measurements at newly established sites in the course of the second survey.

The spatial distribution of declination also exibits characteristic pattern with clearly marked anomalous zone of considerably smaller D values in the center (0°51ʹ.3) in comparison with neighboring sites (1°33ʹ.0 to 2°36ʹ.3). This anomaly is again caused by the presence of serpentines and it spatially coincides with the anomalous zone of the total field intensity. The fact that anomalies in F and D extend over the area which is larger than the one where serpentines occur probably points out that deep complexes of magnetic rocks spread over considerably larger area than the one where their presence can be ascertained on the surface. Further away from the observed anomaly, isolines, especially in the SW part, mostly follow the direction of more important faults.

If we look at the total field intensity changes in the periods between consecutive surveys (Figs. 5 and 6), the following can be noticed. In both cases changes are in the range of about ± 6nT and with respect to the accuracy of proton magnetometer which is ±1nT, they are well above the error limits. Also, since the distance between the observatory and measuring sites is 50–60 km at the most, the assumption that the total field intensity variations are the same over the whole surveyed area seems to be justified, although the possibility of the difference between the amplitudes of short–period variations, which may come from the difference in the

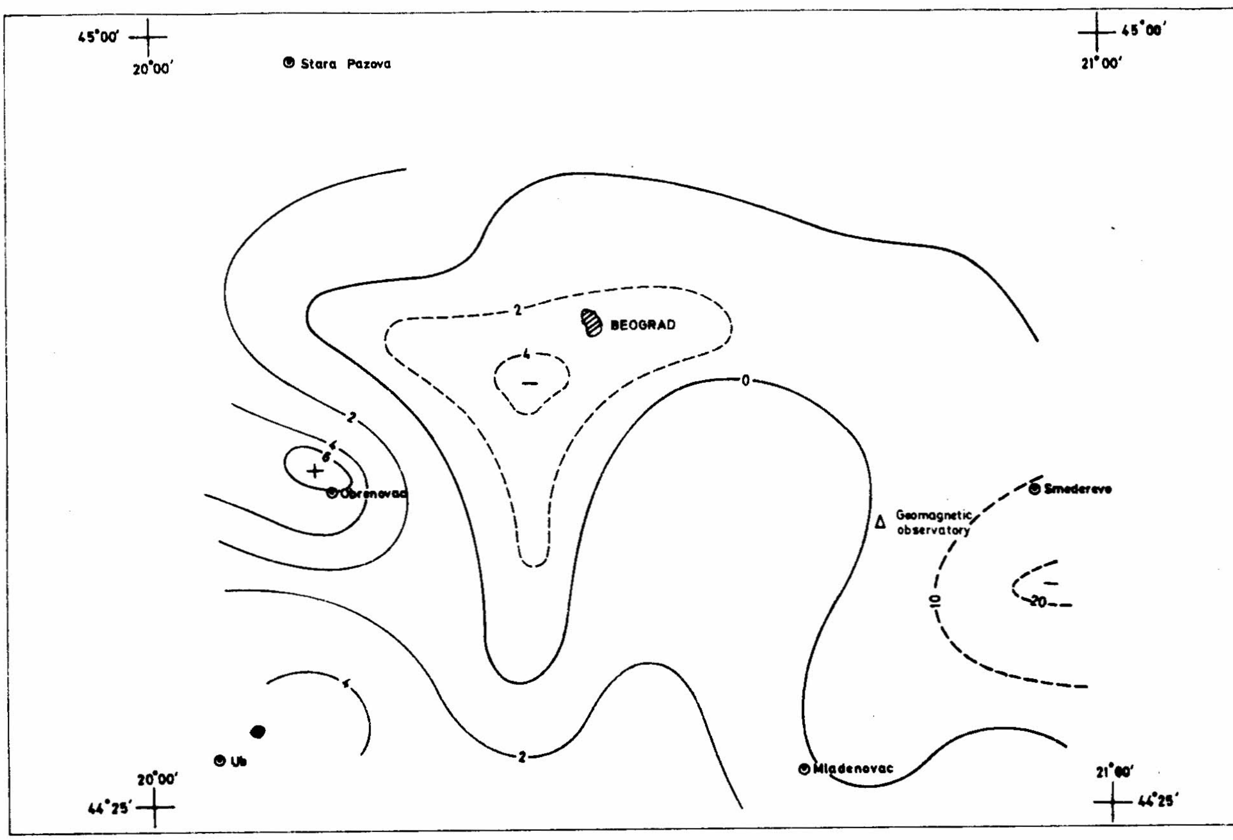

Fig. 5. Total geomagnetic field intensity changes in the period between the first and the second survey, August 1981 – April 1982 (unit: nT)

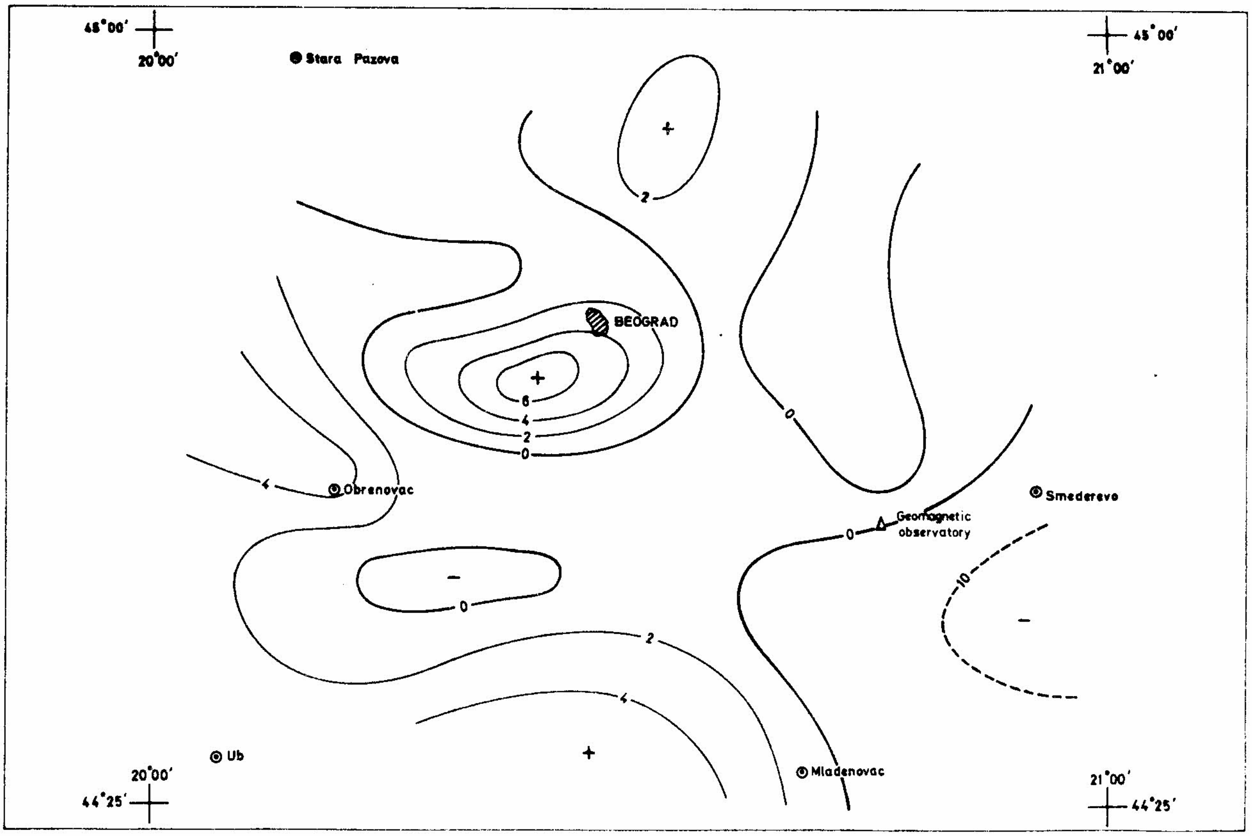

Fig. 6. Total geomagnetic field intensity changes in the period between the first and the third survey, August 1981 – September 1982 (unit: nT)

subsurface local resistivity structure, cannot be ruled out. In any case, we may safely assume all anomalies of ΔF with magnitudes larger than 3nT to be significant. If this is accepted, it remains to find the cause of the observed ΔF anomalies located south and south–west from Belgrade. Since there are no data on geodetic or strain measurements which could be used to establish possible connection between local field changes and tectonic activity, nothing definite can be concluded on this matter. Yet, if certain regularity is looked for, it can be said that in the whole period concerned the same tendency of increase or decrease has been retained in some areas. This could, eventually, point out that there exists particular, relatively constant stress distribution within certain smaller geotectonic units – blocks and characteristic relation between them.

However, taking into account geotectonic and seismological features of the wider area of Belgrade, it is difficult to suppose that the movement of particular blocks and therewith induced stress could be of such an order of magnitude as to cause total geomagnetic field intensity changes of the obtained magnitude. According to the seismological investigations, the highest expected level of seismic activity characteristic for the territory of Belgrade and its vicinity is 7^{o} MCS, which makes it hard to belive that within the area of given characteristics there could exist geotectonic unit whose relative motion might produce the observed local field changes. Besides, it should also be kept in mind that sedimentary, not magnetic, rocks are mainly present in the area of negative total field intensity changes, and it is one more reason why observable F changes, cuased by particular stress distribution, are not very likely to occur.

Having in mind the principal goal of the project within which these investigations were realized, the following can be concluded. In order to be able to get an insight into a relative movement of geographical coordinates using geomagnetic mehtods according to the scheme: movements of blocks– stress accumulation – stress induced changes of rock magnetization – geomagnetic field changes, it is necessary to use more precise instruments, i.e. magnetometers of 0.1 or even 0.01nT accuracy and therefore adequate data reduction methods. Besides, the interpretation of geomagnetic data should be supported by geodetic and strain data, which are not available at the moment. Only under these conditions we might attempt to interpret small magnitude geomagnetic field changes as a consequence of possible relative motion and interaction of tectonic blocks and therewith induced stress variations.

2. MAGNETOTELLURIC INVESTIGATIONS

The magnetotelluric investigations in the surveyed area have been performed with a goal to examine the time–dependent behaviour of the local electrical properties of the upper crustal layers by measuring a short–period variations of the magnetic and telluric fields. To investigate the time–dependent electrical resistivity changes in crustal rocks, as well as the possibility of detecting an anomalous magnetic fields due to electronic current induced in a conducting dilatant region by short–period geomagnetic fluctuations, we operated during past years, three magnetotelluric recording stations for a period of about two weeks yearly. The magnetotelluric fields have been monitored in the vicinity of Lazarevac and Markovac as well as at Grocka. To exclude the contribution rate of the electrical resistivity changes influenced by a seasonal variation in the temperature, the repeated field observations at the mentioned recording sites have been carried out in the same season each year.

2.1. Estimated parameters

The parameters discussed in this paragraph are the geomagnetic transfer–functions and the impedance tensor elements. The transfer functions „A" and „B" have been computed from a linear relations between the variations of three components of the geomagnetic fields as given by:

$$Z = A \cdot X + B \cdot Y.$$

The impedances Z_{xx}, Z_{xy}, Z_{yx} and Z_{yy} have been computed from an assumed linear relationship between telluric and horizontal magnetic components given by:

$$E_x = Z_{xx} \cdot X + Z_{xy} \cdot Y$$

$$E_y = Z_{yx} \cdot X + Z_{yy} \cdot Y.$$

In these expressions Z, X and Y indicate complex Fourier transform estimates of the downward, north ward and eastward magnetic field, respectively. E_x and E_y denote the spectral estimates of the northward and eastward telluric components, respectively.

The impedance tensor elements, as well as the transfer functions, were determined for the periods of 5, 10, 30, 60 and 120 minutes, usually from moderately disturbed records of approximately 10 hours in length, using a techniques of least–square method in calculation.

We have examined changes in the telluric and magnetic fields over the period of three years. Analysis of data from all recording stations revaled changes in amplitude of telluric and magnetic fields, while no significant changes were observed in the impedance tensor elements or transfer functions. The established increasing trend in impedance as well as in transfer functions is about 4–5% per year. On the basis of these data it is not possible to infer a clear and direct correspondence between impedance or transfer function change and a specific tectonic activity.

Bull. Obs. Astron. Belgrade, N° 138 (1988) UDC 523.44–424

SUMMARY REPORT ON THE SECOND INTERNATIONAL WORKSHOP ON "CATASTROPHIC DISRUPTION OF SMALL SOLAR SYSTEM BODIES"

R. Davis
Planetary Science Institute, 2030 E. Speedway, Suite 201. Tucson, Arizona 85719 U S A.

and

P. Farinella
Dipartimento di Matematica, Universita di Pisa, Via Buonarroti 2, 56100 Pisa, Italia

(Received: 2 December, 1987)

SUMMARY: A brief review is presented of the most important topics and achievements discussed at the Workshop.

Belgrade was indeed an appropriate location to hold the Second Workshop on the subject of Catastrophic Disruption. Few cities have been so often "catastrophically disrupted" as has Belgrade for on no fewer than twenty occasions has this city been ravaged. Yet the stanch Belgradians reassembled their city from the "rubble pile" each time. This workshop was one of four concurrent scientific meetings held to commemorate the centennial of the Belgrade Observatory. It addressed topics of laboratory experiments, scaling laws and numerical modeling, observations and analysis, and future directions for research. Emphasis at this meeting was on progress in the field during the two years since the 1985 Pisa meeting on this same subject.

EXPERIMENTS

Only a modest amount of new experimental results were reported at this meeting as compared with the first one. P. Cerroni outlined experiments that she and A. Fujiwara performed in Japan in recent months using cement mortar targets having a strong core surrounded by a weaker mantle material. Collisional outcomes, ranging from only slight damage to the mantle to complete disruption of the target (including the strong core) were described. The results currently are under analysis to determine the fracture plane distribution. E. Ryan presented results from an experimental program using cement mortar targets having strengths of 3.5 x [illegible] ergs/cm^3 and 3.5 x 10^8 ergs/cm^3. Measured size distributions from 35 experiments having collisional specific energies ranging from 1 x 10^6 to 2 x 10^8 ergs/cm^3 were found generally to agree well with predicted distributions with the possible exception of the very catastrophic experiments.

SCALING

E. Ryan also presented results on scaling of collisional outcomes for different impact velocities and target materials using a computerized data base containing all published results on catastrophic experiments. She demonstrated that the experimentally determined impact strength (defined as the collisional specific energy delivered to a body needed to produce a largest fragment with one–half the mass of the original body) is correlated with the static compressive strength for coherent bodies. Also, by applying existing scaling laws incorporating a strain–rate (or impact velocity) dependence, she showed that scaling with impact velocity and material type could represent the entire experimental data base to within the experimental uncertainties.

On the other hand, the existing algorithms for scaling with target size do not lead to satisfactory results when used in numerical models for asteroid collisional evolution or creation of Hirayama families. D.R. Davis described how the strain–rate scaling predicts much lower strain rates (i.e. weaker strengths) for large (> km sized) bodies than those produced in typical laboratory experiments. Weaker strengths imply more collisional grinding which produced a depleted asteroid belt compared to the observed belt for the preferred initial population found by Davis et al., (**Icarus** 62, 30–53, 1985). Furthermore, models for the break–up of the Themis parent body based on scaling of basalt impact strengths do not match the observed size distribution in this classical asteriod family. The above mentioned problems can be obviated by assuming a laboratory–scale impact strength 25–50 times that of basalt - but this seems to imply an implausibly high strength for natural silicates. P. Farinella pointed out that a problem also exists with the scaling of fragment velocities:

ejection velocities determined for family members are typically larger by a factor of 5–10 than those determined in laboratory experiments. Since for bodies dominated by solid state strength the fragment velocities are likely to scale with the square root of the specific binding energy, the velocity vs. size scaling problem is possibly just another manifestation of the strength vs. size scaling problem.

K. Holsapple and K. Housen gave a summary and critical review of existing scaling laws. Their approach is to apply dimensional analysis in conjunction with specific assumptions regarding the relevant physical variables for the projectile and target in order to derive scaling laws in the strength and gravity regimes. They described a revised model for the size distribution of pre–existing fractures in the target and how this might alter the scaling laws. However, they noted that a common feature of all such scaling is that strength decreases with target size in the regime where material bonds are dominant. This result is experimentally verified for cratering explosions, where the crater volume increases faster than predicted from simply energy scaling alone. The discrepancy between predicted and observed fragment velocities described above was also noted in their work. They pointed out that using observed fragment velocities with their scaling laws would imply a transition from the strength to the gravity regime at sizes of $\sim$ 1 km – much smaller than found using other methods.

On a somewhat different but related problem, numerical simulations of planetesimal accretion incorporating a new collisional outcome algorithm, based on the non–dimensional effective late energy parameter of Mitzutani and Takagi, were presented by M. Hayakawa. Such applications illustrate the importance of developing a general algorithm for collisional outcomes, valid for studies involving collisional accretion as well as collisional destruction. Preliminary results from this simulation show that Mars–sized objects accrete from km–sized bodies on the 10^7 year timescale. However, there was no rapid growth of a single body to dominate the size distribution – rather, there was growth of a number of similar sized bodies at every stage of evolution.

ASTEROID OBSERVATIONS AND ANALYSIS

Observations of asteroids and their analyses provide essential constraints for understanding asteroid collisional history. Of particular interest is the development of a new asteroid taxonomy (M. Fulchignoni) and the application of this taxonomy to dynamical families (G. Valsecchi). The large families were found to be compositionally homogeneous, while others, generally smaller and/or different from the „background" families, appear to make little sense cosmochemically. Differences in family membership as calculated by various authors make it difficult to believe that we can reliably identify small families at this time. Progress on the problem of calculating reliable proper elements for asteroids was described by Z. Knežević. His calculations give proper elements that are verified by direct numerical integration to be stable (to within the accuracy needed for family studies) over intervals of up to 10^5 years. Future work will yield new elements for all asteroids which should lead to better identification of dynamical families in the asteroid belt and to better estimates of ejection velocities in family–forming events.

Rotation rates of small asteroids in the Eos and Koronis families were compared with those of similar sized field asteroids (R. Binzel). He argues that differences in the distribution of rotation rates between families is evidence for a difference in their ages with the Koronis family being relatively young. Numerical models of the collisional evolution of rotation rates suggest very old absolute ages, approaching that of the solar system, although there is considerable uncertainty in the modeling. A. Harris reviewed problems associated with determining asteroid pole directions and shapes from lightcurves. Pole directions can be reliably determined with a suitable observation set while extreme caution was advised in trying to disentangle the effects of asteriod shape and albedo features on asteroid lightcurves. Shape effects dominate when the lightcurve amplitude is > 0.2 mag, but for smaller amplitudes it is generally quite difficult to disentangle the two effects. It was discussed whether the very elongated shapes of some Apollo–Amor asteroids might be representative also for very small main–belt asteroids or might be caused by observational selection effects. Finally, an experimental program for measuring phase curves for meteorites using a photometric goniometer was described by F. Capaccioni. About 25 of the 400 meteorites from the Vatican collection have been measured in this program.

A semiempirical method for calculating fragment sizes, velocities, shapes and rotation rates for a catastrophic break–up event was outlined by A. Cellino and P. Paolicchi. This approach is based on modeling the velocity field and its gradient within the target body. Such a model is able to reproduce several results from laboratory experiments and asteroid observations on fragment velocities and rotation rates, but does not address the scaling problems and leads to discrepancies with respect to the experimental and observational evidence in the slope of the derived mass distributions and in the sensitivity of fragment shapes to the input parameters. The predicted fragment rotation rates 're-member' that of the parent body for the largest fragments but are generally higher and more scattered at smaller sizes. This result agrees with data on the rotation rate distribution of small (< 100 km) asteroids and with Binzel's observations of family members.

FUTURE DIRECTIONS

The final session of the workshop was aimed at identifying the outstanding problems in the field and generating suggestions for future experimental programs to address these problems. The consensus was that size scaling – both for the size and velocity distribution of fragments – is a major problem. Without such scaling, we simply cannot reliably apply the extensive experimental data base to study problems such as asteroid collisional history or fragmentation of small satellites. Improved techniques (better proper elements and statistical cluster analysis techniques) for identifying dynamical families was recognized as a major requirement to test the collisional models against observations. Moreover, the existence (or lack there of) of such families serve as constraints on the collisional history of the asteroids.

Several areas were suggested as being fruitful for future experimental work:

1. Experiments using reassembled targets from previously disrupted bodies.
2. Disruption experiments in a pressure chamber to see if pressure loading increases the strength of the target and, if so, at what point does it become significant.
3. Experiments to test whether the outcome is the same for a given impact energy when the energy is delivered by a series of small collisions rather than a single large one.
4. Further experiments using targets with a core/mantle strength difference in order to establish the minimum energy to collisionally strip away the mantle and expose the core, and to find any difference in the size and velocity distributions of fragments with respect to the homogeneous target case.
5. Data on fragment velocities and rotation rates for weak silicate material and ices at various impact speeds and geometries.
6. Explosive disruption of large ($\gtrsim$ meter–sized) bodies to test size scaling.

Finally the problem of how to determine the age of dynamical families was noted. Estimates of family ages ranged from the age of the solar system to an upper bound of only a few million years. Clearly better techniques are needed to determine how long a dynamical family can be recognized after it is created.

The workshop closed with a decision to accept the invitation of A. Fujiwara to consider holding the third international workshop in Kyoto, Japan in 1990. Clearly much work is to be done if this next meeting is to be as fruitful as the first two have been.

Bulletin de l'Observatoire astronomique de Belgrade No.138, 1988.

CONTENTS